The DAMBE Manual

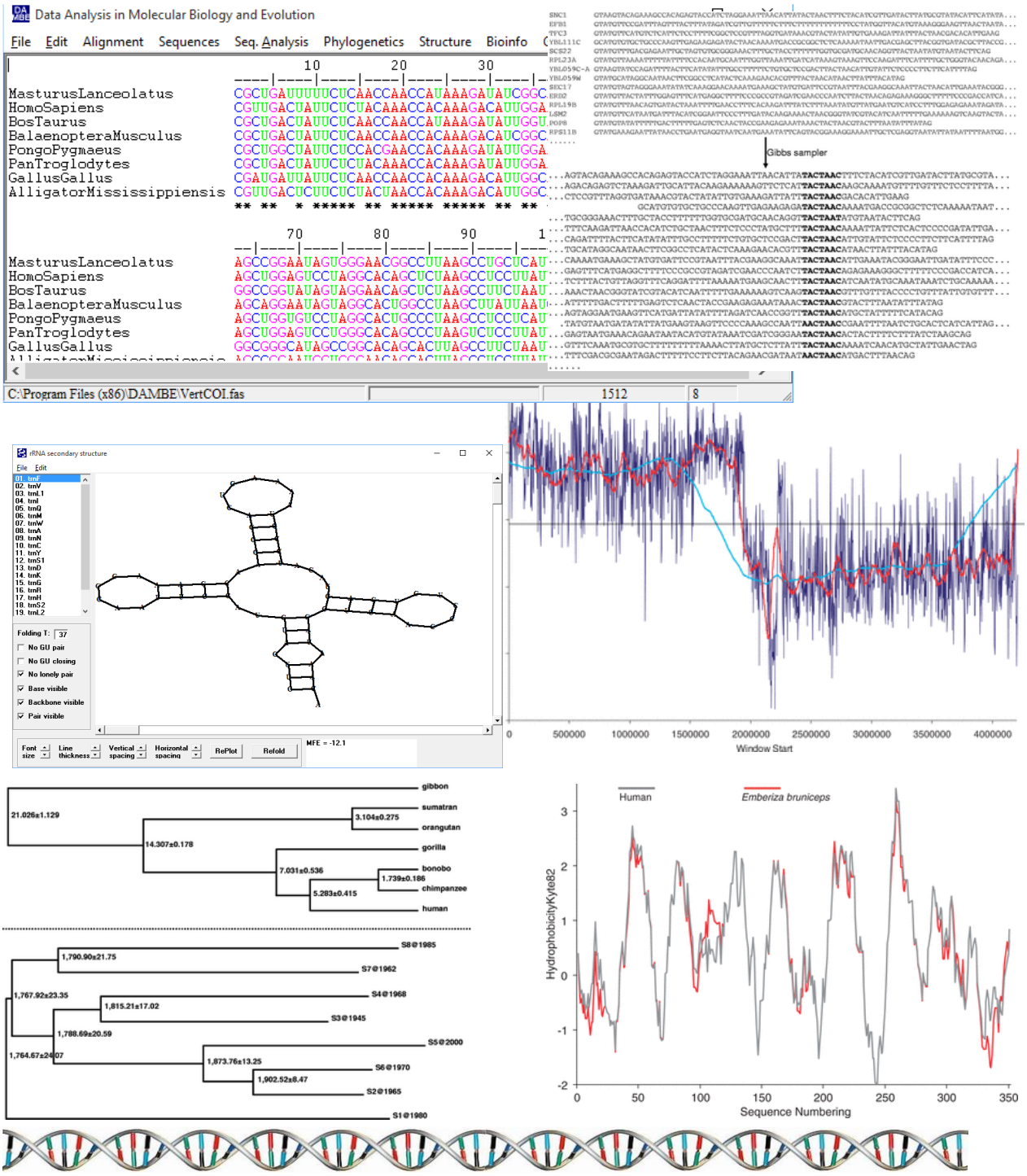

CONTENTS

INSTRUCTION FOR STUDENTS

WHY BIOINFORMATICS?

Bioinformatics is synonymous to computational molecular biology. It has two main objectives. The first is accurate data curation and efficient data delivery, mainly in the form of molecular databases and web interfaces to access the databases. Data curation requires accurate characterization and prediction of genes, gene products, as well as a variety of genetic switches involved in regulating gene expression and function. This objective is exemplified by the databases hosted by NCBI (National Center for Biotechnology Information) and made freely available to the public. Private biopharmaceutical companies typically have their own databases which are not available to the public. This laboratory manual makes extensive use of databases from NCBI.

The second objective of bioinformatics is to develop and use efficient bioinformatics tools to retrieve, parse, organize and analyze the molecular data to reveal relationships that otherwise would be hidden from us. Any data analysis will involve several essential components. First, one abstracts molecular data into variables, e.g., gene expression, protein isoelectric point, index of translation elongation, signal strength of splice sites, substitution rate, evolutionary distances. A variable is typically a vector of numbers. In bioinformatics, a variable is very often a sequence which is a vector of letters, i.e., a vector of four letters of nucleotide sequences or a vector of 20 letters for amino acid sequences. Second, one formulates models to characterize relationship among these variables. Relationships among vectors of numeric values are typically expressed as an algebraic model. Relationships among vectors of letters (e.g., aligned sequences) are typically expressed as a tree or a graph, e.g., a phylogenetic tree. Finally, given alternative ways of modelling the data, we formulate and use criteria to choose the best model among different alternatives.

Bioinformatics tools are equivalent to the fishing fleet operating in the vast oceans of databases – the 'ocean' would be of little value if we do not have the means to make use of it. Just like telescopes and a microscopes can extend our vision, a good computational tool can also enable us to see things that we wouldn't have seen before. We use these bioinformatics tools to examine the molecular data for patterns that have been hidden from us, and to derive new insights that would otherwise be beyond our imagination.

WHY DAMBE?

This laboratory manual makes extensive use of DAMBE (Xia and Xie 2001; Xia 2018a) in illustrating functionalities of bioinformatics algorithms. DAMBE is a general-purpose bioinformatics platform for descriptive and comparative genomics and evolutionary bioinformatics, implementing the complete functionality of about 200 commonly used computational algorithms in bioinformatics and molecular evolution. In addition, it extends its function by integrating widely used bioinformatics tools such as MAFFT (Katoh, et al. 2005; Katoh and Frith 2012) and MUSCLE (Edgar 2004b) for sequence alignment, PhyML (Guindon and

Gascuel 2003; Guindon, et al. 2005) for likelihood-based phylogenetic reconstruction, and ViennaRNA package library (Hofacker 2003) for modeling RNA secondary structure.

Two books (Salemi and Vandamme 2003; Felsenstein 2004) listed DAMBE as one of the most widely used software packages in molecular phylogenetics, but DAMBE also features numerous computational tools beyond phylogenetics. These include position weight matrix for characterizing and predicting sequence motifs, perceptron for two-group classification of sequence motifs, Gibbs sampler for *de novo* motif discovery in nucleotide and amino acid sequences, RNA secondary structure prediction, tRNA anticodon identification, characterization of codon usage bias with RSCU, N_c, CAI and I_{TE}, computing protein isoelectric point, hydrophobicity plot, among many others. The original publication of DAMBE (Xia and Xie 2001) was cited 2409 times by Dec. 21, 2020 according to Google Scholar. An update of DAMBE (Xia 2013b) has been cited 898 times by Dec. 21, 2020. Another DAMBE update (Xia 2018a) have been cited 158 times in slightly over one year. My typical feedback from DAMBE users is that they wish to have known DAMBE earlier. These numbers attest to DAMBE's popularity among active researchers and my commitment to DAMBE users.

DAMBE was actually created more for teaching than for research. It has been installed in various university computer laboratories around the world. We teachers typically would try to convince our students that the teaching materials they receive from us are the best they could ever find, much in the same way as a merchant selling a spade. A spade-selling merchant will not tell us that the spade he sells is good for digging our own graves. Instead, he would try to persuade us into believing that there are treasures hidden somewhere, that the spade is a handy tool for digging up the treasure, that almost everyone has already acquired a spade, and that we would be at a terrible disadvantage if we do not acquire a spade quickly. Now to demonstrate the salesmanship that I have acquired from teaching in various universities, let me share with you the secret that there is indeed much treasure hidden in large molecular databases, that computer programs such as DAMBE are indeed handy tools for digging up the treasure, that almost everyone has already been using these computer programs, and that you would be at a terrible disadvantage if you fail to acquire the efficiency in using them, especially if you are going to be a student in molecular biology or biopharmaceutical or biomedical sciences.

Although DAMBE may be available in computers in university teaching labs, you are encouraged to install the most updated DAMBE on your own computer to take advantage of new functions periodically added to the software. DAMBE is freely available at http://dambe.bio.uottawa.ca/DAMBE/dambe.aspx. Installation requires only a few mouse clicks.

ANSWERS ALL QUESTIONS AT THE END OF EACH LAB

There are questions at the end of each laboratory in this manual. Knowing the answers to all questions will enhance your study in subsequent laboratories. If you are in Ottawa, my office door is always open to you if you have any questions related to this manual or DAMBE. Please email me any questions on the laboratory or on DAMBE if you are not in Ottawa. I response to user enquiries in one day or two.

ACKNOWLEDGEMENT

Many graduate students have contributed to improving this manual. I particularly wish to thank Lisha Tang, and Caitlyn Vlasschaert for going through the manual and identify errors and inconsistencies. Akramalsadat Abolbaghaei, Parisa Aris, Shivapriya Chithambaram, Olga Jarinova, Sam Khalouei, Alibek Kruglikov, Pinchao Ma, Ramanandan Prabhakaran, Manon Ragonnet, Jordan Silke, Anna van Weringh, Huaichun Wang, Juan Wang, Yulong Wei, Huiling Xiong and Xiaoquan Yao have also provided comments, suggestions and corrections.

LAB 1 SEQUENCE DATABASES AND STRING MATCHINGS

SUMMARY

1. Learn two sequence formats: the simplest FASTA format and the very complicated GenBank format
2. Use NCBI Entrez to download a HIV-1 genome (KAL153 which is isolated from Kaliningrad) and extract all coding sequences annotated in the genome
3. Compute nucleotide frequencies and Karlin-Altschul parameters that are essential for accurate computation of E-value in string matching used in BLAST and FASTA.
4. Identify KAL153 subtype by using local BLAST (build a BLAST library from HIV-1 subtype reference sequences and then search *env* and *gag* gene sequences from KAL153 against the BLAST library). Another method for subtype identification is to build a phylogeny, which is the subject in a latter laboratory.

To be a good bioinformatician, one must be (1) familiar with bioinformatic resources in public databases otherwise you would be like a whale-hunter without knowing where the ocean is, and (2) capable of using and developing a variety of Bioinformatic tools to retrieve the data from these databases and to analyze the data to facilitate the process of converting information to knowledge. Indeed, an overwhelming amount of undigested information may not only dazzle our eyes, but also confuse our mind. It is for this reason that many computer programs have been developed in the last decade to facilitate the harvesting of organized and valuable knowledge from the bewildering jungle of molecular information. This first laboratory is to 1) introduce you to sequence data with a few sequence formats and 2) develop your skill in using bioinformatic tools to address biological questions.

1.1 REPRESENTATIVE DATABASE AND WEB INTERFACE: NCBI, GENBANK, AND ENTREZ

NCBI hosts the vast ocean of data including GenBank and many other databases accessed through the web portal Entrez. Consider human data alone. The Human Genome Project started in 1990 and the first draft was published by the Human Genome Project (International Human Genome Sequencing Consortium 2001) and Celera (Venter, et al. 2001). Human sequences in GenBank total 14,792,487,417 bases in 2010 (Benson, et al. 2011), and the 1000 Genomes Project (The 1000 Genomes Project Consortium 2010, 2012) will generates terabytes of human sequences. This huge amount of data offers unprecedented opportunities to understand human genetic variation, especially those variations that cause diseases. The GenBank also contains sequences for 380,000 organisms by 2010 (Benson, et al. 2011).

All these terabytes of sequences from the genomes of organisms will soon be dwarfed by the sequence data generated by RNA-Seq, the sequencing of the whole transcriptome of organisms in different cell types and different time points, facilitated by the next-generation sequencing technologies (Morin, et al. 2008; Birol, et al. 2009; Ahn, et al. 2010; Goya, et al. 2010; Griffith, et al. 2010; Kridel, et al. 2012; Roth, et al. 2012). Such data have rendered the DNA microarray and SAGE data obsolete, so I have removed all teaching material related to microarray and SAGE data.

The explosion of molecular sequence data spawned the development of the International DNA Databases with three participating members, the GenBank in USA, the EMBL (European Molecular Biology Laboratory) databases in Europe, and the DDBJ (DNA Data Bank of Japan) in Japan. The sequence information submitted to each of these three centers is exchanged and synchronized daily to ensure the homogeneity of sequence information among the three centers. NCBI assumed responsibility for the GenBank DNA sequence database in October 1992. In addition to GenBank, NCBI supports and distributes a variety of other databases for the medical and scientific communities.

NCBI databases are equivalent to a gigantic shopping mall. We need a custom-friendly corridor and storefront for us to browse around and to pick what we need. The web portal Entrez is the user-friendly corridor and storefront for NCBI databases. Many different types genomic, transcriptomic, and proteomic databases are organized and presented via the Entrez portal, which is NCBI's search and retrieval system. A powerful and unique feature of Entrez is the ability to retrieve related sequences, structures, and references. The journal literature is available through PubMed, a Web search interface that provides access to over millions of journal papers in MEDLINE and contains links to full-text articles at participating publishers' Web sites.

1.2 ANNOTATED SEQUENCES

Terabytes of sequence data are now generated by genomic sequencing projects. A sequence in a database is equivalent to a word in a dictionary. A good dictionary features not only a comprehensive list of words, but also an authoritative explanation of the words. Similarly, a good sequence database such as GenBank features not only a comprehensive list of sequences, but also annotations of the sequences such as start and end sites of the exons and introns, transcription and translation initiation and termination sites, rRNA and tRNA genes, functions of proteins, etc.

The annotation process is analogous to decoding the meaning of a lengthy text. Two approaches can be taken in the decoding. First, if you already have a good dictionary, you can check individual words against the dictionary. Molecular biologists have already worked out the meaning of a large number of genes that are annotated and deposited in NCBI. One uses BLAST (Altschul, et al. 1990; Altschul, et al. 1997) or FASTA (Pearson 1990) algorithms to query new sequences against the large but still limited 'gene dictionaries'. The other approach is when we already understand the language reasonably well, and can infer the meaning of a new word based on the context it appears (e.g., is it a noun, a verb, etc.). This *de novo* gene prediction is represented by GenScan (Burge and Karlin 1997), GLIMMER (Salzberg, et al. 1998), and Contrast(Flicek 2007).

Just as different dictionaries could have different explanations for the words, different sequence databases could also differ in sequence annotations. It has been agreed that a gene sequence contains three pieces of information that are the most fundamental to biologists: 1) the function of the gene product, 2) the biological processes the gene product participates in, and 3) cellular localization. A gene sequence annotated with these three pieces of information is said to be GO-annotated, where GO stands for gene ontology (Gene Ontology Consortium 2008, 2021)

1.3 AMBIGUOUS CODES, INDEL, AND MISSING SYMBOLS IN SEQUENCES

There are two scenarios where ambiguous codes can arise. First, it is simply not resolved in sequencing, which may be due to poor sequencing quality or to the existence of polymorphic sites. Second, the site is intentionally degenerated, e.g., codons AAA and AAG degenerated to AAR or the four Ala codons degenerated to GCN, where 'N' stands for a base that is present but unresolved. The ambiguous codes are well defined (Table 1-1) and does not cause confusion.

Table 1-1. **IUB codes of nucleotides.**

Code	Meaning	Complement
A	A	T
C	C	G
G	G	C
T/U	T	A
M	A or C	K
R	A or G	Y
W	A or T	W
S	C or G	S
Y	C or T	R
K	G or T	M
V	A or C or G	B
H	A or C or T	D
D	A or G or T	H
B	C or G or T	V
X/N	G or A or T or C	X
-	Gap (not G or A or T or C)	-

There are two approaches of treating these ambiguous codes. The first is to treat an 'R' as A or G each with a probability of 0.5. When comparing a aligned site between two sequences, with A in one sequence and R in another, this would be interpreted as A/A match and A/G match each with a probability of 0.5. Similarly, an A/N match would be interpreted as A/A match, A/C match, A/G match and A/T match each with a probability of 0.25. The second approach will make use of nucleotide frequencies from all input sequences. If nucleotide

frequencies of all sequences are P_A, P_G, P_C, and P_T, then an 'N' is taken to have a probability of A, G, C, and T with probabilities P_A, P_G, P_C, and P_T, respectively.

While the treatment of ambiguous codes are reasonable for computing nucleotide frequencies, it can cause serious problem in computing sequence divergence. For example, suppose we have four identical sequences (S1, S2, S3 and S4) of length 100 in Fig. 1-1A. The sequence divergence, as measured by the proportion of sites differing between the two sequences (P_{ij}), should be 0 between each pair of sequences. However, if S3 and S4 have some ambiguous sites as indicated in Fig. 1-1B, then the P_{ij} could be substantially greater than 0 (Fig. 1-1C). Only maximum likelihood methods in molecular phylogenetics, which we will learn in the later part of the course, can properly handle the ambiguous codes in sequence comparisons.

```
(A)         10         20         30         40         50
    ----|----|----|----|----|----|----|----|----|----|----|----|
S1 CGCTGATTTTTCTCAACCAACCATAAAGATATCGGCACCCTTTATTTAGTATTTGGTGCA
S2 CGCTGATTTTTCTCAACCAACCATAAAGATATCGGCACCCTTTATTTAGTATTTGGTGCA
S3 CGCTGATTTTTCTCAACCAACCATAAAGATATCGGCACCCTTTATTTAGTATTTGGTGCA
S4 CGCTGATTTTTCTCAACCAACCATAAAGATATCGGCACCCTTTATTTAGTATTTGGTGCA
(B)
S1 CGCTGATTTTTCTCAACCAACCATAAAGATATCGGCACCCTTTATTTAGTATTTGGTGCA
S2 CGCTGATTTTTCTCAACCAACCATAAAGATATCGGCACCCTTTATTTAGTATTTGGTGCA
S3 CGCTGATTTTNNNNNNNNNNCCATAAAGATNNNNNNNNNNTTTATTTAGTATTTGGTGCA
S4 CGCTGATTTTTCTCAANNNNNNNNNNAGATATCGGCACCCTTTATTNNNNNNNNNTGCA
(C)
```

P_{ij}:Proportion of sites differ between sequences i and j

$$P_{12} = 0; P_{13} = P_{14} = P_{23} = P_{24} = \frac{10\times0.75}{60} = 0.125; P_{34} = \frac{16\times0.75+20\times0.75}{60} = 0.45$$

Fig. 1-1. Fictious sequences illustrating the problem of treating ambiguous codes in computing sequence divergence. (A) Four sequences, S1, S2, S3 and S4 are identical. (B) The same four sequences but with some with ambiguous codes in sequences S3 and S4. (C) While correct P_{ij} should be 0, the P_{ij} values computed from sequences with ambiguous codes in (B) are greater than 0. Only maximum likelihood methods, which we deal with later, can handle ambiguous codes properly.

Indels and missing values in sequences have been a source of confusion in sequence comparisons. Aligned sequences typically have insertions or deletions (indels) represented by symbol '-'. An indel can be of length 1, 2 or greater. We have a vague notion that 1) longer indels probably occur less frequently than shorter ones, 2) frameshifting indels most likely occur less frequently than frame-preserving indels, and 3) an indel occurs less frequently than a nucleotide substitution. However, it is difficult to formulate an indel substitution models for sequence comparisons. For this reason, a '-' is typically considered missing for convenience in the likelihood-based inferences on sequence evolution. As we will learn later, likelihood methods can handle missing values quite elegantly, but it cannot handle indels without a properly formulated indel substitution model. As we do not have a satisfactory method to handle indels, we might as well treat it as missing information.

1.4 SEQUENCE FORMATS

NCBI uses both machine-readable sequence formats such as ASN.1 and XML and the human-readable formats such as GenBank and FASTA formats. FASTA format is one of the simplest sequence formats, and GenBank format is one of the most complicated sequence formats. These two file formats, as well as many other sequence formats, can be directly read into DAMBE.

Aside from machine-readable ASN.1 and XML formats, sequence files in GenBank can be retrieved in one of two plain text formats via the Internet. One format is the FASTA format, which is one of the simplest sequence formats, and the other is the GenBank format, which is one of the most complicated sequence formats. These two file formats, as well as many other sequence formats, can be directly read into DAMBE.

1.4.1 FASTA format

Files in the FASTA format contain just plain sequences and sequence labels, with optional descriptions that can be added one space after the sequence label, i.e.,

>SeqName1 Optional description here in the same line. Anything after the first space is ignored
ACCGGTTT……
>SeqName2 The sequences in the file can contain indels, ambiguous codes or missing values.
ACUGGCTT……

A database with sequences in FASTA format is equivalent to a word list with no explanations. The FASTA format is typically used when we know nothing about the sequence other than the sequence itself. All automatic sequencers can generate sequences in FASTA format. Sequence annotation typically start from BLASTing or aligning these sequences against known and annotated sequences in GenBank, i.e., checking the meaning of a new word (a sequence) against a gene dictionary.

1.3.2 GenBank format

In contrast, the GenBank format represents the most complicated sequence format typically with extensive sequence annotation contained in the FEATURES table section. A database with sequences in GenBank format is equivalent to the Oxford English Dictionary where one finds comprehensive annotation of individual words. Sequence annotation represents a key step in the genomic sequencing pipeline.

Sequence files in the GenBank format typically have the file type of .GB or .gbk. Each sequence record has a unique ACCESSION number that is permanent. An ACCESSION number typically contains six characters (one letter and 5 digits, e.g., U49845) or eight characters (two letters and six digits) and the corresponding LOCUS name is usually the ACCESSION number prefixed with the initials of the genus and species names. For example. SCU49845 is a sequence from the yeast *Saccharomyces cerevisiae*. A GenBank format starts with a LOCUS name, which was originally designed to be informative in addition to being unique. However, the only rule for LOCUS name now is that it is unique. When a sequence is updated, e.g., if the original contains unresolved bases that have been subsequently resolved, then the version number will be increased, e.g., U49845.1 $\rightarrow$ U49845.2.

The sequences curated by NCBI personnel in collaboration with INSDC (International Nucleotide Sequence Database Collaboration) are stored in the RefSeq database. These sequences have rather unique ACCESSION numbers containing 9 or 12 alphanumeric characters (i.e., two letters, an underscore, plus six or nine digits):

NT_123456, or NT_123456789 constructed genomic contigs
NG_123456, or NG_123456789 non-transcribed genomic region or incomplete/unannotated
NM_123456 or NM_123456789 mRNAs
NR_123456 or NR_123456789 non-coding RNA
NP_123456 or NP_123456789 proteins
NC_123456 or NC_123456789 chromosomes
XM_123456 or XM_123456789 mRNAs
XR_123456 or XR_123456789 non-coding RNA
XP_123456 or XP_123456789 proteins

These sequences are generally referred to as NCBI-curated or RefSeq sequences. Many submitted genomes each have two ACCESSION numbers, one assigned for the original submission by laboratories that sequenced and submitted the genome, and the other assigned after NCBI scientists have checked and curated the genome. You should use the NCBI curated genome whenever possible.

You may be wondering what differences there are between NM and XM, NR and XR, and NP and XP. XM_123456 identifies an mRNA derived from a well-annotated genome, while NM_123456 may refer to an mRNA from a mutant. Those start with X (e.g., XM, XR, XP) are called model RefSeq sequences. If an *E. coli* strain is sequenced 10 times and if one particular site in a coding sequence is nucleotide A in 9 of the 10 times, and G only once, then we would **predict** the site to be A, and the associated XM_123456 will have A at that site. In this context, a model sequence is a predicted (most representative) sequence.

Familiarity with NCBI data source is essential for a bioinformatician. Every sequence submitted to GenBank/EMBL/DDBJ is assigned a permanent and unique accession number that one can use to retrieve the sequence. The genomic sequence of the KAL153 HIV-1 viral strain, which will be used in this lab, has an accession number AF193276. When we need to retrieve this sequence, we tell a database of HIV-1 sequences that we wish to see AF193276, and our faithful database genie will go to fetch the associated genomic sequences right away.

Each of the GenBank sequences may contain multiple coding regions (CDS), multiple introns and exons, and multiple rRNA and tRNA genes. These different sequence elements within a contiguous sequence are specified in what is known as the FEATURES table in GenBank files (Fig. 1-2). For each annotated genomic elements, e.g., CDS, or exon, the FEATURES table specifies its location (starting and ending sites on which DNA strand). Software tools use information in the FEATURES table to extract various sequence elements (e.g., all CDSs, all

exons, 100 nt upstream of CDSs, exon-intron junctions, etc.). For example, the yeast gene *SNC1* has a coding sequence (CDS) made of two exons. The start and end sites of the first exon is specified by "87286..87387", and the second exon is specified by "87501..87752". The intron sequence between these two sequence segments, i.e., starting from 87388 and ending at 87500.

```
LOCUS       NC_001133             230218 bp    DNA     linear   CON 17-FEB-2017
DEFINITION  Saccharomyces cerevisiae S288c chromosome I, complete sequence.
...
SOURCE      Saccharomyces cerevisiae S288c
...
REFERENCE   1  (bases 1 to 230218)
  AUTHORS   Goffeau,A., Barrell,B.G., Bussey,H., Davis,R.W., Dujon,B.,
            Feldmann,H., Galibert,F., Hoheisel,J.D., Jacq,C., Johnston,M.,
            Louis,E.J., Mewes,H.W., Murakami,Y., Philippsen,P., Tettelin,H. and
            Oliver,S.G.
  TITLE     Life with 6000 genes
  JOURNAL   Science 274 (5287), 546 (1996)
...
FEATURES             Location/Qualifiers
     source          1..230218
...
     CDS             join(87286..87387,87501..87752)
                     /gene="SNC1"
                     /locus_tag="YAL030W"
```

Fig. 1-2. Partial display of chromosome I in the yeast (*Saccharomyces cerevisiae*) strain S288c.

In addition to sequence annotation specified in the FEATURES table, GenBank also include associated information such as classification of the organism and publications directly related to the genomes. This is particularly useful to many bioinformaticians who do not have a strong biological background. The references allow them to quickly gain familiarity with the background knowledge.

1.5 EXTRACT CDS, INTRONS, OR OTHER SEQUENCE ELEMENTS

Extracting sequence elements from GenBank files is an essential skill in bioinformatics. I will give you three examples. First, my student Caitlin Vlasschaert was interested in alternative splicing of the human USP4 gene which contains 22 exons but exon 7 is often skipped. She hypothesized that the skipped exon has flanking introns with weak splicing signals (Vlasschaert, et al. 2017). This would require the extraction of exon-intron junctions for a detailed analysis. Second, another student of mine, Yulong Wei, wishes to know whether highly expressed bacterial genes have stronger termination signals made of stop codon and flanking nucleotides. This would require the extraction of stop codon and flanking nucleotides from highly expressed and lowly expressed genes (Wei, et al. 2016; Wei and Xia 2017). Third, my students Jordan Silke and Yulong joined their effort to characterize translation initiation and elongation efficiency in bacterial species, so they need to extract Shine-Dalgarno (SD) sequences from protein-coding genes and anti-SD sequences from small subunit rRNA, as well as tRNA sequences to obtain their relative abundance in transcriptomes (Wei, et al. 2017; Wei, et al. 2019). It is through this type of studies that scientists are now able to engineer a gene so that it can be efficiently translated in bacterial, fungal, or human cells. Such expertise came handy in the production of mRNA vaccines that need to be efficiently translated in human cells (Xia 2021).

The main objective of this lab is to learn simple sequence data retrieval and processing, and to gain practical application of string matching. We will retrieve the KAL153 viral genome by using its accession number AF193276, extract all protein-coding genes, compute nucleotide frequencies and Karlin-Altschul parameters for accurate computation of E-value in string matching, and investigate whether KAL153 is a recombinant.

1.6 WORKING WITH THE KAL153 GENOME

(If there is any problem with the databases at NCBI Entrez, then just download the **KAL153_AF193276.gb** file at http://dambe.bio.uottawa.ca/teach/bps4104_download/KAL153_AF193276.gb).

Browse to Entrez cross-database search at http://www.ncbi.nlm.nih.gov. Close to the top of the page you will see a dropdown box 'All databases'. Choose 'Nucleotide' and enter 'AF193276' as the search term. When the sequence in GenBank format is displayed, click 'Send|File|Create file' to save the HIV-1 KAL153 genome in GenBank format to your personal directory (I will omit the details of how to download and save the sequences,

but trust that you will figure it out by yourself. Ask me or TA if you cannot). Name the file KAL153.gbk or something informative (If you do not know the accession number, you may enter 'KAL153' as query).

1.6.1 Extracting coding sequences from a GenBank file

Start DAMBE, and click 'File|Open standard sequence file'. In the 'File of type' dropdown listbox (Fig. 1-3), choose 'GenBank' file format. Choose the saved KAL153.gbk file and click the 'Open' button.

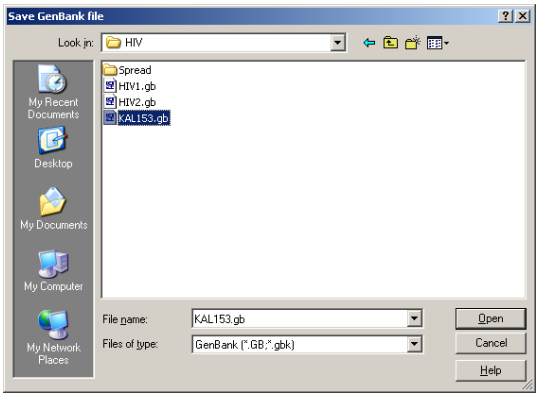

Fig. 1-3. File open dialog in DAMBE. Different sequence formats can be selected by clicking the 'Files of type' dropdown box.

A large dialog box appears (Fig. 1-4) for you to choose which sequence elements to extract. Choose CDS and optionally check 'Include location ID' so that you know where each CDS starts along the genome. Click OK. When prompted for type of sequences, choose 'Protein-coding nucleotide sequences' and select translation table 1 (standard genetic code, which is the default. There are now 18 different genetic codes). Examine the extracted CDSs. The default number of sequences and sequence length display in DAMBE can be changed by clicking 'Tools|Options'.

Save the file in FASTA format by clicking 'File|Save or convert sequence file' and choose 'Pearson/FASTA' in the 'Save as type' dropdown box save it to file **KAL153CDS.fas**. We will need this file later. The '.fas' file type is for sequence files in FASTA format, which, in contrast to the very detailed GenBank format, is the simplest possible sequence format. All automatic sequences output sequences in FASTA format. If you wish to save only a subset of sequences, click 'File|Save a subset of sequences'. We will save the *env* and *gag* sequences into a separate file. In the ensuing dialog box, provide a file name, e.g., **KAL153_Env_Gag.fas**. Choose env and gag and click the '→' button. Click 'Go!' to save.

When you click the 'Save as type' dropdown box, you will see a long list of available sequence formats that DAMBE can convert to. Some of them (e.g., MEGA, PHYLIP, PAUP/Nexus) require aligned homologous sequences. They are used mainly for comparative sequence analysis including building phylogenetic trees and dating speciation or gene duplication events.

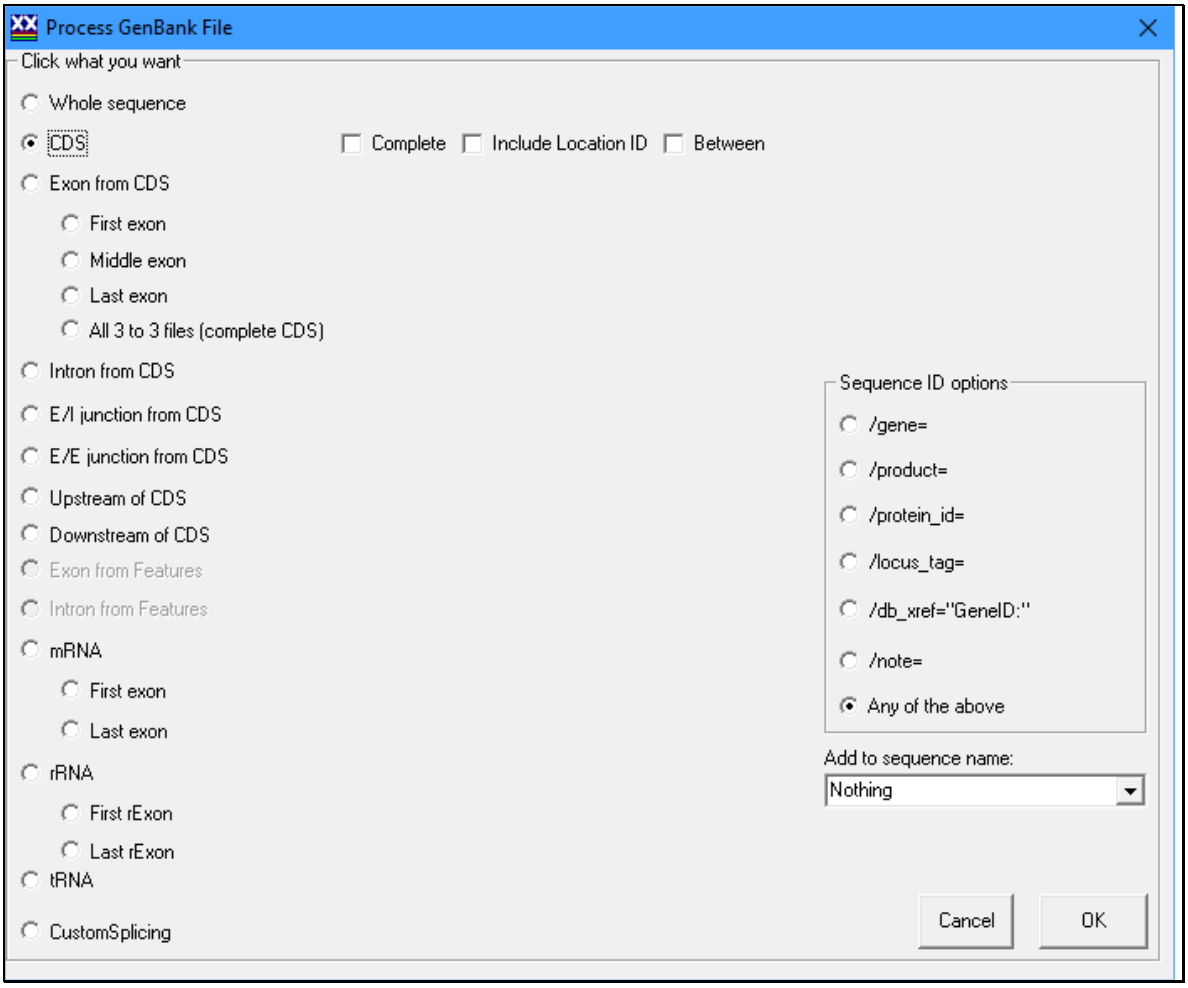

Fig. 1-4. Sequence extraction dialog box in DAMBE for GenBank files.

1.6.2 Computing nucleotide frequencies

Recall that, for a rigorous BLAST search, we should compute our own Karlin-Altschul parameters (λ, K and H) for computing an accurate E-value. Computing these parameters require s two types of input. The first is nucleotide frequencies and the second is match/mismatch scores. Here we use DAMBE to compute nucleotide frequencies. DAMBE organizes the functions that describe sequences under the 'Seq.Analysis' menu. The first group of submenus are functions for nucleotide sequences, the second for codon sequences and the third for amino acid/protein sequences. To calculate nucleotide frequencies, click 'Seq.Analysis|Nucleotide & di-nuc frequencies'. In the ensuing dialog box (Fig. 1-5), click the 'Add all' button, and optionally di-nucleotide frequencies. Click the 'Go' button.

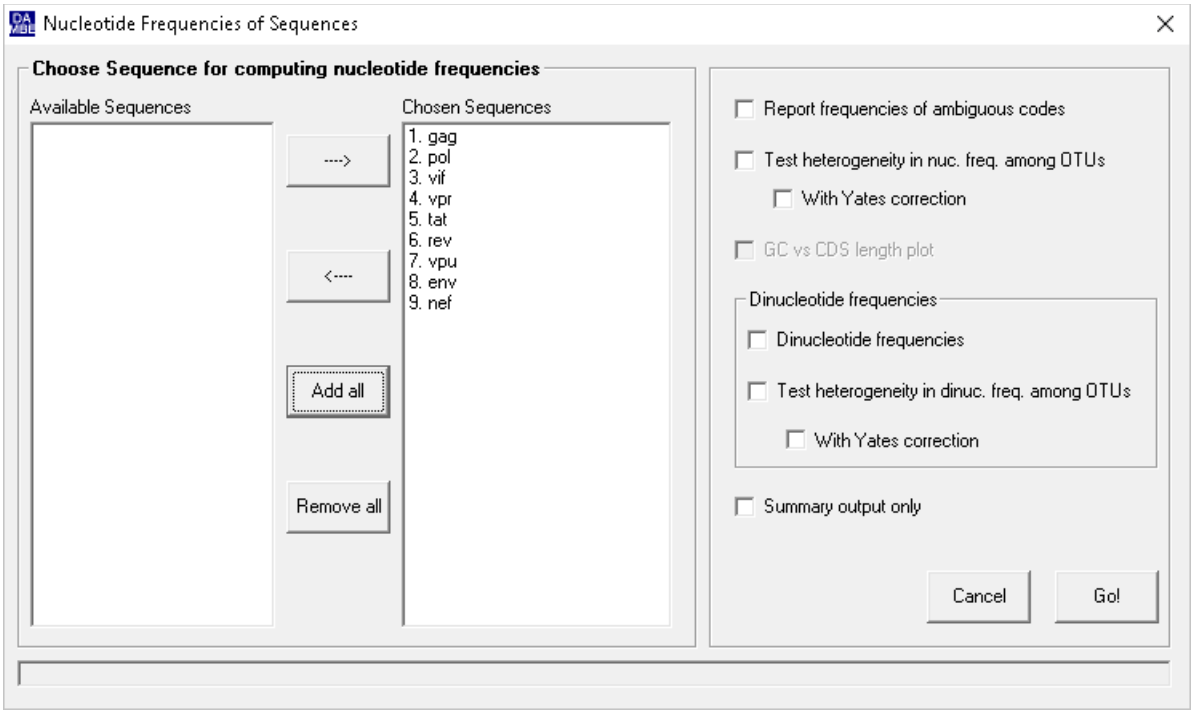

Fig. 1-5. Dialog box for computing nucleotide frequencies in DAMBE.

The resulting nucleotide frequencies are shown in Table 1-2. The first four columns are observed counts. They are summed to 'Sum(ACGT)'. The X^2-tests, with X^2 value s and the associated p values (ProbX2), are performed for each gene against the null hypothesis that nucleotide frequencies are all equal to 0.25. The last four columns are the nucleotide frequencies for each input sequences. The global nucleotide frequencies from pooling all sequences together are also in the output.

Table 1-2. Nucleotide counts and frequencies for input sequences. The global frequencies for A, C, G and T are 0.3647, 0.1777, 0.2402 and 0.2174. The X^2-test is against the null hypothesis of equal nucleotide frequencies.

SeqName	A	C	G	T	Sum(ACGT)	X2	ProbX2	PA	PC	PG	PT
Gag	552	292	367	286	1497	123.4490	0.0000	0.3687	0.1951	0.2452	0.1910
Pol	1173	496	685	658	3012	340.1040	0.0000	0.3894	0.1647	0.2274	0.2185
Vif	216	98	138	127	579	52.6610	0.0000	0.3731	0.1693	0.2383	0.2193
Vpr	96	51	78	66	291	14.9380	0.0019	0.3299	0.1753	0.2680	0.2268
Tat	81	66	63	51	261	7.0000	0.0719	0.3103	0.2529	0.2414	0.1954
Rev	107	80	96	68	351	10.1280	0.0175	0.3048	0.2279	0.2735	0.1937
Vpu	91	26	64	56	237	36.2320	0.0000	0.3840	0.1097	0.2700	0.2363
Env	652	306	417	446	1821	137.3640	0.0000	0.3580	0.1680	0.2290	0.2449
Nef	190	123	172	124	609	22.7830	0.0000	0.3120	0.2020	0.2824	0.2036

1.6.3 Computing Karlin-Altschul parameters

Click 'Alignment|Karlin-Altschul parameters' and we will see the options for computing these parameters for either nucleotide or amino acid sequences by clicking the 'Nuc' or 'AA' option button. The default is nucleotide, and is what we need for this lab. The dialog shows sample input: 1) a match-mismatch score matrix, and 2) nucleotide frequencies. You should replace the nucleotide frequencies with your own nucleotide frequencies computed before, and optionally change the match/mismatch scores (but never let mismatch scores greater than match scores). The sample input has a score of 1 for a match, a score of -1 for a transition difference and a score of -3 for a transversional difference. You can either modify the sample input or paste into the box your own s_{ij} matrix and nucleotide frequencies. Click the 'Get L, K, H' button to calculate λ, K and H parameters. For amino

acid sequences, the sample input has a PAM30 matrix as the s_{ij} matrix. Click the 'Get L, K, H' button will calculate λ, K and H parameters appropriate for the s_{ij} matrix and the specific amino acid frequencies.

1.6.4 Which subtype does KAL153 belong to? Is it recombinant?

1.6.4.1 Subtypes in HIV-1 M group

There are nine subtypes labelled as A, B, C, D, F, G, H, J, and K in the M group of HIV-1. Their genomic sequences can be retrieved from either GenBank hosted at NCBI, HIV Databases hosted by Las Alamos National Laboratory at http://www.hiv.lanl.gov/, or my University of Ottawa download page for teaching at http://dambe.bio.uottawa.ca/teach/bps4104_download/download.aspx. It is important to know which subtype in the HIV-1 M group (where M stands for 'major') your HIV-1 strain belongs to because different subtypes may have different viral properties and respond to AIDS drugs differently. Identification of subtypes are typically done by sequencing the *env* and *gag* genes and then following one of two approaches. The first is simply to BLAST your *gag* and *env* sequences against the reference set of subtype sequences. If your query sequence matched subtype A sequence much better than all other subtypes, then your query belong to subtype A. The second is to construct a phylogenetic tree with all subtypes and the new HIV-1 sequence and see which subtype clusters together with your new HIV-1 sequence. If your new sequence is clustered with subtype A with high confidence, then your HIV-1 sequence belongs to subtype A.

1.6.4.2 Retrieve reference subtype sequences

To retrieve subtype reference sequences from Las Alamos HIV Databases, browse to http://www.hiv.lanl.gov/content/sequence/NEWALIGN/align.html, choose 'Subtype reference' in 'Alignment type' field, 'ENV' or 'GAG' in the 'Pre-defined region of the genome, 'M group without recombinants (A-K)' in the subtype field, and click the 'Get Alignment' bottom to retrieve the aligned sequences in FASTA format. Save the retrieved sequences in files such as **RefEnv.fas** and **RefGag.fas**. These sets of reference sequences are aligned, but have five problems. First, they were not updated since 2010. Second, they are inconsistent with the sequence annotation in the NCBI GenBank files. Third, contains multiple inframe stop codons which should not appear in functional coding sequences. Fourth, the alignment quality appears poor. Fifth, some sequences are very short and may be partial sequences. For this reason, it is better to extract the *env* and *gag* sequences from GenBank files and filter out poor and incomplete sequences. I have done this and deposited the resulting *env* and *gag* sequences at http://dambe.bio.uottawa.ca/teach/bps4104_download/download.aspx in two files: **RefGag.fas** and **RefEnv.fas**. Please download these two files and save in a directory, so that we can perform subtype identification by using BLAST.

1.6.4.3 Use BLAST to identify subtypes

(All input and output files in this section need to have no space in the file name or directory name. You will have an error if you have a file such as C:\My Documents\MyFile.fas because there is a space in 'My Documents', or C:\Temp\Test File.fas because there is a space in 'Test file.fas'.)

Create local BLAST libraries: BLAST libraries facilitate repeated searches by preprocessing the target (database) sequences so that search results can be returned quickly in response to a user query. We will create two BLAST libraries, one from **RefEnv.fas** and the other from **Ref.Gag.fas**.

DAMBE uses the NCBI program makeblastdb.exe to create BLAST libraries. Start DAMBE and click 'Alignment|BLAST'. In the dialog box (Fig. 1-6), select **RefEnv.fas** and specify the directory where the resulting BLAST library will be stored. Click the 'OK' button and the library will be created. Do the same for **RefGag.fas**.

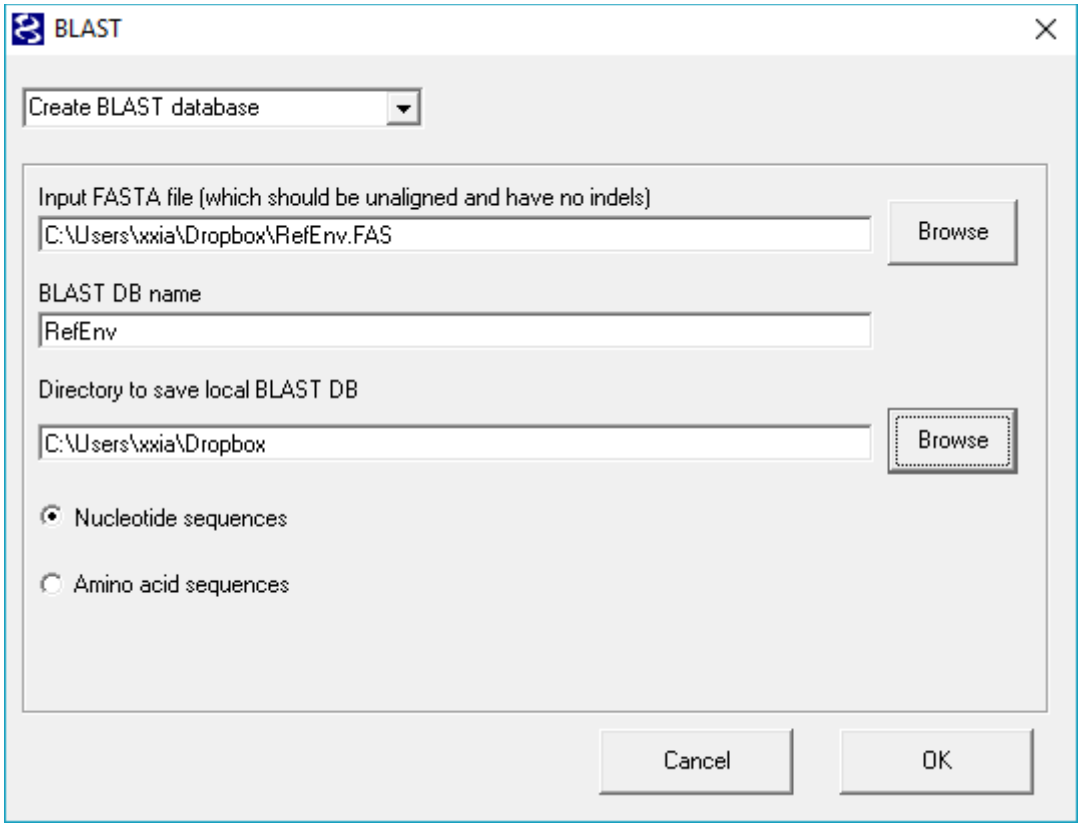

Fig. 1-6. Dialog box for creating a local BLAST library.

BLAST against a BLAST library: DAMBE uses NCBI's blastn.exe and blastp.exe to do nucleotide and protein BLAST searches. Click 'Alignment|BLAST'. In the ensuing dialog box, choose BLAST in the top dropdown box (Fig. 1-7). Use **KAL153_env_gag.fas** as the input FASTA file, and the previously created BLAST library **RefEnv** as the 'Local BLAST DB'. The other options are all self-explanatory as you have already learned E-value and word size in the lecture. The 'Ungapped BLAST' will not allow indels and usually should not be checked. The 'Strand' has three options: plus, minus and both. 'minus' means search the complementary strand.

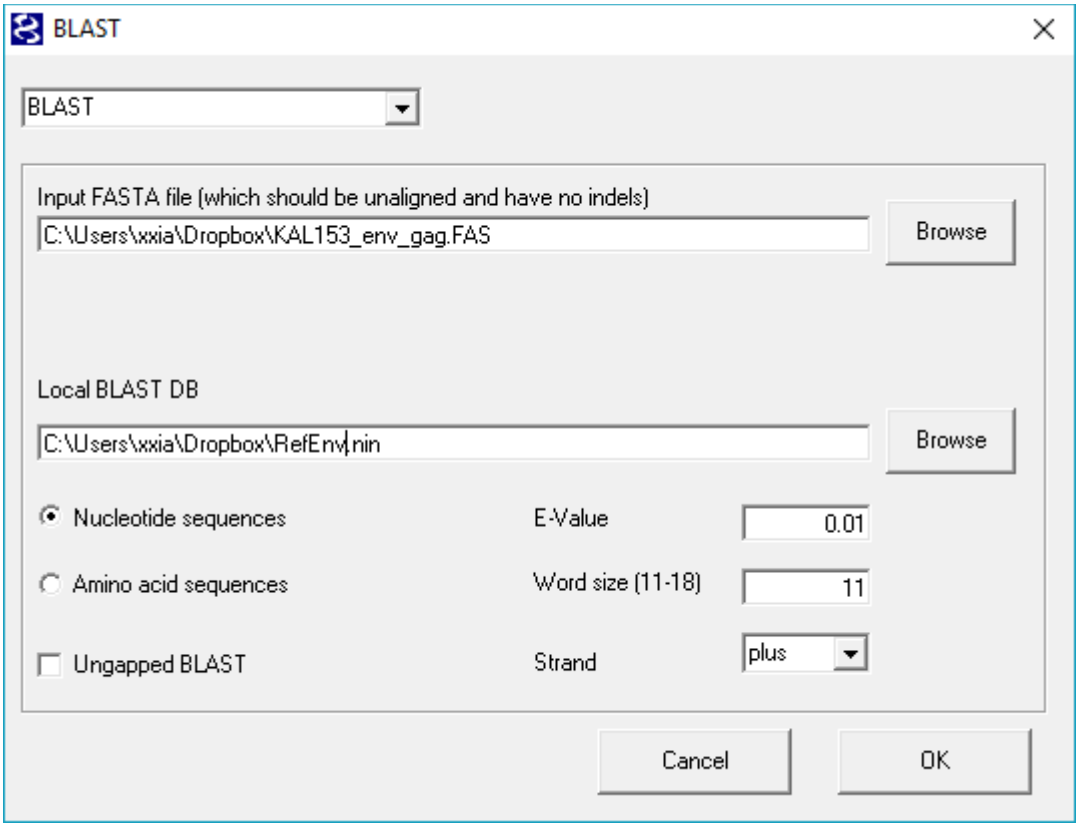

Fig. 1-7. Options for basic local BLAST in DAMBE.

Click 'OK' and you will obtain the BLAST result for the query sequence KAL153_env of which a short version is shown in Table 1-3. The matching quality is ranked from the highest BitScore to the lowest. We see that KAL153 *env* matches subtype B best. Perform the same BLAST against the **RefGag** library and record which subtype is hit with the highest BitScore. You will need these information to answer one of the lab questions.

Table 1-3. Partial output from BLAST KAL153 *env* sequence against *env* sequences of reference subtypes.

SubType	QueryStart	QueryEnd	DB_SeqStart	DB_SeqEnd	E-Val	BitScore
B	31	1820	43	1868	0	2342
B	23	1820	32	1865	0	2074
B	42	1820	60	1868	0	2017
B	1	22	1	22	0.002	36.2
D	25	1820	34	1856	0	1652
D	31	1820	40	1859	0	1628
F2	23	1820	53	1871	0	1600
D	25	1820	34	1844	0	1585
D	23	1820	32	1832	0	1578
A1	1	1817	1	1835	0	1555
C	91	1820	100	1832	0	1513
H	27	1803	27	1818	0	1506
A2	32	1802	33	1802	0	1474
J	26	1820	26	1859	0	1472
F2	23	1820	32	1847	0	1471

LECTURE QUESTIONS:

1. What are the main functions of the BLAST and FASTA programs? What are the main differences between BLAST and FASTA algorithms?
2. Use the FASTA algorithm to align the following two sequences. You should fill in the Query Table, the Target-Query Table, produce the alignment, state how values in the Target-Query Table have guided you in generating the alignment, and evaluate the significance of the alignment by assuming equal nucleotide frequencies (For such short sequences.

   Target: GACGAATA
   Query: GAATACGC

3. Given an mRNA of 500 nucleotides with $P_A = P_T = 0.1$, and $P_C = P_G = 0.4$, calculate the probability of the sequence having no NlaIII restriction site (GTAC). What is the E value (expected number of random matches) if you search this restriction sites against the mRNA?
4. Human mitochondrial genome (NC_001807) is 16571 nt long and its nucleotide frequencies are 0.3086, 0.3133, 0.1316, and 0.2466 for A, C, G and T, respectively. What is the probability that the HindIII endonuclease with the restriction site AAGCTT will cut the mitochondrial genome?
5. When E-value is very small, it can be interpreted approximately as the probability of finding exactly one match that is equally good or better than the reported match. Give mathematical justification based on the Poisson distribution with the Poisson parameter being the E-value.
6. Given (1) two nucleotide sequences with one being 100 bases long and the other being 1000 bases long and (2) a match length of 10 bases long (i.e., an exact match of 10 consecutive letters), compute the expected number of matches and the probability of having at least one match, assuming equal nucleotide frequencies.
7. The following match is returned from searching of a query sequence against a genomic sequence, with the effective query and effective database lengths being 23 and 500000 bases long, respectively. The gap open and gap extension penalties are 5 and 2, respectively, and match and mismatch scores are 1 and -2, respectively. Compute the E-value using $\lambda = 1.37$ and $K = 0.711$.

```
Query: atgaataacg--attat---caacgacaaaacaaaaccac
       ||||||||||  |||||   |||  |||||| ||||||||
Sbjct: atgaataacgttattatttccaataacaaaataaaaccac
```

LAB QUESTIONS:

8. What are Karlin-Altschul parameter λ and K for 1) equal nucleotide frequencies and BLAST default match/mismatch scores (1 for match and -3 for mismatch), and 2) nucleotide frequencies from KAL153 coding, a score of 1 for matching, -1 for a transition difference and -3 for a transversion difference?
9. Is KAL153 a recombinant? From which two HIV-1 subtypes? Is the evidence strong (provide BitScore values for the best-hit subtype and the second best-hit subtype)

LAB 2 MAKING SENSE OF GENOMES: POSITION WEIGHT MATRIX

INTRODUCTION

We know that the genome is shared among all our somatic cells which nevertheless look, behave and function quite differently. These morphological, physiological and functional diversifications are achieved mainly through genetic switches (regulatory motifs) present in the genome that are turned on and off in different cell types during their development. Many of these switches are present in the 5' upstream or 3' downstream of individual genes (e.g., transcription and translation start and termination sites， promotor and transcription factor binding sites, etc.). Some are also present inside genes (e.g., 5' and 3' splice sites and branchpoint site), and some could be up to 1 million bases away from the gene (e.g., enhancers). To study these regulatory motifs we need to gain the skill of manipulating genomic sequences, such as extract different sequence elements in order to discover and characterize such motifs.

Position weight matrix (PWM) is for characterizing a set of known motifs, e.g., five nucleotides flanking the start codon in mammalian genes. It has two purposes. The first is to know what is special about the motif for it to be recognized by the cellular machinery, e.g., the start codon motif recognized by the translation machinery, or the splice site motif recognized by the spliceosome. The second purpose is to use PWM to scan a sequence to detect the presence of such motifs.

PWM also serve as a key component in *De novo* motif discovery algorithms such as Gibbs sampler. *De novo* motif discovery refers to the process of finding a motif in a sequence but we do not know what the motif is like and where it is located in the sequence. We will learn Gibbs sampler in a later laboratory.

Two approaches to understand the meaning of a nucleotide sequence

There are two main approaches to understand the meaning of a sequence. The first is to check against the existing 'gene dictionary'. You may not find an exact match, but a near-exact match can be helpful, in the same way when you look for 'favour' but find 'favor' in the dictionary. Such checking against the 'gene dictionary' is almost exclusively done by using BLAST or FASTA suites of programs, and has become more and more useful with the improvement of gene dictionaries (in the form of BLAST databases).

The second approach to annotate a sequence is gene prediction based on known gene features (Burge and Karlin 1997; Salzberg, et al. 1998). For example, to scan for the presence of a protein-coding gene in a mammalian sequence, one would first search for an open reading frame (ORF), check for the presence of 1) Kozak consensus (Rcc**AUG**G) flanking the putative start codon, 2) 5' and 3' splice sites defining the exon-intron boundary and the branchpoint site near the 3' splice site, and 3) poly(A) signal after the stop codon. This approach becomes essential when we find no match in the 'gene dictionary' or when we find a match with no explanation.

The effectiveness of the gene prediction approach depends on how well we know the genomic language. An expert in English, when presented with an English sentence containing a new word, can almost instantly point out if the new word is a noun or a verb or whether the word serves as a subject or object. In contrast, a person knowing no English could infer little. For this reason, gene prediction algorithms typically need to be trained by existing knowledge about genes.

Finding and specifying the meaning of a sequence is called sequence annotation. All NCBI-curated genomic sequences represent well-annotated sequences from which we can extract coding sequences, exons, introns, rRNAs, tRNAs and upstream and downstream sequences for detailed analysis. A more rigorous type of gene annotation is called GO annotation, i.e., sequence annotation according to gene ontology (GO). A GO-annotated gene contains the three minimum pieces of information: 1) the function of the gene product, 2) the biological processes the gene product participates in, and 3) cellular localization. We will not have time to learn GO-annotation in this course.

Extraction of annotated gene features from GenBank files

Extracting sequence elements from GenBank files is an essential skill in bioinformatics. For example, in order to let *E. coli* produce a human protein, we need not only to insert the human gene into the *E. coli* genome, but also to add a Shine-Dalgarno sequence to facilitate the localization of the initiation codon, to optimize its codon usage to increase translation elongation efficiency, and to incorporate a strong promoter to facilitate transcription. To optimize codon usage, we need to extract the tRNAs and use codons recognized by the most abundant tRNAs. We can also extract the highly expressed *E. coli* genes to find their codon usage as a reference.

To have a good Shine-Dalgarno sequence, we again can do two things involving sequence extraction. First, we can extract the small subunit rRNA to obtain its 3' sequences. Second, we can extract the sequences upstream of highly expressed *E. coli* genes, identify the Shine-Dalgarno sequence and obtain their consensus. One may also be interested in knowing what is the best 5' UTR for loading ribosomes during translation (Xia, et al. 2011) and therefore need to extract the 5' UTR sequences. Extraction of intron splice sites have revealed a strong correlation between a strong splice site and protein production (Ma and Xia 2011) and advanced our understanding of alternative splicing through exon skipping (Vlasschaert, et al. 2016). The first author of the paper, Caitlyn Vlasschaert, is one of the former BPS4104 students, and she published two papers in her first year as an MSc student at University of Ottawa.

Extracting sequence fragment is also necessary for making inter-specific comparisons. For example, to study the evolution or functional changes of the coding sequences of the elongation factor EF-1α, it is necessary to splice out the CDS regions of EF-1α and join them together, and repeat this process for more than one species in order to make inter-specific comparisons. Similarly, to study the evolution of introns of EF-1α, one would need to splice out the introns from a variety of organisms and make comparisons among them.

Position weight matrix

Extracting specific sequence components is always associated with specific analysis to address specific biological problems. In this lab, we will extract the sequence fragments at the exon-intron junctions and use position weight matrix (PWM) to characterize 5' and 3' splice sites. Such a PWM can then be used to scan sequences for putative 5' and 3' splice sites to aid sequence annotation. It has also been found that 5' and 3' splice sites with a high PWM score (PWMS) are more efficient in recruiting spliceosome than those with a low PWMS and that splice sites with a strongly negative PWMS are spliced by non-spliceosome mechanisms (Ma and Xia 2011). PWM has been numerically illustrated in Xia (2007a, Chapter 5), and reviewed much more thoroughly, with particular reference to the associated statistical significance tests in Xia (2012).

OBJECTIVES

Extracting exon-intron junctions: Specifically, we will extract the 5' splice sites from intron-containing genes in the yeast (*Saccharomyces cerevisiae*), e.g., 5 nucleotide sites on the exon side and 12 nucleotide sites on the intron side. While we know that a spliceosome intron typically starts with GT, there are often GT dinucleotides that do not represent the beginning of an intron. The spliceosome must have used additional information to decide whether a particular GT represents the beginning of an intron, and this additional information is likely in the sequences flanking the GT dinucleotide.

Characterize the sequence features of the 5' splice site by PWM: We will learn whether there are significant signals in nucleotides flanking the GT dinucleotide at the beginning of intron and how we can use PWM to find similar signals in new sequences.

PROCEDURES

A brief peek into a GenBank file

We will work with the genome of the yeast *Saccharomyces cerevisiae*. The GenBank file **Sc.gbk** file is available at http://dambe.bio.uottawa.ca/teach/bps4104_download/download.aspx. The file (about 25 MB) contains annotated genomic sequences for 16 chromosomes of the yeast. Right-click the **Sc.gbk** link, choose 'Save target as' and save to **Sc.gbk** in your personal directory. You can download the chromosome sequences from NCBI, but it may take longer.

It is a good idea to have a look at the file which is in plain text. Click 'File|Load text file into display', browse to the directory you saved the **Sc.gbk**, and click the 'Open' button. Each annotated chromosome has its own LOCUS and ACCESSION (which may be the same or different). The 'DEFINITION' tells us that this LOCUS is for the first chromosome of the yeast. PageDown to 'FEATURES' table and note that the first chromosome consists 230208 nucleotides numbered from 1 to 230208. PageDown further and you will find the first annotated coding sequences (CDS) in chromosome 1 for gene *PAU8*, which spans sites from 1807 to 2169 on the complementary strand. Click 'Edit|Find' and input 'join(' to find CDSs resulting from the joining of several exons separated by introns. The first intron-containing gene is *SNC1*, whose CDS results from the joining of two exons, one spanning sites from 87287 to 87388 and the other from 87502 to 87753. The single intron naturally spans the sites from 87389 to 87501. If we wish to obtain its 5' splice site, with 5 nucleotides on the exon side and 12 nucleotide from the intron side, then we simply extract sites spanning 87384 to 87400.

Extracting annotated sequence elements with DAMBE

Click 'File|Open standard sequence file'. The standard Windows file open dialog appears for you to browse to and open **Sc.gbk**. A dialog appears with a long list of options such as CDS, tRNA, rRNA, etc., for you to choose what to extract from the input file. You have already learned how to extract CDSs from a GenBank file in the first lab, but let's practice it once more. Click 'CDS' and then click OK. A dialog appears with three options: non-protein sequence, amino acid sequence, and protein-coding nucleotide sequence. Choose the last and choose the relevant translation table out of 17 implemented genetic codes. In our case with the yeast nuclear genome, choose 1 (the default). Click the GO button. The sequences will be displayed. Recall that we computed CAI for HIV-1 CDSs in our last laboratory. You may practice CAI computation for the yeast genes. Save the CDSs to file **Sc_CDS.fas**

To appreciate the importance of inputting the correct genetic code, click 'Sequece|Work on amino acid sequene'. DAMBE will translate the codon sequences into amino acid sequences. There should be no '*' (which indicates an inframe stop codon) embedded in the sequence (which is typical of functional protein-coding genes). Click 'Sequence|Work on codon sequences' to restore the original codon sequences. Now choose a wrong genetic code by clicking 'Sequences|Change Seq.Type' and changing the genetic code to vertebrate mitochondrial (VertMtDNA). Now again click 'Sequences|Work on amino acid sequences', and you may see a number of '*' embedded in the sequence resulting from translation based on a wrong genetic code (translation table). On the other hand, if your sequences do have an embedded stop codon UGA (common in pseudogenes), and you choose translation table 4, then the stop codon will be mistranslated into tryptophan.

Practice with extraction of introns from CDS specifications by opening **Sc.gbk** and choosing 'Intron from CDS'. Have you noticed anything common among the introns? Spliceosome in the yeast is simpler than that in multicellular eukaryotes and the intron splice signals are consequently stronger in the yeast than in multicellular eukaryotes. There are only major-class introns in the yeast, and they generally start with GT dinucleotide and end with AG dinucleotide.

Characterize 5' and 3' splice sites with position weight matrix (PWM)

Open the **Sc.gbk** file again. Note that DAMBE keeps four most recently opened files under the 'File' menu. If you have opened **Sc.gbk** recently, just click it under the 'File' menu. When presented with a dialog for you to choose which sequence feature to extract (Fig. 2-1), click 'E/I junctions from CDS'. Extract 5 nucleotides on the exon side and 12 nucleotides on the intron side by entering '5,12' (which is in fact the default). Click 'Non-protein sequences' when prompted for sequence type. Some sequences may be identical and you may be asked if you wish to merge identical sequences. Click 'No'.

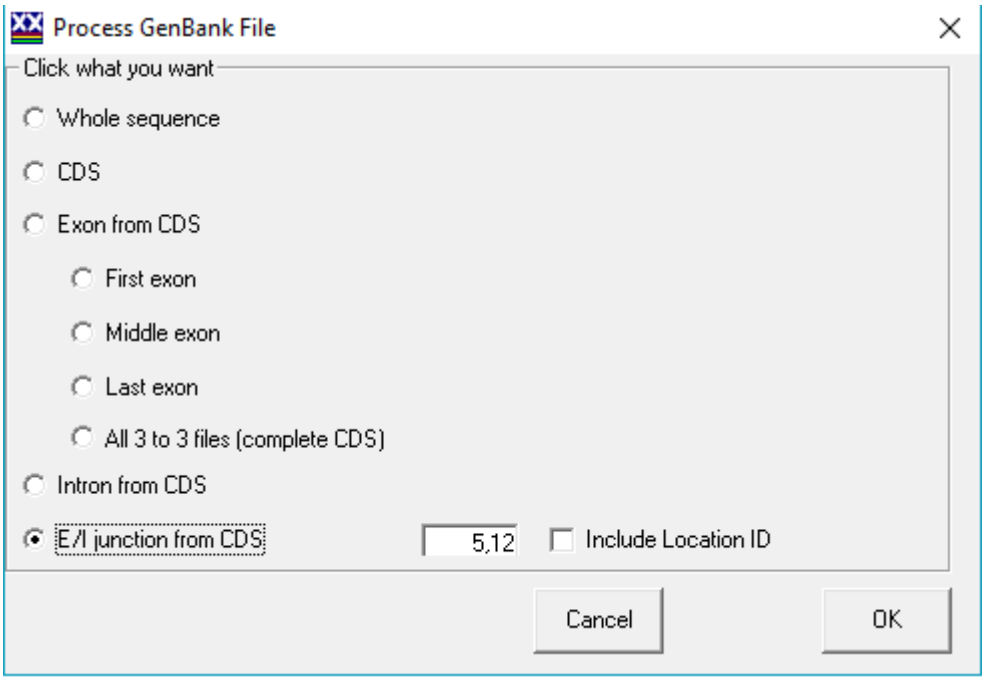

Fig. 2-1. DAMBE dialog (middle section omitted) for extracting exon-intron junctions.

The 5' splice sites (5'SS) sequences (17 nt) will be displayed. DAMBE also automatically extracted the 3' SS and you will be asked to save the 3'SS sequences to a file. Just enter an informative file name such as **Sc3SS.fas**. Also, it is a good idea to save the displayed 5' SS sequences by clicking 'File|Save or convert sequence format' to save the 5'SS to a file such as **Sc5SS.fas**.

The displayed 5'SS sequences share the dinucleotide GT at sites 6 and 7. You will almost immediately notice that site 8, 9, 10 and 11 are dominated by A, T, A, and T, respectively. PWM quantifies what you see and sometime reveals what you don't see by eyeballing. Computation and interpretation involving the position weight matrix were detailed in Xia (2007a, Chapter 5). Now click 'Bioinfo|Position weight matrix'. In the ensuing dialog box (Fig. 2-2), leave all the options unchanged and Click the 'Run' button.

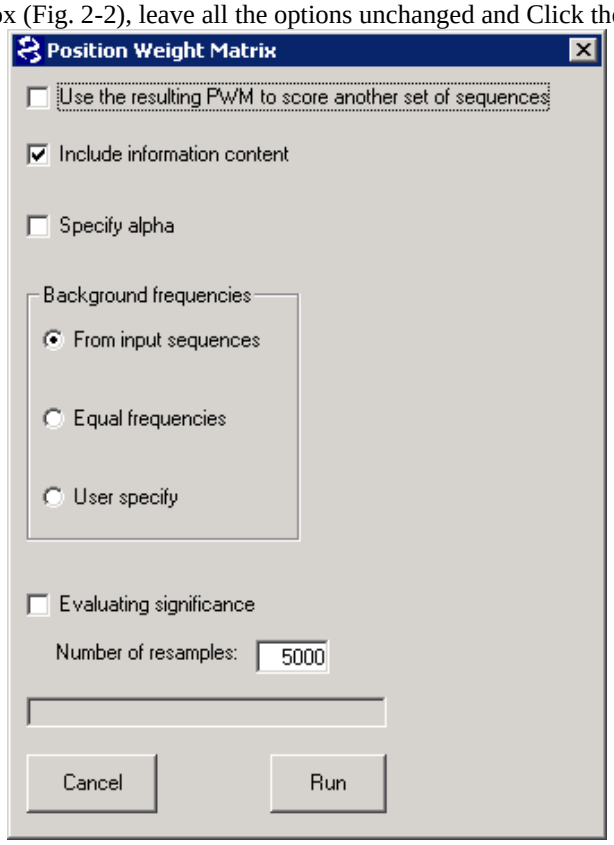

Fig. 2-2. Dialog box for computing position weight matrix.

The result will be displayed in two parts, one in graphs and the other in text. The graphic part includes two charts (Fig. 2-3). The strongest signals are presented at the 5' end of the intron from sites 6 to 11 in the consensus form of GTATGT, which is revealed in both site-specific frequency distribution (Fig. 2-3a) and PWM (Fig. 2-3b). You might have noticed that the PWM plot (Fig. 2-3b) not symmetric above and below the 0 PWM line, i.e., PWM values can be smaller than -8 but is never greater than 2.3. There is easily understandable if you remember that each PWM value is $\log_2(P_{ij}/P_i)$, where P_{ij} is the frequency of nucleotide i (i = A, C, G, or T) at site j, and P_i is the background frequency of nucleotide i. To avoid taking the logarithm of 0, we typically would add a very small value to P_{ij}, e.g., 0.0001. The range of P_{ij}, instead of being (0, 1), in computationally (0.0001, 1). If P_i = 0.25, then the maximum PWM value is $\log_2(1/0.25)$ = 2. The minimum of PWM value is $\log_2(0.0001/0.25)$ = -11.2877.

The key difference in information between the site-specific frequency (Fig. 2-3a) and PWM plot (Fig. 2-3b) is that the latter takes background frequencies into consideration. It is for this reason that one needs to consider carefully what background frequencies to use. In this particular case, it would seem reasonable to use nucleotide frequencies in yeast introns as background frequencies. You may extract intron sequences from the yeast genome, click 'Seq.Analysis|Nucleotide and di-nuc frequencies to get the pooled nucleotide frequencies of yeast introns and re-run PWM by choosing 'User specify' under 'Background frequencies' (Fig. 2-2).

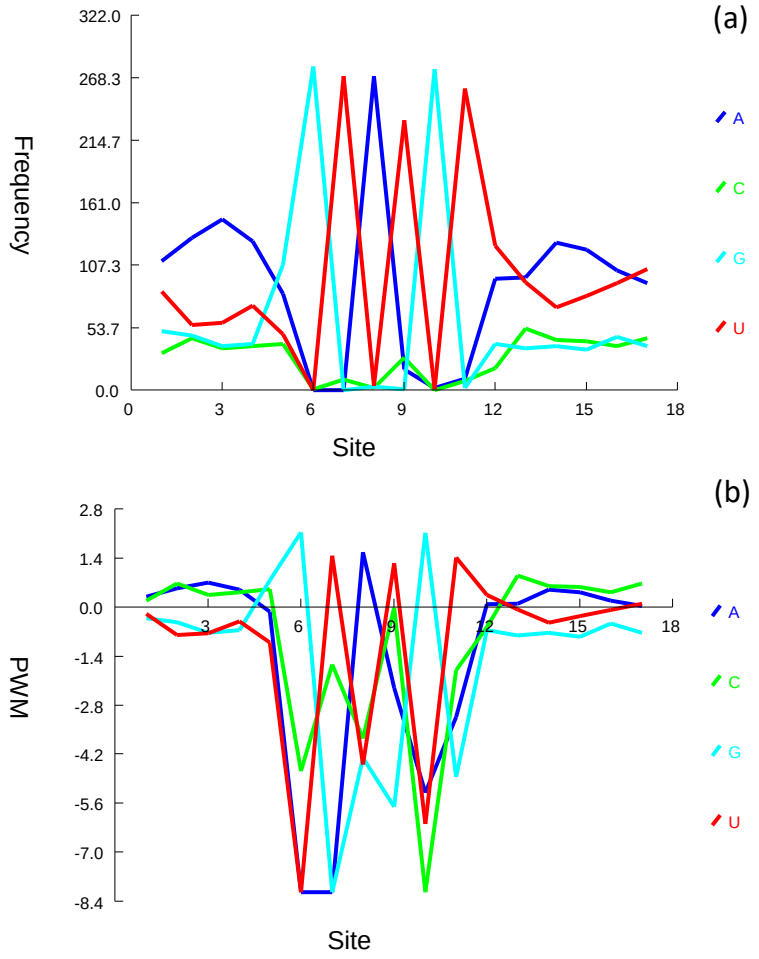

Fig. 2-3. Graphic output from PWM analysis of the 17-bp 5'SS from yeast intron-containing genes. (a) Site-specific nucleotide frequency distribution. (b) PWM plot where nucleotides with PWM values greater than 0 are over-represented and those smaller than 0 underrepresented, and is equivalent to a sequence logo with background frequency taken into consideration.

The test output includes several tables. Table 0 shows the background frequencies used if the user did not specify background frequencies. Table 1 shows site-specific frequencies (which can be used to re-create Fig. 2-3a), including χ^2-tests testing nucleotide frequencies at each site against the background frequencies. These tests do not control for familywise error rate, so another set of tests based on false discovery rate (FDR) is also included. The FDR test is numerically illustrated in Xia(2012) and Xia(2013a). Table 2 shows the resulting PWM which can be used to recreate Fig. 2-3b. The final part of the output is a list of position matrix scores (PWMSs) for each 17mer. PWMS is used to assess the relative likelihood of two hypotheses: (1) the sequences have no site-specific patterns, designated as θ_{No}, and (2) the sequences have site-specific patterns (i.e., a motif), designated as θ_{Yes}. We compute the likelihood for each hypothesis, designated as L_{No} for θ_{No} and L_{Yes} for θ_{Yes}. The odds ratio is the ratio of L_{Yes}/L_{No}. An odds ratio of 1 means that the two hypotheses are equally likely. The log-odds is the logarithm of an odds ratio. A log-odds of 0 means that the two hypotheses are equally likely. PWMS values are log-odds.

A PWM not only summarizes the site-specific patterns, but also facilitates the computation of PWMS. Take for example the PWM in Table 2-1, which results from characterizing the mammalian translation initiation sites (the translation initiation AUG plus three bases upstream). The PWMS for a sequence ACCAUG is computed as

$$PWMS_{ACCAUG} = 0.9284 + 1.0279 + 1.1967 + 1.9941 + 2.3190 + 1.6783$$

Table 2-1. A position weight matrix with the sequence length of 6.

Site	A	C	G	T
1	0.9284	-0.0167	0.7350	-0.4293

2	0.4731	1.0279	-0.0072	0.1086
3	-0.0761	1.1967	0.3856	-0.3954
4	1.9941	-0.7772	-0.8254	-0.9879
5	-0.8980	-0.8743	-0.8254	2.3190
6	-0.8980	-0.8743	1.6783	-0.9879

A 5'SS with a high PWMS value indicates a strong signal. Almost all introns in highly expressed yeast genes have high PWMS values because there is selection pressure for these genes to be spliced efficiently. A 5'SS with no selection would be subject to mutation and would have site-specific frequencies similar to those of the background frequencies, and the expected PWMS values for such genes is close to 0. What is puzzling is that some 5'SS have PWMS that are strongly negative, which means that such introns are under selection pressure to have their 5'SS not recognized by spliceosomes. Some of these genes are known to be spliced by mechanisms other than spliceosome (Ma and Xia 2011).

Now perform the same PWM analysis for the 3'SS that you have saved in file **Sc3SS.fas**.

Scan sequences for splice site signals

A PWM derived from a good set of motif sequence can be used to scan for motif signals in new sequences. For example, we can use the PWM in Table 2-1 to scan sequences with a sliding window of 6 bases, e.g., from site 1 to site 6, from site 2 to site 7, and so on. The resulting window-specific PWMS can be used to judge whether the 6-mer is a putative translation initiation site. Similarly, we can use our PWM derived from 5'SS or 3'SS to scan for the presence of splicing signals. One interesting finding by experimental biologists is that most spliceosome proteins are recruited to yeast mRNAs with no introns, and one may hypothesize that those intron-less mRNAs may happen to contain false 5'SS signals. You may use your PWM to scan yeast intron-less genes to see which 17mer may have a high PWMS, and you would predict that those 17mers with high PWMS values are where the spliceosome proteins are recruited.

The option to use the resulting PWM to scan another set of sequences is available at the top of the PWM dialog box in Fig. 2-2. Click 'Bioinformatics|Position weight matrix' and check 'Use the resulting PWM to scan another set of sequences'. Click 'Run'. You will be asked for the file name containing the sequences that you wish to scan. Choose the saved **Sc_CDS.fas**. You will have the same output as before but with an additional table showing the 17mer with the highest PWMS in each CDS. While a high PWMS in a true splice sites represent a true splice signal, a high PWMS in an intronless gene implies a false signal. Unfortunately, the spliceosome proteins are attracted to splice signals, whether they are false or true. These PWMS values can be used to test our hypothesis that many spliceosome proteins are recruited by intron-less yeast mRNAs with strong but false splice site signals.

Limitations of PWM

PWM cannot detect site dependence. For example, if nucleotides at two positions form base pairs, then the information is contained in the two positions jointly but not individually. The two sites can classify the eight sequences below into four groups, but a conventional PWM will conclude that the two sites are not informative.

…A…T…
…A…T…
…C…G…
…C…G…
…G…C…
…G…C…
…T…A…
…T…A…

One way to extend PWM to site dependence is to recode sites as doublets. For example, if site-dependence occurs only between neighboring sites, then we can modify PWM to detect the neighboring site dependence, by using the 16 dinucleotides instead of the four nucleotides. For example, a 6-mer CCCGGG contains five dinucleotides, i.e., CC, CC, CG, GG, GG. An further extension of this is that we may take a nucleotide at position i and another nucleotide at position i+k as a dinucleotide.

MORE QUESTIONS

1. If you have CDS sequences from a vertebrate nuclear genome, will DAMBE translate them into amino acid sequences properly when you choose the vertebrate mitochondrial genetic code? Give reasons.
2. What are the major differences between translation tables #1 and #4?
3. What is the minimum specification of the FASTA format?
4. Extract all yeast intron sequences (Click 'Intron from CDS' when prompted for what sequence features to extract). What dinucleotides flank the introns at the 5' and 3' ends in yeast?
5. What is the consensus motif at the 5' end of yeast introns based on the PWM from 5'SS sequences? List the first 6 nucleotides.
6. Which yeast CDS has the highest 5'SS signal based on PWMS? (All such signals in CDSs are false signals that can confuse spliceosome.)
7. Download a bacterial genome (e.g., *Escherichia coli* or Bacillus subtilis) and extract 50 nucleotides upstream of all CDSs. Is there any genetic switch (functional motif) that might be hidden in these sequences? Address this question by performing a PWM analysis on these 50 sites.

LAB 3 GIBBS SAMPLER AND YEAST INTRON PROPERTIES

INTRODUCTION

Genetic switches

A genome with its encoded genes come to life only when the genes are activated or inactivated over time in response to the changing cellular environment leading to the production of different proteins and RNAs at the right time in the right location. How can a genome respond to the changing cellular environment? It can do so because it features many genetic switches that can be flipped on or off by cellular machineries. Even simple genomes such as that of the phage λ have such genetic switches (Ptashne 1986).

Genetic switches are specific sequence motifs in nature. These include transcription and translation initiation and termination sites, transcription factor binding sites, intron-splicing sites, intron branching-point site, poly-A site, etc., as well as a set of very important but yet poorly defined set of signals for epigenetic modification of DNA. Finding these genetic switches in a genome not only increase our understanding of how genomes work, but also have practical applications because many genetic switches are drug-targets.

Some sequence motifs can be experimentally characterized. Such characterized motifs can then be used to construct a position weight matrix to scan other sequences for the presence of such motifs. However, often we will just have a set of sequences and have no idea what the motif would look like and where it might be in the sequence. We only have a vague idea that some genetic switch is located somewhere in all or most of these sequences, but we do not know what and where. Gibbs sampler is one of the Monte Carlo algorithms for finding such motifs.

Gibbs sampler and its application in molecular biology

Monte Carlo method was envisioned by the famous mathematician Stanislaw Ulam, following the successful assembly of the first electronic computer ENIAC in 1945, and further developed by physicists and mathematicians working on nuclear weapon projects in the Los Alamos National Laboratory in mid-1940s (Metropolis 1987). The term 'Monte Carlo method' was coined by Nicholas Metropolis to designate this class of computational algorithms. While the development and application of the method unsurprisingly followed the operation of ENIAC in 1945, the physicist Enrico Fermi is known to have independently developed and applied the method nearly 15 years earlier with mechanical calculators (Metropolis 1987).

Gibbs sampler simplifies computation in parameter estimation when analytical solution is very difficult or impossible to obtain. In biology, it has been used in the identification of functional motifs in proteins (Neuwald, et al. 1995; Mannella, et al. 1996; Qu, et al. 1998), biological image processing (Samso, et al. 2002), pairwise sequence alignment (Zhu, et al. 1998) and multiple sequence alignment (Holmes and Bruno 2001; Jensen and Hein 2005). However, the most frequent biological application of Gibbs sampler in bioinformatics remains in the identification of regulatory sequences of genes (Lawrence, et al. 1993; Thijs, et al. 2001; Thijs, Marchal, et al. 2002; Thijs, Moreau, et al. 2002; Coessens, et al. 2003; Qin, et al. 2003; Thompson, et al. 2003; Thompson, et al. 2004; Aerts, et al. 2005).

The core component of a Gibbs sampler is PWM (position weight matrix). The implementation of the Gibbs sampler algorithm has been numerically illustrated before (Xia 2007a, Chapter 7; 2012). For relevant statistical tests for the derived PWM, one should consult Xia (2012).

Identifying genetic motifs with Gibbs sampler

Imagine three scenarios. In the first, suppose you have performed microarray (Schena 1996; Schena 2003) or SAGE (Velculescu, et al. 1995; Saha, et al. 2002) or RNA-Seq analysis of a yeast strain over time, and identified a set of protein-coding genes that increase and decrease gene expression synchronously. Are these co-expressed genes co-regulated? They may be co-regulated if they share regulatory sequences in their 5'-UTR. But how would we know if they share regulatory sequences in the 5'-UTR? With the bioinformatic skills you have gained, you could extract, say, 2000 nt upstream of the initiation AUG that may well contain the regulatory sequence. However, the regulatory sequences could be just a few bases long and may be anywhere in the 2000-nt sequence. What are these regulatory sequences? Where are they located? If there are indeed shared sequence motifs hidden somewhere in these 2000-mers, then they most likely will be found by Gibbs sampler and displayed with information on their exact locations.

In the second scenario, imagine that you have done a control/treatment experiment on two groups of goldfish in which the treatment is exposure to estrogen. You identified a set of genes that are upregulated. You wish to

know if they share estrogen response elements (ERE) in 5' UTR, but do not know what ERE looks like and where in 5' UTR it is located. Again you can extract 5'UTR from these upregulated genes and subject them to Gibbs sampler to discover shared regulatory motifs.

In the third scenario, imagine that you have extracted the intron sequences from a fungal species and wish to know where the branchpoint site (BPS) is located. You know, from previous experiments, that a BPS is only a few bases long, but it could be anywhere between 5'SS and 3'SS, although we know that they generally are close to 3'SS. Of course you could run experiment for each intron by mutating sequentially nucleotide sites along the intron between 5'SS and 3'SS. The site that, upon mutation, leads to failed splicing is likely the BPS. However, this is very tedious. Can we simply run the intron sequences through a Gibbs sampler to identify all the BPSs? Note that all three scenarios raise the same problem, i.e., identify a motif that we do not know what or where. We will try to solve the problem in this laboratory.

You will be given a set of yeast (*Saccharomyces cerevisiae*) intron sequences. We know that each intron, if it is to be spliced properly by the spliceosome, should contain a 5'SS, a 3'SS, and a branchpoint site (BPS). We have learned quite a bit about 5'SS and 3'SS of yeast genes. Your task today is to find out what the BPS is and where it is located in each intron. Fig. 3-1 shows the input and output of Gibbs sampler in a nutshell.

Fig. 3-1. Application of Gibbs sampler in motif discovery. The sequences shown are reverse complement of a subset of erythroid-specific gene sequences, which has been tested for the presence of GATA box or TATC box in reverse complement (Rouchka 1997).

The main output of Gibbs sampler is typically of two parts. The first is the sequences with aligned motifs as shown in Fig. 3-1b. The second is a position weight matrix (or a site-specific frequency matrix from which a position weight matrix can be derived) derived from the aligned motifs so that we can use it to scan new sequences for the presence and location of such motifs.

In short, the input to Gibbs sampler for motif prediction is a set of sequences, the majority of which contain one or more motifs of interest (Fig. 3-1a). The output is a set of sequences with aligned motifs (Fig. 3-1b) together with a position weight matrix that can be used in future motif prediction.

There are two slightly different applications of Gibbs sampler in motif prediction. The first assumes that each sequence contains exactly one motif (Lawrence, et al. 1993) and the associated algorithm is called site sampler. The second is more flexible and allows each sequence to have none or multiple motifs (Neuwald, et al. 1995) and the algorithm is termed motif sampler. It is unfortunate that these two terms, now in common use, do not really tell us the difference between the two methods if we do not already know the difference already. In identifying the nature and location of BPS in yeast introns, the site sampler should be used because each yeast intron is expected to have exactly one BPS.

OBJECTIVES

Gain the skill of using Gibbs sampler to identify functional motifs by applying it to the identification of branchpoint sequence (BPS) in yeast introns: The BPS could potentially be located anywhere in an intron, although it is more likely located closer to the 3' splice site than the 5' splice site. How to find it if we have only a set of intron sequences but know nothing else about the BPS?

Bioinformatic analysis of the BPS and flanking distances: The BPS break the yeast intron into two parts, i.e., the upstream part stretching from the 5' splice site to BPS, referred to in literature as the S1 sequence, and the downstream sequence from BPS to the 3' splice site referred to as the S2 sequence. The lengths of S1 and S2 sequences are referred to as S1 and S2 distances.

If there is no constraint on the location of BPS, i.e., if the location of BPS does not affect intron splicing efficiency, then S1 and S2 distances are expected to be equal. If BPS is constrained to be close to the 3' splice

site, then the S2 distance is expected to (1) be smaller than the S1 distance and (2) vary less than the expectation based on random placement of BPS along the intron sequences. Similarly, if BPS is constrained to be close to the 5' splice site, then the S1 distance would expected to (1) be smaller than the S2 distance, and (2) vary less than the expectation based on random placement of BPS along the intron sequences.

PROCEDURES

Start DAMBE and read in the YeastAllIntron.FAS file in DAMBE's installation directory (it is one of the sample files that come with DAMBE). The file contains all documented yeast introns located within the coding sequences.

We will first practice how to copy column-based output from DAMBE to EXCEL. This is needed for subsequent data analysis on S1 and S2 distances. We will then use Gibbs sampler implemented in DAMBE to find what the BPS is and where it is located in each intron. Once BPS is identified, S1 and S2 are defined and can be further studied.

Copy column-based output from DAMBE to EXCEL

When the yeast intron sequences are displayed on the screen, what we see is equivalent to a two-column output, i.e., the first column being sequence names and the second column being sequences. We will copy these two columns into an EXCEL sheet.

Highlight all sequences, but not the numbering (Fig. 3-2), and click 'Edit|Copy to EXCEL'. Now the sequence name and the sequences are all copied into Windows clipboard ready to be copied into any Windows programs.

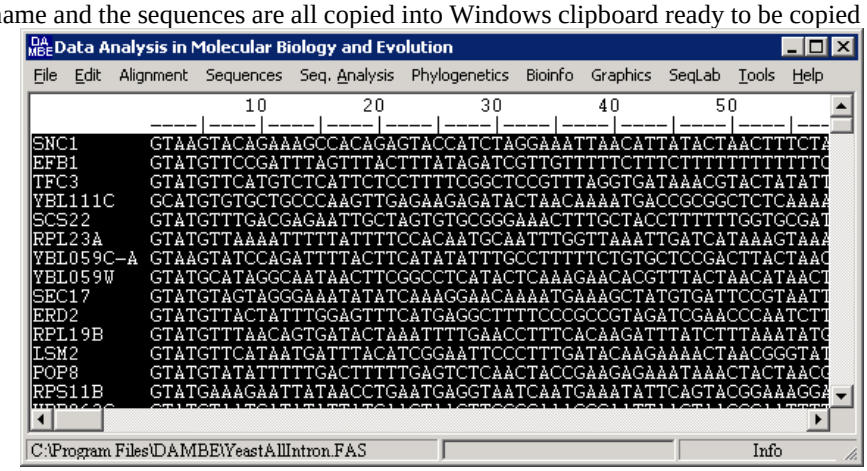

Fig. 3-2. Highlight column-based output in DAMBE for copying and pasting into EXCEL.

Launch EXCEL and label one EXCEL sheet as S1S2 (i.e., double-click the tag 'Sheet 1' and change it to 'S1S2'). We will generate and store all relevant S1 and S2 distances in this sheet. In the first cell of the first column (i.e., the A1 cell), enter 'SeqName' (without the single quotes) for sequence name. In the first cell of the second column (i.e., the B1 cell), enter 'Sequence'. Now click the second cell of the first column (i.e., the A2 cell) and click, in EXCEL, 'Edit|Paste'. The sequence name and the sequences in the clipboard will be pasted into EXCEL in two columns.

Now in the C1 cell, enter 'SeqLen' as we want this column to contain intron length. In the C2 cell, enter '=LEN(B2)' and press the 'Enter' key in your keyboard (Fig. 3-3). The cell will display the number 113 which means that the intron sequence in the B2 cell is 113 nucleotides long. Now move the mouse over the B2 cell to its lower right corner so that the fat empty cross becomes a thin solid cross. Hold down the left mouse button and drag down all the way to the last intron. The 'C' column will now contain the length of all introns.

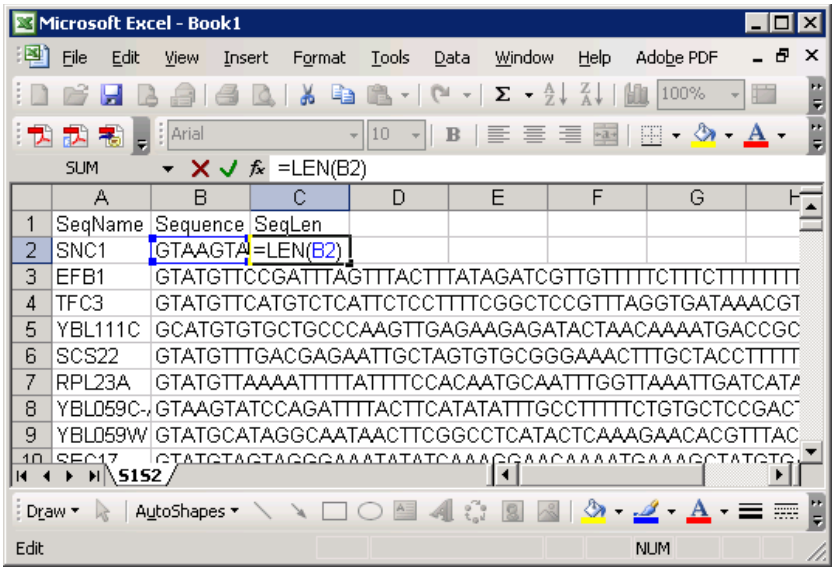

Fig. 3-3. Entering the 'LEN' function to obtain the length of the intron sequence in the B2 cell.

Running Gibbs sampler in DAMBE

Now come back to DAMBE. Click 'Bioinfo|Gibbs sampler'. A dialog appears for you to set options (Fig. 3-4). Suppose we do not know the length of BPS, so we will leave the 'Motif width' as the default (i.e., 6). This is a good value for a first try. We could increase it or decrease it after we have seen the output. The other entries are explained in the textbook (Xia 2007a, Chapter 7). Click the 'Run' button to start running the algorithm. Gibbs sampler, being a Monte Carlo algorithm, is slow, so you will have at least several minutes to discuss with your lab mates on what the output would look like.

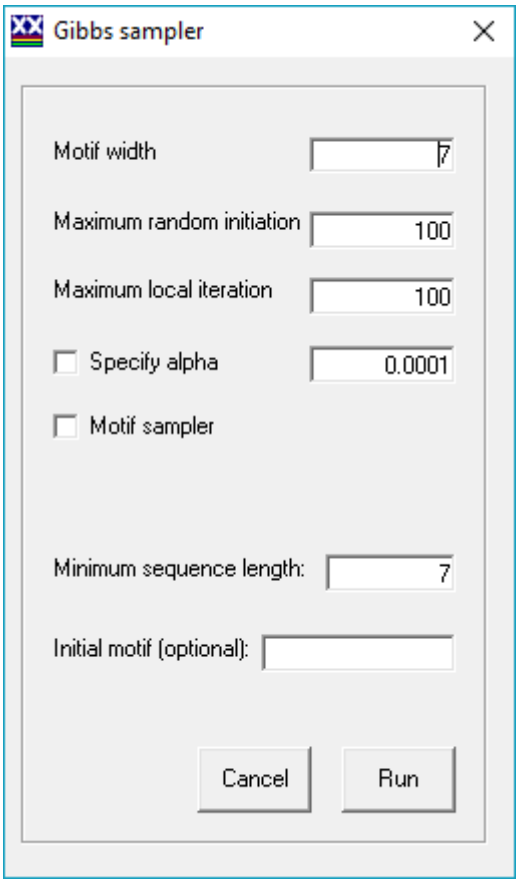

Fig. 3-4. Setting options for Gibbs sampler in DAMBE.

Once DAMBE has finished running Gibbs sampler, the output will be presented in four parts. The first part shows the global nucleotide frequencies. The second part shows the site-specific nucleotide frequencies for the motifs found (Fig. 3-5). We notice that the Gibbs sampler converged after only 24 iterations. If it fails to converge, then we have to increase the number of iterations (Fig. 3-4).

Gibbs sampler reached convergence after 24 iterations.

Final site-specific counts:

	A	C	G	U
1	275	0	4	0
2	0	272	0	7
3	0	0	1	278
4	275	1	3	0
5	278	0	1	0
6	0	276	0	3

Final site-specific frequencies:

	A	C	G	U
1	0.98330	0.00059	0.01491	0.00121
2	0.00116	0.97201	0.00062	0.02621
3	0.00116	0.00059	0.00419	0.99407
4	0.98330	0.00416	0.01133	0.00121
5	0.99401	0.00059	0.00419	0.00121
6	0.00116	0.98630	0.00062	0.01192

Fig. 3-5. Partial output from Gibbs sampler after running it on yeast intron sequences.

The partial output (Fig. 3-5) shows that the 6-mer motif is ACUAAU. The site-specific frequencies can be used to derive a position weight matrix to rapidly scan other sequences for the presence of such motifs.

The third part of the output shows the motifs in aligned format (Fig. 3-6), with the two down arrows indicating the start and end of the motif which is ACUAAC in most intron sequences. We also note that the nucleotide just upstream of ACUAAC is U in most cases, so yeast BPS might be UACUAAC, i.e., a 7-mer instead of a 6-mer. You may re-run Gibbs sampler by changing the 'Motif width' from the default 6 to 7.

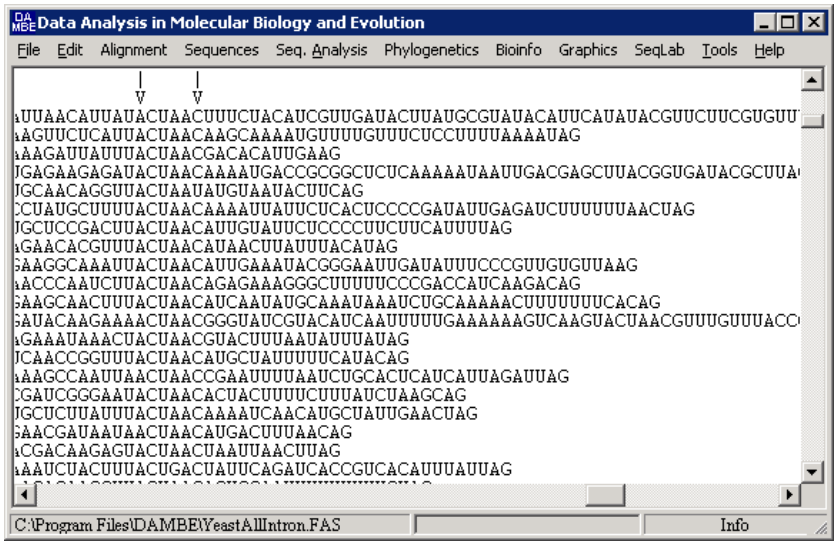

Fig. 3-6. Partial output from running Gibbs sampler on yeast intron sequences, with the shared motifs shown in aligned format. Note that you may need to drag the horizontal bar to the far right in order to see the aligned motifs shown.

The fourth part of the output (Table 3-1) shows the motifs found, where they start in the intron sequence and the position weight matrix scores (PWMSs). Note that a position weight matrix score may be presented in two ways. Sometimes it is presented as a likelihood ratio (i.e., the likelihood that there is a site-specific pattern, designated as L_{Yes}, and the likelihood that there is no site-specific pattern, designated as L_{No}), but sometimes it is presented as the base-2 logarithm of the likelihood ratio. The two likelihood values for the motif ACUAAC

are computed as follows, with P_A, P_C, P_G and P_U being in the first part of the output and the site-specific P_{A1}, P_{C2}, P_{U3}, etc., in the second part of the output (Fig. 3-5).

$$L_{Yes} = p_{A1}p_{C2}p_{U3}p_{A4}p_{A5}p_{C6}$$
$$L_{No} = p_A^3 p_C^2 p_U \quad \text{.....(3.1)}$$

The reported PWMS for ACUAAC in the output from earlier versions of DAMBE is the likelihood ratio of L_{Yes}/L_{No}, without taking the base-2 logarithm (This has been changed in the most recent version so that the reported PWMS is $\log2(L_{Yes}/L_{No})$. When you use the output to re-compute PWMS, the resulting PWMS may not be exactly the same as those in Table 3-1, for two reasons. The first is the rounding error in the output (e.g., you do not want to output a number with 40 digits after the decimal), and the second is because of the addition of pseudocounts in the computation. The necessity of pseudocounts is explained and numerically illustrated in the textbook (Xia 2007a, Chapters 5 and 7) and in more detail in a review (Xia 2012).

Table 3-1. Partial output from Gibbs sampler running on yeast intron sequences, displaying the found motif, start location in the intron (Start) and position weight matrix scores (PWMS).

SeqName	Motif	Start	PWMS
SNC1	ACUAAC	46	3216.0441
EFB1	ACUAAC	327	3216.0441
TFC3	ACUAAC	72	3216.0441
YBL111C	ACUAAC	30	3216.0441
SCS22	ACUAAU	68	18.1104
RPL23A	ACUAAC	455	3216.0441
YBL059C-A	ACUAAC	52	3216.0441
YBL059W	ACUAAC	46	3216.0441
SEC17	ACUAAC	72	3216.0441
ERD2	ACUAAC	58	3216.0441
RPL19B	ACUAAC	338	3216.0441
…	…	…	…

Studying S1 and S2 distances

The column of data in Table 3-1 headed by 'Start' gives us S1 distances directly. For example, the BPS in the intron of gene SNC1 starts at position 46 which means that there are 45 nucleotides before the BPS, i.e., S1 distance equals 45. Similarly, the S2 sequence starts 6 nucleotides after the start site, i.e., the BPS ends at 51, i.e., it includes the sequence from site 52 to the end. So the S2 distance is 113-51 which equals 62.

To facilitate computation, highlight the last part of the output and click 'Edit|Copy to EXCEL'. Go back to the EXCEL sheet labeled 'S1S2' and paste the content into cell D1. Now the EXCEL sheet S1S2 looks like in Fig. 3-7.

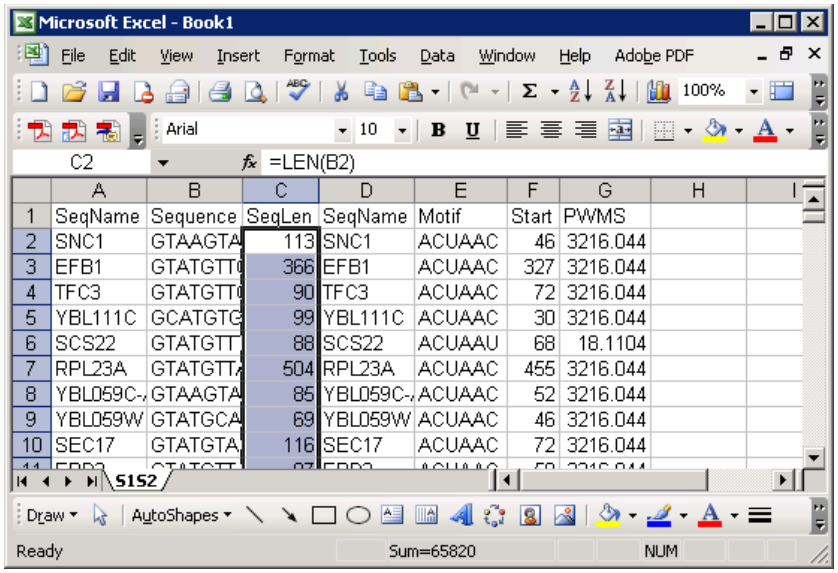

	A	B	C	D	E	F	G	H
1	SeqName	Sequence	SeqLen	SeqName	Motif	Start	PWMS	
2	SNC1	GTAAGTA	113	SNC1	ACUAAC	46	3216.044	
3	EFB1	GTATGTT	366	EFB1	ACUAAC	327	3216.044	
4	TFC3	GTATGTT	90	TFC3	ACUAAC	72	3216.044	
5	YBL111C	GCATGTG	99	YBL111C	ACUAAC	30	3216.044	
6	SCS22	GTATGTT	88	SCS22	ACUAAU	68	18.1104	
7	RPL23A	GTATGTT	504	RPL23A	ACUAAC	455	3216.044	
8	YBL059C-	GTAAGTA	85	YBL059C-	ACUAAC	52	3216.044	
9	YBL059W	GTATGCA	69	YBL059W	ACUAAC	46	3216.044	
10	SEC17	GTATGTA	116	SEC17	ACUAAC	72	3216.044	

Fig. 3-7. EXCEL sheet showing the procedure for obtaining S1 and S2 distances.

Now enter 'S1D' in cell H1 and 'S2D' in cell I1. In cell H2, enter '=F2-1'. In cell I2, enter '=C2-H2-6'. Highlight both cell H2 and cell I2 and move the mouse cursor to the lower right corner of cell I2 so that the fat empty cross changes to the thin solid cross. Drag all the way down to the last intron. Now you have both S1 and S2 distances ready for further analysis.

The simplest analysis of S1D and S2D is simply to scatter-plot them against intron length. To do so in EXCEL, highlight the three columns and click the graph icon. I will leave you to interpret the data as this is where bioinformatics ends and biostatistics begins.

MORE QUESTIONS

1. Is position weight matrix a component in Gibbs sampler?
2. Does yeast intron length depend mainly on S1 distance or S2 distance? What does your result suggest regarding the distance of the yeast BPS to the 3' splice site? (hint: does the result suggest that S2 might be functionally constrained, i.e., BPS needs to be close to the 3' splice site so that S2 is relatively fixed?)
3. Is yeast BPS a 6-mer, 7-mer, or 8-mer based on your research? (This is not an easy question. The strength of a site pattern is reflected in PWM. When you look at the four values in each row corresponding to A, C, G and T, a strong site pattern will have both value(s) much smaller than 0 and value(s) much greater than 0 (i.e., a large variance), whereas a week pattern will have the four values closer to zero (a small variance). An intuitive way of determine the length of a site pattern is simply to plot the site-specific variance versus the site. Fig. 3-8 below shows such a plot. You may notice that the last six sites have stronger site pattern than the first two. So we may conclude that those six sites have the strongest signal, although there might be more neighbouring sites contributing to the motif recognition. You may produce similar plot after running Gibbs sampler with, say, 12mer. An alternative approach is simply to use F/L where L is the motif length used in Gibbs sampler. (The length of a regulatory motif is difficult to determine when it may border another motif, either upstream or downstream. This does happen often.)
4. What are the mean and median of the S1 and S2 distances?

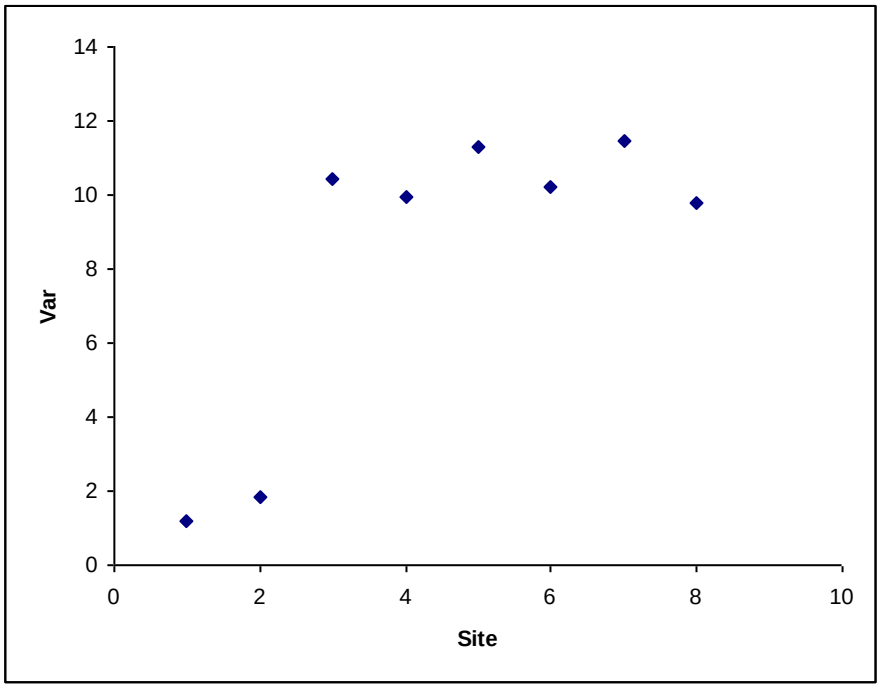

Fig. 3-8. Var-Site plot for the PWM from running Gibbs sampler on 8mer.

LAB 4 TRANSCRIPTOMIC DATA ANALYSIS

INTRODUCTION

Our topic today is transcriptomic data analysis. Transcriptomic data is equivalent to RNA-Seq data. There are many different types of molecular data. However, they may be categorized into just three types: genomic data, transcriptomic data and proteomic data. Our major focus today is the transcriptomic data. We will learn what transcriptomic data is, how it is stored in NCBI, and how to use them to solve practical questions.

This quick-start guide has three parts. First, it guides you through the conversion of FASTQ to FASTQ+ or FASTA+ format. Second, it demonstrates a variety of data quality visualization functions. Third, it takes you through the process of generating gene expression. These represent the most fundamental aspects of transcriptomic data analysis and serve as an entry point for more specific data analysis using transcriptomic data.

In biological literature, the word "transcriptome" has been used with different meanings. Ideally, a transcriptome is defined at the level of cell type and time. For example, we may obtain transcriptomic data from a colony of E. coli or a colony of yeast cells at a specific point in a yeast cell cycle. However, transcriptomic data from multicellular eukaryotes is often obtained from a sample of heterogeneous cells.

Most of the transcriptomic data are generated by the so-called next-generation sequencing (NGS). A good sequencer is characterized with three features, read length, read accuracy and speed. We typically expect anything labelled with "next generation" as something better than the first generation. However, here we have an exception. NGS not only generates sequences that are shorter than before, but also less accurate than before. The "next-generation" refers to the much-increased speed in sequencing. You can generate a large number of sequences in a very short time.

NGS is equivalent to second-generation sequencing, so that newest sequencing technology is known as the third-generation sequence. Unfortunately, the sequence quality of the third-generation sequencing is even poorer than that from NGS. However, the third-generation sequencing does have a major advantage in that it generates much longer reads than NGS.

Because NGS generates short sequences, the database for their storage was originally called short read archives or SRA for short. In the early stage of NGS, the reads were often just 20 or 30 bases long. Over time, the length of the reads increases, so now SRA has become known as sequence read archive instead of short read archive. Transcriptomic data is equivalent to RNA-Seq data. A read in transcriptomics is synonymous to a sequence.

There are two pronounced differences between transcriptomic data analysis and genomic data analysis. Firstly, transcriptomic data is large in size because NGS is very fast. It is common for a single transcriptomic study to generate hundreds of gigabytes or even terabytes of sequence data. Secondly, read quality from NGS is poor, so we always needs to assess read quality of transcriptomic data. We typically do not assess sequence quality in genomic analysis.

File format of transcriptomic data

Transcriptomic data comes in two formats. If you generate transcriptomic data in your lab, then your transcriptomic data are in plain-text FASTQ format. If you download transcriptomic data from NCBI's SRA database, then your data is in a compact machine-readable SRA format. Each SRA file contains either one FASTQ file (for single reads) or two (for pair-end reads). NCBI has created a set of programs for using SRA file directly as input. However, in most data analysis, one would need to convert SRA files to FASTQ files.

The FASTQ format might have reminded you of the FASTA format that you are already familiar with. Like FASTA format, FASTAQ format also starts with a sequence ID in the first line. However, instead of a ">" symbol proceeding the sequence name, FASTQ format has an "@" proceeding the sequence name. The second line is the actual sequence. However, we have the third and the fourth line that that are not present in FASTA format. The third line starts with a plus sign and can be followed by almost anything. The fourth line is the quality line, with each character representing the quality of each corresponding nucleotide in the second line. Therefore, each sequence in FASTQ format takes four lines:

```
@SEQ_ID1.1
NATTTGGGGTTCAAAGCA...
+
0''*((((***+))%%%+...
@SEQ_ID2.1
```

```
GATTTGGGGTTCAAAGCA...
+
%''*((((***+))%%%+...
```

One-letter quality notation

The most frequently used quality score is Phred quality score. Phred is a computer program for base-calling for traditional automatic DNA sequencers based on the 4-flourescent dye method. Base-calling is not guaranteed to be correct. For this reason, there is an error associated with base-calling. P is defined as the base-calling error probability. The worst case is when you have no certainty at all about what base might be at the site. If you make a random guess, and if nucleotide frequencies are equal, then the chance that you are correct is 1/4 or 0.25. The chance that you are wrong would then be 1-0.25=0.75.

P values are typically quite small, much closer to 0 than to 0.75. Using a small P for base quality is not convenient for two reasons. First, we interpret integers such as 1, 2, 3, etc., better than a small decimal value. For example, it is easy to say that 2 is greater than 1, but it is harder to say that 0.0001432 is greater than 0.0001431. Second, the base-calling error probability P values are clustered close to 0, and we want to space them out. Phred quality score (Q) serves these two purposes. It takes the following form:

$$Q = -10\log_{10} P\,; P = 10^{-\frac{Q}{10}}$$

Keep in mind that Q values are rounded to integer values from 0 to 93. If the quality scores vary from 0 to 9, then we can just write the quality score underneath the nucleotides, represented by the blue text. However, when quality score is greater than 9, then each number occupies more than a single space, so the quality score and the nucleotide will not be aligned properly. Therefore, one needs to find an alternative way of representing quality score by a single letter.

There are 94 printable characters in ASCII codes. The first one is the exclamation mark (!) with an ascii code of 33. The next is the quotation mark (") with an ascii code of 34. The next ones are the number sign (#), the dollar sign ($), and so on until the last tilde symbol (~), with corresponding ascii codes 35, 36, and so on all the way to the last tilde symbol that is 126. These characters are used to represent Phred score from 0 to 93. The greater the number, the higher the quality.

Different applications of transcriptomic data

Different types of transcriptomic data can be used in different ways, but they all involve mapping transcriptomic reads to genes in a known genome. The most frequent use of transcriptomic data is to characterize gene expression or differential gene expression. If we are studying life cycles of baker's yeast, we would synchronize yeast cells at the same developmental stage, and then take snapshots of transcriptome to see how gene expression changes during the yeast cycle. If we study the effect of a carcinogen in skin cancer induction in mammals, we may shave part of the mouse skin, apply the carcinogen to the skin and being to take snapshots of transcriptome of control and treatment skin samples over time to identify the difference in gene expression following the carcinogen application. For example, normal skin cell and cancerous skin cell exhibit different gene expression patterns. In most cases, those genes responsible for triggering apoptosis are silenced in cancer cells, so the cells refuse to die. By analyzing and comparing transcriptomic data, one can find what genes are overexpressed or suppressed in cancer cells relative to normal control cells.

The second most frequent application of transcriptomic data is characterizing splicing sites, intron-specific splicing efficiency, and alternative splicing. Some genes are transcribed but not spliced and exported to cytoplasm unless a certain environmental trigger is present. We observe the presence of mRNA but no protein. Different introns differ in splicing efficiency. Highly expressed genes typically have strong 5' and 3' splice sites and branchpoint sites and are spliced efficiently. In contrast, lowly expressed genes often have weak splicing signals and spliced inefficiently. Many genes undergo alternative splicing, most through exon skipping. Different splicing isoforms can be easily detected by transcriptomic data analysis.

How transcriptomic data can be used in research depends on the creativity of the researcher. My students have used transcriptomic data to characterize the 3' end of small subunit ribosome RNA in bacterial species. Small subunit rRNA, large subunit rRNA and 5.8S rRNA are transcribed together and processed to generate functional individual rRNA molecules. Strangely enough, after so many years of rapid development of molecular biology, we still do not know how the 3' end of small subunit rRNA is processed. The 3' end of small subunit

rRNA was experimentally verified for only a handful of bacterial species. If the 3' end of many transcriptomic reads are mapped to site i in the ribosomal gene, but never beyond, then we know that the rRNA ends at site i.

In designing mRNA vaccines against viral pathogens such as SARS-CoV-2, one needs to optimize codon usage by maximizing the usage of codons decoded by the most abundant tRNA. For example, the spike protein mRNA in the Pfizer and Moderna vaccines has been optimized in codon usage. However, what tRNA species is the most abundant in muscle cells where the vaccine mRNA is to be translated? My students have also used transcriptomic data to characterize cellular tRNA pools to understand the cellular optimization of translation efficiency.

DATA AND SOFTWARE

Data files

Original source files

The original transcriptomic data file is SRR1536586.sra downloaded from GenBank to illustrate two aspects of transcriptomic data analysis: 1) quality assessment of transcriptomic data, and 2) characterization of gene expression. The file is small by RNA-Seq standard, with only 198 MB. It is from a wild-type *E. coli* K-12 colony, and represents one of the four data sets with three others being from three *E. coli* K-12 mutants (Pobre and Arraiano 2015) that lacks RNase II, RNase R, and PNPase, respectively. You can download SRR1536586.sra directly from NCBI Entrez by using an NCBI utility called prefetch. However, to avoid internet traffic jam, I have already downloaded it locally. It is available at:

http://dambe.bio.uottawa.ca/teach/bps4104_download/SRR1536586.sra

The original publication (Pobre and Arraiano 2015) aimed to understand how the RNase mutants would affect RNA degradation. If you wish to compare the gene expression between the wild-type and the mutant, or between mutants, then you should also download the other three SRA files (SRR1536587.sra, SRR1536588.sra, SRR1536589.sra) and repeat what is detailed below for the other three files.

Processed files

Some of the data processing is time-consuming, so I have included a few processed files. If a protocol converts File X to File Y and if the protocol is slow, I have included File Y so that you don't have to wait in the lab to get results. You may just download them following the links below:

1. http://dambe.bio.uottawa.ca/teach/bps4104_download/SRR1536586.fasP: This is the file in FASTA format that represents identical reads with a single sequence in the format of SeqID_N, where N is the number of identical sequences.
2. http://dambe.bio.uottawa.ca/teach/bps4104_download/SRR1536586.zip: This file contains a BLAST database generated from the SRR1536586.fasP file above. You do not need this file. It is included just in the rare case when you have done something wrong before the step on quantifying gene expression.

Software ARSDA and DAMBE

In addition to DAMBE, we will introduce a new software ARSDA (Xia 2017) which stands for Analysis of RNA-Seq Data. ARSDA has two advantages over other transcriptomic data analysis software. Firstly, it can dramatically reduce RNA-Seq file size without losing any sequence information. This is possible because many sequence reads from a transcriptomic study are identical. Take for example the transcriptomic data for *Escherichia coli* K12 in the file SRR1536586.sra (where SRR1536586 is the SRA sequence file ID in NCBI/DDBJ/EBI). The file contains 6,503,557 sequences of 50 nt each, but 195310 sequences are all identical (TGTTATCACG GGAGACACAC GGCGGGTGCT AACGTCCGTC GTGAAGAGGG), all mapping to sites 929-978 in *E. coli* 23S rRNA genes. A more dramatic example is the file SRR922264.sra (from another *E. coli* transcriptomic study) in which one forward read has 1,606,515 identical copies stored in the file as separate entries (The file contains 9,690,570 forward reads and same number of reverse reads). The current approach at NCBI/DDBJ/EBI stores individual reads in SRA or FASTQ files as separate entries. There is no sequence information lost if all these identical sequences are stored by a single sequence with a sequence ID such as UniqueSeqX_1606515 (i.e., SequenceID_CopyNumber). Such storage scheme also leads to dramatic saving in analysis time. At present, all software packages for RNA-Seq analysis will take these identical reads and search them individually against the *E. coli* genome (or coding sequences). The SequenceID_CopyNumber storage

scheme reduces all these separate searches of identical sequences to a single one. The new FASTQ+ and FASTA+ formats generated and used by ARSDA differ from the corresponding FASTQ and FASTA file formats only in the use of SequenceID_CopyNumber as sequence ID.

The second advantage in ARSDA is in its explicit and rational allocation of reads to paralogous genes leading to more accurate quantification of gene expression. This method is missing in other software packages for RNA-Seq data analysis (Langmead, et al. 2009; Trapnell, et al. 2009; Langmead, et al. 2010; Roberts, et al. 2011; Langmead and Salzberg 2012; Trapnell, et al. 2012; Dobin, et al. 2013; Roberts, et al. 2013; Deng, et al. 2014). The rationale for the allocation has been numerically illustrated in detail (Xia 2017, 2018b).

Some of ARSDA's functions make use of several NCBI programs for sequence matching and for processing SRA files (sratoolkit). These programs are included in the ARSDA distribution for your convenience. Some of ARSDA functions such as gene expression quantification involves reading genomic data in GenBank format and extracting coding sequences, exons, introns, rRNAs and tRNAs, and are better done jointly with DAMBE (Xia 2018a) which features extensive data analysis. Both ARSDA and DAMBE are freely available at dambe.bio.uottawa.ca/Include/software.aspx, and can be installed with just a few mouse clicks.

OBJECTIVES

Quality assessment of transcriptomic data

There are three types of quality assessment involving transcriptomic data: global quality assessment, read quality assessment and site-specific quality assessment

Conversion of FASTQ to FASTA+ to speed up all downstream analysis

Many reads in a transcriptomic data set are identical and can be represented by a single sequence with the sequence name indicate the number of identical copies in the format of SequenceID_CopyNumber. This dramatically decreases file size and speeds up all downstream data analysis. All transcriptomic data analyses can be carried out with this file instead of the original file of large file size.

Quantification of gene expression from transcriptomic data

All transcriptomic data analyses including differential gene expression, alternative splicing, transcription start and end site, mature 5' and 3' ends of RNA species, etc., is ultimately related to quantification of gene expression. Quantification of gene expression from transcriptomic data is the most fundamental skill in transcriptomic data analysis.

PROCEDURES

All functions in this quick start guide can be performed on a 64-bit computer with 16 GB of RAM when no other memory-hungry programs are running. If you do not have such a computer available, you may take advantage of the processed data files I mentioned above.

File conversion among SRA, FASTQ and FASTA files

The SRA file downloaded from NCBI contains the original FASTQ file and the result of a global base-calling quality assessment based on the FASTQ file. Because the quality assessment from the original FASTQ file is time-consuming, NCBI has done this quality evaluation for all FASTQ files and then pack this result together with the FASTQ file into an SRA file. This SRA file, like a BLAST data file, encodes AAAA as 0, AAAC as 1, and so on so that the resulting SRA file is much smaller than the original FASTQ file. Single-read sequencing will generate one set of sequences. Pair-end sequencing will generate two set of sequences. Therefore, an SRA file can contain either one FASTQ file for single-read method or two FASTQ files for paired-end method. SRA files can be analyzed directly, but far more methods are available for FASTQ and FASTA files. Therefore, the most fundamental skill in RNA-Seq analysis is to restore FASTQ or FASTA files from SRA files.

To convert the downloaded SRR1536586.sra to FASTA format, launch ARSDA, and click 'File|Dump .SRA file to FASTA'. In the ensuing dialog (Fig. 1), fill in the two entries by browsing to the input file (e.g., SRR1536586.sra) and output directory and click the 'OK' button. This will generate a SRR1536586.fasta file of 764MB. This is larger than the original SRR1536.SRA file. If the input SRA file contains paired-end reads, then two FASTA files will be generated, one for the forward reads and one for the reverse reads. A FASTA file does not have information on base quality. If you wish to perform specific base-quality analysis, you need to restore

the SRA file to the original FASTQ file by clicking 'File | Dump .SRA file to FASTQ'. The resulting FASTQ file will take up about 1.5 GB in disk space.

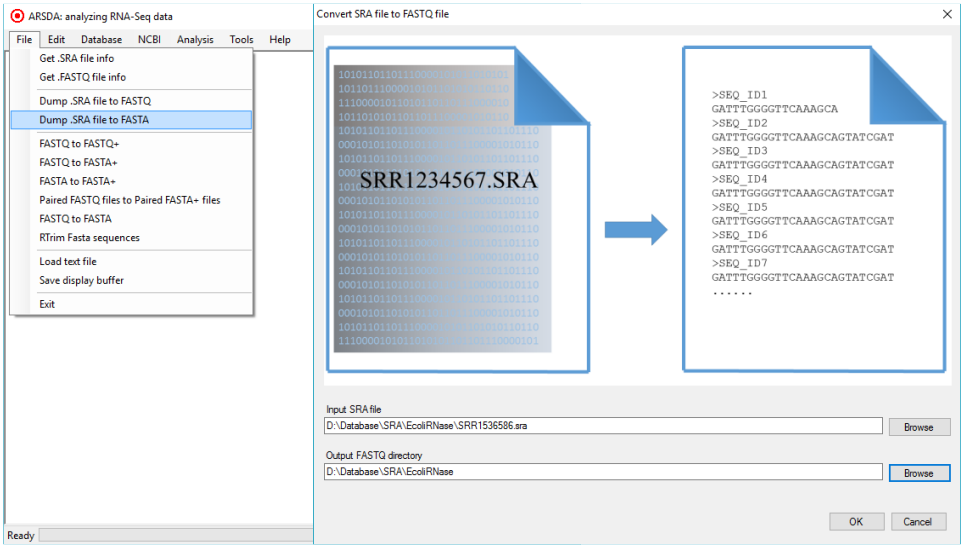

Fig. 1. ARSDA's main menu system displaying the function for dumping SRA file to FASTA. The output entry is a directory.

Three ways to visualize sequence quality

Global base-calling quality

Data for global base-calling quality is already present in the downloaded SRA file and needs little computation (because it has already been computed by NCBI). To visualize the quality report within an SRA file, click 'File|Get .SRA file info' and browse to the input SRA file (Fig. 2). Leave the default option of 'Graphic display of quality of reads' and click 'OK'.

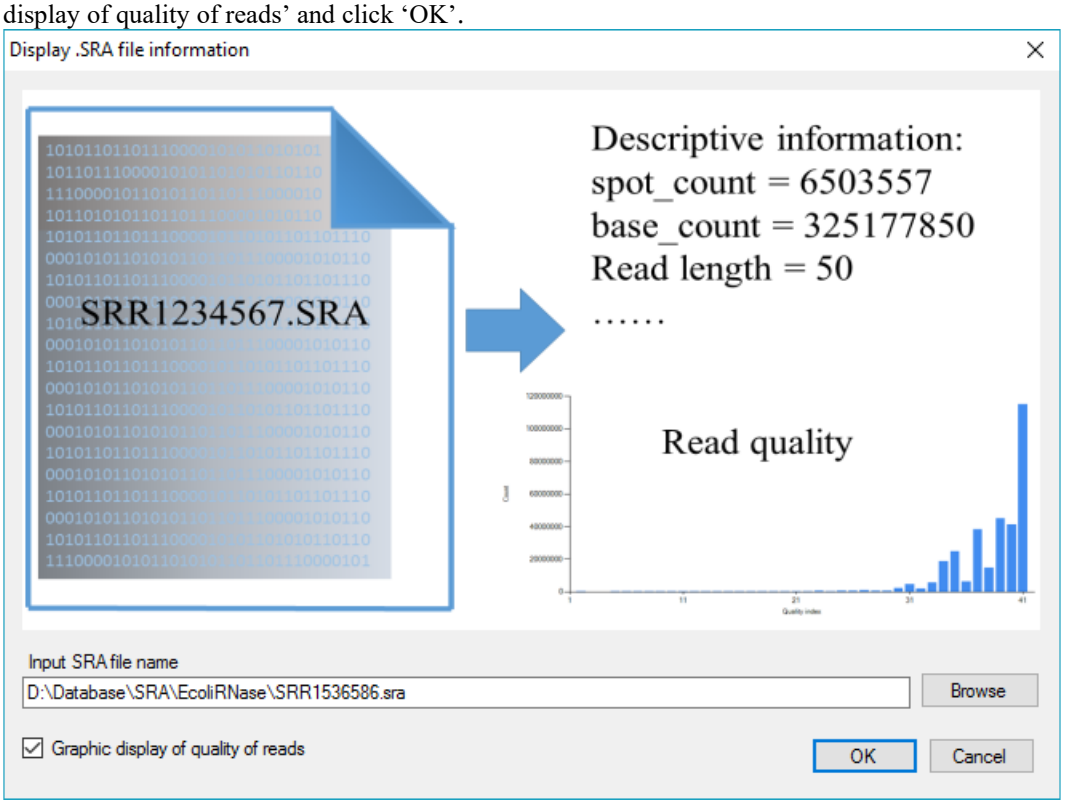

Fig. 2. Input for visualizing global base-calling quality based on information stored within individual SRA files**.**

The output (Fig. 3) shows the frequency distribution (Y-axis) of base-calling quality ('Quality index in X-axis). Good quality corresponds to large 'Quality index'. A 'Quality index' of 41 in an .sra file is equivalent to an error probability of base-calling (P) of 0.000079433, i.e., it is equal to $-10*\log_{10}(P)$. In contrast, base quality in a FASTQ file is represented by symbols from '!' to '~' corresponding to ASCII codes from 33 to 126, so a 'Quality index' of 41 in Fig. 3 would be represented by character 'I' corresponding to the ASCII value of 73 [$=-10\log_{10}(P) + 32$].

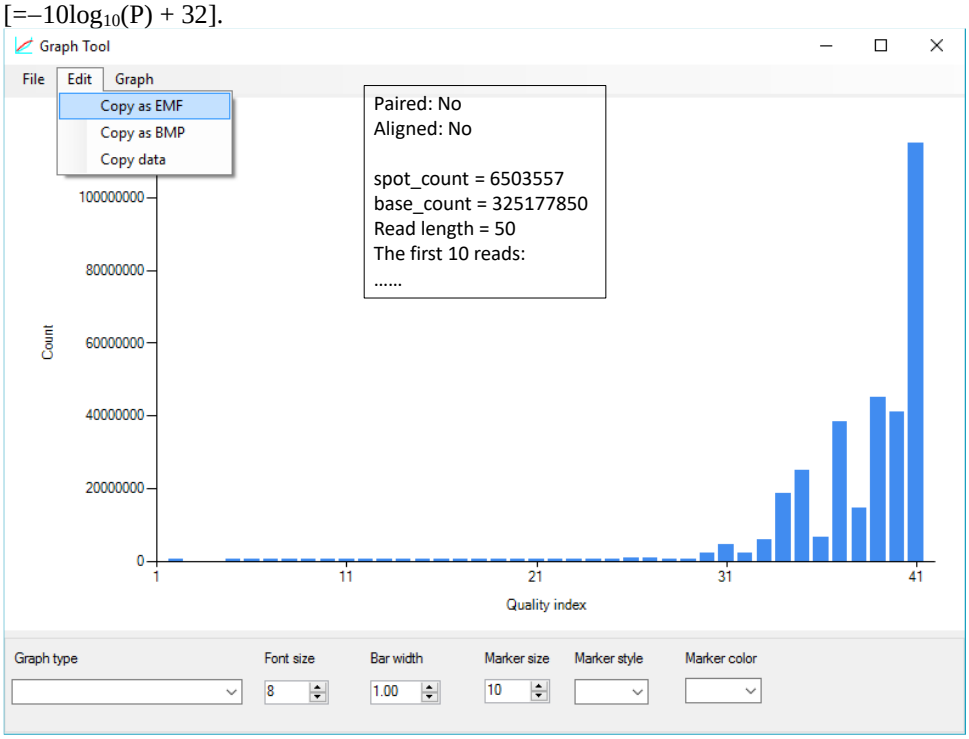

Fig. 3. Output for visualizing global read quality based on information stored within individual SRA files. One can copy and paste high-resolution image to graphic programs such as Microsoft PowerPoint by clicking 'Edit|Copy as EMF'. Alternatively, one may copy and paste the graphic data to EXCEL and re-generate graphs in EXCEL. The inset shows part of the text output.

Among a random selection of 10 SRA files, the global base-calling quality in SRR1536586 is the second best. Some files, especially those with long reads of 250 bases, are often quite poor.

Read-specific quality and site-specific quality

The SRA file does not include results for these two types of quality assessment, so we need to do this very time-consuming quality evaluation ourselves from the FASTQ file that we generated in the section on file conversion. The FASTQ file is large, about 1.5 GB. Processing this large file during the quality evaluation may take about half an hour to finish. Hopefully, NCBI will do these two types of quality evaluation in the future and pack the results into SRA files as well.

Read-specific quality: A read with many low-quality bases is better excluded from the analysis. For this reason, it is important to know how many poor-quality reads there are in the RNA-Seq data and what threshold one should use to exclude them. A read with 50 bases has 50 individual base quality values, and a read quality is simply the average of these 50 values.

Site-specific quality: The sequencing by synthesis step in RNA-Seq by Illumina and the like is particularly error prone so that the base quality decreases rapidly with read length. A researcher with long reads of 250 bases would wish to know whether all bases are good or only the first 150 bases are good. A sequencer manufacturer would want to know the optimal read length to extract so that the sequencer will not waste time to generate long but poor reads (which would be embarrassing to the sequencer manufacturer). Site-specific base quality helps to address this problem.

The read-specific and site-specific qualities can be obtained by clicking 'File|Get FASTQ file info', which displays the dialog in Fig. 4. Browse to the input FASTQ file, click 'OK', and ARSDA will start a lengthy process of reading and processing the input file. For large FASTQ files, ARSDA read them in chunks so there is no high-memory requirement for this function. For the SRR1536586.fastq, ARSDA may take half an hour before generating the output.

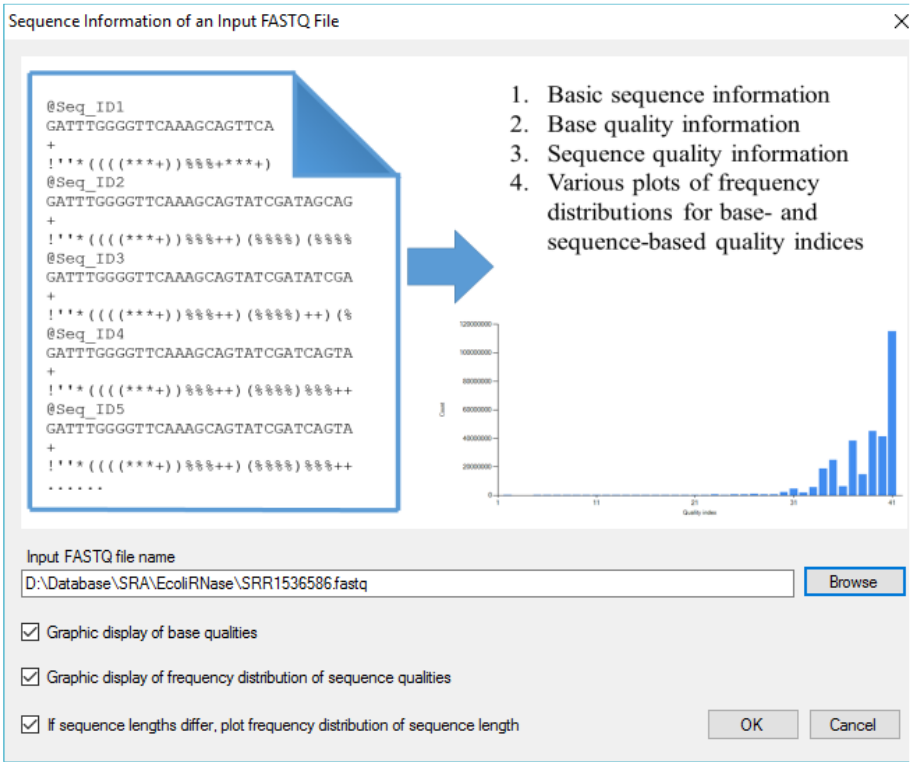

Fig. 4. Dialog box for accessing read-specific and site-specific quality characterization.

The output is of three parts. The first is the same as in Fig. 3, and will not be repeated here. The second is read-specific quality distribution, which plots reads with and without ambiguous codes separately for sequences (Fig. 5 for SRR1536586.fastq). As I mentioned before, this data set is of high quality, and it is helpful to contrast it with another data set that is of lower quality (Fig. 6 for sequences in the file SRR2056426.sra, which is also for *E. coli*, but is of paired-end reads with read length of 250 nt). In general, quality decreases rapidly with sequence length. For paired-end reads, the reverse read is much worse than the forward read.

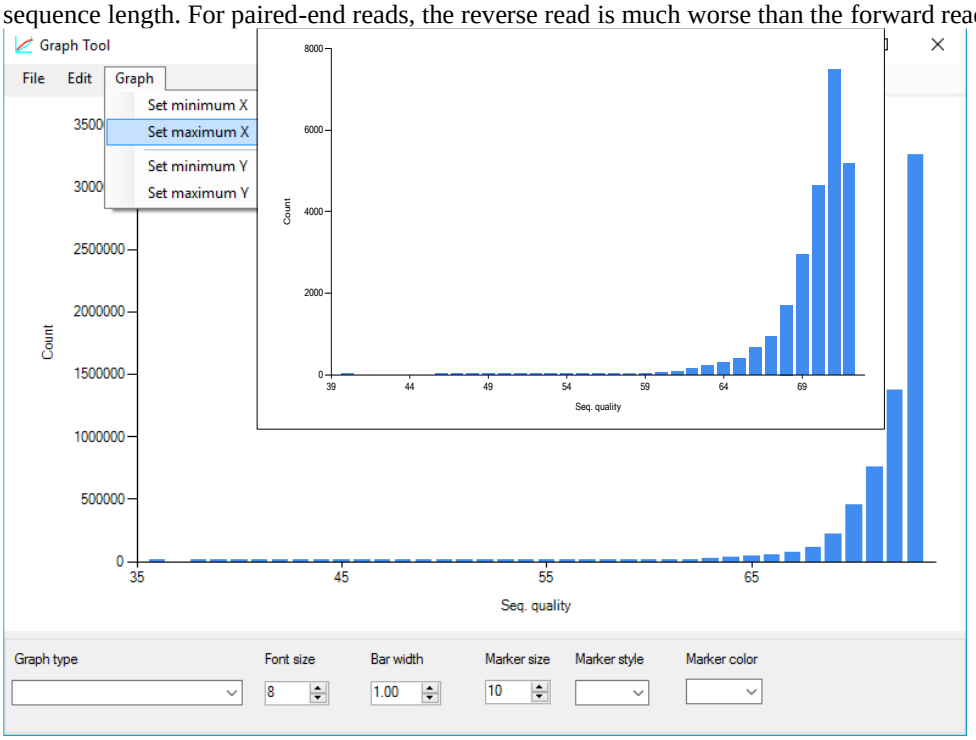

Fig. 5. Frequency distribution of the quality of individual reads for all reads with fully resolved bases in file SRR1536586.sra. The inset is an equivalent plot for sequence reads with at least one unresolved base.

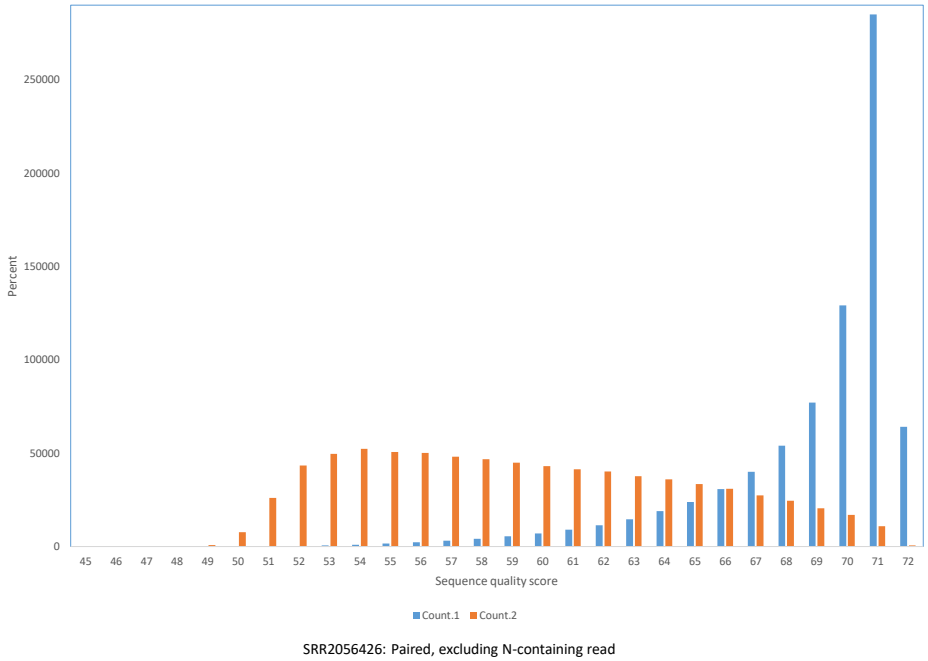

Fig. 6. Frequency distribution of the quality of individual reads for sequences in SRR2056426.sra with paired-end reads. The reverse read (Count2, in orange) is generally poor in quality. The graph includes only sequences without ambiguous codes, otherwise the quality would be even worse.

The site-specific quality distribution (Fig. 7 for SRR1536586.fastq) shows the change of base-calling quality with sites. The values for the first 15 or so sites can be ignored as the sequencing machine needs to have enough data to assign appropriate base-calling qualities. Fig. 7 shows the decreasing trend of base-calling quality with sites. However, because this data set have only short reads (50 nt) and is of high quality even among RNA-Seq data set with read length of 50, the decrease is not alarming. It might help to contrast this pattern with RNA-Seq data in a file with longer reads, such as SRRSRR2056426.sra with paired-end reads and read length of 250 (Fig. 8).

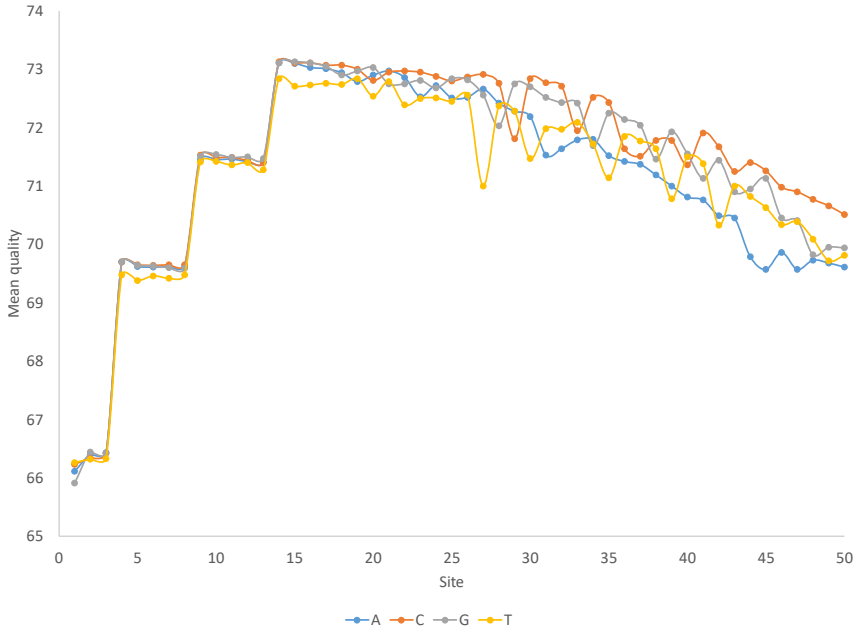

Fig. 7. Site-specific quality for sequences in SRR1536586.sra, including only sequences without ambiguous codes (otherwise the quality would be worse). The quality score of the first ~15 sites may be ignored because the sequencing machine needs to accumulate enough information to generate quality scores properly.

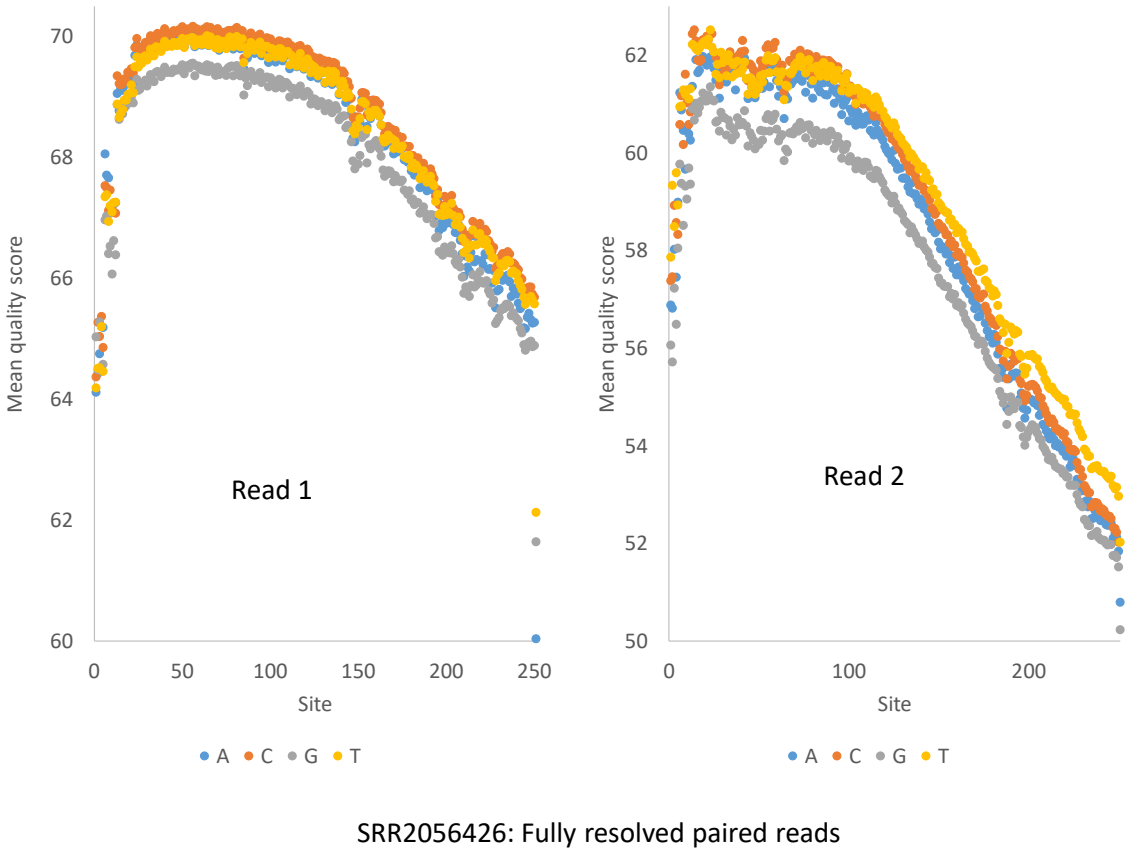

Fig. 8. Quality of individual reads for sequences in SRR2056426.sra with paired-end reads. The reverse read (Read 2) is generally poor in quality. The graph includes only sequences without ambiguous codes, otherwise the quality would be even worse. The quality score of the first ~15 sites may be ignored because the sequencing machine needs to accumulate enough information to generate quality scores properly.

Convert FASTA files to FASTA+ files

FASTA+ is the condensed file format by representing identical read with a single sequence. This step is slow. To reduce waiting time, I have already done this step and the resulting file can be downloaded from the link at http://dambe.bio.uottawa.ca/teach/bps4104_download/SRR1536586.fasP. I use the "fasP" as file extension for FASTA+ files. You may skip this section unless you have a computer with at least 16 GB of memory.

To convert the FASTA file to FASTA+ file, click 'File|FASTA to FASTA+', enter the input and output file names (Fig. 10), and click 'OK'. The conversion is a rather lengthy process. ARSDA will create a dictionary of unique sequences as well as a count for each unique sequence. This dictionary is necessarily large and is the only function in ARSDA that requires 16GB or more RAM. However, the conversion needs to be done only once for data storage, but the saving in storage space, internet traffic and computation time in downstream data analysis is tremendous. For example, one can use this file to obtain gene expression for coding sequences or tRNAs, and it reduces the computation time from many hours to a few minutes. This conversion will make RNA-Seq data analysis feasible in every biological laboratory.

The output also includes a table showing how many reads are represented only once, twice, etc., and part of the table is replicated in Table 1. Some sequences are represented many times. As I mentioned before, one 50mer mapped to sites 929-978 in *E. coli* 23S rRNA gene is represented 195310 times in the SRR1536586.sra file. The SRA file (and the FASTA file derived from it) lists these 195310 sequences individually. The resulting FASTA+ file lists them by a single entry (S17_195310) in FASTA+ format where 'S17' means that the read is the 17th unique sequence in the read dictionary and it has 195310 identical copies in the FASTA file. This condensed representation of UniqueSeqID_N leads to dramatic reduction in file size, from the original FASTA file of 764 MB to the new FASTA+ file of only MB, and the FASTA+ file will be only about 68 MB. This FASTA+ can be used for all subsequent data analysis or transmitted to your collaborators instead of the original file of large size.

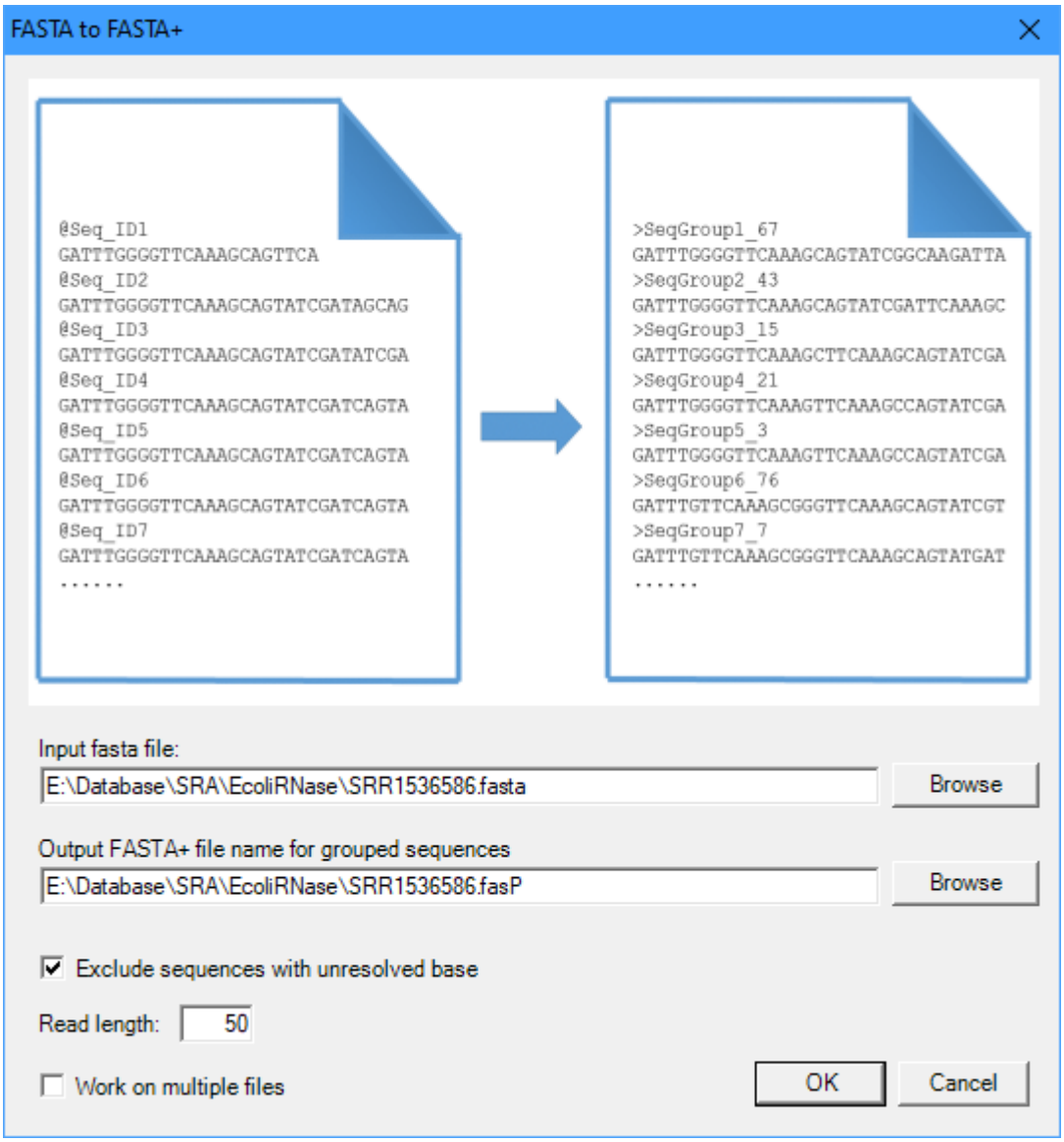

Fig. 10. User interface in ARSDA for converting a FASTA file to a FASTA+ file. For a set of N sequences represented as SequenceID_N, the quality score for each site is the average of N quality values. The interface for converting FASTA file to FASTA+ file is the same except that FASTQ will be replaced by FASTA. I use "fasP" file extension to FASTA+ files.

Table 1. Part of read-matching output from ARSDA, with 195310 identical reads matching a segment of large subunit (LSU) rRNA, 86308 identical reads matching another segment of LSU rRNA, and so on. Results generated from ARSDA analysis of the SRR1536586.sra file from GenBank.

Gene	N_{copy}	Gene	N_{copy}
LSU rRNA	195310	SSU rRNA	30417
LSU rRNA	86308	LSU rRNA	29508
LSU rRNA	58400	5S rRNA	28187
SSU rRNA	47323	LSU rRNA	24982
LSU rRNA	45695	SSU rRNA	23286
LSU rRNA	36258	LSU rRNA	19991
5S rRNA	33674	SSU rRNA	19268

The interface for converting FASTQ file to FASTQ+ file is similar to that in Fig. 10. A transcriptomic study typically generates a number of files (e.g., one for wild type and several for various treatments). The dialog in Fig. 10 include a "Work on multiple files" option. One can check this option, select all FASTA files and let the computer run over night to generate FASTA+ files. To save disk space and speed up data analysis even further, one can pack the FASTA+ file into a BLAST database. I have created a BLAST database that you can download as http://dambe.bio.uottawa.ca/teach/bps4104_download/SRR1536586.zip, but you can create the BLAST database yourself. All bioinformaticians need to create local BLAST databases often. For example, if you are in a biopharmaceutical company working on transgenic genes or vaccine mRNA, you would need to create microRNA database to check if your transgene might be targeted by certain microRNAs. Similarly, if you are working on transgenes in crop species, you need to create a database of allergens to make sure that your transgene does not encode something that would cause severe allergic responses. For this reason, many bioinformatics software packages include a function for converting FASTA files to BLAST databases.

Convert FASTA+ file to a BLAST database

I have already done this part which results in the SRR1536586.zip with the URL link provided previously. Download this file, unzip the content and save the resulting six files in a directory with no space in the directory name (e.g., not something like "C:\users\John Doe\data" because a space is present between "John" and "Doe"). You can skip this section unless you have already generated your own FASTA+ file or have downloaded the SRR1536586.fasP file.

Suppose that you have the SRR1536586.fasP (I use "fasP" as a file extension for FASTA+ files) on your computer. Click ‘Database|Create BLAST DB’ and browse to and open the SRR1536586.fasP file (Fig. 11). Enter the 'Output database name' and the 'Directory to save output BLAST database'. This directory should contain no space as I mentioned above. Click ‘OK’ and a BLAST database with SRR1536586 as database name is creased in the specified directory.

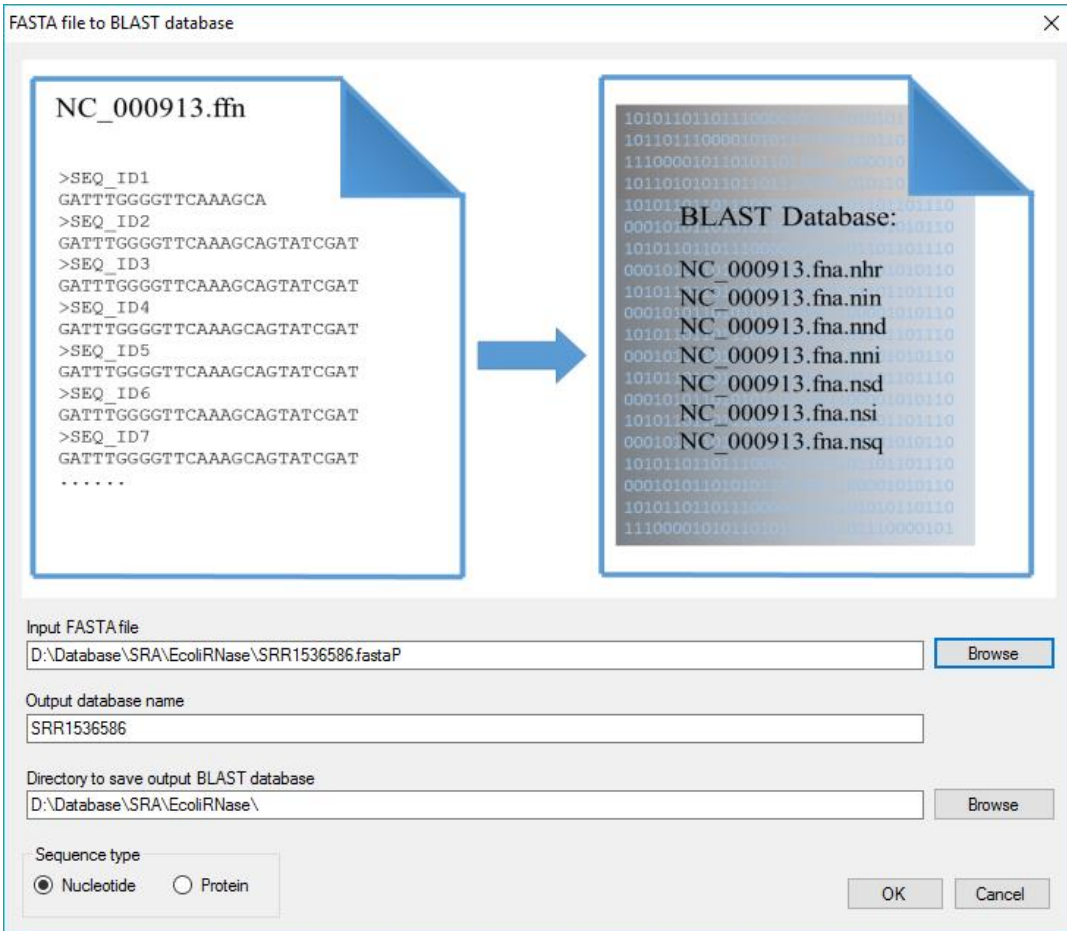

Fig. 11. Input and output for generating a BLAST database from a FASTA file. The latest version has an additional checkbox for processing multiple files.

Quantifying gene expression (FPKM)

Characterizing gene expression involves a process of assigning reads to genes and normalizing the read count for each gene to FPKM (Fragment per kilobases per million matched reads, sometimes 'fragment' is replaced by 'read' leading to RPKM). A gene with many reads mapped to it is more expressed than a gene with few or no read mapped to it. The normalization allows comparisons not only between genes of different sequence lengths but also between experiments with different number of total matched reads.

ARSDA maps transcriptomic reads to genes to quantify gene expression. This implies two sources of information: 1) genes whose expression needs to be quantified, and 2) transcriptomic reads that will be mapped to the genes. The first source of information depends on what genes one wants to quantify their expression. For quantifying gene expression of protein-coding genes of E. coli K12, one may use DAMBE to extract all coding sequences of an E. coli K12 genome as input. This is what we will do in this lab. If one is interested only in the expression of tRNA genes, one may use DAMBE to extract all tRNA genes from an E. coli genome as input. The second source of information is always the transcriptomic data. We will use the BLAST database derived from SRR1536586.fasP which in turn was originally derived from the downloaded SRR1536586.sra file.

Download E. coli K12 genome, extracting coding sequences and save in FASTA format

Download *E. coli* GenBank file NC_000913.gbk for E. coli K-12 strain MG1655 by browsing to https://www.ncbi.nlm.nih.gov/nuccore/NC_000913. Click 'Send to | File | GenBank (full) | Create File' and save it to NC_000913.gbk.

Launch DAMBE, click 'File|Open standard sequence file' to open the NC_000913.gbk. DAMBE can extract coding sequences (CDSs), exons, introns, rRNAs or tRNAs (Fig. 12). Select 'CDS'. In 'Sequence naming options', choose '/locus_tag'. You might have already learned that '/gene' name is often not unique because two paralogous genes could have the same gene name. However, locus tag is always unique. Click 'OK' to extract CDSs and save the CDSs in FASTA format to EcoliCDSGeneLoc.fas (or whatever file name you wish to name it, but remember where it is located).

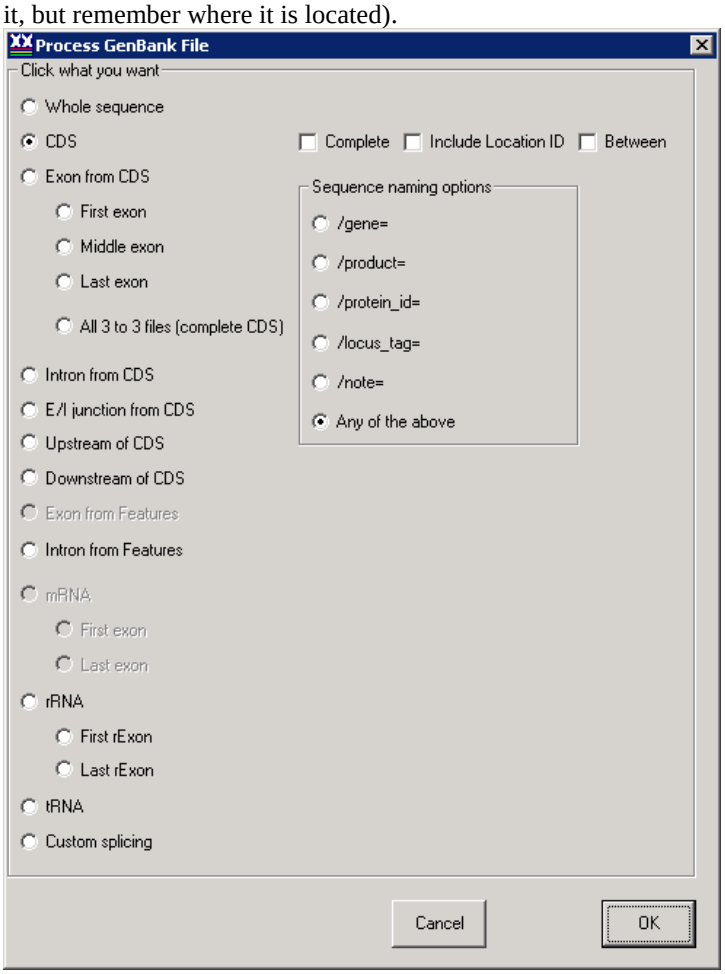

Fig. 12. Sequence extraction dialog box in DAMBE for GenBank files.

Quantifying gene expression

Now we have everything needed to characterize gene expression. Close DAMBE and other memory-hungry programs (DAMBE is not memory-hungry) and go back to ARSDA. Click ‘Analysis|Gene expression from BLAST database’ (NOT ‘Gene expression from SRA database’ which is extremely slow). The ensuing dialog (Fig. 13) shows two parts that should have already been similar to you because all dialogs in ARSDA were designed with a similar genre. The top of the dialog is a graph summarizing what the function will accomplish. The key output is the 'Gene expression' which requires information from two sources. One is a list of genes for quantifying gene expression, and the other is the BLAST database containing transcriptomic data used to quantifying gene expression.

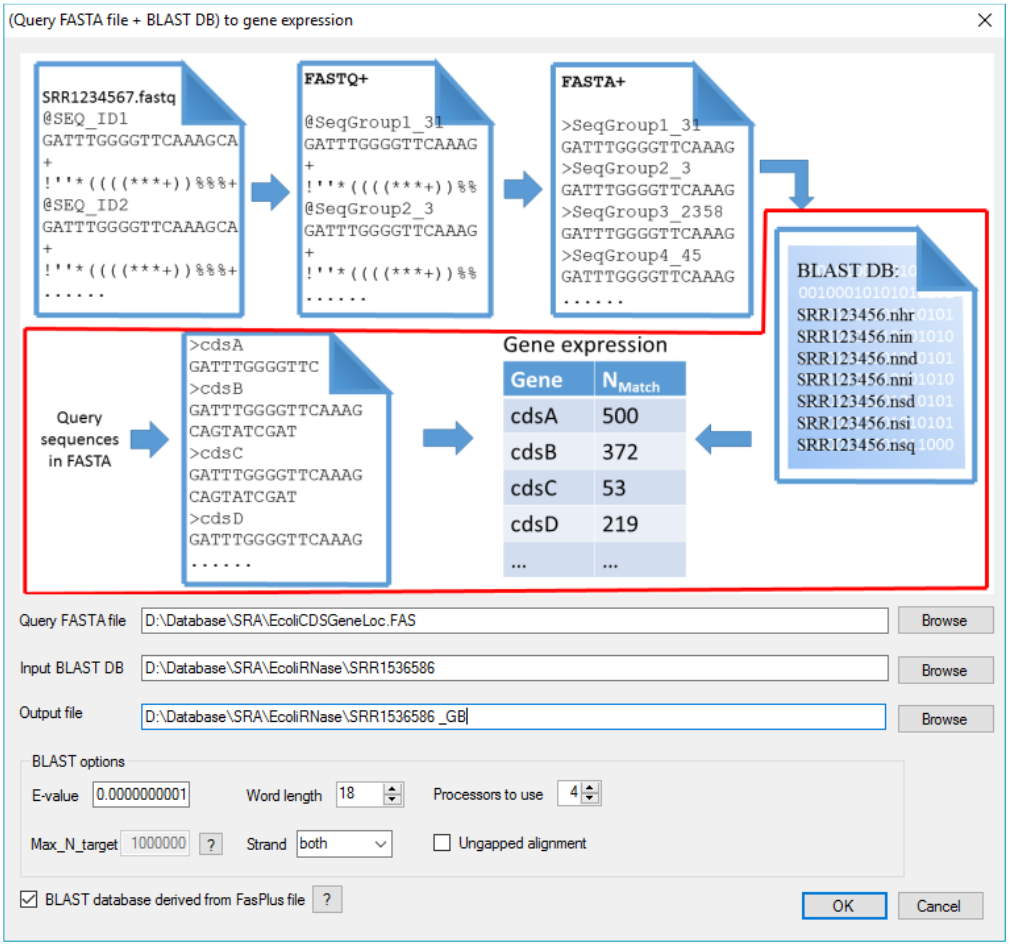

Fig. 13. Input specification for characterizing gene expression.

The lower part of the dialog demands input. In the ‘Query FASTA file’ input field, enter, or browse to, the EcoliCDSGeneLoc.fas file that we have just created from extracted *E. coli* CDSs. In 'Input BLAST DB', browse to the directory of the BLAST database you have created (or where you have unzipped the SRR1536586.zip file) and click SRR1536586 (or whatever BLAST database name you have used in Fig. 11) in the file open dialog (Fig. 13). Note that I have set the E-value very small. This is important because we do not want to have false positives when mapping reads to *E. coli* genes. The 'Word length' was set to 18. The smallest word length in BLAST is 11. Increasing it to 18 increases speed. The 'Processors to use' field is set to 4 in the dialog in Fig. 13, but you can increase or decrease it depending on how many processors your computers have. The 'Strand' field was set to 'both'. The 'BLAST database derived from FasPlus file' was checked because our BLAST database was indeed created from a FASTA+ file. This tells ARSDA that a sequence represent N identical reads. A single match to the gene means N matches. If this option is not checked, then a match between a read and a CDS represents just a single match. Click ‘OK’ and gene expression for all *E. coli* K12 CDSs will be generated. Part of the output is shown is Table 2.

Table 2. Partial output of gene expression, with the gene locus_tag (together with start and end sites) as gene ID.

Gene ID	SeqLen	Count	Count/Kb	FPKM
b0001|190_255	66	76	1151.515	389.894
b0002|337_2799	2463	2963	1203.004	407.328
b0003|2801_3733	933	1121	1201.501	406.819
b0004|3734_5020	1287	1782	1384.615	468.82
b0005|5234_5530	297	97	326.599	110.584
b0006|C5683_6459	777	113	145.431	49.242
b0007|C6529_7959	1431	143	99.93	33.836
b0008|8238_9191	954	1561	1636.268	554.028
b0009|9306_9893	588	289	491.497	166.417
b0010|C9928_10494	567	100	176.367	59.716
b0011|C10643_11356	714	13	18.207	6.165
b0013|C11382_11786	405	2	4.938	1.672
b0014|12163_14079	1917	6863	3580.073	1212.186
b0015|14168_15298	1131	1671	1477.454	500.255
…	…	…	…	…

Assignment

1. Extract all tRNA genes from the downloaded *E. coli* K12 genome and quantify their gene expression. (Don't overinterpret the result because the RNA sample was treated in various ways which may distort the relative abundance of tRNA species. For this reason, it is always important to read the detailed description of methods and materials used in the original research project).

LAB 5 CODON USAGE BIAS

INTRODUCTION

Genetic codes are degenerate. For example, glycine is coded by four synonymous codons (GGN, where N stands for any nucleotide) and lysine is coded by two synonymous codons (AAR, where R stands for either A or G). Some synonymous codons are used much more frequently than others. Differential usage of synonymous codons is termed codon usage bias.

This laboratory has two parts. The first part is on codon usage bias and indices frequently used to measure the codon usage bias. These indices are often used as an indirect measure of gene expression because experimental data have repeated demonstrated a close correlation between gene expression and codon bias indices (Comeron and Aguade 1998; Coghlan and Wolfe 2000).

Because eukaryotic viruses and bacteriophages generally do not have their own translation machinery, they typically evolve codon usage in response to their host tRNA pools. Several students in my laboratory have made significant contributions along this line of enquiry, including HIV-1 codon adaptation to human T-cell tRNA pool (van Weringh, et al. 2011), codon adaptation in *E. coli* phages in response to host tRNA pool and the effect of phage-encoded tRNA on this adaptation (Chithambaram, et al. 2014a, b; Prabhakaran, et al. 2014), and how codon adaptation in phages is mediated by other processes such as translation initiation (Prabhakaran, et al. *2015*).

The second part is for identifying tRNA anticodon, which is often necessary to understand codon usage bias. Two factors are known to affect codon usage bias. The first is the mutation bias (Muto and Osawa 1987; Xia 2005), i.e., AT-biased mutation will increase the usage of A-ending and T-ending codons. The second is the tRNA-mediated selection to improved efficiency and accuracy in translation (Ikemura 1981a; Bulmer 1987; Ikemura 1992; Xia 1998a; Xia, et al. 2007; Carullo and Xia 2008; Xia 2008). Different synonymous codons in a codon family are often translated by different tRNA species (isoaccepting tRNAs) which exist in different concentrations in the cell. It is understandable that, if many tRNAs are available to translate glycine codons GGC and GGU but few tRNAs are available to translate glycine codons GGA and GGG, then translation efficiency can be improved by coding glycine by GGC and GGU codons. The correlation between codon usage bias and differential tRNA availability was discovered in 1970s (Garel 1974; Garel, et al. 1974; Chavancy, et al. 1979).

We need to refresh our memory on tRNA notations before proceeding. An uncharged tRNA (i.e., it does not carry an amino acid) is simply written as $tRNA^{AA}$, where the superscripted AA is the amino acid that the tRNA anticodon is supposed to code. For example, $tRNA^{Gly}$ means an uncharged tRNA with an anticodon that matches one of the glycine codons (GGA, GGC, GGG and GGU). To specify an uncharged tRNA with the anticodon, the notation such as $tRNA^{Gly/CCC}$ is used, where CCC is the anticodon forming the Watson-Crick base pairing with the Gly codon GGG. An alternative notation is $tRNA^{Gly}_{CCC}$ which, being more cumbersome to write, will not be used here.

Different types of tRNAs are charged by their respective aminoacyl-tRNA synthetases (aaRS). A charged tRNA is written in the generic form as AA2-$tRNA^{AA1}$, where AA2 is the amino acid that is actually attached to the tRNA. In most cases, AA1 = AA2, i.e., we will typically have charged tRNAs such as Gly-$tRNA^{Gly}$, Ala-$tRNA^{Ala}$, Cys-$tRNA^{Cys}$, etc. However, sometimes one may take, for example, a Cys-$tRNA^{Cys}$ and modify the attached Cys to Ala, so we now have Ala-$tRNA^{Cys}$. Such a modification is exactly what was done in the classical Raney-nickel experiment (Chapeville, et al. 1962) that showed that Ala-$tRNA^{Cys}$ will incorporate Ala at the site of a Cys codon in the mRNA. This is strong proof that amino acid incorporation in ribosome is specified by the anticodon of the tRNA, but not by the amino acid actually carried by the tRNA.

GlnRS or AsnRS may be absent in some prokaryotes (Schon, Hottinger, et al. 1988; Curnow, et al. 1997; Curnow, et al. 1998), plants (Schon, Kannangara, et al. 1988) or organelles such as chloroplasts and mitochondria in eukaryotes (Schon, Kannangara, et al. 1988; Chen, et al. 1990). The production of Gln-$tRNA^{Gln}$ and Asn-$tRNA^{Asn}$ are produced in two steps. First Glu-$tRNA^{Gln}$ and Asp-$tRNA^{Asn}$ are formed by misacylation and then transformed to Gln-$tRNA^{Gln}$ and Asn-$tRNA^{Asn}$ by transamidation (Ibba, et al. 1997; Stortchevoi 2006). This represents a rare case in which an error (i.e., misacylation) is essential for survival.

Codon usage bias

Many unicellular organisms, especially bacterial species, need to grow and replicate rapidly in order not to be out-competed by others. For example, an *E. coli* cell replicates one every 20 minutes with unlimited nutrients.

To replicate a cell, not only does the genome need to be replicated, but a large amount of proteins have to be produced, with some proteins produced in nearly half a million copies in an *E. coli* cell. For such highly expressed proteins, it is very important for them to have efficient coding strategy to maximize the rate of transcription (Xia 1996) and translation (Ikemura 1981a; Bulmer 1987; Ikemura 1992; Xia 1998a; Xia, et al. 2007; Carullo and Xia 2008; Xia 2008).

One way to increase translation efficiency is to have most used codons to match the most abundant cognate tRNA. For example, the amino acid glycine can be coded by GGA, GGC, GGG and GGU codons. However, Gly-tRNA$^{Gly/GCC}$ (which can translate GGC and GGU codons) is very abundant in *E. coli* cells whereas Gly-tRNA$^{Gly/UCC}$, Gly-tRNA$^{Gly/CCC}$, and Gly-tRNA$^{Gly/ACC}$ are either rare or absent. This would lead us to predict that *E. coli* should use GGC and GGU codons to code Gly, which turns out to be true (Ikemura 1981a, 1992; Xia 1998a).

When scientists in a biopharmaceutical company want to produce a certain human protein (e.g., insulin) in a bacterial species (e.g., *E. coli*), they will not just cut out the DNA coding the human protein and insert it into the *E. coli* gene with an *E. coli* promoter. Instead, they will study the relative abundance of *E. coli* tRNA species and make sure that the codon usage of the human gene is modified in such a way that maximizes translation efficiency and accuracy. For example, if the human gene codes Gly with GGA and GGG, these GGA and GGG codons will be modified to GGC and GGU codons before the gene is inserted into the *E. coli* genome (Recall that *E. coli* has many tRNAs translating GGC and GGU codons but relatively few tRNAs translating GGA and GGG codons).

Scientists used to consider Human Immunodeficiency Virus 1 (HIV-1) as having poor codon-anticodon adaptation. For example, according to a recent compilation of tRNAs in human genome (Chan and Lowe 2009), the AUC codon can be translated by 17 tRNA^{Ile} species, i.e., 14 tRNA$^{Ile/IAU}$ and 3 tRNA$^{Ile/GAU}$, AUU can be translated by 14 tRNA$^{Ile/IAU}$ species, whereas AUA can only be translated by only 5 tRNA$^{Ile/UAU}$ species. In agreement with this, human genes code Ile mostly by AUC and least by AUA. In contrast, HIV-1 genes code Ile mostly by AUA and least by AUC (Haas, et al. 1996; Nakamura, et al. 2000). However, HIV-1 has recently been shown to package non-lysyl tRNAs in addition to the tRNA^{Lys} needed for priming reverse-transcription and integration of the HIV-1 genome. tRNAs decoding codons which are highly used by HIV-1 but avoided by its host are overrepresented in HIV-1 virions. In particular, tRNAs decoding A-ending codons, required for the expression of HIV's A-rich genome, are highly enriched (van Weringh, et al. 2011). Because the affinity of Gag-Pol for all tRNAs is non-specific, HIV packaging is most likely passive and reflects the tRNA pool at the time of viral particle formation. Codon usage of HIV-1 early genes is similar to that of highly expressed host genes, but codon usage of HIV-1 late genes were better adapted to the selectively enriched tRNA pool, suggesting that alterations in the tRNA pool are induced late in viral infection. If HIV-1 genes are adapting to an altered tRNA pool, codon adaptation of HIV-1 may be better than previously thought.

The coding strategy is reflected in codon usage bias which is often measured by two indices, the relative synonymous codon usage (RSCU) and the codon adaptation index (CAI). RSCU measures codon usage bias for each codon family. It is essentially a normalized codon frequency so that the expectation is 1 when there is no codon usage bias. A codon is overused if its RSCU value is greater than 1 and underused if its RSCU value is less than 1. It is computed directly from input sequences. In contrast, the computation of CAI requires a set of known highly expressed genes as a reference.

Relative synonymous codon usage (RSCU)

The general equation for computing RSCU is

$$RSCU_{ij} = \frac{CodFreq_j}{\frac{\left(\sum_{j=1}^{NumCodon_i} CodFreq_i\right)}{NumCodon_i}} \quad \text{.....(5.1)}$$

where i refers to a codon family and j refers to a specific codon within the family. For example, i may refer to the alanine codon family with four codons (GCU, GCC, GCA, and GCG) and j to a specific codon such as GCU. In this case, the numerator is the frequency of GCU and denominator is the summation of the four codon frequencies divided by the number of codons in the codon family, i.e., 4.

For biology students, it is always easier to learn by numerical examples. Suppose we counted the codon frequencies of one particular protein-coding sequence and have obtained the codon frequencies (Table 5-1). The RSCU for the GCU codon is computed, according to equation (5.2), as

$$RSCU_{GCU} = \frac{52}{\frac{(52+91+103+2)}{4}} = 0.84 \quad \text{.....(5.2)}$$

which is displayed in Table 5-1. You should cover up the last column in Table 5-1 and finish the computation of the rest of the RSCU values.

Table 5-1. Data for illustrating the calculation of RSCU. AA-amino acid; N-codon frequency.

Codon	AA	N	RSCU
GCU	Ala	52	0.84
GCC	Ala	91	1.47
GCA	Ala	103	1.66
GCG	Ala	2	0.03
GAA	Glu	78	1.64
GAG	Glu	17	0.36
...	...	...	...

CAI (Sharp and Li 1987; Xia 2007b) is a measure of translation elongation rate, formulated on the basis of our understanding of highly expressed genes. First, highly expressed genes tend to use cheap but abundant amino acids, i.e., you can't mass-produce a protein when its component amino acids are rare and expensive to make). Second, because the tRNA pool in the cytoplasm where translation occurs does not feature different tRNA species in equal amount, highly expressed genes tend to use codons recognized by the most abundant tRNA to code each amino acid. This leads to highly biased codon usage in highly expressed genes, especially in rapidly replicating organisms such as *Escherichia coli* and *Saccharomyces cerevisiae* (Xia 1998a). CAI is computed with a reference set of highly expressed genes. We will study CAI in more detail and learn its formulation in one of the future lectures.

The maximum CAI is 1 and the minimum is 0. In general, the higher the CAI value, the more efficient the mRNA can be translated. Viruses that cause acute diseases, such as influenza A viruses (which is also single-stranded RNA viruses with a high mutation rate), often replicate fast and need to translate their mRNAs efficiently, especially those coding mass produced structural proteins. In contrast, viruses that replicate and kill host cells slowly and cause chronic disease tend to have their genes with smaller CAI values.

CAI is known to be an excellent predictor of gene expression in prokaryotes and unicellular eukaryotes. Caveats in computing CAI, factors affecting CAI, and correct interpretation of CAI output have been reviewed in detail (Xia 2007a, Chapter 9). The implementation of CAI in DAMBE avoids most of the problems shared in other computer programs computing CAI (Xia 2007b).

While RSCU characterizes codon usage bias in each codon family, CAI quantifies the codon usage bias in one gene. It is based on (1) the codon frequencies of the gene and (2) the codon frequencies of a set of known highly expressed genes. I will illustrate its computation with the data in Table 5-2. The last column in Table 5-2, headed by w, is the weight factor and computed according to the following equation:

$$w_{ij} = \frac{RefCodFreq_{ij}}{RefCodFreq_{i.\max}} \quad \text{.....(5.3)}$$

For example, the first value, 0.375, for codon UGA is obtained by simply dividing the RefCodFreq for UGA (i.e., 6) by the maximum RefCodFreq in the stop codon family (i.e., 16). You should cover up the last column and compute the rest of the w values based on the data in the RefCodFreq column in Table 5-2.

With the w values, we can now compute the CAI value of any protein-coding sequence. Table 5-2 displays the codon frequency of one particular protein-coding gene. Its CAI value can be obtained by the following equation:

$$CAI = e^{\left(\frac{\sum_{i=1}^{n}[CodFreq_i \ln(w_i)]}{\sum_{i=1}^{n} CodFreq_i}\right)} \quad \text{.....(5.4)}$$

$$= e^{\left(\frac{1\times\ln(0.606)+15\times\ln(1)+8\times\ln(0.752)+...}{1+15+8+...}\right)}$$

where n is the number of sense codons (excluding codon families with a single codon, e.g., AUG for methionine and UGG for tryptophan in the standard genetic code). It is important to exclude codon families with a single codon. Note that for such codons (e.g., AUG and UGG in the standard genetic code), their corresponding w_{ij} value will always be 1 regardless of codon usage bias of the gene. If a gene happens to use a high proportion of methionine and tryptophan, then it will have a high CAI value even if the codon usage is not at all biased. The CAI program in EMBOSS (Rice, et al. 2000) does not exclude codon families with a single codon. One should be cautious in interpreting results from such programs.

Table 5-2. Data for illustrating the computation of CAI. AA-one-letter notation of amino acid; CodFreq-codon frequency of the gene whose CAI is to be computed; RefCodFreq-codon frequency of the reference set of genes known to be highly expressed; w-the weight factor computed from RefCodFreq.

Codon	AA	CodFreq	RefCodFreq	W
UGA	*	0	6	0.375
UAG	*	0	4	0.250
UAA	*	0	16	1.000
GCA	A	1	195	0.606
GCU	A	15	322	1.000
GCG	A	0	81	0.252
GCC	A	8	242	0.752
UGC	C	3	123	1.000
UGU	C	3	112	0.911
GAU	D	9	69	1.000
GAC	D	11	40	0.580
GAG	E	11	289	0.863
GAA	E	14	335	1.000
UUU	F	3	118	0.554
UUC	F	9	213	1.000
…	…	…		…

Note that the exponent is simply a weighted average of ln(w). Because the maximum of w is 1, ln(w) will never be greater than 0. Consequently, the exponent will never be greater than 0. Thus, the maximum CAI value is 1. The minimum CAI depends on the smallest w in each codon family. If the smallest w in each codon family is very close to zero, then the minimum CAI will also be very close to zero (when a gene happen to use the rarest codon to code its amino acids).

To eliminate or alleviate the problems above, a new implementation of CAI has been published (Xia 2007b). However, there is still another problem with computing CAI, in particular, it does not take into account the background mutation bias. An improved Index of Translation Elongation (I_{TE}) has been developed recently and implemented in the latest version of DAMBE (Xia 2015).

One may wonder where the reference set of highly expressed genes comes from. Early reference sets of genes include known highly expressed genes such as ribosomal proteins. The first large-scale compilation is derived from TransTerm (Brown, et al. 1994; Dalphin, et al. 1996), which also outputs CAI values for genes from species with a reference set of highly expressed genes. Such genes, together with associated parameters such as CAI, are compiled for each species in a file named ****.dat, where '****' is usually a four letter code made from the organism's genus and species. For example, the codon usage table for Homo sapiens is Hsap.dat. The subset of genes with the highest CAI values are found in the file named ****_H.dat. TransTerm also outputs these files in GCG format (Dalphin, et al. 1996), named as ****.cod. Note that gene sequences in the ****_H.dat files are not necessarily highly expressed genes because their expression is not verified by gene expression studies.

These ****.dat files can be formatted as codon frequency tables that can be used as the reference set of genes for computing CAI values. The first large-scale distribution of the reformatted codon frequency tables came with the release of EMBOSS (Rice, et al. 2000). The EMBOSS-reformatted codon frequency tables are stored in files

named E*.cut where the prefix E is presumably for EMBOSS and the file type 'cut' is for codon usage table. The * part in the file is typically a species designation, but unfortunately is not standardized. Because EMBOSS is open-source, and consequently because everybody can contribute to it with little restriction, there was an undesirable proliferation of E*.cut files. For example, you will find Ehum.cut, Ehuman.cut, Eco.cut, Eeco_h.cut, Eecoli, Emus.cut, etc. In some cases, the species is easy to tell. For example, the first two file names in the previous sentence refer to human, the next three refer to *Escherichia coli*, with the middle one referring to highly expressed *E. coli* genes (i.e., from genes with high CAI values, not from genes experimentally verified to be highly expressed), and the last refers to Mus musculus. Names ending with cp refer to chloroplast genes. For example, Emzecp.cut is from maize chloroplast genes. File names ending with mt are from mitochondrial genes. For example, Eyscmt.cut is derived from the yeast (*Saccharomyces cerevisiae*) mitochondrial genes.

There are two major problems with the EMBOSS compilation of reference genes. First, the nonstandard species designation, coupled with a lack of documentation typically associated with open-source software, has led to a profound confusion as to which file refers to which species. Second, the reference set of genes are supposed to be highly expressed, but it is difficult to define highly expressed genes in multicellular eukaryotes because a gene may be highly expressed only in a certain tissue at a certain time. For these reasons, my laboratory has initiated a large-scale compilation of tRNA anticodons for each species and uses the frequencies of the cognate codons as a reference to compute CAI values. This is based on the rationale that a gene with its codon usage maximizing the use of the most abundant cognate tRNA must be a highly expressed gene (Ikemura 1981b; Gouy and Gautier 1982; Xia 1998a).

You may have already noted that, in contrast to RSCU which is codon-specific, CAI is gene-specific. It makes no sense to say that a hemoglobin gene has a RSCU value of 2, neither does it make sense to say that a codon (e.g., GCU) has a CAI value of 0.8.

Codon usage bias and tRNA abundance

The tRNA sequences are essential in the translation hypothesis. Each tRNA can be viewed as an adaptor with one end attached to an amino acid and the other end matching the cognate codon. The latter is called the anticodon loop.

The anticodon in almost all tRNA sequences from all species share the regular feature of being flanked by two nucleotides on either side to form a loop that is held together by a stem. For example, the anticodon loop (AC loop) of tRNA-Ala in M. musculus is 24AUUGAUUUGCAUUCAAU40 where the starting and ending numbers indicate the position of the AC loop in the tRNA sequence (numbered from 1), with the anticodon (5'-UGC-3') flanked by two nucleotides on either side (bolded) to form a loop that is held together by a stem made of the first and the last four nucleotides. Such a regular AC loop and its anticodon can be easily identified by dynamic programming. A few tRNA sequences have an anticodon flanked by three nucleotides, e.g., tRNA-Val in Erpetoichthys calabaricus and tRNA-Ser1 in the blue whale, Balaenoptera musculus. Some tRNA sequences have a suspicious AC loop. For example, the AC loop of tRNA-Trp is 26GAGCCUUCAAAGCCC42 with a stem that has a mismatch. For such tRNA sequences with an irregular AC loop, DAMBE will flag them out and we will need to check the sequence manually.

Different tRNA species do not exist in the same amount. Some amino acids have many tRNA species, while others have few, carrying them. Within the same codon family, e.g., the glycine codon family GGN, some codons are recognized by more codons than others. In *E. coli*, GGC and GGU have more tRNAs to translate them than GGA and GGG. For this reason, highly expressed *E. coli* genes code almost all glycine residues by GGC and GGU codons. This increases the rate of translation (Xia 1998a, 2005; Carullo and Xia 2008; Xia 2008).

How would we know the relative abundance of different tRNA species? Fortunately for us, there is a high correlation between relative tRNA abundance and the copy number of tRNA genes in the genome of prokaryotic species and unicellular eukaryotes (Ikemura 1992; Percudani, et al. 1997; Kanaya, et al. 1999; Duret 2000). So we will use the copy number of tRNA genes in the genome as an index of relative tRNA abundance.

In this lab, we will work on *E. coli* genome. All tRNA genes will be extracted and the anticodon identified by DAMBE. You will look at the output to find cases where DAMBE may fail to identify the correct codon and manually identify the anticodon. You may have computed CAI before, but the information on tRNA genes will greatly enhance our understanding of CAI and codon usage.

OBJECTIVES

Use RSCU and CAI to characterize codon usage

RSCU is a codon-specific index for codon usage, whereas CAI is a gene-specific index for codon usage. Both are related to gene expression, especially in prokaryotes and unicellular eukaryotes.

Understand the relationship between tRNA abundance and codon usage

Through a detailed study of tRNA genes in *E. coli* genome, you will develop a good understanding of the relationship between relative tRNA abundance and codon usage bias.

PROCEDURES

Computing CAI and RSCU

Read into DAMBE the *E. coli* CDS sequences saved in a previous laboratory. If you did not have a saved file containing *E. coli* CDS sequences, then download the E coli K12 genome in GenBank format by using Entrez, and save to file EcoliK12.gbk. Start DAMBE, and click 'File|Open standard sequence file'. In the 'File of type' dropdown listbox, choose 'GenBank file' format. Choose the saved *E. coli* file (EcoliK12.gbk) and click the 'Open' button. Choose CDS and click 'OK'. Save the file to your personal directory in FASTA format.

Calculate CAI: Click 'Seq.Analysis|Codon usage|Codon adaptation index (CAI). A dialog box will be displayed for you to choose options (Fig. 5-1). The upper panel should display two listboxes with the left showing sequences available for analysis and the right showing sequences selected to compute CAI. You may choose one or a subset of sequences and click the '-->' button. In our case, we will compute CAI for all CDSs, so click the 'Add all' button to move all sequences to the right. Leave the 'Detailed output' checkbox unchecked (otherwise it will produce too much output). In 'Choose a species' dropdown box, choose 'Escherichia coli K12 (high) which will use the highly expressed *E. coli* genes as the reference set. The same reference set of genes can also be used for any *E. coli* or *Shigella* strains because what is highly expressed in *E. coli* K12 is also almost always highly expressed in similar strains.

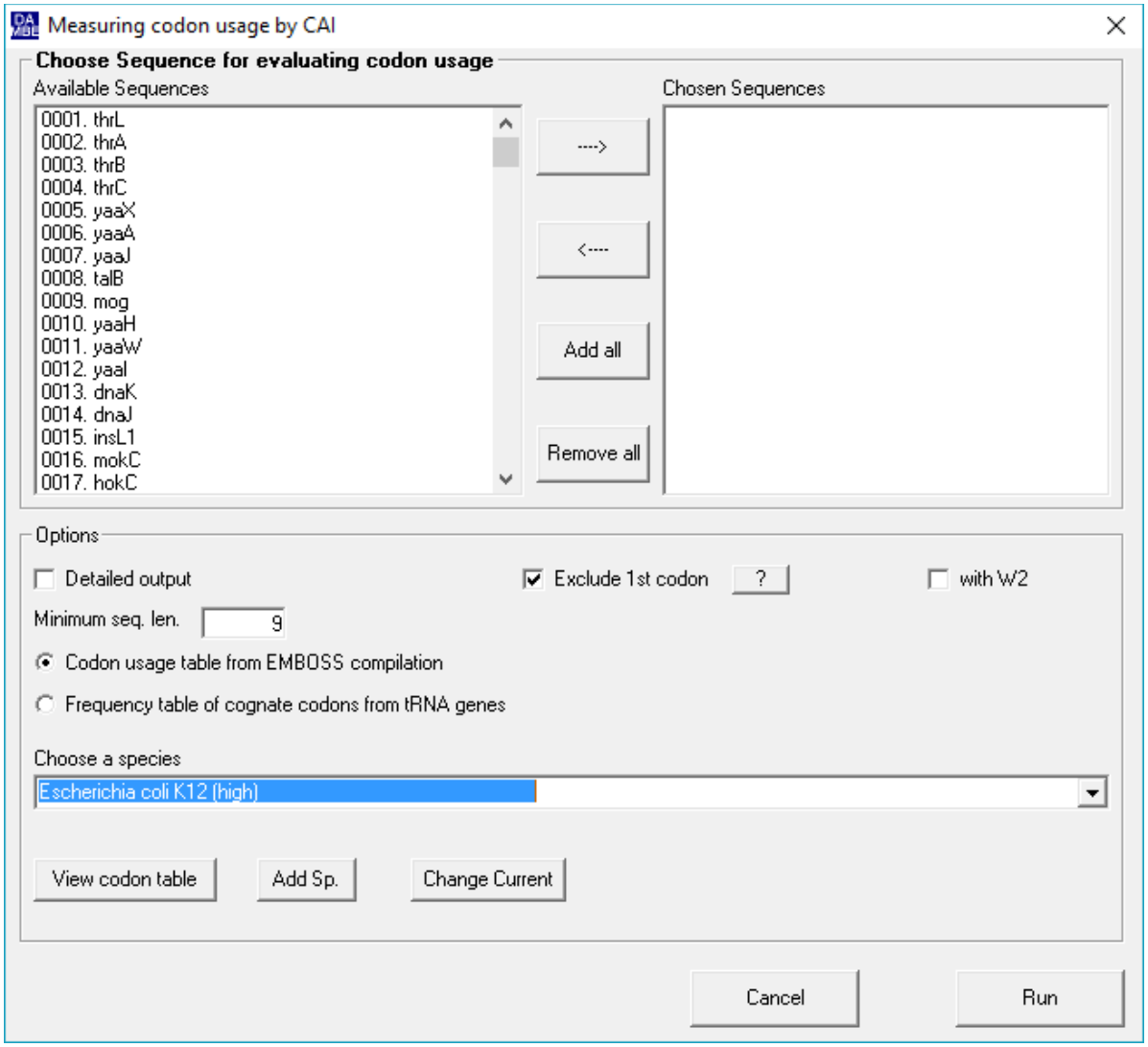

Fig. 5-1. Dialog box for computing codon adaptation index (CAI). The first codon is typically excluded, especially for prokaryotes, because a start codon could be AUG, GUG, UUG or even CUG and may be mistranslated.

The number of species in the dropdown box is quite limited because only a small number of extensively studied species have a set of highly expressed genes. Some bacterial species cannot even be cultured, so there is no way to find out what genes are highly expressed in their cells. For such species, it is impossible to compute the conventional CAI. An alternative is available for those with genomic sequences available. One could extract all tRNAs and identify all anticodons, and then use codons forming Watson-Crick base pairing with the anticodons as a reference set. This alternative is provided through the option button labeled 'Frequency table of cognate codons from tRNA genes' and detailed in my book (Xia 2007a, Chapter 9). However, we will not use this alternative in this laboratory.

Three buttons, labeled 'View codon table ', 'Add Sp.' and 'Change Current', are for viewing the codon usage of highly expressed genes, add a new species with a known set of highly expressed reference genes, and change the reference gene set for the currently selected species, respectively. Some species have multiple sets of highly expressed reference genes compiled by different researchers from different data sources. Different reference sets will generate somewhat different CAI values, but the relative magnitude of CAI should stay the same.

If you click the 'View codon table' button when Eeco_h is selected in the 'Choose species' dropdown box, the codon usage data for the highly expressed reference gene set will be displayed (Fig. 5-2). You will notice that the TAA stop codon is used much more frequently in highly expressed genes than the other two stop codons (TAG and TGA). You will also note that nucleotide frequencies at the third codon position are often not a good predictor of the codon usage bias. For example, C-ending codon is the rarest in the alanine codon family, but the several two-fold codon families (Fig. 5-2). You may not need to tough the 'Add sp' button or the 'Change current'

button until you begin your own research and find your species is either not listed in the dropdown box or listed with a rather unrepresentative reference set. In that case, you may compile your own reference set of highly expressed genes so that you can compute CAI with your own reference set of highly expressed genes.

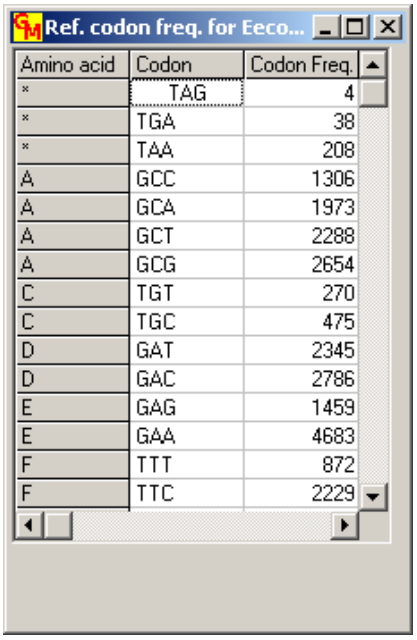

Amino acid	Codon	Codon Freq.
*	TAG	4
*	TGA	38
*	TAA	208
A	GCC	1306
A	GCA	1973
A	GCT	2288
A	GCG	2654
C	TGT	270
C	TGC	475
D	GAT	2345
D	GAC	2786
E	GAG	1459
E	GAA	4683
F	TTT	872
F	TTC	2229

Fig. 5-2. The reference set of highly expressed genes in *Escherichia coli* (Some genes in the reference may be replaced by others leading to differences in the actual numbers.

Now that we have gotten thoroughly familiar with the dialog box in Fig. 5-1, click the 'Run' button. The CAI value will be computed for each gene and displayed in the format in Table 5-3. In addition to the conventional CAI, the slight modification, designated CAI2, is also displayed (Table 5-3). CAI2 is defined as

$$\frac{\sum_{i=1}^{n}[CodFreq_i w_i)]}{\sum_{i=1}^{n} CodFreq_i} \qquad (5.5)$$

which avoids the problem associated with $w_i = 0$. You may ignore it in this lab.

Which three genes have the highest CAI values? Which three the lowest? What are the main differences in codon usage between those with high CAI values and those with low CAI values? To address these questions, you should first sort the genes by CAI values. We will do this in EXCEL and take this opportunity to learn how to get data in DAMBE's display to EXCEL sheet. (Note that CAI is computed with a set of genes known to be highly expressed. Changing this reference set of genes could also change the CAI values. DAMBE will generally use the most accurate compilation of highly expressed genes and the CAI values you have may not be the same as shown here.)

When the CAI is displayed, highlight the output table (Fig. 5-3). Click 'Edit|Copy to EXCEL'. Now launch EXCEL, click a cell and click the 'Paste' button (or just press Ctrl-V). The table will be copied into EXCEL is four columns. Now highlight all the data and click 'Data|Sort' in EXCEL to sort the data by CAI.

Table 5-3. Output of CAI for each gene. You may ignore CAI2.

SeqName	SeqLen	CAI	CAI2
thrA	2463	0.55097	0.70581
thrB	933	0.53635	0.70278
thrC	1287	0.60688	0.73973
yaaX	297	0.47696	0.66049
yaaA	777	0.53883	0.68732
yaaJ	1431	0.48754	0.66228

talB	954	0.75838	0.83941
mog	588	0.58178	0.72263
…	…	…	…

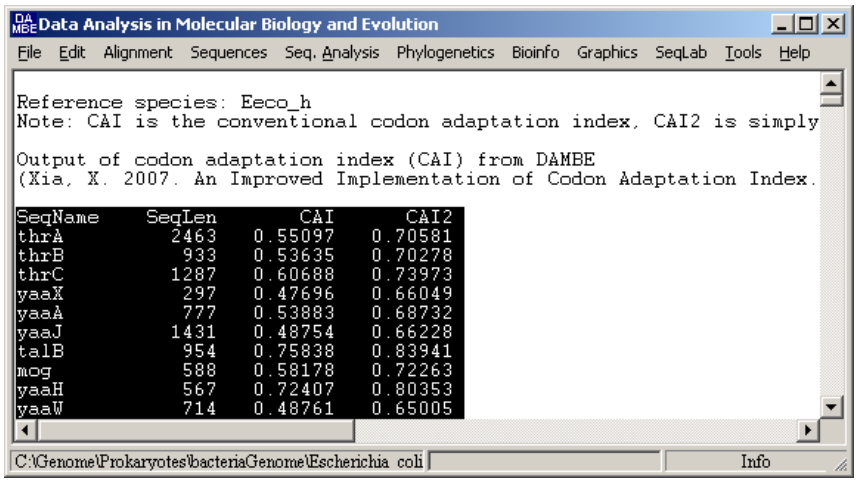

Fig. 5-3. Transfer tables from DAMBE to EXCEL.

Some genes are very short with few codons. Avoid such genes because they may not be true genes. Even if they are, the few codons they contain may not reveal any clear patterns. Instead, find three high-CAI genes and three low-CAI genes with sequence length at least 500 bases long. Click 'File|Save a subset of sequences' to save these six genes with extreme CAI values in FASTA format. These genes will be used to practice the computation of RSCU.

Calculate RSCU: We want to obtain pooled RSCU for the three high-CAI genes and that for the three low-CAI genes and compare their differences. Our prediction is that highly expressed genes should maximize, within each codon family, the usage of codons efficiently translated by tRNAs and minimize the usage of codons that have few tRNAs to translate them. For this reason, they should have more biased codon usage with RSCU deviating substantially from 1, than lowly expressed genes with RSCU staying relatively closer to 1. Will this prediction be supported?

Click 'File|Read standard sequence file' to read the FASTA file containing the six genes with extreme CAI values. Click 'Seq.Analysis|Codon usage|RSCU'. Click the three high-CAI genes to the right listbox, and then click the 'Run' button. When the results are displayed, copy and paste the table into another EXCEL sheet. Do the same for the three low-CAI genes. Table 5-4 shows the results ready for comparison.

Table 5-4. Contrast of RSCU between genes with high CAI value (RSCU_H) and genes with low-CAI value (RSCU_L).

Codon	AA	ObsFreq	RSCU_H	Codon	AA	ObsFreq	RSCU_L
UGA	*	0	0	UGA	*	1	1
UAG	*	0	0	UAG	*	0	0
UAA	*	3	3	UAA	*	2	2
GCU	A	72	2.549	GCU	A	22	1.419
GCG	A	14	0.496	GCG	A	9	0.581
GCC	A	5	0.177	GCC	A	7	0.452
GCA	A	22	0.779	GCA	A	24	1.548
…	.	..	…	…	.	..	….

Examine the output for the six genes. With the alanine codon family shown in Table 5-4, we see that genes with high-CAI have more biased codon usage with highest RSCU being 2.549 for the GCU codon and the lowest being only 0.177 for the GCC codon. In contrast, for the low-CAI genes, the highest and lowest RSCU is 1.419 and 0.452, spanning a much smaller range.

What can you infer about the tRNA carrying alanine? There could be $tRNA^{Ala/AGC}$, $tRNA^{Ala/CGC}$, $tRNA^{Ala/GGC}$, and $tRNA^{Ala/UGC}$ in the *E. coli* genome. Which $tRNA^{Ala}$ species is likely to be the most abundant in *E. coli* cell? Given that GCU is the most frequently used codon, we may predict that $tRNA^{Ala/AGC}$ may be the most abundant. How can we test this prediction? It would be nice if we could quantify the abundance of the four $tRNA^{Ala}$ species. Unfortunately this is extremely tedious experimentally. One alternative is based on the observation that tRNA abundance is highly correlated with the copy number of tRNA genes. So we may predict that the $tRNA^{Ala/AGC}$ gene not only should be present in the *E. coli* genome, but also have more copies than other $tRNA^{Ala}$ species.

An alternative hypothesis, termed wobble versatility hypothesis (Carullo and Xia 2008; Xia 2008; Xia 2013c), makes predictions differently concerning the tRNA anticodon, based on the assumption that the tRNA anticodon should maximize its wobble capacity. For four-fold degenerate codon families such as the alanine codon family, it predicts that there should be $tRNA^{Ala/GGC}$ translating GCC and GCU codons and $tRNA^{Ala/UGC}$ translating GCA and GCG codons. Testing these different hypotheses and their predictions obviously would require us to extract tRNA genes from the *E. coli* genome and identify the anticodons. We will learn these techniques in the next section.

The alanine codon family is consistent with our prediction that highly expressed genes should exhibit more codon usage bias than lowly expressed genes. Is this pattern generally true for other codon families? Fig. 5-4 plots the RSCU for the high-CAI genes (RSCU_H) and the low-CAI genes (RSCU_L) versus the 64 codons. It is quite clear that high-CAI genes (representing highly expressed genes) have RSCU values deviating much more from 1 than the low-CAI genes (representing lowly expressed genes). We conclude that highly expressed genes are under strong selection to maximize translation efficiency and accuracy which has driven their evolution towards optimizing their codon usage. In contrast, such selection should be weak for lowly expressed genes whose codon usage may largely depend on mutation bias.

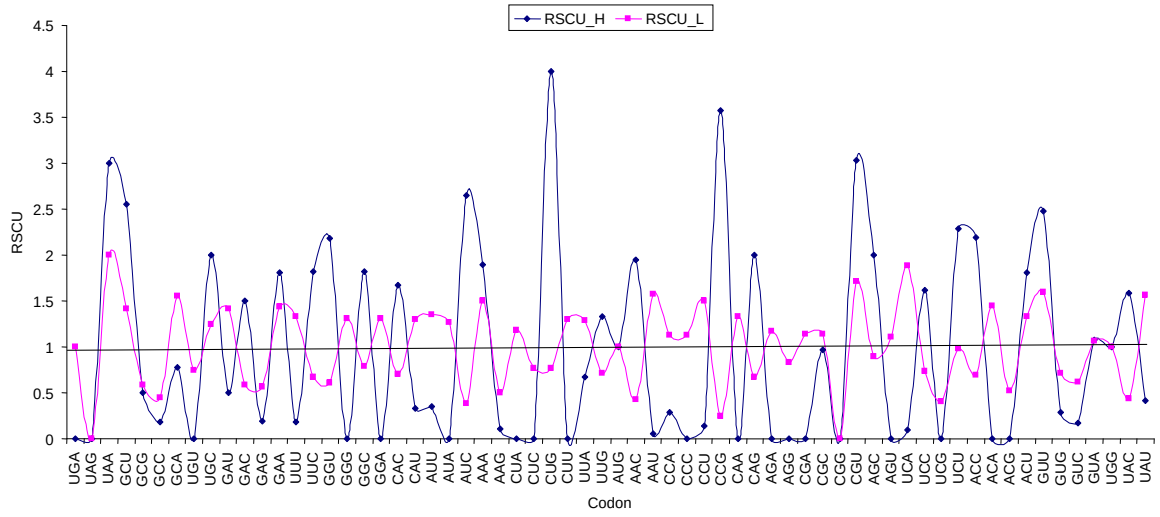

Fig. 5-4. RSCU for high-CAI and low-CAI genes (RSCU_H and RSCU_L, respectively), plotted over the 64 codons.

Identifying tRNA anticodon

Extract and save tRNA sequences: (If you have not done so already) Download the *E. coli* K12 substr. MG1655 genomic sequence (RefSeq: NC_000913) by using Entrez. Save the file to EcoliK12.gbk in your local directory.

Read EcoliK12.gbk into DAMBE by clicking 'File|Open standard sequence file'. In the 'File of type' dropdown listbox, choose GenBank file format. In the ensuing dialog box prompting you what to extract, choose tRNA. In 'Sequence ID options', you should choose '/gene' or '/product'. These two contains information on what amino acid the tRNA is carrying. For example, choosing '/gene' will lead to sequence ID such as alaX, and alaW for two $tRNA^{Ala}$ genes that may have the same sequence but are located in different sites of the genome. If you choose '/product' as sequence ID, then the corresponding sequence name will both be 'tRNA-Ala' which is longer but less informative than alaX and alaW. If DAMBE subsequently identified these tRNAs as carrying a different amino acid, then it is your job to investigate whether DAMBE is correct or GenBank annotation correct by folding the tRNA sequences to identify the anticodon loop.

In the ensuing dialog box asking you to specify the sequence type, choose 'Non-protein-coding'. When the sequences are displayed, click 'File|Save or convert sequences' to save the tRNA sequences to a file named EcoliK12tRNA.fas.

Note that *E. coli* K12 contains six identical $tRNA^{Lys}$ genes and four identical $tRNA^{Asn}$ genes. We will have a closer look at the effect of these tRNA genes on codon usage bias.

Identify tRNA anticodon by using DAMBE: Click 'Seq.Analysis|tRNA anticodon and AC loop'. You will be asked for a temperature because RNA fold differently in different temperature. For mammalian species or their parasites and commensals, input 37 (degrees Celcius) which is the default. For avian species and their parasites/commensals, enter 39. For poikilotherms, a 20 is perhaps a good guess. Click the Yes button to run. Examine the output. Are all tRNA anticodons identified correctly? How would you know if they are identified correctly? Note that DAMBE's identification is based on the sequence only, whereas the GenBank identification is based on much more information. So any discrepancy between DAMBE and GenBank can be assumed to be a misidentification by DAMBE.

It is important for you to check the result and to learn how to manually identify the AC loop and anticodon. Suppose a $tRNA^{Val}$ gene has the same sequence

GGGUGAUUAGCUCAGCUGGGAGAGCACCUCCCUUACAAGGAGGGGGUCGGCGGUUCGAUCCC
GUCAUCACCCACCA

The anticodon is typically near the middle of the sequence, and should be flanked by two nucleotides on either side to form an anticodon loop held together by a stem (Fig. 5-5). If we know that the amino acid carried by the tRNA, then it is easy to identify the anticodon. For example, valine is coded by GUN, so the anticodon of $tRNA^{Val}$ should be NAC. There are only two NAC's in the sequence, but only the second one follows the anticodon loop structure, i.e., **CCUCC**CU**UAC**AA**GGAGG**. Note that anticodons tend to be flanked by two pyrimidines (e.g., CU) on the 5' side and two purines (e.g., AA) on the 3' side. The seven nucleotide anticodon loop is held by a stem formed by base-pairing between CCUCC and GGAGG. DAMBE is supposed to infer the anticodon from the sequence only, so any five-nucleotide loop held together by a stem, located somewhere near the center of the sequence, may be taken as a putative anticodon loop. Do the same manual identification for other tRNA sequences that might have a misidentified anticodon loop.

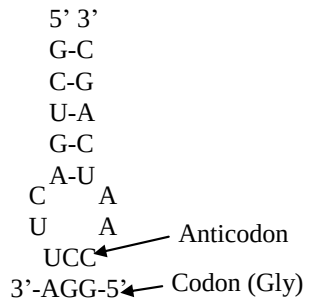

Fig. 5-5. Anticodon loop of $tRNA^{Gly/UCC}$.

Note that *E. coli* K12 contains six identical $tRNA^{Lys}$ genes with anticodon UUU forming Watson-Crick base-pair with the AAA codon. Lysine is coded by a two-fold codon family with AAA and AAG codons. Given that all $tRNA^{Lys}$ genes have the anticodon pairing with the AAA codon, we should expect AAA codon to be used more frequently than AAG codons. Although the wobble U in the tRNA anticodon can also pair with G in RNA secondary structure, such U/G base-pair is considered energetically less favorable than U/A pair, i.e., we should expect the AAA codon to be used more often to code lysine than the AAG codon. Check your RSCU results for the high-CAI genes to see if this is true. If the AAG codon is used just as frequently as the AAA codon, then our assumption that U/A is energetically more favorable than U/G pair may be wrong.

Also note that *E. coli* K12 has four identical $tRNA^{Asn}$ genes all with anticodon GUU forming Watson-Crick base-pair with AAC codons. Asparagine is coded by a two-fold codon family with AAC and AAU codons. Given that all $tRNA^{Asn}$ genes have the anticodon pairing with the AAC codon, we should expect AAC codon to be used more frequently than AAU codons. Although the wobble G in the anticodon can pair with both C and U in RNA secondary structure, such U/G base-pair is considered energetically less favorable than U/A pair, i.e., we should expect the AAC codon to be used more often to codon lysine than the AAU codon. Check your RSCU

results for the high-CAI genes to see if this is true. If the AAG codon is used just as frequently as the AAA codon, then our assumption that U/A is energetically more favorable than U/G pair may be wrong.

Look at other tRNAs and other codon families and find exceptions to this rule of codon-anticodon adaptation. Discuss with each other, or ask me or a TA, to find answers to such exceptions. Remember that a good scientist can explain all the commonly observed phenomena in his field, but only a great scientist can also explain rare and exceptional phenomena.

MORE QUESTIONS

1. Someone states that the pig hemoglobin gene has a RSCU value of 2. Does it make sense to you?
2. Someone states that the GGA codon of the pig hemoglobin gene has a CAI value of 0.75. Does it make sense?
3. What is the maximum value for RSCU?
4. What is the maximum value for CAI?
5. A researcher wants to use CAI as a measure of the elongation efficiency of protein-coding genes in phage lambda parasitizing *E. coli* cells. Which species should we use to derive the reference set of genes?
6. Compare the codon usage between the three genes with the highest CAI values and another three with the lowest CAI values. Highlight the differences you can detect. (For a fair comparison, you should use sequences of similar lengths, e.g., ~1000 nt.)
7. Hand in the tRNA sequences for which DAMBE has misidentified the anticodon, together with the result of your manual identification.
8. What information can we use to infer the tRNA anticodon?
9. Does CAI measure the rate of transcription of protein-coding genes?
10. Is the first codon site of Leu codon CUG a two-fold degenerate site?
11. Why does lysine usage tend to be low in GC-rich genomes relative to AT-rich genomes?
12. Why do transitions occur more frequently than transversions in protein coding genes?
13. Fig. 5-6 below shows the relationship between the CAI and protein production (Ghaemmaghami, et al. 2003) in yeast (*Saccharomyces cerevisiae*) genes. Why don't all genes with high CAI values have high protein production?

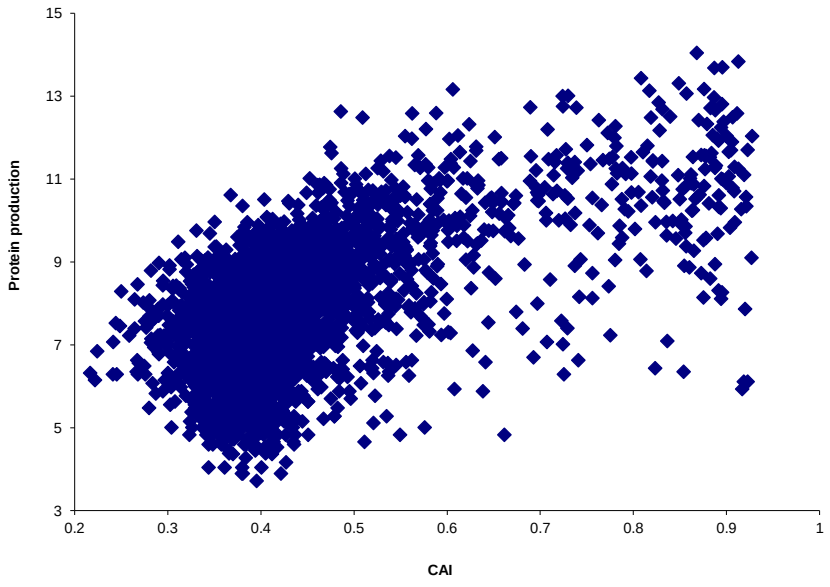

Fig. 5-6. Relationship between CAI and protein production in the yeast.

LAB 6 RNA SECONDARY STRUCTURE, MINIMUM FOLDING ENERGY, AND IRES

INTRODUCTION

Biological functions of nucleotide and protein sequences are often related to their secondary structure. Whether a transcribed 'tRNA' sequence is functional depends on whether it can be folded into proper structure. Different mRNAs have different 5' UTRs that often differ dramatically in their efficiency in loading ribosomes onto the mRNA, leading to different translation initiation efficiency and protein production. This difference is often related to the secondary structure that form at the 5' end of the mRNAs (Zid, et al. 2009). Some genes are transcribed but translated only under special circumstances. For example, some yeast genes are transcribed but only translated under nutrient depletion to help the yeast to find new nutrient sources. This is achieved by their unique secondary structure (or the shared lack of secondary structure) in the 5' UTR or these genes (Gilbert, et al. 2007; Xia and Holcik 2009). As efficient protein production directly affects the profit of biopharmaceutical industry, optimization of the 5' UTR, especially its secondary structure, represents research efforts of many biopharmaceutical industry including the production of vaccines which needs to be produced in large quantity in a short time in response to emerging infective agents such as Influenza viruses. For this reason, characterizing secondary structure is a crucial bioinformatic skill useful in a variety of circumstances.

RNA secondary structure

RNA molecules, e.g., tRNA, rRNA, mRNA, siRNA, snRNA, etc., typically need to fold into secondary and tertiary structures to perform their biological function. The 5' UTR of many mRNA in eukaryotic species or viral pathogens of eukaryotic cells often contain particular sequences that allow translation initiation by internal ribosomal entry without involving cap-dependent scanning mechanism. The sequences in 5' UTR of mRNA that facilitate internal ribosomal entry are known as internal ribosomal entry sites (IRESs). While many viral IRESs are known to contain special secondary structures, many eukaryotic IRESs are devoid of secondary structure.

The secondary structure of RNA molecules are formed by three kinds of base-paring, G/C, A/U and G/U, with the G/U being the weakest, leading to what is called a stem-loop structure. Functional RNA molecules in bacteria living in hot springs typically have higher percentage of GC and more G/C pairs than RNA in bacterial species living in habitats with a low temperature. This contrast is particularly strong at the stem region, which makes sense because it is mainly the stem that maintains the secondary structure. RNAs from organisms in high temperature also have longer stems than that from organisms in low temperature.

Minimum folding energy (MFE)

The stability of secondary structure formed by an RNA is typically measured by minimum folding energy (MFE), which is expressed as the amount of energy required to break the secondary structure. The more negative MFE is, the more stable the secondary structure.

It is important to keep in mind that the structure of any macromolecule is almost always dynamic instead of static. It is like the walk of a drunkard along a trail, jerking left and right but still is most likely to stay in the middle of the trail. However, the probability that we will actually observe him right in the middle of the road at any particular time point is quite small. Similarly, an RNA molecular will jerk into non-minimum-energy states quite often.

5' UTR secondary structure and translation economy

While the filthy rich can afford a great deal of wasteful expenditure, a pauper would have to economize his budget. The same principle applies to cellular and subcellular systems. For example, a 5' UTR with a strong secondary structure will require eIF-4A or equivalent helicases to unwind such secondary structure. When nutrient is unlimited and ATP is plenty, such ATP-consuming unwinding is not a serious problem. However, when nutrient is limited and ATP is scarce, a 5' UTR with a strong secondary structure would become wasteful.

One can immediately derive a prediction from this hypothesis. That is, when nutrient is limited, mRNAs with increased translation should have 5' UTRs with weak secondary structure, whereas mRNAs with strong secondary structure should exhibit dramatically reduced translation. Zid et al (2009) tested this prediction by using DAMBE to calculate MFE of the 5' UTR of translationally up- and down-regulated mRNA in nutrient limited Drosophila melanogaster. The result strongly supported the prediction. Translation of mRNAs that have

a 5' UTR with a strong secondary structure is dramatically decreased with nutrient limitation, whereas those translationally up-regulated mRNAs almost all have 5' UTR with a weak secondary structure.

Internal ribosomal entry site

A number of genes in eukaryotic genomes are known to be transcribed, properly spliced, but translated only at specific environmental conditions, e.g., nutrient depletion. How is this translational regulation achieved? mRNAs from these genes typically have a long 5' UTR that forms stable secondary structure that prevents the small ribosomal subunit from scanning down to find the initiation AUG, hence blocking the cap-dependent translation. It is inferred that such mRNAs must be translated by internal ribosomal entry, i.e., the small ribosomal subunit would bypass the cap and bind to mRNA downstream of the stable secondary structure (but upstream of the initiation codon).

During the last few years, several papers have been published in Nature and Science proposing the following hypothesis. The ribosomal small subunits are recruited by translation initiation factors binding to 5' UTR. If an RNA sequence forms the secondary/tertiary structure that mimics the structure of translation initiation factors positioned on mRNA, then the RNA secondary/tertiary structure may function in the same way as the translation initiation factors in recruiting the ribosomal complex. Several papers in structural biology presented RNA structures that indeed mimic that of the translation initiation factor complex.

Marilyn Kozak criticized this hypothesis vehemently, claiming that these pretty structural pictures are nothing more than being pretty. She has got a good point, as no one is able to show that RNA sequences forming such structures can actually facilitate internal ribosomal entry.

Over years many so-called internal ribosomal entry sites (IRESs) have been characterized by the experimental setup in Fig. 6-1 (Many use bicistronic sequences but the principle is the same), with the hairpin loop blocking the cap-dependent translation. Various candidate RNA segments have been inserted between the hairpin loop and the initiation AUG. An RNA segment that allows the translation of the downstream coding sequence is then designated as an IRES. IRES activity is characterized by how much protein is produced from the coding sequence.

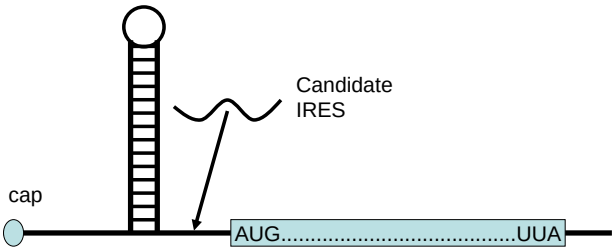

Fig. 6-1. Typical mRNA construct for identifying IRES.

Biologists have always been taught to link structures to functions, but numerous studies have failed to find either sequence similarity or structural similarity among the characterized eukaryotic IRESs. Does this means that RNA structure has nothing to do with IRES activity? Answering this question is your objective in this lab.

OBJECTIVES

(1) Compute MFE for these IRESs and
(2) Check if there is any relationship between MFE and IRES activities.

PROCEDURES

In the course download page at http://dambe.bio.uottawa.ca/teach/bps4104_download/download.aspx, you will find the following files needed for you to accomplish the lab objectives. The data contained in this data have been used in Xia and Holcik (2009) which you should read to gain more background information.

1. ScIRESwithRC.fas: a set of experimentally verified IRES sequences from the yeast, *Saccharomyces cerevisiae*, together with the reverse complements of some of the IRESs, in FASTA format.

2. DmIRES60.fas: a set of experimentally verified IRES sequences from the fruit fly, *Drosophila melanogaster*, together with the reverse complements of some of the IRESs, in FASTA format.

3. IRES.xls: experimentally measured IRES activities for the fruit fly and the yeast sequences in files #1 and #2. The original unit is number of proteins per mRNA.

You access the MFE function in DAMBE by clicking 'Structure|RNA minimum folding energy'. You are on your own to choose the options, but you need to justify what you have chosen in the assignment below. The unit for MFE is KJ/mol.

ASSIGNMENT

Write a mini-manuscript. Outline in the 'Introduction' section the objective of testing if there is any relationship between MFE and IRES activities. The manuscript, including 'Methods', 'Results', 'Discussion' and 'References' sections, should be no more than three pages (single-spaced. The 'References' section will not be counted towards the page limit). You may include tables and graphs which also will not be counted towards the page limit. You may read Xia and Holcik (2009) to gain more background information.

LAB 7 PROTEIN ISOELECTRIC POINT AND ACID-RESISTANCE

INTRODUCTION

Proteins are the workhorses in a living cell. They can perform a variety of tasks because of their diverse properties. Protein isoelectric point (pI) is just one of many properties of proteins. Although we focus on isoelectric point in this laboratory, the same large-scale comparative studies illustrated in this laboratory can be performed on other properties as well.

Protein pI

Protein pI is the pH at which a protein carries no net electric charge. One can infer if a protein carries positive or negative charges given pI of the protein and pH of the solution. The protein would carry a net positive charge if the protein pI is higher than the solution pH, and a negative charge if the protein pI is smaller than the solution pH.

Protein pI determines electrostatic interactions within between protein domains with the same protein, between different proteins, and between proteins and other cellular components. Protein pI also contributes to cellular localization. Proteins binding to RNA and DNA often have a positively charged domain forming nonspecific electrostatic interaction with the negative phosphate backbone of nucleotide acids. This is true for nearly all transcription factors. Positively charged peptides and proteins under physiological pH can be readily taken up by the liver and kidney. Thus, a protein drug intended for liver or kidney diseases should be designed to be positively charged. Positively charged peptides and proteins can also cross the blood-brain barrier by a mechanism related to receptor-mediated transcytosis (Terasaki, et al. 1991; Tamai, et al. 1997). Thus, a protein drug intended for the brain should be positively charged, but should not be taken up or degraded by the liver or the kidney.

The isoelectric point of a protein is determined by its ionizable groups such as carboxyl groups and amino groups. Since the charge of these groups depends on pH, a protein molecule can have different charges according to pH. The pH at which the number of negative charges is the same as the number of positive charges of the protein molecule is the isoelectric point of the protein, i.e., the pH at which the protein carries no net charge. Isoelectric point is typically abbreviated as pI.

A protein will carry positive charges if its pI is greater than its physiological pH, and negative charge is its pI is smaller than its physiological pH. The electrostatic repulsion between proteins is smallest at this point and the solubility is consequently the lowest. Proteins with low solubility may aggregate and precipitate which is often bad for the cell. The 'amyloid precursor protein' causing Alzheimer disease and the prion protein causing the mad cow disease are examples of the undesirable protein aggregation and precipitation.

If an organism has its cellular pH at 7, should its proteins, especially those mass-produced ones, have isoelectric point at 7? What distribution of protein isoelectric points would you expect to find in *Escherichia coli* that live in the intestine with its environmental pH about 8-9? What about Helicobacter pylori which lives in the acidic environment of mammalian stomach?

Acid-resistance in Helicobacter pylori and its protein isoelectric point

Helicobacter pylori (Fig. 7-1) is a human pathogen causing gastric and duodenal ulcers and gastric cancer (Hamajima, et al. 2004; Hunt 2004; Menaker, et al. 2004; Siavoshi, et al. 2004). It is an acid-resistant neutralophile (Scott, et al. 2002) capable of surviving for at least 3 hours at pH 1 with urea (Stingl, et al. 2001) and maintaining a nearly neutral cytoplasmic pH between pH 3.0 and 7.0 (Matin, et al. 1996; Scott, et al. 2002; Stingl, Uhlemann, et al. 2002). These properties allow it to resist the acid shock in human gastric fluid that has a pH averaging about 1.4 over a 24-h period (Sachs, et al. 2003) and infect the gastric mucosa. The buffering action of the gastric epithelium and limited acid diffusion through the gastric mucus was previously thought to protect the bacterium against stomach acidity, but both empirical studies (Allen, et al. 1993) and theoretical modeling (Engel, et al. 1984) have suggested that the protection is rather limited (Matin, et al. 1996). Recently it has also been shown that mucus does not hinder proton diffusion and a trans-mucus pH gradient is abolished when the luminal pH drops to < 2.5 (Baumgartner and Montrose 2004). It is therefore necessary for *H. pylori* to have acid acclimation mechanisms to colonize the gastric mucosa successfully (Sachs, et al. 2003).

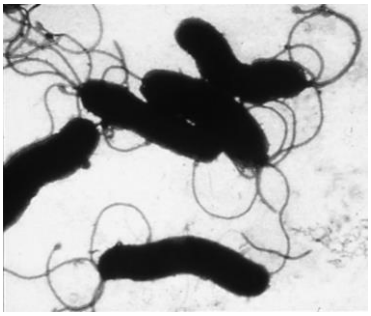

Fig. 7-1. Microscopic image of *H. pylori* (From Paul Stokes Hoffman, University of Virginia).

Two acid-resistance mechanisms in *H. pylori*: *H. pylori* has evolved two mechanisms protecting itself against the acidic environment in the mammalian stomach, schematically illustrated in Fig. 7-2. The first involves the urease gene cluster ureABIEFGH. The constitutively expressed cytoplasmic urease, a heterodimer with its two subunits coded by ureA and ureB, respectively, catalyzes urea to generate $2NH_3 + CO_2$ to buffer against the H+ influx into either the periplasm or the cytoplasm (Mobley, et al. 1991; Rektorschek, et al. 2000; Stingl, Altendorf, et al. 2002; Sachs, et al. 2003) and to facilitate the extrusion of H^+ from the cytoplasm in the form of NH_4^+ (Stingl, Altendorf, et al. 2002). However, urease is an apoenzyme requiring a nickel to be active. The ureEFGH gene cluster, whose expression is acid-induced, codes for nickel-sequestrating proteins that insert nickel into the urease, leading to increased and sustained urease activity (Williams, et al. 1996; Sachs, et al. 2003; Wen, et al. 2003).

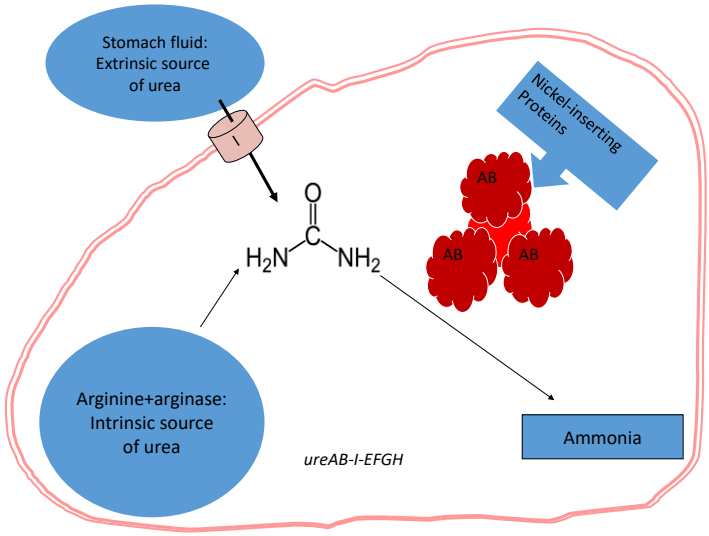

Fig. 7-2. Schematic illustration of the acid-resistance mechanisms in *H. pylori* mediated by genes in the urease gene cluster ureAB-I-EFGH.

The urease, once activated, naturally needs a constant supply of urea as its substrate, and the cell has two sources of urea supply, one intrinsic and one extrinsic (Fig. 7-2). The extrinsic source refers to urea present in saliva and stomach fluid. The exposure to gastric acid results in a large increase in urea influx into the cell due to the pH-gating of the urea channel protein UreI (Weeks, et al. 2000; Bury-Mone, et al. 2001). The intrinsic source comes from efficient conversion of arginine to urea in the cytoplasm by the highly expressed arginase in *H. pylori* (Mendz and Hazell 1996). For this reason, arginine is underused in *H. pylori* proteins and the positively charged membrane in *H. pylori* is mainly maintained by a surplus of positively charged lysine residues (Xia and Palidwor 2005).

The second acid-resistant mechanism in *H. pylori* is the restriction of acute proton entry across its membranes by having a high frequency of positively charged amino acids in the inner and outer membrane proteins (Scott, et al. 1998; Sachs, et al. 2003; Valenzuela, et al. 2003). This is supported by recent discovery of a basic proteome (Tomb, et al. 1997), a set of basic membrane proteins (Baik, et al. 2004) in *H. pylori*, and an extensive genomic analysis (Xia and Palidwor 2005).

Evolutionary hypotheses on the high pI values of *H. pylori* proteins: Given that *H. pylori* has many proteins with high pI values relative other bacterial species that do not live in acidic environment, one is naturally tempted to conclude that the high pI values in the *H. pylori* proteins represent an adaptation to the acidic environment. However, there are at least four possible hypotheses for the origin of the basic proteome in *H. pylori* (Xia 2007a, Chapter 10).

The first hypothesis invokes natural selection and adaptation, i.e., *H. pylori* inhabits the acidic environment in mammalian stomach with a high concentration of H^+ that may get into the cytoplasm and disrupt cellular pH homeostasis. So *H. pylori* needs a lot of positively charged proteins (especially membrane proteins) to alleviate the influx of H^+ into cytoplasm. It is therefore beneficial for the organism to accumulate basic amino acid residues in its proteins, especially in its membrane proteins. This hypothesis is known as the acid-adaptation hypothesis (Xia and Palidwor 2005), i.e., *H. pylori* acquired its high-pI proteins as an adaptation in response to the acidic environment.

The second hypothesis argues that parasitic bacterial genomes typically evolve towards AT-richness because spontaneous mutations are generally AT-biased based on comparisons between pseudogenes and their functional counterparts (Li, et al. 1981; Gojobori, et al. 1982; Li 1983). *H. pylori* has a relatively AT-rich genome, e.g., the genomic GC% of *H. pylori* 26695 is only 38%, in contrast to the genomic GC% of 50% in *E. coli* substr DH10B. This potentially mutation-mediated AT-richness will lead to an increase in A-rich codons such as the lysine codon AAA and AAG (and a consequently increased usage of lysine). The increased lysine usage in proteins then increases protein pI. Because *H. pylori* and its sibling species are all parasites, their most recent common ancestor might have already practiced parasitism and acquired AT-richness and increased frequency of lysine codons before it became a parasite in the mammalian stomach. Therefore, with an overrepresentation of its lysine residues in its proteins, it is already pre-adapted to acidic environment. This hypothesis is termed exaptation hypothesis (Xia and Palidwor 2005), i.e., the process in which an originally neutral trait has subsequently acquired a beneficial function. A well known example of exaptation is the brain-specific RNA gene BC200 resulting from the exaptation of a presumably neutral SINE repeat (Smit 1999).

The third hypothesis states that nucleotide C is rare in mammalian cells and a mammalian parasite should therefore minimize the usage of C as a building block of its RNA and DNA. Minimizing C in an organism with a DNA genome has the necessary consequence of reduced G, with a consequent increase in A and T. This will also contribute to increase AT and increased lysine codon. Thus, originally an adaptation to a C-rare environment predisposed the organism to tolerate an acidic environment. Such a mechanism is called preadaptation in evolution (Xia and Palidwor 2005), i.e., a trait originally selected for one function but that subsequently gained a different function beneficial to the carrier of the trait. An often cited example of preadaptation is the rudimentary feather that presumably has been selected for thermoregulation in nonavian dinosaurs but preadapted their carriers to subsequent evolution of flight.

The fourth hypothesis is more complicated. As mentioned previously, a protein in a solution with a pH equal to the protein pI is not charged. If highly expressed proteins happen to have their pI equal to the cytoplasmic pH, then there is no electrostatic repulsion among these proteins when they are mass-produced. Because the proteins are not charged, their solubility is at the lowest, and they may aggregate and precipitate, which is often harmful to the cell. The 'amyloid precursor protein' causing Alzheimer disease and the prion protein causing the mad cow disease are examples of the undesirable protein aggregation and precipitation. *H. pylori* living in an acidic environment maintains its cytoplasmic pH around 5. This suggests that *H. pylori* proteins should avoid having pI = 5. Avoiding pI = 5 can be achieved by either shifting protein pI much below 5 or much above 5. Shifting below 5 would require a huge amount of glutamic and aspartic acids (and their codons) and is likely difficult to achieve evolutionarily because selection favoring such codons would have to battle against the AT-biased mutation in *H. pylori.* It is easier evolutionarily to evolve protein pI above 5 because of the AT-biased mutation (lysing codon is A-rich and increases with AT-biased mutation).

OBJECTIVES

Compare pI profiles between *Escherichia coli* and *H. pylori*

Proteins have many different properties and isoelectric point is one of them. *E. coli* thrives in a slightly basic environment in mammalian intestine, whereas *H. pylori* is a pathogen inhabiting the strongly acidic environment of mammalian stomach. Characterizing genomic and proteomic differences between different organisms and interpreting the difference with reference to their respective environment belong to the field of comparative and functional genomics/proteomics.

The word 'proteome' has been used in two different meanings: (1) the collection of all protein sequences coded in the genome of an organism, and (2) the collection of all proteins found in a cell type at a specific time. In the first, a proteome is a genomic property and does not change over developmental time or differ among different cell types (unless there are mutations). In contrast, in the second, a proteome is a cellular property and changes over developmental time and typically differ among different cell types. In this laboratory, the word proteome means the genome-encoded proteome.

Learn to appreciate natural selection and adaptation

An evolutionary lineage often has to respond to many different environmental challenges over time. Those that fail to respond effectively will become extinct, and those that do will thrive. Many human bacterial pathogens have evolved to overcome challenges our defense system has imposed upon them, such as iron-binding proteins that leave little free iron for the invading bacteria, antibodies that kill antigen-carrying bacteria, lysozyme in the tear and saliva that damage bacterial cell walls, etc. A very acidic stomach can eliminate a large array of bacterial species that chance to enter our mouth. We will have a glimpse of how *H. pylori* is able to overcome the acidic environment and colonize our stomach.

PROCEDURES

Comparison in pI profile between *E. coli* and *H. pylori*

Download *Escherichia coli* K12 genome and obtain the proteome: Download the *Escherichia coli* K12 genome in GenBank format by using Entrez and save to file EcoliK12.gbk (if you have not done so already).

Start DAMBE, and click 'File|Open standard sequence file'. In the File of type dropdown listbox, choose GenBank file format. Choose the saved *E. coli* file and click the 'Open' button.

Choose CDS and click OK. The translation table for *E. coli* is 11. What is a translation table? What is a genetic code? How many translation tables have been implemented in DAMBE? How many translation tables have been documented by molecular biologists? Why do we need to specify the translation table for computing pI?

Check the initiation codon and the termination codon of some of the sequences. In prokaryotic species, although AUG is the most efficient initiation codon, other codons such as CUG, GUG and UUG are also used as initiation codons. The frequency of those non-AUG initiation codons are used far more frequently in prokaryotes than in eukaryotes. The main reason for the difference between prokaryotes and eukaryotes in initiation codon usage is that the translation machinery in prokaryotes depends mainly on the match between the Shine-Dalgarno (SD) sequence of mRNA and the anti-SD sequence of the small subunit rRNA for localization of the translation initiation site (Shine and Dalgarno 1975). It relies relatively little on the initiation codon itself, with the consequence that the initiation AUG can mutate into other NUG with little deleterious effect. In contrast, the initiation AUG is a key component of the eukaryotic translation initiation signal for localizing the translation initiation site and mutations occurring at the initiation AUG can severely affect the efficiency and accuracy of translation initiation (Kozak 1978; Kozak and Shatkin 1979; Kozak 1986, 1997).

In prokaryotes, CUG, GUG and UUG codons have two meanings. When they are positioned at the beginning of a CDS and used as an initiation codon, they mean methionine. When they occur elsewhere, they assume the conventional meaning according to the genetic code, with CUG and UUG coding for leucine and GUG coding for valine.

Click 'File|Save or convert sequence format' to save the CDS sequences in FASTA format to file EcoliCDS.fas.

Translate all CDS to amino acid sequences by clicking 'Sequences|Work on amino acid sequence'. Click OK. Click 'File|Save or convert sequence format' to save the CDS sequences in FASTA format to file EcoliCDSaa.fas.

Compute pI: Click 'Seq.Analysis|Protein isoelectric point'. In the next dialog box (Figure 3), click the 'Add all' button. Click the 'Run' button. Click the 'Yes' button to graphically visualize the distribution of the pI values. Repeat the steps for the *H. pylori* genome. Record any differences in the isoelectric point profile between *E. coli* and *H. pylori*. What might be the cause for the difference in pI profiles between the two species?

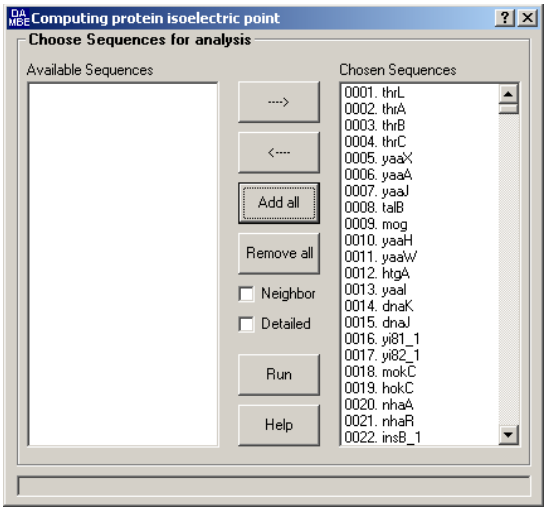

Fig. 7-3. Dialog box for computing protein isoelectric point in DAMBE.

Testing evolutionary hypotheses

A prediction arising from this simple observation is that organisms tend to avoid having proteins, especially those highly expressed ones, with their pI equal to intracellular pH because of the negative (purifying) selection against protein aggregation and precipitation. Because most living organisms have physiological pH nearly neutral, their pI profiles should exhibit a saddle-shaped curve with relatively few proteins at their physiological pH but with a peak at the acidic pH range and another peak at the basic pH range. For *E. coli* living in mammalian intestine where the pH is about 8-9, we should expect relatively few proteins with pI in the range of 8-9. Is this true based on your observation? For *H. pylori* inhabiting the acidic environment in mammalian stomach, the cellular pH can often reach 5, which would lead us to expect *H. pylori* proteins to avoid having pI = 5. Is this what you observed?

E. coli and *H. pylori* differ in many ways each of which could potentially explain the difference in their proteomic pI profile. For this reason, a better comparison is between *H. pylori* and one or more of its close relatives that do not live in acidic environment. One of the close relatives with its genome sequenced is *H. hepaticus* which is a parasite in mammalian liver.

Now go to the NCBI genome database, download the *H. hepaticus* genome, and obtain its proteomic pI profile. If the acidic environment is the sole contributor to the pI profile, then we expect the pI profile of *H. hepaticus* to be similar to that of *E. coli*. However, if phylogenetic relatedness determines the pI profile (i.e., two closely related species share the pI profile because they share a common ancestor and have not yet had time to evolve substantial divergence in pI profile), then the pI profile of *H. hepaticus* should be similar to that of *H. pylori*. What is your conclusion based on comparison of pI profiles among *E. coli*, H. polyri and *H. hepaticus*?

MORE QUESTIONS

1. What amino acids is pI computation based on?
2. What are the possible causes for proteins coded in the *H. pylori* genome to have high pI values relative to those living in an environment with pH ≈ 7?
3. The *H. pylori* genome is AT-rich which might result from AT-biased mutations. Is AT-richness likely to affect pI in *H. pylori* proteins (give reasons)?
4. List two amino acid residues that strongly increase pI and another two that strongly decrease pI.
5. Have you noticed any difference between the *E. coli* pI profile and *H. pylori* pI profile? Can you make sense of the difference?
6. Summarize the differences in pI profiles among *E. coli*, H. polyri and *H. hepaticus*. Do you think that the difference is more attributable to the acidic environment or to the phylogenetic relationship?

LAB 8 SEQUENCE ALIGNMENT

INTRODUCTION

Sequence alignment is essential for molecular phylogenetics and comparative sequence/genome analysis. It serves three purposes. The first is to study functional divergence. Given two homologous genes with their products differing in function, one naturally wishes to know how much of the functional difference can be accounted for at the sequence level. Sequence alignment allows one to quickly identify sequence differences that might lead to functional divergence. The second purpose of sequence alignment is to build phylogenetic trees and to date evolutionary events, e.g., when gene duplication occurred or when human and chimpanzee diverged from each other. The third is to perform phylogeny-based comparative genomic analysis.

Sequence alignment is of two kinds: the local alignment and the global alignment. The local alignment algorithms are used in BLAST and FASTA for homology searches of query sequences against BLAST databases. The global alignment, the subject of this laboratory, is used to align homologous sequences for comparative studies. Although ClustalW (Higgins and Sharp 1988; Thompson, et al. 1994) was once the most frequently used program for multiple sequence alignment, it has almost been entirely replaced by two better alternatives, MAFFT (Katoh, et al. 2005; Katoh, et al. 2009) and MUSCLE (Edgar 2004a). Consequently, I have removed ClustalW from DAMBE but included MAFFT and MUSCLE.

During the evolution of protein-coding genes, an entire codon or multiple codons may be deleted or inserted, but it is much rarer to see an insertion or deletion (often abbreviated as indel) of one or two nucleotides because such indel events lead to frameshifting mutations that almost always disrupt the original protein function and are strongly selected against. However, alignment of protein-coding nucleotide sequences often produce indels of one or two bases as alignment artifacts. For this reason, the alignment of protein-coding nucleotide sequences is typically done in two steps. First, the nucleotide sequences are translated into amino acid sequences. These amino acid sequences are then aligned and the nucleotide sequences are then aligned against the aligned amino acid sequences.

Here is a simple illustration. Suppose we are to align the following two protein-coding sequences designated S1 and S2, respectively:

```
S1 ATG CCG GGA TAA
S2 ATG CCC GGG ATT TAA
```

Step 1: Translate the sequences into amino acid sequences (one-letter notation) to get:

```
S1 MPG*
S2 MPGI*
```

Step 2: Align the amino acid sequences:

```
S1 MPG-*
S2 MPGI*
```

This alignment implies a deletion of an amino acid (and its associated codon) just before the termination codon

Step 3. Align the protein-coding nucleotide sequences against alignment amino acid sequences. This is done by essentially mapping the codon sequences to the alignment amino acid sequences. Keep in mind that a gap in the alignment amino acid sequences correspond to a triplet gap in nucleotide sequences:

```
S1 ATG CCG GGA --- TAA
S2 ATG CCC GGG ATT TAA
   *** **  *** *   ***
```

This alignment, designated Alignment 1, has 10 matches, 2 mismatches, and 1 gap of length 3. Recall that the main objective of sequence alignment is to identify homologous sites and it is important to note that different alignments imply different interpretations of sequence homology. With the alignment above, sites 6 of the two

sequences (G in S1 and C in S2) is interpreted as a homologous site, so is site 9 (A in S1 and G in S2). These interpretations are not established facts. They are only inferences of what might have happened.

Aligning protein-coding nucleotide sequences against aligned amino acid sequences assumes that all sequences are from functional genes. So the minimum requirement for carrying out this procedure is that there is no embedded stop codon in the sequence.

What is the negative aspect of this approach? What would you miss if the frameshifting mutations actually happened and the protein-coding gene is still functional? (Hint: if two homologous protein-coding sequences differ by a frameshifting mutation, then there will always be a fragment of the protein sequences with no meaningful alignment.)

Depending on the scoring scheme, a nucleotide-based sequence alignment, i.e., without using aligned amino acid sequences as a mapping reference, may well generate the following alignment designated Alignment 2, with 12 matches, 0 mismatch and two gaps of lengths 1 and 2, respectively:

```
S1 ATG CC- GGG A-- TAA
S2 ATG CCC GGG ATT TAA
   *** **  *** *   ***
```

Note three different interpretations of the homologous sites between Alignment 1 and Alignment 2. First, the nucleotide G at site 6 of S1 is now interpreted to be homologous to the nucleotide G at site 7 of S2. Second, the nucleotide A at site 9 of S1 is now interpreted as homologous to the nucleotide A at site 10 of S2. Which of the two alignments makes more sense to you? (Hint: Is it likely for a protein-coding gene to remain functional after two consecutive frameshifting indel mutations?)

If Alignment 1 is correct but we used a nucleotide-based alignment method and end up with Alignment 2, then the estimation of the genetic distance between the two sequences will be biased. The genetic distance measures the evolutionary dissimilarity between two sequences, often estimated by ignoring the indel sites. It is an index of the sequence divergence time used frequently in molecular phylogenetics. In this particular case, if we perform site-wise deletion of indels, then S1 and S2 would appear more similar to each other for Alignment 2 than for Alignment 1. Biased estimation of the genetic distance often results in failure in molecular phylogenetic reconstruction (which will be covered in later laboratories).

For sequence alignment involving RNA genes, it is often necessary to incorporate information on the secondary structure to aid the alignment (Xia 2000b; Xia, et al. 2003). However, this is a bit too complicated and will not be practiced in this laboratory.

OBJECTIVES

How to align homologous nucleotide and amino acid sequences

We will use MAFFT and MUSCLE alignment programs included in DAMBE to perform sequence alignment. DAMBE has functions built upon these two programs, such as automatic codon-based alignment. The hands-on experience will enhance our understanding of the alignment algorithms.

Align protein-coding nucleotide sequences against aligned amino acid sequences

Most frameshifting indels in published sequence alignment of protein-coding nucleotide sequences are alignment artifacts. Aligning these nucleotide sequences against aligned amino acid sequences avoid such artificial indels.

A preview of building phylogenetic trees using aligned sequences

Sequences are aligned, in most cases, for the purpose of building phylogenetic trees. We will have a preview of phylogenetic reconstruction, by using distance-based methods, with the sequences we align in this lab.

PROCEDURES

We will use protein-coding sequences, translate the sequences into amino acid sequences and use the nucleotide and amino acid sequences to learn how to perform global sequence alignment. We will also use the same set of sequences to practice alignment of codon sequences which is done in three steps behind the scene: 1) protein-coding sequences are translated in to amino acid sequences, 2) the amino acid sequences are aligned, and 3) the

original codon sequences are aligned against the aligned amino acid sequences. This last function has been implemented in DAMBE since 2000, with detailed description in my first book (Xia 2000a). However, the early alignment functions are not as good as MAFFT (Katoh, et al. 2009) or MUSCLE (Edgar 2004a, b). Current version of DAMBE includes these two alignment programs and uses them for all alignment functions.

Align nucleotide and amino acid sequences

Download and save the http://dambe.bio.uottawa.ca/teach/bps4104_download/RefGag.FAS. Open the file into DAMBE. The sequences in the file are from protein-coding genes of Simian Immunodeficiency Viruses (SIV). What is the genetic code for these protein-coding genes? If you enter a wrong genetic code, then the protein-coding nucleotide sequences will not be translated correctly into amino acid sequences. Protein-coding genes of all mammalian viruses share the same genetic code as the host nuclear genetic code, i.e., the standard genetic code. If you have chosen a wrong genetic code, then the translation may generate wrong amino acid sequences. Similarly, if you clone a vertebrate mitochondrial gene into *E. coli*, the mRNA from the mitochondrial gene will also be translated incorrectly by the *E. coli* translation machinery.

Click 'Alignment|MAFFT'. A dialog box appears (Fig. 8-1) for you to specify alignment options. DAMBE allows you to align a single set of sequences already read into DAMBE, or a large number of sequences sets in multiple files, with each set containing N homologous sequences. Suppose you are working with 50 vertebrate mitochondrial genomes. Each vertebrate mitochondrial genome contains 13 protein-coding genes named COX1, COX2, etc., so you could obtain 13 files named COX1.FAS, COX2.FAST, etc., ..., with each file contain homologous sequences from one gene from 50 vertebrate genomes. DAMBE allows you to input all these 13 files to be aligned in one operation. The first option box is for you to make such a choice of whether to align the sequence already in DAMBE or other sequences separately stored in files. For our practice, we will align the sequences in SIV_Subset.FAS that are already in DAMBE.

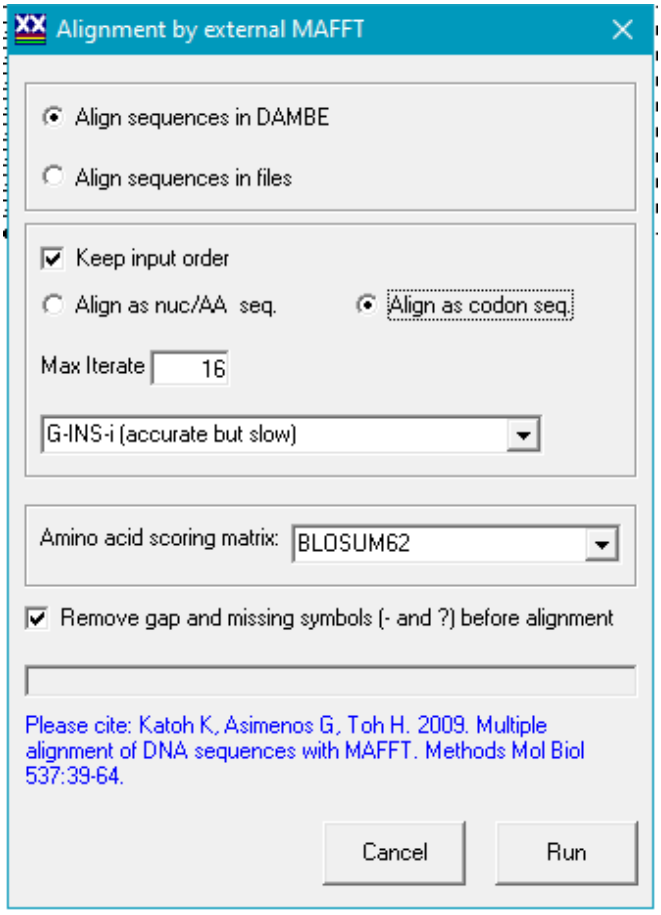

Fig. 8-1. Setting options for sequence alignment in DAMBE.

The 'Keep in order' checkbox, if checked, will keep the aligned sequences in the same order as the input file. If unchecked, closely related sequences tend to be listed next to each other in the final aligned file. This is because the progressive multiple alignment starts from tips of a tree, so closely related species are aligned first.

The 'Align as nuc/AA seq.' and 'Align as codon seq.' radio buttons are all relevant to protein-coding sequences that can be aligned either as nucleotide sequences or as codon sequences. If our input sequences are nucleotide but not protein-coding, then the 'Align as codon seq.' radio button will not be visible. Similarly, if the input sequences are proteins, then the 'Align as codon seq.' radio button will be invisible. We will first align the sequences as nucleotide sequences, so click the radio button 'Align as nuc/AA seq.' You will see why this may not be a good approach for protein-coding sequences.

The 'Max Iterate' option is typical of progressive multiple alignment. A guide tree is first built from pairwise alignment scores, pairwise alignment is then done alone the guide tree to generate a multiple alignment. This multiple alignment is then used to build another tree as a guide tree to generate another, presumably improved alignment. This continues until there is no further improvement or until the maximum number of iterations has been reached. You could increase or decrease the default 16.

A guide tree is necessary to reduce the multiple alignment problem to a pairwise alignment problem. However, this causes the chicken-egg problem in multiple sequence alignment. To obtain a good guide tree, we need to have a good multiple alignment, but to have a good multiple alignment we need to have a good guide tree. The iteration is alleviate this problem so that we will progressively obtain better trees and better alignment.

The next option controls alignment quality. You should always choose the algorithm that is 'accurate but slow' unless you are alignment very long sequences.

The 'Remove gap ...' option is relevant if your input sequences already contain gaps (e.g., if they have been aligned before). For our sequences, it is not relevant because there are no gaps in the sequences.

Click the 'Go' button to align. You will realize that sequence alignment is slow, so be patient. Once the alignment is displayed, have a look at the alignment. You may observe indels (insertions or deletions) of length one or two when your alignment is not based on codons. In our case, the sequence H2B05GHD contains two indel events, one of length one and the other of length two. These frameshifting indels are almost certainly alignment artefacts, because a protein-coding gene hit by frameshifting mutations twice remaining functional is extremely unlikely. In contrast, indels of length three occur frequently, and in most cases do not affect the function of the protein deleteriously. Of course, there are exceptions. For example, about 70% of cystic fibrosis cases are caused by a single deletion of a single codon for phenylalanine at the amino acid site 508.

Save the aligned sequences by clicking 'File|Save or convert sequences'. Use a descriptive file name such as SIV_Subset_MAFFT_nuc.FAS to indicate that the sequences were aligned with MAFFT on nucleotide sequences (not only codon sequences).

Align protein-coding nucleotide sequences against aligned amino acid sequences

In order to avoid introducing indels of length one or two as alignment artefacts, one typically takes an alternative approach to align protein-coding sequences. This is done is three steps. First, one translates the protein-coding nucleotide sequences into amino acid sequences. This is why it is extremely important to specify the genetic code correctly when reading in the sequences. Second, one aligns the amino acid sequences. Third, one maps the protein-coding nucleotide sequences against the aligned amino acid sequences. DAMBE automates these three steps.

We now practice this alternative sequence alignment approach for protein-coding sequences. Read in the SIV_Subset.FAS file into DAMBE. Make sure to specify the genetic code as standard code. Click 'Alignment|MAFFT'. You will again see the dialog box in Fig. 8-1 appears. This time we leave the 'Align as codon' radio botton selected (which is DAMBE default for protein-coding sequences).

The default protein match-mismatch matrix is BLOSUM62. It is compiled from sequences that have about 62% sequence divergence, so it offers a good compromise for sequences with some diverged more than 63% and some less than 62%. There are several other matrices that you can choose from the dropdown list. All of them try to weight amino acid pairs according to the empirical substitution frequencies between amino acids. If you have very similar sequences, you may choose BLOSU80. If you have highly diverged sequences, then choose BLOSOM30. My book (Xia 2020) includes detailed explanation on the derivation of various kinds of match-mismatch matrices. You can download the book for free from our university library.

Click the 'Go' button to align. Once the alignment is done, save the aligned amino acid sequences to a file named SIV_Subset_MAFFT_Codon.FAS to indicate that you have aligned the protein-coding nucleotide sequences by mapping the nucleotide sequences against the aligned amino acid sequences. Note that all indels should now be multiples of three instead of having indel lengths of one or two.

MAFFT and MUSCLE are the two most popular sequence alignment programs currently in use. Just like MAFFT, MUSCLE is also included in DAMBE. You have used MAFFT for sequence alignment, and may repeat the exercise with MUSCLE. When you click 'Alignment', choose MUSCLE instead of MAFFT.

I should emphasize here that occasionally the protein-coding sequences, even functional, may be sequenced poorly and contain frameshifting indels as sequencing artefact. Some sequences may also be pseudogenes that naturally contains frameshifting indels. Before you do codon-based alignment, it is always a good idea to read in the protein-coding sequences, and click 'Sequence|Working on amino acid sequence' to translate the nucleotide sequences into amino acid sequences. Inspect the sequences to make sure that there is not embedded stop codons (which are translated into '*'). You may press CTRL-F and enter '*' (without the quotation marks) to search for the presence of '*'. Its presence in a sequence indicates that the protein-coding sequence is either sequenced poorly or is a pseudogene. In such cases, it is not a good idea to use codon-based alignment. If you do not find any '*' in the sequence, you may then restore the sequences to codon sequences by clicking 'Sequence | Work on codon sequences' and then proceed with the codon-based sequence alignment.

A preview of molecular phylogenetics

The main purpose of sequence alignment is to build phylogenetic tree. Molecular phylogenetics is the topic in the next few lectures, so we will give it a laboratory preview. There are four categories of molecular phylogenetic methods: distance-based, maximum parsimony, maximum likelihood and Bayesian inference. Here we will use only the distance-based method.

Because third codon position in protein-coding genes often evolve so fast that substantial substitution saturation would occur between highly diverged taxonomic groups (Xia, et al. 1996; Xia 1998b), molecular phylogeneticists often believe that amino acid sequences would generate more reliable trees than nucleotide sequences. We will use aligned nucleotide and aligned amino acid sequences to check this belief.

Download the http://dambe.bio.uottawa.ca/teach/bps4104_download/VertCOX2.FAS and save it to your local directory. These are COX2 gene sequences from eight vertebrate mitochondrial sequences. We will align the sequences first as nucleotide sequences, and then as amino acid sequences. We will then use both the aligned nucleotide sequences and aligned amino acid sequences to build phylogenetic trees to see if they differ and which of the two trees makes more sense.

Read the sequences into DAMBE and specify the genetic code as 'VertMtDNA' (the second on the genetic table list). Align it first as nucleotide sequences (not 'Align as codon'), and save the aligned nucleotide sequences to VertCOX2_aln_nuc.FAS file.

Now click 'Sequence | Sequence manipulation'. In the ensuing dialog, click 'All gaps' to delete all gaps in the aligned sequences so that we can translate the sequences to amino acid sequences. Click 'Run'. Once the sequences are displayed, click 'Sequence | Work on amino acid sequence' to translate the sequences into amino acid sequences. Click 'Yes' when asked if all sequences start with a start codon. If you click 'No', then DAMBE will spend extra time judging which of the three possible reading frame is the most likely.

Once sequences are translated into amino acid sequences, perform alignment of the amino acid sequences by using either MAFFT or MUSCLE, and save the sequences to VertCOX2_aln_AA.fas. Now that we have both aligned nucleotide and aligned amino acid sequences, we can make phylogenetic comparisons.

Read in the VertCOX2_aln_nuc.FAS file. Click 'Phylogenetics | Distance methods | Sequences aligned'. The next dialog asks you if you want to use nucleotide-based or codon-based distances. Click 'Yes' to use nucleotide-based distances. The next dialog (Fig. 8-2) shows the options for distance-based phylogenetic methods. For any distance-based method involving nucleotide sequences, one needs to specify (1) the genetic distance to be used and (2) the phylogenetic algorithm that uses the distance matrix to build the tree to facilitate the reproduction of the result. We will use the default MCCompositeTN93 distance the FastME algorithm (Desper and Gascuel 2002, 2004).

There are several options that you can choose for the FastME algorithm. There are three choices you can make with regard to the initial tree option. First, the 'User tree' will ask for a preliminary tree of the species which will be optimized. Second, the 'GME' option stands for a greedy minimum evolution algorithm. It starts with a three-species tree, adds a new taxon to one of the existing branches of the tree and checks which resulting tree has the shortest tree length. The shortest four-species tree is then used to add the fifth species. Third, the 'BME' option stands for balanced minimum evolution. It gives sister subtrees equal weight instead of a weighting scheme proportional to the number of species in the subtree. Other acronyms in the options include NNI (nearest neighbor interchange), and OLS (ordinary least-squares method). You should just leave everything as default. Click the 'Run' button to build the tree.

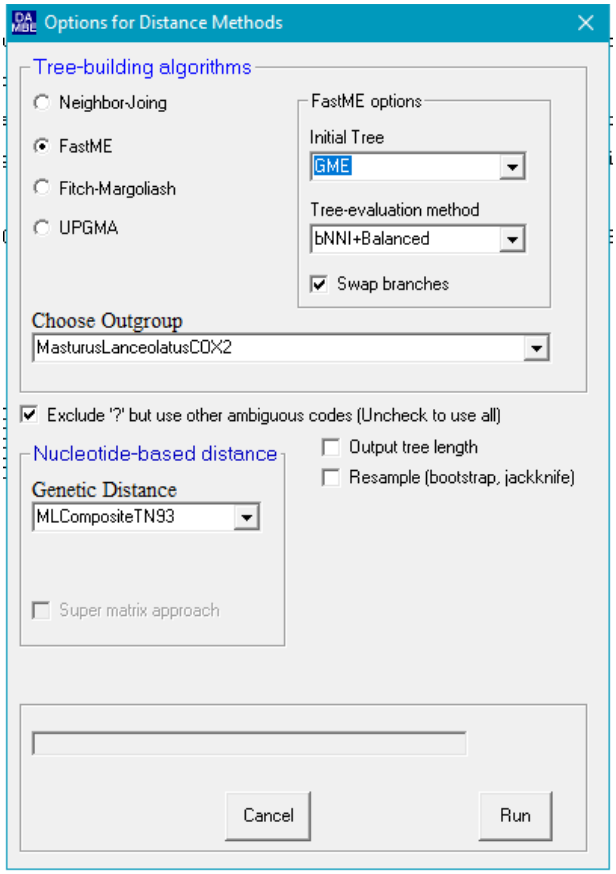

Fig. 8-2. Setting options for distance-based phylogenetic methods in DAMBE.

The correct phylogenetic relationship among the species, based on many genes and many morphological characters and fossil evidence, is shown in Fig. 8-3. Is your distance-based tree, built from aligned nucleotide sequences, the same as that in Fig. 8-3?

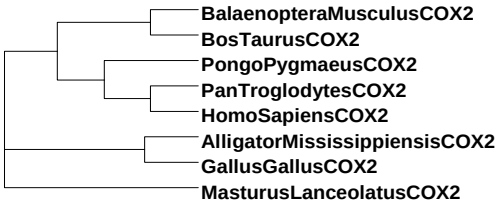

Fig. 8-3. Well-established phylogenetic relationship among eight vertebrate species.

Now repeat the phylogenetic reconstruction with the aligned amino acid sequences in the saved file VertCOX2_aln.AA.FAS. Read the aligned amino acid sequences into DAMBE. Click 'Phylogenetics | Distance methods | Sequences aligned'. As DAMBE already has the information that you are working on aligned amino acid sequences, only genetic distances relevant to amino acid sequences will be shown in the 'Genetic distance' dropdown box. The default genetic distance is 'Poisson P' which you should try first before trying alternative distances. Set the other options as before, i.e., as shown in Fig. 8-2. Click the 'Run' button to build the tree. Is the resulting tree more similar to that in Fig. 8-3 than that from the aligned nucleotide sequences?

MORE QUESTIONS

1. With the constant gap penalty, how much memory would be needed for the scoring matrix in aligning two sequences with lengths of M and N nt long, respectively, if we use only integers in the scoring scheme and four bytes are used to hold an integer? (The memory requirement would be at least three times more if we distinguish between gap open and gap extension.)

2. Complete the following scoring matrix and backtrack matrix, with 2, and -1 being the match and mismatch scores, respectively, and -3 being constant gap penalty. Obtain the sequence alignment and the alignment score. Identify cell with two possible arrows indicating two alternative optimal alignments. There may be several such cells, but you need only to find one along the backtrack path.

		A	A	T	T	C	A	G
	0	-3	-6	-9	-12	-15	-18	-21
A	-3			-4	-7	-10	-13	-16
A	-6			1	-2	-5	-8	-11
T	-9	-4	1	6	3	0	-3	-6
C	-12	-7	-2	3		5	2	-1
A	-15	-10	-5	0	2	4	7	4
G	-18	-13	-8	-3	-1	1	4	

3. What is the advantage of aligning protein-coding nucleotide sequences against aligned amino acid sequences?
4. What is the minimum requirement for aligning protein-coding nucleotide sequences against aligned amino acid sequences?
5. What are the main differences in dynamic programming between local and global sequence alignment?
6. Given the following two alignments labeled (1) and (2), provide the simplest possible scoring scheme that will give Alignment 1 a higher alignment score than Alignment 2 and give the alignment score for Alignment 1 and Alignment 2 according to the scoring scheme.

(1)	(2)
ACG--T	AC-G-T
ACGGCT	ACGGCT

LAB 9 CHOOSING THE BEST-FIT SUBSTITUTION MODEL

INTRODUCTION

Many factors can modulate the substitution rate of nucleotide sequences, such as transition bias (Xia, et al. 1996) and rate heterogeneity among codons (Xia 1998b), and of amino acid sequences, such as genetic codes and functional constraints (Xia and Li 1998). To trace the evolutionary history back to time t_0, we need to know how nucleotide or amino acid sequences have come to their current states, i.e., how the sequences have changed during the interval from time t_0 to present.

. There are substitutions for nucleotide, amino acid or codon sequences, but we focus on substitution models for nucleotide frequencies because, once you understand substitution models for nucleotide sequences, it is quite easy to understand those for amino acid or codon sequences. A nucleotide substitution model summarizes our understanding on how DNA changes over time. It is typically expressed as a transition probability matrix in the framework of a Markov chain. A value in a transition probability matrix shows the probability of a nucleotide or amino acid in the leftmost column staying the same or changing into another one over a time interval. Different substitution models differ in the transition probability matrix. Those frequently used ones, including the JC69 (Jukes and Cantor 1969), K80 (Kimura 1980), TN84 (Tajima and Nei 1984), HKY (Hasegawa, et al. 1985), TN93 (Tamura and Nei 1993), and general time reversible or GTR (Tavaré 1986) models, as well as their relationships, are shown in Fig. 9-1. As you can see, different substitution models differ by two sets of parameters: 1) the frequency parameters (π_i in Fig. 9-1) and 2) rate parameters (a_i in Fig. 9-1). In the most complicated 12-parameter model, π_i's are themselves variables that changes over time.

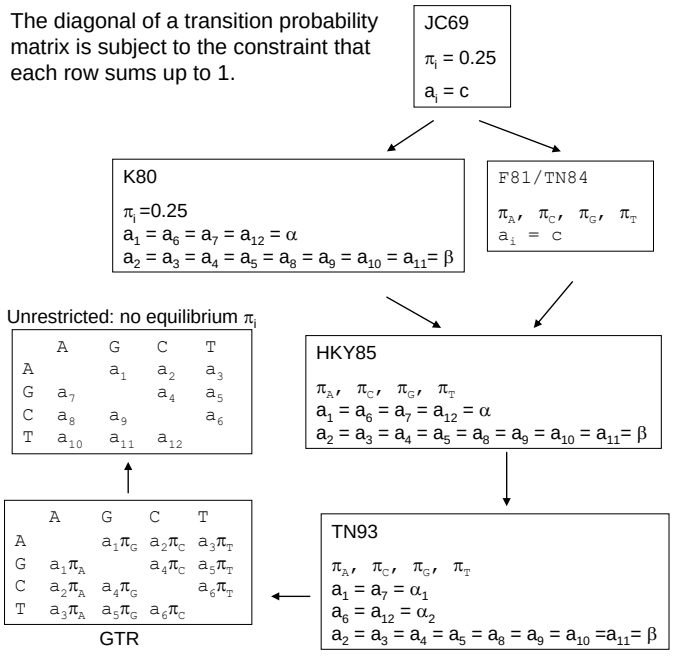

Fig. 9-1. Relationship among frequently used substitution models.

It might help with some illustrations of the two sets of parameters that characterize all substitution models. The simplest nucleotide substitution model is the JC69 model (Jukes and Cantor 1969) which assumes that frequency parameters are all equal to 0.25, so we do not need any data to estimate them. In other words, for the JC69 model, the number of frequency parameters that we need to estimate from sequence data is 0. The JC69 model also assumes that substitutions between any two nucleotides have the same rate, so it is a one-rate model. If you have sequences whose frequencies differ substantially from 0.25, or if transitions occur more frequently than transversions, then the assumptions of JC69 are violated and you should not use JC69 for your sequences.

If your sequences do have equal nucleotide frequencies, but transitions and transversions occur at different rate (typically transitions occur much more frequently than transversions), then you should use the K80 model (Kimura 1980) which let transitions have one rate and transversions another rate. So K80 model is a two-rate model in contrast to JC69 which is a one-rate model. However, both JC69 and K80 assume equal nucleotide

frequencies. To be more descriptive, you may refer to JC69 as a one-rate, equal-frequency model, and K80 as a two-rate, equal-frequency model. If transition rate and transversion rate are in fact the same, then K80 is reduced to JC69. Thus, JC69 is a special case of K80. When one model is a special case of another more general model, we say the two models are nested.

Here is a concrete example of nested models. Suppose Model 1 is $Y = aX$, and Model 2 is $Y = aX^b$. If b is in fact equal to 1, then Model 2 is reduced to Model 1. The two models are nested with Model 1being a special case of Model 2. We will learn that, for nested models, we can use likelihood ratio tests for model selection.

On the other hand if different nucleotides do change into each other with the same rate, but sequences differ in frequencies, then you can use the F81/TN84 model (Tajima and Nei 1984) which is also a one-rate model but differs from the JC69 model in that the former allow nucleotide frequencies to be different. So you may refer to F81/TN84 as a one-rate, different-frequency model. Thus, JC69 and F81/TN84 are also nested because JC69 is a special case of F81/TN84. If the nucleotide frequencies are in fact equal, then F81/TN84 is reduced to JC69. Note that, in F81/TN84, we need to estimate THREE nucleotide frequencies from the nucleotide sequence data. The reason that it is three instead of four is that, once we know three frequencies (e.g., P_A, P_C, P_G), the 4th (e.g., P_T) is determined (i.e., not free) because $P_T = 1 - P_A - P_C - P_G$.

If your sequences not only have different nucleotide frequencies, but the transition rate also differs from the transversion rate, then you cannot use JC69, K80 or F81/TN84. Instead, you should use HKY85 (Hasegawa, et al. 1985) or F84 (Felsenstein 2004), the two being equally general). These two are two-rate, different-frequency models. If the two rates are in fact equal, then HKY85 and F84 are reduced to F81/TN84. If the frequencies are in fact equal, then HKY85 and F84 are reduced to K80.

If your sequences not only have different nucleotide frequencies and different the transition and transversion rates, but the two transition rates (i.e., A ↔ G and C ↔ T) are also different, then you should not use any of those models mentioned above because now you have three rates: two for the two types of transitions and one for all transversions. Instead, you should use TN93 (Tamura and Nei 1993) which allows the nucleotide frequencies to be different as well as the three rates to be different. So TN93 is a three-rate, different-frequency model. If the two transitions in fact have the same rate, then TN93 is reduced to HKY85.

If your sequences not only have different frequencies, but all nucleotides change each other with different rates, then you should use GTR (for General Time-Reversible) which have six rates (Tavaré 1986).

All models that we have mentioned so far are time-reversible models. Time-reversible means that a nucleotide (say A) change into any other nucleotide is balanced by other nucleotide changing to A. This means that you can have all kinds of changes, but the frequencies will stay the same. If the ancestral sequence have frequencies for A, C, G, T being 0.1, 0.4, 0.4, 0.1, then all descendent sequences are also expected to have the same frequencies.

There are cases in which time-reversibility is violated. For example, if there is a high tendency for spontaneous mutation of C to U (or methylated C to T), then C will become fewer and fewer and T become more and more in descendent sequences. If C to T mutations occur frequently in the vertebrate lineages, but rarely in invertebrate lineages, then you may have frequencies for A, C, G, T being 0.1, 0.4, 0.4, 0.1 in some lineages but 0.4, 0.1, 0.1, 0.4 in others. In this case, you should not use time-reversible models but instead should use the Unrestricted model (which in practice is almost never used in teaching or research because it has too many parameters to be practical).

With the conceptual framework above, it is not difficult to understand substitution models for amino acid and codon sequences. Now we know that all substitution models are characterized by the frequency parameters and rate parameters. For amino acid sequences, there are 19 frequency parameters to estimate from the data, but the rate parameters are a bit complex. We know that some amino acid replacements occurs very frequently, e.g., between Gly and Ala, but others occur rarely, e.g., between Gly and Tyr. So different amino acid substitutions should have different rates, but there would be 20*19/2 rates assuming time-reversibility which are too many to estimate for any real amino acid sequence alignment. As a sub-optimal alternative, we typically use an empirical substitution matrix (e.g., a Blosum or Dayhoff matrix) as an approximation to the rates.

For codon sequences, we typically ignore the termination codons because any substitution from a sense codon to a termination codon is typically highly deleterious with an extremely low fixation probability. There are 61 sense codons for the standard genetic code, so we have 60 frequency parameters to estimate from the data. We also have 61*60/2 rate parameters which are simply monstrous. Instead, a typical codon-based substitution model will only estimate the transition and transversion rates and the synonymous and nonsynonymous rates. In other words, GGA ↔ GGG and GGC ↔ GGT will have the same rate because both substitutions involve a transition and both are synonymous (they both code Gly). However, GGA ↔ GGG and GGA ↔ GGT will have different rates because the former involves a transition and the latter a transversion. Also, GGG ↔ GGA and

GGG ↔ GAG will have different rates because, although both involve a G ↔ A transition, the former is synonymous and the latter is nonsynonymous.

Substitution models are the foundation of the maximum likelihood method and the distance-based method in molecular phylogenetics. A genetic distance in molecular phylogenetics is often prefixed with the substitution model from which it is derived, e.g., JC69 distance is derived from the JC69 substitution model (Jukes and Cantor 1969). The maximum likelihood method for phylogenetic analysis (Felsenstein 2004, 2014), which has increased its popularity in recent years with the increasingly faster computers, assumes a substitution model for computing the likelihood of the tree. Recently, scientists have tried to reconstruct ancestral protein-coding sequence based on substitution models, synthesize the reconstructed protein, and explore its function and evolution (Chang, Jonsson, et al. 2002; Chang, Kazmi, et al. 2002; Ugalde, et al. 2004). If the substitution model is good, then the likelihood of the reconstruction being correct is increased. Given that substitution models are used widely in molecular phylogenetics, we need to develop an appreciation of the differences among different substitution models and to understand how to choose one substitution model over others in practical applications.

In this laboratory, we will first take a guided empirical approach to understanding the various nucleotide substitution models implemented in DAMBE. In short, we will take a set of aligned sequences and characterize nucleotide frequencies and substitution patterns, which are then used as the basis for choosing substitution models.

Characterizing nucleotide frequencies may seem straightforward – you only need to count the number of A, C, G and T, designated N_A, N_C, N_G and N_T, in the sequences, and obtain the estimated frequencies by N_A/N, N_C/N, N_G/N and N_T/N, where $N = N_A + N_C + N_G + N_T$. However, for a set of aligned sequences, there are often conserved sites and variable sites. For example, 18S rRNA sequences have conserved domains and variable domains, with the nucleotide frequencies in the former differing from those in the latter. Because substitutions occur frequently at the variable domains but rarely at the conservative domains, it is the nucleotide frequencies at the variable domains that are the most relevant for substitution models (Xia, et al. 2003). However, the variable domains also experience insertions/deletions (indels) and a site containing indels are often deleted from analysis, resulting in nucleotide frequencies at the conserved domains dominating in estimating overall nucleotide frequencies. This can lead to bias in phylogenetic estimation (Xia, et al. 2003).

Characterizing an empirical substitution pattern also seems straightforward – you compare two sequences and count the differences. For example, if one sequence has A at site 11, and the other sequence has G at the same site, then we record an A→G or G→A transition if the tree is rooted or just an A↔G transition if the tree is not rooted so we do not know the direction of change. However, empirical substitution patterns based on all pairwise comparisons can be misleading. For illustration, suppose we have five sequences, with the first four sequences very similar to each other, but the 5th sequence is very different from the rest. If we perform all possible pair-wise comparisons, then nearly all differences are between the 5th sequence and the other four sequences. In other words, any difference between the 5th sequence and the other four sequences is counted four times. To alleviate this problem, we would build a phylogenetic tree, reconstruct ancestral sequences and perform pairwise comparisons between neighboring nodes along the tree. Thus, for the tree in Fig. 9-2, there are only seven pairwise comparisons in contrast to 10 possible pairwise comparisons for five OTUs. If OTU5 represents the odd sequence, then its unique differences will only contribute to the comparison between IN8 and OTU5 (Fig. 9-2).

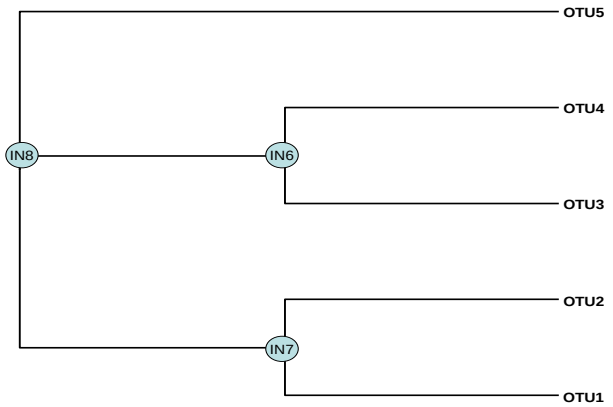

Fig. 9-2. Seven pairwise comparisons between neighboring nodes: OTU1-IN7, OTU2-IN7, IN7-IN8, IN8-IN6, IN6-OTU3, IN6-OTU4, IN8-OTU5, where 'IN' stands for internal node.

The empirical characterization of the substitution pattern by counting the observed number of substitutions represents an intuitive approach to help us select substitution models for phylogenetic analysis. DAMBE can also evaluate alternative substitution models by using statistically more rigorous likelihood ratio tests and information-theoretic indices.

The likelihood ratio test in model selection can be used for nested models. For example, the JC69 model is a special case of the K80 model (i.e., when there is no transition bias). Given a set of OTUs and a topology, we can compute the log-likelihood of the tree (lnL) based on the JC79 model ($\ln L_{JC69}$) and that based on the K80 model ($\ln L_{K80}$). If the sequences are sufficiently long, then twice of the difference in lnL between the two models follows approximately the χ^2 distribution, with the degree of freedom equals the difference in the number of parameters. For the JC69 and K80 models, the difference in the number of parameters is 1, so the degree of freedom for the χ^2-test is 1.

The information-theoretic indices represent an alternative approach and can be used between any two models, nested or not. This approach is also advantageous over the likelihood ratio test even in the case when the two models are nested. For example, the likelihood ratio test does not reject the simpler model at the significance level of 0.05 (e.g., when p = 0.051), it does not necessarily mean that the simpler model should then be preferred. In such cases, one is wise to choose the model based on the information theoretic indices.

OBJECTIVES

Gain familiarity with the assumptions of nucleotide-based substitution models

Substitution models can be nucleotide-based, amino acid-based or codon-based. They are all based on Markov chain models with rate ratio parameters and frequency parameters. For nucleotide-based models which are the focus in this laboratory, the rate ratio parameters refer to the relative probability of different nucleotides substituting each other in the evolutionary process and the frequency parameters refer to the frequencies of the four nucleotides. Different nucleotide-based substitution models differ in their assumption concerning the frequency and rate ratio parameters. We will use a set of aligned mitochondrial gene sequences from vertebrate species to gain insights into these frequency and rate ratio parameters.

Develop skills to choose appropriate substitution models for molecular phylogenetic studies

The universal criterion for choosing any mathematical model for data description and analysis is that the model should be the simplest but sufficient, or 'as simple as possible, but not simpler' in Einstein's words. We will use a set of aligned mitochondrial gene sequences from vertebrate species to illustrate how to choose an appropriate model for data analysis.

Apply the skill learned to practical phylogenetic analysis

The result of molecular phylogenetics depends significantly on the substitution models used. We will illustrate how different substitution models result in different phylogenetic trees by using mitochondrial genes from a set of vertebrate species, and how the correct choice of the substitution model will produce the correct tree.

PROCEDURES

The empirical approach

We will use a set of aligned sequences from eight vertebrate species in this laboratory. The sequences are saved in the VertCOI.FAS file that is included with DAMBE.

Checking frequency parameters

Launch DAMBE and open the VertCOI.FAS file. Click 'Seq.Analysis|Nucleotide frequencies'. A dialog box (Fig. 9-3) is displayed for you to set options. The left listbox shows sequences available for analysis. Click the 'Add all' button to move all sequence to the 'Chosen sequences' listbox as we want to include all sequences in analysis. Check the 'Test heterogeneity in nuc. freq. among OTUs' checkbox and the 'With Yates correction' checkbox. These options are for testing the heterogeneity in nucleotide frequencies among sequences. If

sequences differ significantly from each other in nucleotide frequencies, then a time reversible substitution model may not be appropriate.

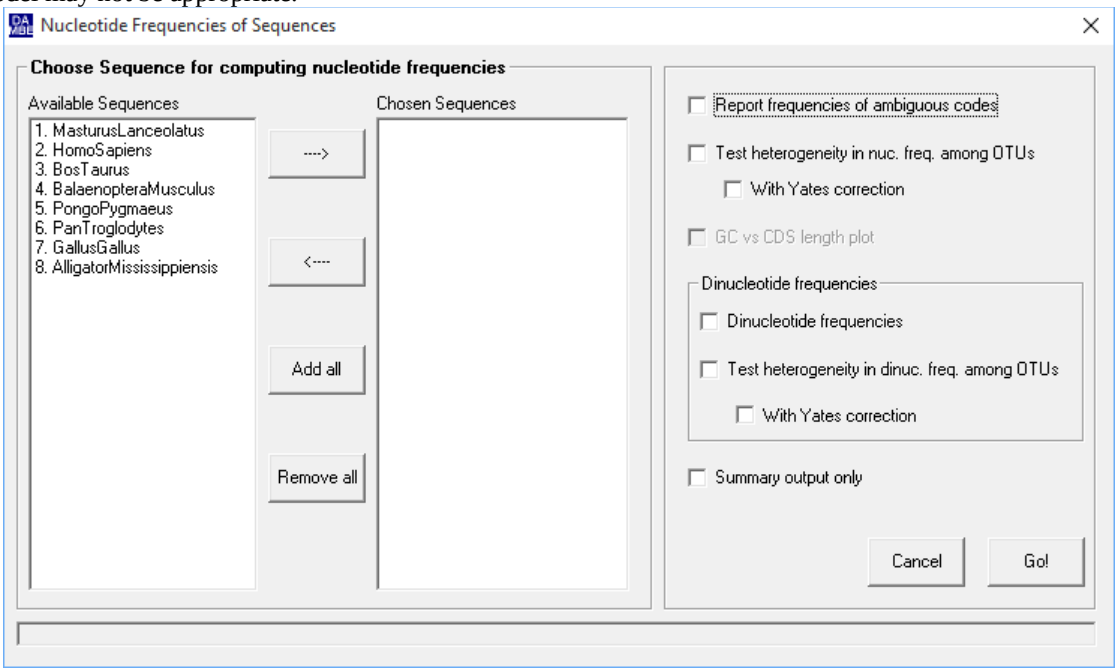

Fig. 9-3. Dialog box for setting options for analyzing nucleotide frequencies.

We will not analyze dinucleotide frequencies. So leave those checkboxes for dinucleotide frequencies unchecked.

Click the 'Go!' button to run the analysis. The results are present in 'Part Ia' and 'Part Ib' (You may wonder why there is no Part II. The Part II output is for analyzing dinucleotide frequencies). Table 9-1 shows the partial output for Part Ia, which tests whether nucleotide frequencies differ from 0.25 for each sequence. Note that nucleotide frequencies do differ significantly from 0.25, with p values all smaller than 0.0001 (Table 9-1). What substitution models are inappropriate for this set of sequences given the rejection of the null hypothesis of $\pi_i = 0.25$? We can reject JC69 and K80 models because they assume equal nucleotide frequencies.

The Part Ib output presents significant tests of the null hypothesis that nucleotide frequencies are not different among different sequences. This null hypothesis is rejected ($p < 0.01$, Table 9-2). One needs to be cautious with the p values obtained by a simply contingency table analysis because the data points are not independent. Imagine that sequences A and B differ significantly from each other in nucleotide frequencies. If we add 20 sequences that are closely related to sequence A (and consequently with nucleotide frequencies nearly identical to sequence A), then a test of difference in nucleotide frequencies among the 22 sequences may not report a significant difference among the sequences, i.e., the difference between sequences A and B is obscured. However, nucleotide frequencies can change substantially in a short time, so we may consider the nucleotide frequency data from the eight species as quasi-independent.

Table 9-1. Partial output for testing the null hypothesis of $\pi_A = \pi_C = \pi_G = \pi_T = 0.25$.

Species	P_A	P_C	P_G	P_T	X^2	P
Masturus lanceolatus	0.2361	0.2685	0.1925	0.3029	40.196	0.0000
Homo sapiens	0.2698	0.3016	0.1620	0.2665	66.926	0.0000
Bos Taurus	0.2844	0.2546	0.1653	0.2956	63.222	0.0000
Balaenoptera musculus	0.2837	0.2632	0.1620	0.2910	64.905	0.0000
Pongo pygmaeus	0.2652	0.3003	0.1620	0.2725	66.534	0.0000
Pan troglodytes	0.2652	0.2956	0.1667	0.2725	59.053	0.0000
Gallus gallus	0.2718	0.3135	0.1581	0.2566	78.640	0.0000
Alligator mississippiensis	0.2851	0.2870	0.1574	0.2705	70.122	0.0000

Table 9-2. Testing heterogeneity of nucleotide frequencies among different sequences.

Statistic	Value	DF	p
Chi-square	42.96	21	0.0032
Likelihood ratio chi-square	46.96	21	0.0009
Cramer's V	0.0344		

A significant difference in nucleotide frequencies among the sequences means that time-reversible models may not be appropriate. However, my own simulation (not published) suggests that the efficiency of time-reversible models in recovering the true tree is little affected by nucleotide frequency differences among the sequences as long as Cramer's V is smaller than 0.15. Note that Cramer's V is equivalent to a correlation coefficient. It does not depend on sample size. In contrast, p value is strongly dependent on sample size.

If Cramer's V is greater than 0.15, then we may consider using a nucleotide substitution model that would accommodate the inherent nonstationary substitution process. For distance-based methods, the paralinear distance (Lake 1994) and the LogDet distance (Lockhart, et al. 1994) have been claimed to accommodate nonstationarity, although the claim has not been verified.

There is a subtle difference between the paralinear and the LogDet distances. To highlight the difference, we reproduce the distance between two nucleotide sequences 1 and 2 below:

$$d_{12} = -\frac{1}{4}\ln\left(\frac{\det J_{12}}{\sqrt{\prod_{i=1}^{4} p_{1i}\prod_{i=1}^{4} p_{2i}}}\right) \quad \text{.....(9.1)}$$

where J_{12} is the observed substitution matrix, p_1 and p_2 are nucleotide frequencies for sequences 1 and 2, respectively and detJ12 means the determinant of J_{12}. In the formulation of the paralinear distance, J_{12} are in numbers, and p_1 and p_2 are reconstituted from J_{12} (Lake 1994). Consequently, p_1 and p_2 are based on aligned sites only, i.e., sites with no indels. This causes a new problem in analyzing the sequences with conserved and variable domains typical of rRNA genes. Both substitution and indel events occur almost exclusively in just a few variable domains of the 18S rRNA sequences (Van de Peer, et al. 1993). The variable domains have nucleotide frequencies different from the conserved domains in the 18S rRNA gene, which is also true in the 28S rRNA gene (Zardoya and Meyer 1996). In phylogenetic analyses involving the distance and maximum likelihood methods, we need to have the frequency parameters most appropriate for the underlying substitution model. It would seem obvious that the most appropriate estimate of the frequency parameters should be from the sites where substitution occurs, i.e., from the variable domains. However, variable domains in the 18S rRNA sequences are poorly represented in the aligned sites because of the presence of many indels in these domains. Thus, p_1 and p_2 in equation (9.1) are mainly based on invariable domains and consequently are not appropriate for phylogenetic reconstruction. PAUP (Swofford 2000) uses this original formulation for calculating the pairwise Lake/LogDet distances.

An alternative is to use the LogDet distance (Lockhart, et al. 1994) which defines J_{12} as a substitution matrix in proportions summing up to 1, and p_1 and p_2 as vectors of proportions summing up to 1. This permits the computation of empirical frequencies from all sites, including sites containing indels. Both DAMBE and the DNADIST program in PHYLIP (Felsenstein 2014) use all sites in computing p_1 and p_2. This approach allow sites in the variable domains of the 18S rRNA sequences to be better represented in computing nucleotide frequencies, and is the approach that we have taken in analyzing the 18S rRNA sequences.

Checking rate parameters

While the sequences are still in DAMBE, click 'Seq. Analysis|Nucleotide substitution pattern|Detailed output'. The dialog shows two listboxes, with the left showing the sequences available for analysis and the right showing sequences that you have chosen to do the analysis. Click the 'Add all' button to move all sequences to the right

(Fig. 9-4), and click the 'Go!' button. DAMBE will characterize nucleotide substitution patterns from all pairwise comparisons.

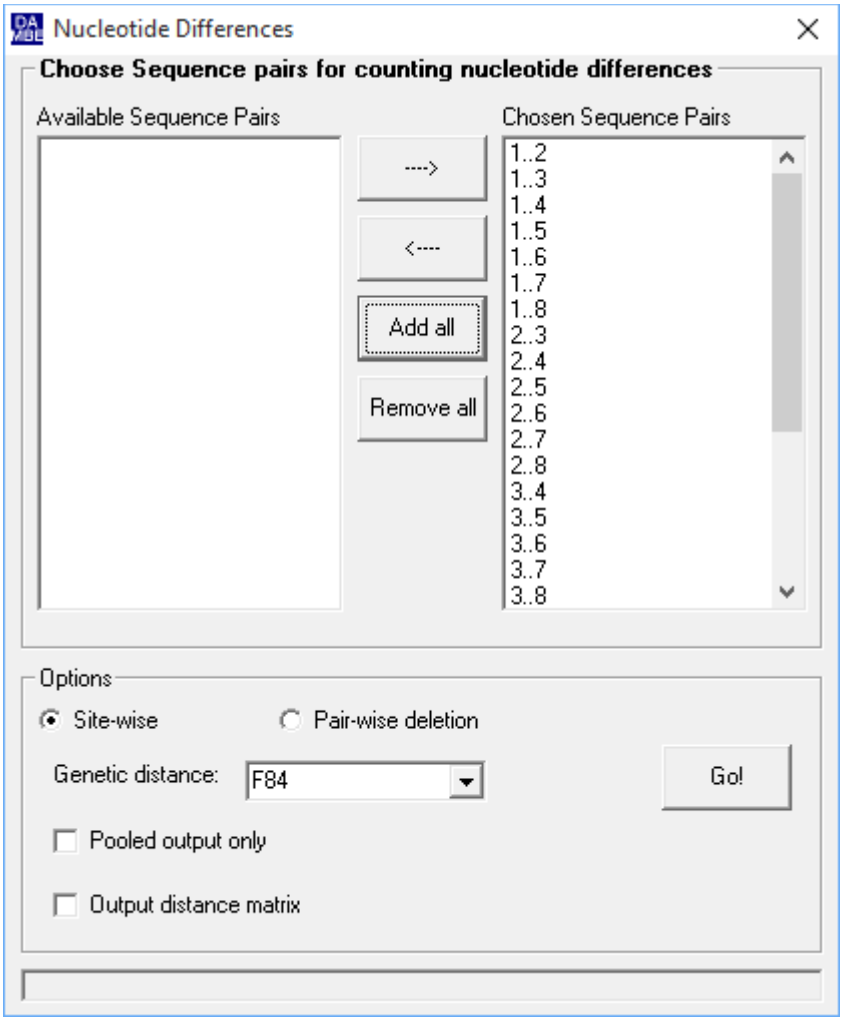

Fig. 9-4. Dialog box for characterizing nucleotide substitution pattern.

Once DAMBE finishes documenting the substitution patterns, you will be asked if you want to see the number of transitions and transversions plotted against the K80 or F84 distances. This is for visualizing substitution saturation which would erase historical information written in nucleotide sequences. For pairs of highly diverged taxa experiencing high substitution saturation, transversions will outnumber transitions. If sequences evolve according to the JC69 or K80 models, transversions will be twice as many as transitions for pairs of sequences experiencing full substitution saturation. Such sequences would be of little use for reconstructing phylogenetic relationships because all historical information written on the nucleotide sequences has been over-written a number of times. If the plot shows that both transitions and transversions fall on a straight line with transitions consistently outnumbering transversions, then the sequences have not experienced substitution saturation and are good for phylogenetic analysis.

Fig. 9-5 shows transitions and transversions plotted against the F84 distance. Note more transitions than transversions for recently diverged sequences (with small F84 distances), but the number of transversions gradually catch up for more diverged sequences (with large F84 distances).

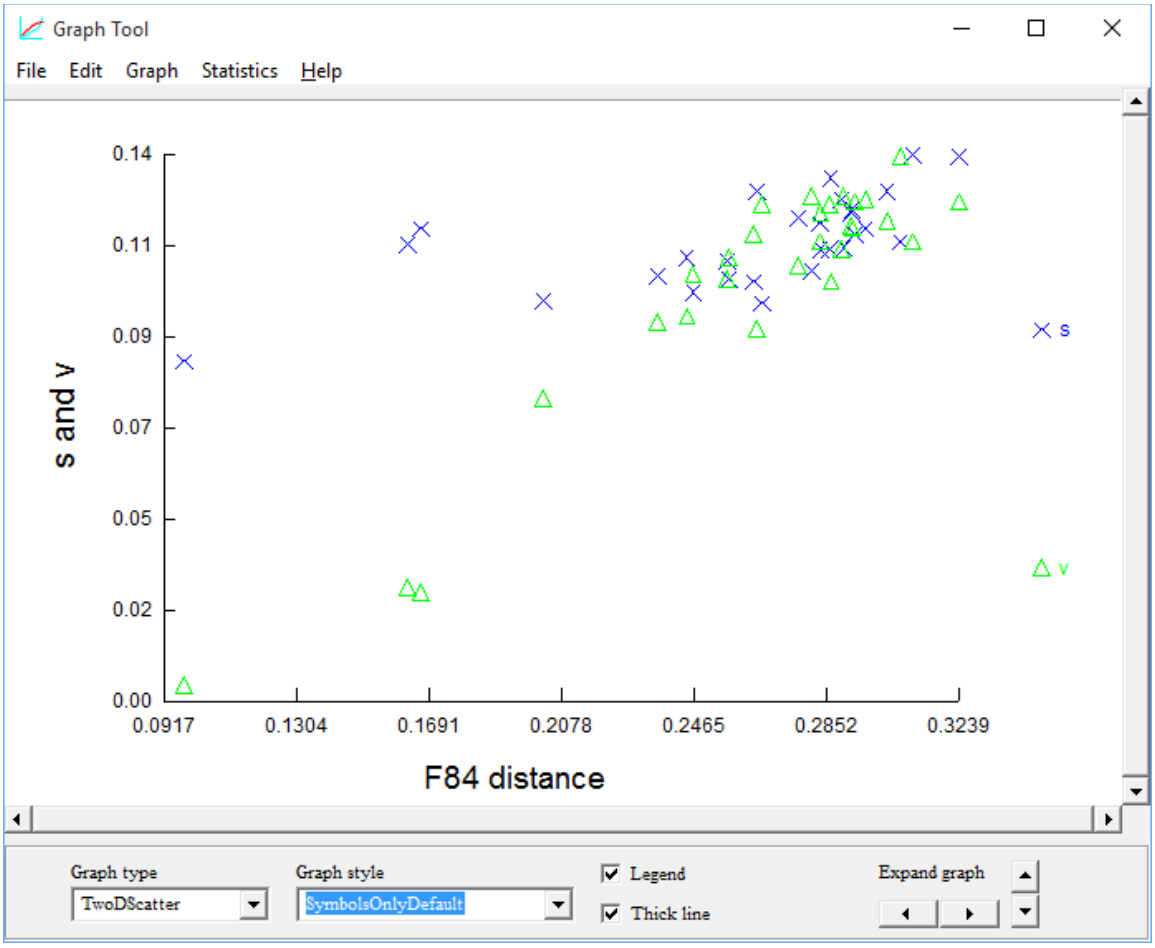

Fig. 9-5. Plot of transitions (s) and transversions (v) against the K80 distance.

The output from the analysis of substitution patterns is of two parts in similar formats. Part 1 shows results from all pairwise comparisons of which one, between fish (*Masturus lanceolatus*) and human (*Homo sapiens*), is shown in Table 9-3a. Part 2 displays results pooled from all pairwise comparisons (Table 9-3b). The column headed by 'AA' lists the number of sites when both sequences are A, and the column headed by 'AG' lists the number of sites when one sequence is A and the other is G, and so on. So the number of 288 under column heading of 'AA' in the row marked by 'Obs' means that there are 288 nucleotide sites being A in both the *Masturus lanceolatus* vs. *Homo sapiens* sequences.

The expected numbers (Exp in Table 9-3) are calculated in a way analogous to the equal input model such as F81/TN84, where nucleotide frequencies can be different but all substitutions are equally likely. We use 1) nucleotide frequencies (π_i, where i = A, C, G and T), 2) number of identical sites (N_I) and 3) number of different sites (N_D). Take data in Table 9-3a for example.

$$\pi_A = \frac{2\times 288 + 60 + 72 + 57}{2\times 1512} = 0.252976$$

$$\pi_C = 0.28505291;\ \pi_G = 0.177248677;\ \pi_T = 0.284722222 \qquad (9.2)$$

$$N_I = 288 + 317 + 213 + 331 = 1149$$

$$N_D = 60 + 124 + 72 + 57 + 32 + 18 = 363$$

The expected numbers of AA, CC, GG, and TT are

$$AA = N_I\left(\frac{\pi_A^2}{\pi_A^2 + \pi_C^2 + \pi_G^2 + \pi_T^2}\right) = 285.3017 \qquad (9.3)$$

$$CC = 362.2396;\ GG = 140.0590;\ TT = 361.3997$$

Table 9-3. Output from the analysis of nucleotide substitutions. (a) comparison between the *Masturus lanceolatus* vs. *Homo sapiens* sequences, (b) results pooled over all pairwise comparisons.

		Identical			Transition			Transversion			
		AA	CC	GG	TT	AG	CT	AC	AT	CG	GT
(a)	Obs(1)	288	317	213	331	60	124	72	57	32	18
	Exp(2)	285	362	140	361	44	79	71	70	49	49
(b)	Obs(1)	8919	8992	5930	9261	1417	3438	2299	1322	457	301
	Exp(2)	9308	10398	3504	9892	1117	1984	1924	1877	1181	1152

(1) observed

(2) expected assuming the JC69 model.

Similarly, the expected numbers of AG, CT, AC, AT, CG and GT are

$$AG = N_D \left(\frac{\pi_A \pi_G}{\pi_A \pi_G + \pi_C \pi_T + \pi_A \pi_C + \pi_A \pi_T + \pi_C \pi_G + \pi_G \pi_T} \right) = 43.8572 \qquad (9.4)$$

$CT = 79.3825$; $AC = 70.5315$; $AT = 70.4497$; $CG = 49.4182$; $GT = 49.3608$

Inspecting the observed substitution patterns can help us choose appropriate substitution models for analyzing the data. Note that the two transitions (A↔G and C↔T) are quite different from each other. Only TN93 and GTR models accommodate such rate differences between the two types of transitions, so we can exclude substitution models such as JC69, K80, F84, HKY85, etc. We also note that the four types of transversions differ substantially in their frequencies of occurrence, so we can exclude the TN93 model that consider all four types of transversions to have the same rate. In short, to fit our data, we should use GTR. We will arrive at the same conclusion by inspecting the pooled data in Table 9-3b.

Phylogenetic reconstruction using distance-based methods

While the sequences are still in DAMBE (if you are not sure, click 'Sequences|View sequences|Plain view'), click 'Phylogenetics|Distance-based method|Nucleotide sequences'. A dialog box (Fig. 9-6) is displayed for you to set the options. You may use the default tree-building algorithm (FastME) and its associated options. FastME does not assume a molecular clock and consequently produces an unrooted tree. Choose *Masturus lanceolatus* as outgroup. The selection of outgroup affects the drawing of the tree but does not affect the phylogenetic relationship among species with the unrooted tree.

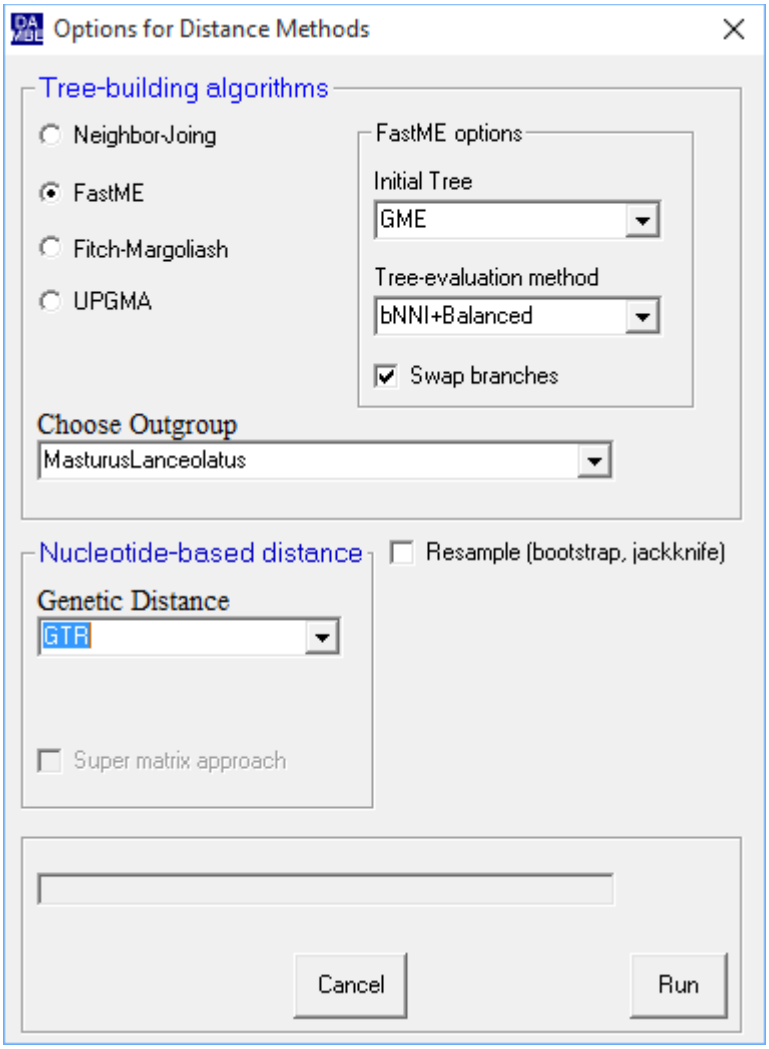

Fig. 9-6. Setting options for distance-based methods in molecular phylogenetics.

For evolutionary distance, we will choose GTR because it treats allow all six types of substitutions to have different rates. Click 'Run' to generate the tree (Fig. 9-7) which has internal nodes numbered for later use. You should learn two more tricks. One is to copy the tree to programs such as PowerPoint for presentation and publication, and the other is to save the tree for future phylogenetic analysis.

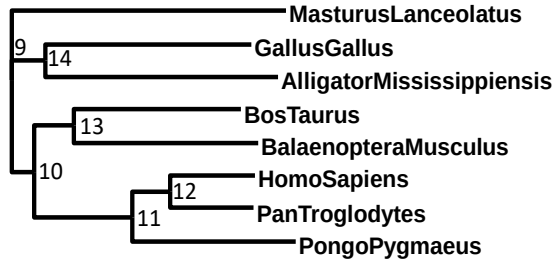

Fig. 9-7. The tree panel in DAMBE.

You can copy and paste the tree to PowerPoint slides or any other graphic programs including EXCEL and WORD, either in fixed-resolution bitmapped format or in high-resolution Windows metafile format. Appendix 1 summarizes the copying and pasting of trees between DAMBE and PowerPoint.

To save a tree for future viewing or for use with other phylogenetic functions, click 'File|Save tree for future viewing'. Give a file name, and the tree will be saved in text format with the file extension of '.dnd' (for dendrogram). Save the tree that is constructed with the correct substitution model to VertCOI.dnd.

Characterizing empirical substitution patterns with a tree: We have previously characterized empirical substitution patterns by performing all possible pairwise comparisons, and we have mentioned that such comparisons are not independent. For example, if we have seven sequences whose evolution is well described by the JC69 model, but one sequence which has accumulated a large number of C↔T substitutions, then we will have seven pairwise comparisons all with a large number of C↔T substitutions. To alleviate this problem, one can use a tree to reconstruct ancestral sequences in the internal nodes, and perform pairwise comparisons between neighboring nodes along the tree. We can now do this because we already have a tree that we are happy with.

Construct ancestral states of internal nodes: An unrooted tree with N OTUs has (N – 2) internal nodes which represent hypothesized ancestral organisms. Here we are to reconstruct the ancestral sequences for these internal nodes. This is useful in many cases, e.g., fitting the rate heterogeneity by gamma distribution, estimating the proportion of invariant sites, etc. However, our immediate purpose of reconstructing the ancestral sequences is to facilitate pairwise comparisons between neighboring nodes along the tree.

Click 'Phylogenetics|Maximum Likelihood|DNAML+'. This function does not use information in sites with indels or ambiguous nucleotides, and you are advised to sitewise delete all such sites. Because our sequences do have such sites, you should click the 'Yes' button to quit. Now click 'Sequence|Sequence manipulation|Delete|Ambiguous nuc, AA or codon'. You will be asked whether you want to perform sitewise deletion or not. Click 'Yes' (which means that any site that contains even a single ambiguous nucleotide/aa/codon will be deleted. Some sequences may become identical after this operation and you are asked if you want to combine identical sequences into one. You should choose no because our tree in the VertCOI.dnd has all the species.

Now click again 'Phylogenetics|Maximum Likelihood|DNAML+' and this time click the 'No' button to proceed. The main difference between DNAML and DNAML+ is that the former implements only one substitution model, i.e., the F84 model, whereas the latter implements a variety of substitution models from the simplest JC69 to the complex GTR model. The former is also faster than the latter, partly because the convergence criterion is more stringent in the latter than in the former. In the resulting dialog box shown in Fig. 9-8, choose the 'User tree' in the 'Running mode' dropdown box, and browse to the directory where you have saved the VertCOI.dnd file. Click to open the VertCOI.dnd file. A tree editing panel will display the tree contained in the VertCOI.dnd file. This is mainly for the purpose of safeguarding against opening a wrong tree which will crush DAMBE. Click 'File|Export and exit' to get back to the dialog box in Fig. 9-8. Check the 'Ancestral state reconstruction' checkbox. In the 'Sub. model' dropdown box, choose GTR that is appropriate for the set of sequences. Click the 'Run' button to reconstruct the sequences.

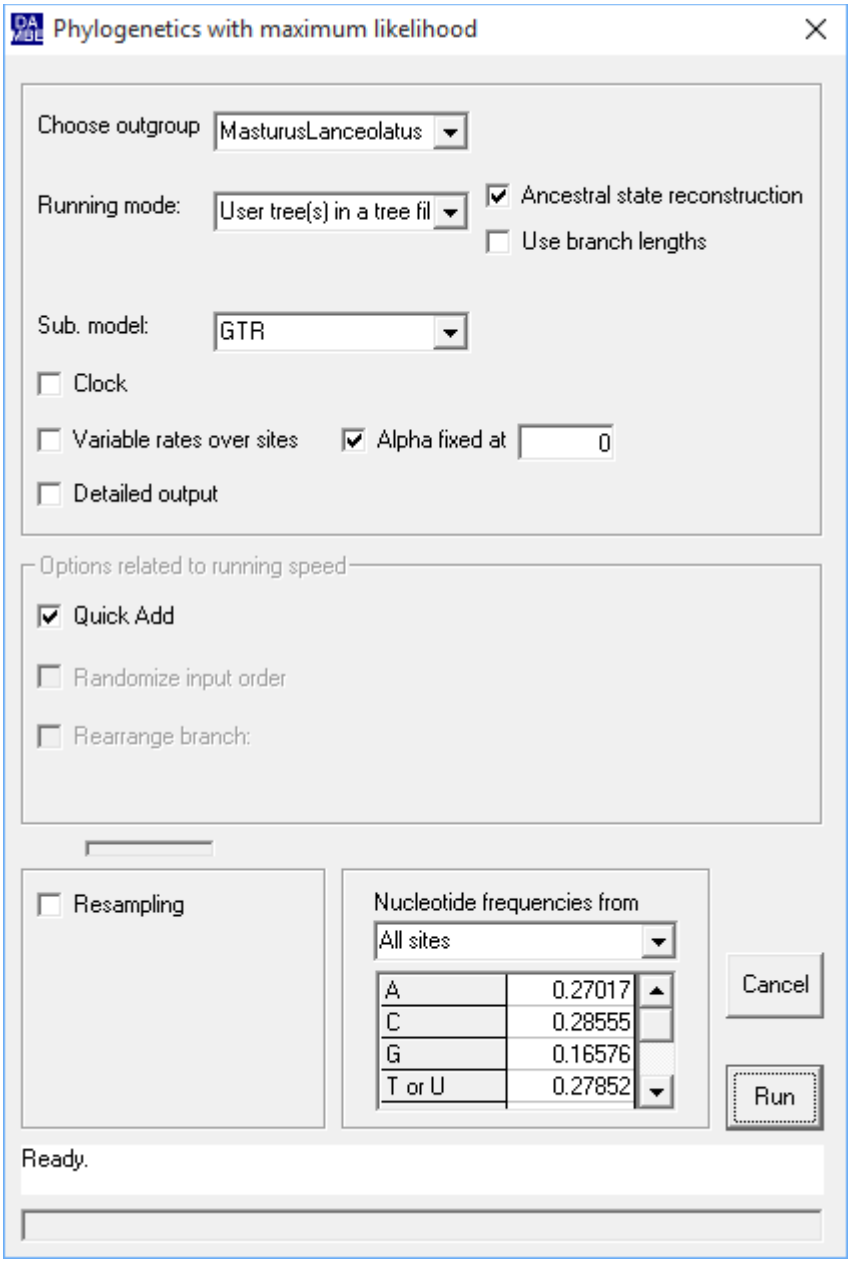

Fig. 9-8. Setting options for reconstructing ancestral sequences.

The reconstructed sequences for the internal nodes, labeled 'node #9-#14', are displayed together with the original sequences (Fig. 9-9). You might wonder which internal node is 'node #9', which is 'node #10' and so on. You will find that out soon, but I have already labelled the internal nodes in Fig. 9-7.

The algorithm involved in reconstruction of ancestral sequences is complicated, but the principle is simple. For any internal node, its nucleotide state at a particular site depends on the states of its three neighboring nodes or, to be more explicit, depends on the probabilities associated with the four nucleotide states of its three neighboring nodes. There are currently two approaches to reconstruct ancestral sequences, the maximum parsimony approach (MP) and the maximum likelihood approach (ML). Each site is typically reconstructed independently. In MP, we first traverse the tree to obtain a 4-element cost vector for each internal node and then decide which nucleotide state would minimize the site-specific cost. In ML, we replace the cost vector by a 4-element likelihood vector and then decide which nucleotide will maximize the site-specific likelihood.

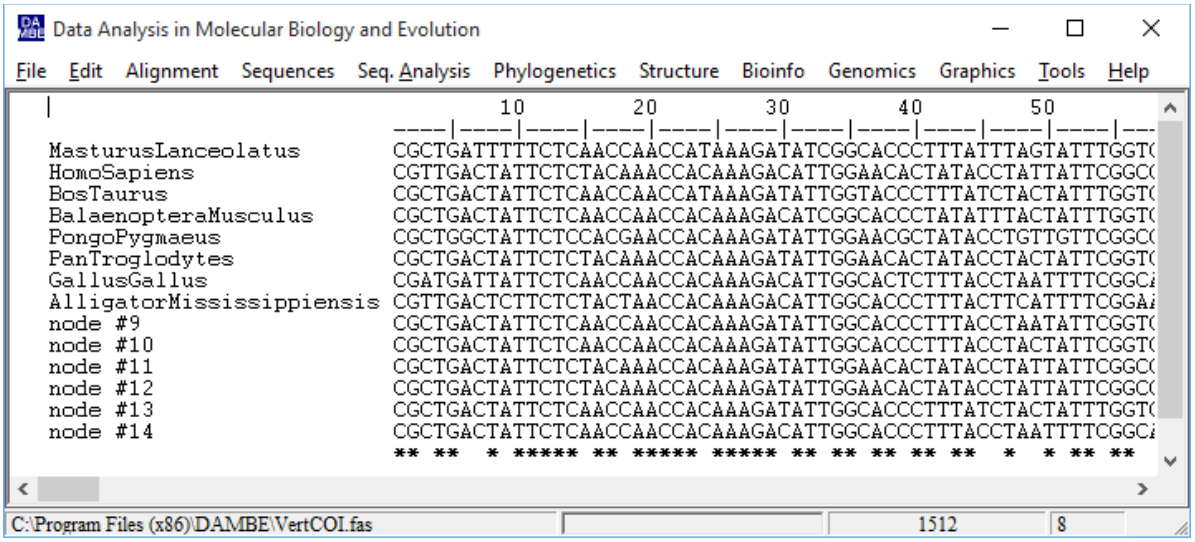

Fig. 9-9. Display of reconstructed ancestral sequences together with the sequences of the nine extant species.

Pairwise comparisons between neighboring nodes along a tree: While the sequences are displayed as in Fig. 9-9 with reconstructed ancestral sequences, click 'Seq. Analysis|Nucleotide substitution pattern|Detailed output'. You will see a dialog box (Fig. 9-10) similar to that in Fig. 9-4 but with many fewer pairs. As you might have guessed, sequences from *Masturus lanceolatus* to *Alligator mississippiensis* are labeled form 1 to 8 and internal nodes are labeled from 9 to 14. Note that for an unrooted tree, there are (2n – 2) nodes (including the terminal nodes or leaves). Our sequence set has 8 sequences, so there are 14 nodes (= 2×8-2).

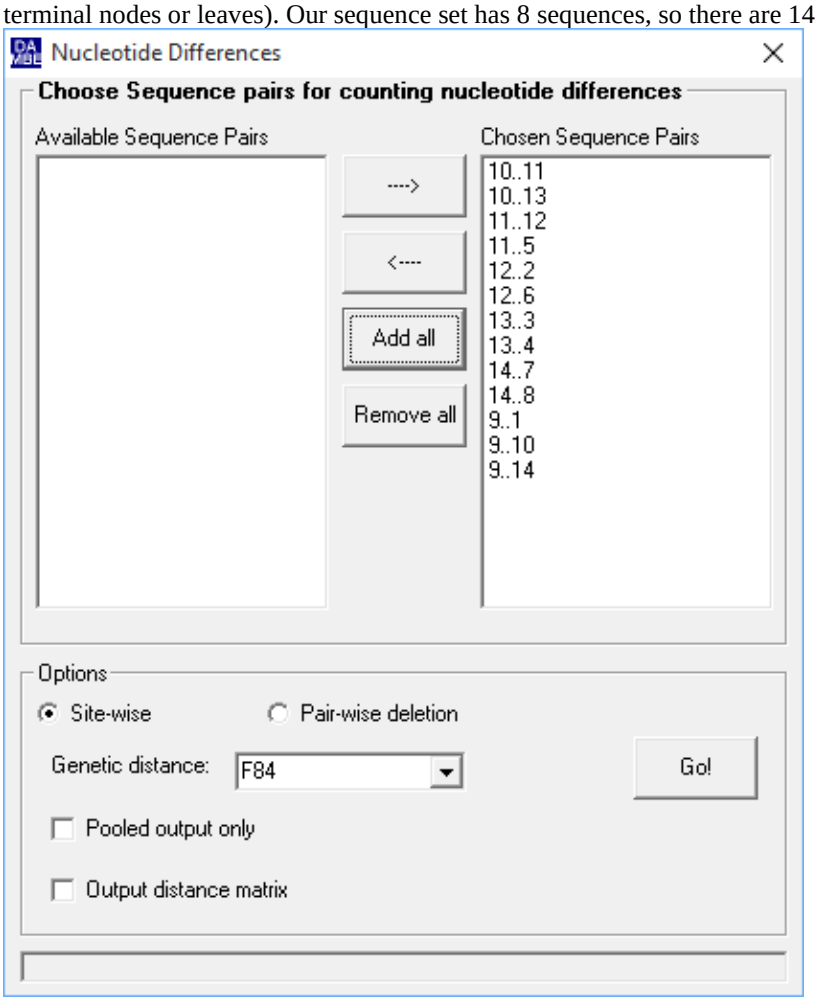

Fig. 9-10. Dialog box for phylogeny-based characterizing nucleotide substitution pattern.

A sequence pair represented by '9..1' means a comparison between the *Masturus lanceolatus* sequence and its ancestral sequence 'node #9', i.e., the internal node connected to *Masturus lanceolatus* is numbered 9 which is connected to the internal nodes numbered 10 and 14 (Fig. 9-10) and so on. These pieces of information will allow you to label the internal nodes on the tree (as I have done in Fig. 9-7).

Click the 'Go!' button will produce results from individual pairwise comparisons as well as the result pooled over all pairwise comparisons.

The statistical model-testing approach

To find the best substitution models for phylogenetic analysis, we need a set of aligned sequences and a tree either from this set of sequences or from alternative sources. In the latter case, it is essential to ensure that the species names in the tree file is the same as those in the sequence file.

Launch DAMBE and open the VertCOI.FAS file. We will first create a phylogenetic tree from this set of sequences. Click 'Phylogenetics|Distance methods|Nucleotide sequences', and click the 'Run' button, leaving everything as default, although it is OK to choose options different from the default. Once the tree is displayed in the tree panel, click 'File|Save tree in text' to save the tree in text format to a file. You may use any name that you can remember, but VertCOI.dnd is a good choice.

Now click 'Phylogenetics|Find best nuc. Substitution model'. In the ensuing dialogbox, click the 'No' button to continue. Don't click 'Yes' because the function will then quit. Click the 'Tree from tree file' option button in the dialog box (Fig. 9-11), and read in the tree file VertCOI.dnd that you have saved in before. Te tree will be displayed in the tree panel. Click 'File|Export/Exit' to quit the tree panel.

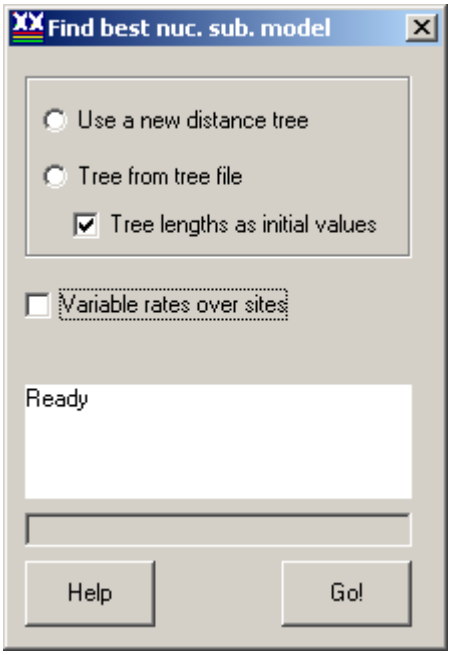

Fig. 9-11. Options for selecting the best nucleotide substitution model.

You are back to the dialog box (Fig. 9-11). Click 'Go' and you will have output in two parts. Part 1 (Table 9-4) shows the information-theoretic indices. The number of parameters (N_p) equals the number of rate ratios plus the estimated nucleotide frequencies. For JC69 and K80, the equilibrium frequencies are assumed to be all equal (=0.25). F80 has one rate ratio (the transition/transversion ratio), and TN93 has two rate ratios as well as three estimated frequencies (The fourth is not estimated from the data as it is constrained by the summation of the frequencies equal to 1). For detailed information and application of the information-theoretic indices, one should consult Burnham and Anderson(2002), but a simple formulation with applications can be found in my MPE paper (Xia 2009). In short, the best model is one with the smallest information-theoretic index. In Table 9-4, GTR consistently has the smallest information-theoretic indices and is taken as the best model for this data set. This is consistent with our previous empirical approach by counting the various types of substitutions.

Table 9-4. Information-theoretic indices from DAMBE for choosing substitution models.

Model	N_p(1)	lnL(2)	AIC(3)	AICc(4)	BIC(5)	r1(6)	r2(6)	r3(6)	r4(6)	r5(6)
GTR	8	-4397.13	8810.264	8810.35	8853.771	2.280	0.173	0.308	0.786	0.913
TN93	5	-4417.34	8844.685	8844.72	8871.877	3.970	1.757			
T92	2	-4431.36	8866.73	8866.737	8877.606	2.785				
HKY85	4	-4431.34	8870.675	8870.699	8892.429	2.775				
F84	4	-4429.51	8867.028	8867.052	8888.782	0.907				
F81	3	-4470.31	8946.614	8946.628	8962.929					
K80	1	-4440.97	8883.941	8883.943	8889.379	2.760				
JC69	0	-4479.55	8959.092	8959.092	8959.092					

(1) N_p: number of parameters: number of rate ratios plus the estimated frequencies.
(2) lnL: log-likelihood
(3) AIC: Akaike information criterion
(4) AICc: corrected AIC
(5) BIC: Bayesian information criterion (also known as Schwarz criterion in statistical software packages such as SAS)
(6) estimated rate ratios

The second part of the DAMBE output related to model selection is the result of likelihood ratio tests based on nested models (Table 9-5). The results can be derived from values in Table 9-4 which contains the log-likelihood and the number of parameters for each model. The GTR model is significantly better than all other models based on the likelihood ratio tests (Table 9-5). For this particular set of sequences, the chosen model (GTR) is the same based on either the information-theoretic indices or on the likelihood ratio tests.

Table 9-5. DAMBE output of the likelihood ratio tests between nested nucleotide substitution models, with their log-likelihoods shown as lnL_G (for the general model) and lnL_S (for the special model). $X2 = 2\Delta(lnL_G\text{-}lnL_S)$, and DF is the difference in the number of parameters for the two involved models.

Comparison	lnL_G	lnL_S	X2	DF	P
GTR..JC69	-4397.13	-4479.55	164.8275	8	0.0000
TN93..JC69	-4417.34	-4479.55	124.4072	5	0.0000
T92..JC69	-4431.36	-4479.55	96.3622	2	0.0000
HKY85..JC69	-4431.34	-4479.55	96.4166	4	0.0000
F84..JC69	-4429.51	-4479.55	100.0637	4	0.0000
F81..JC69	-4470.31	-4479.55	18.478	3	0.0004
K80..JC69	-4440.97	-4479.55	77.1512	1	0.0000
GTR..F81	-4397.13	-4470.31	146.3495	5	0.0000
TN93..F81	-4417.34	-4470.31	105.9292	2	0.0000
HKY85..F81	-4431.34	-4470.31	77.9386	1	0.0000
F84..F81	-4429.51	-4470.31	81.5857	1	0.0000
GTR..K80	-4397.13	-4440.97	87.6763	7	0.0000
TN93..K80	-4417.34	-4440.97	47.2561	4	0.0000
T92..K80	-4431.36	-4440.97	19.2111	1	0.0000
HKY85..K80	-4431.34	-4440.97	19.2654	3	0.0002
F84..K80	-4429.51	-4440.97	22.9125	3	0.0000
HKY85..T92	-4431.34	-4431.36	0.0544	2	0.9732
F84..T92	-4429.51	-4431.36	3.7014	2	0.1571
GTR..T92	-4397.13	-4431.36	68.4652	6	0.0000
TN93..T92	-4417.34	-4431.36	28.045	3	0.0000
GTR..HKY85	-4397.13	-4431.34	68.4109	4	0.0000
TN93..HKY85	-4417.34	-4431.34	27.9906	1	0.0000
GTR..F84	-4397.13	-4429.51	64.7638	4	0.0000
TN93..F84	-4417.34	-4429.51	24.3436	1	0.0000
GTR..TN93	-4397.13	-4417.34	40.4202	3	0.0000

MORE QUESTIONS

1. If you have a set of aligned nucleotide sequences that differ substantially in nucleotide frequencies, e.g., one has frequencies for A, C, G and T equal to 0.1, 0.4, 0.4, 0.1, respectively, and another has corresponding frequencies equal to 0.4, 0.1, 0.1, 0.4, what substitution model would be appropriate for describing the substitution process involving the sequences? (Answer: This excludes all time-reversible models. One should use a substitution model for non-stationary process.)
2. If a set of aligned sequences has equal nucleotide frequencies but transitions occur much more frequently than transversions, which substitution model would be appropriate for phylogenetic analysis of these sequences?
3. You examined nucleotide frequencies of a set of aligned sequences. Every sequence has A, C, G, and T frequencies close to 0.1, 0.4, 0.4, and 0.1, respectively. Without checking substitution patterns, what substitution models would be inappropriate and what might be appropriate for the sequences?
4. Why would transversions outnumber transitions in sequences that have experienced full substitution saturation? What is the expected number of transitions over transversions for sequences having experienced full substitution saturation, assuming equal nucleotide frequencies?
5. CpG-specific methyltransferase methylates the C in CpG dinucleotide and increase the CpG $\rightarrow$ TpG transitions. DNA methylation activity is low in invertebrate genomes but high in vertebrate genomes. If you are studying a set of aligned sequences including both invertebrate and vertebrate species, what substitution model would be appropriate for modeling the evolutionary process?
6. What are the main advantages of using information-theoretic indices over the likelihood ratio test?

LAB 10 MOLECULAR PHYLOGENETICS

INTRODUCTION

Molecular phylogenetics has two objectives (Fig. 10-1): 1) characterizing the branching patterns (cladogenic events, specifically the speciation and gene duplication events) in evolution, and 2) dating of these speciation or gene duplication events that may help us understand functional divergence of genes. Phylogenetics can also help us to identify common ancestors such as the mitochondrial 'Eve' (because mitochondrial genomes are maternally inherited) or the Y-chromosome 'Adam' (because Y-chromosome is passed down from father to son). The universal common ancestor for all living organisms is termed cenancestor which may or may not be identifiable (Xia and Yang 2013). In this laboratory we focus on the first objective, i.e., the characterization of branching patterns (i.e., phylogenetic relationships).

One recent application of the phylogenetic methods by one of the former BPS4104 students is the elucidation of the temporal sequence of gene duplication involving three paralogous genes, USP4, USP15 and USP11 (Vlasschaert, et al. 2015). Caitlyn Vlasschaert took BPS4104 in 2014, started her MSc with me in September 2014, and published her first paper in 2015.

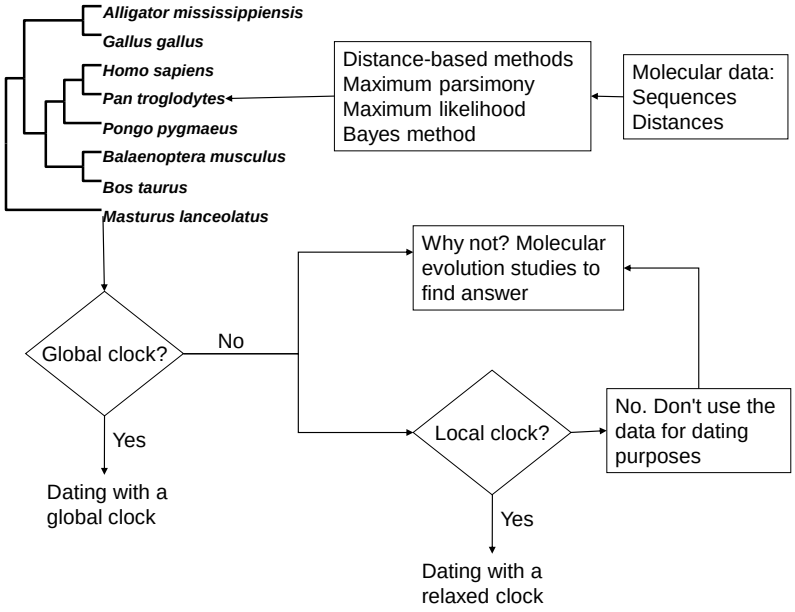

Fig. 10-1. Outline of hypothesis testing concerning the molecular clock.

Major categories of phylogenetic methods

What are the molecular phylogenetic methods currently used to elucidate phylogenetic relationships? Four categories of phylogenetic methods are widely used in molecular phylogenetics: the distance-based approach popularized by MEGA (Kumar, et al. 2016), the maximum parsimony (MP) approach popularized by PAUP (Swofford 1993; Swofford 2000), the maximum likelihood (ML) approach popularized by DNAML in the PHYLIP package (Felsenstein 2014) and the Bayesian inference (BI) popularized by MrBayes and BEAST (Huelsenbeck and Ronquist 2001; Drummond and Rambaut 2007). The main difference between ML and BI is that the former makes inferences entirely on the basis of information in the data, whereas the latter makes inferences by incorporating prior information. While the BI approach has become increasingly popular (Aris-Brosou and Xia 2008) and has contributed many phylogenetic trees in publications, I still have not seen much contribution it makes towards resolving difficult phylogenetic controversies.

The plethora of sequence formats for phylogenetic analysis

Associated with the large number of phylogenetic methods is a proliferation of sequence formats. For example, PHYLILP, MEGA, and PAUP all have their own sequence format. DAMBE reads and writes sequence files in 25 standard sequence formats including the annotation-rich GenBank files, MEGA, PHYLIP, NEXUS,

FASTA, the binary trace files, and NeXML files (Vos, et al. 2012) for comparative sequence analysis. NeXML format is an extensible sequence format for richly annotated comparative data to facilitate interoperability (Vos, et al. 2012). This new data format was formulated with the participation of two Canadian scientists. It has already been used for large-scale archiving of comparative data by TreeBASE (Boettiger and Lang 2012), and is likely to become a standard in future evolutionary bioinformatic data analysis.

Phylogenetic methods we will learn in this lab

In this laboratory we will learn the distance-based, MP and ML methods used in molecular phylogenetics. Instead of using MEGA, PAUP and DNAML, we will learn all this methods by using DAMBE because (1) DAMBE features perhaps the most extensive implementation of distance-based methods, (2) it has a simple yet extremely fast MP method, and (3) it implements DNAML with several enhancements. There are some major differences among and within these different categories of methods. It is important to know the nuance of the differences.

Distance-based methods

The distance-based methods always have two components, i.e., the estimation of the pairwise genetic distance and the tree-building algorithm (e.g., UPGMA, neighbor-joining, Fitch-Margoliash and FastME) based on the genetic distances. For this reason, the genetic distance and tree-building algorithm constitute the minimum specification of a distance-based method in publication

The genetic distance: There are two approaches to estimate genetic distances, the independent estimation (IE) approach and the simultaneous estimation (SE) approach, with distances obtained by the SE approach performing much better in phylogenetic reconstruction than those obtained by the IE approach (Tamura, et al. 2004). There are two SE approaches, one based on the least-squares (LS) approach (Xia 2009) and the maximum likelihood (ML) approach (Tamura, et al. 2004). The SE distance obtained with the ML approach is known as the maximum composite likelihood distance, and is implemented in MEGA4 based on the TN93 substitution model (Tamura, et al. 2007). The same distance is labeled as MLCompositeTN93 in DAMBE which also implements the distance based on the F84 model, designated as MLCompositeF84. The corresponding distances based on the LS approach for TN93 and F84 models are designated as LSCompositeTN93 and LSCompositeF84, respectively, in DAMBE. The DNADist program in the PHYLIP package (Felsenstein 2014) represents an early attempt to obtain genetic distances using the SE approach. It generates the MLCompositeF84 distance but requires the user to input the transition/transversion ratio. It is important to keep in mind that a specification that the genetic distance is computed with the F84 model (or TN93) is insufficient for publication because IE distances based on the F84 model could be quite different from SE distances based on the same substitution model.

The tree-building algorithm: The tree-building algorithm typically works in three steps. First a new topology is generated. Second, branch lengths (b_i) of the topology are evaluated, typically by the least-squares method or by the Fitch-Margoliash method (Note that the Fitch-Margoliash method for branch length evaluation is different from the Fitch-Margoliash criterion for choosing the best tree). Third, a criterion is computed so that the algorithm can decide which tree is the best tree based on the criterion. Commonly used criteria in distance-based methods are the minimum evolution criterion (i.e., a tree with the shortest tree length, which equals Σb_i, is the best tree) and the Fitch-Margoliash criterion (which consists of a set of slightly different least-squares criteria, with the best tree having the smallest sum of squares). Distance-based trees built in this way are said to be based on a global criterion, with examples including FastME and Fitch-Margoliash methods.

The neighbor-joining method uses the minimum evolution criterion, but the criterion is applied locally, not globally. In other words, the algorithm does not build different fully resolved N-taxa trees and choose the shortest tree as the best tree. Instead, it clusters two taxa together if that clustering leads to the shortest partially resolved tree compared to other alternative two-taxa clustering. The UPGMA method is even more local in term of apply the minimum evolution criterion – it groups any two taxa that have the shortest distance. Thus, theoretically, the FastME method should produce better trees than the neighbor-joining method which in turn should outperform the UPGMA method. In practice, the neighbor-joining performs extremely well.

The maximum parsimony (MP) method

The MP method, together with the maximum likelihood (ML) method, is character-based instead of distance-based. The most advanced implementation of the MP method is PAUP (Swofford 1993; Swofford 2000). The most parsimonious tree is one that can explain the nucleotide or amino acid differences in aligned sequences

with the fewest number of substitutions. It is the only method in which the exhaustive search and branch-and-bound search algorithms have been used in practice.

The main problem with the MP method is that it can be inconsistent. In statistical terms, an estimator (e.g., a mean, a variance, a tree topology, i.e., the branching pattern of a phylogenetic tree) is evaluated with three criteria: (1) consistency, (2) efficiency, and (3) bias. Consistency means that the estimator will approach the true value when the sample size increases to infinity. Efficiency is measured by the variance associated with the estimator. The smaller the variance, the more efficient the estimator is. An estimator that hits the bull's eye (the true value) is efficient, and one that spreads the bullets around the bull's eye is not. Bias is the expected deviation from the bull's eye. For point estimators such as mean or variance, bias is measured by the degree of underestimation or overestimation. A desired estimator is one that is consistent, efficient and unbiased. For illustration, suppose we want to estimate the variance of body height of a population of male freshmen based on a sample of n individuals. The maximum likelihood estimator of the variance is

$$s^2 = \frac{\sum_{i=1}^{n}(x_i - \bar{x})^2}{n} \qquad (10.1)$$

The estimator, however, is biased (The unbiased estimator has its denominator being n-1 instead of n). However, the estimator is consistent because, when n increases to infinity, the difference between n and n-1 becomes increasing negligible. You may also note that the unbiased maximum likelihood estimator with n as the denominator leads to a smaller variance than the unbiased estimator with n-1 as the denominator. In this sense, the maximum likelihood estimator is more efficient, but the efficiency in this particular case is gained at the cost of a bias.

The MP method has been demonstrated to be inconsistent (Felsenstein 1978), and the inconsistency is largely due to the so-called long-branch attraction which refers to the phenomenon when two highly diverged non-sister taxa are clustered together erroneously as sister taxa. It is associated most frequently with the maximum parsimony method, but can also occur with the distance-based or maximum likelihood method.

The maximum likelihood (ML) method

The ML method was championed by Joe Felsenstein and popularized by his DNAML program in the PHYLIP package (Felsenstein 2014). The criterion in maximum likelihood is that the estimate that maximizes the probability of observing the data is the best estimate. For example, if you want to estimate the proportion of males (p) in a fish population and you catch 10 fish with 5 being males, then your ML estimate of p is 0.5. Of course there is nothing preventing you from claiming that p = 0.1, but it is more likely to observe 5 males out of 10 fish with p = 0.5 than with p = 0.1.

Maximum likelihood methods are always model-based. For example, in the example of estimating p above, we typically would assume a binominal distribution in order to computing the likelihood of observing 5 males out of 10 fish with a given p. In molecular phylogenetics, the observation is the set of aligned sequences, and the equivalent of p is the topology. The best topology is one that maximizes the likelihood of observing the set of aligned sequences.

The performance of the ML method in molecular phylogenetics mainly depends on two factors, the substitution model and the thoroughness in searching through the tree space. The ML method is slower than the distance-based or MP methods and consequently can only evaluate a relatively limited number of possible trees in practice. For this reason, a 'ML' tree may be worse than a distance-based or MP tree. Theoretically, it should be the best method when one has sufficient data and sufficient computing power.

For detailed information on these different methods, as well as a simple numerical illustration of the Bayesian inference, please consult my book (Xia 2007a, Chapter 13).

Bootstrapping and jackknifing

Publications in molecular phylogenetics often would report not only a reconstructed tree, but also information on how confident we are about the tree. One frequently used measure of confidence about tree topology (actually confidence about subtrees) is by the resampling methods such as bootstrapping and jackknifing (Efron 1982), first introduced to phylogenetics by Felsenstein (Felsenstein 1985).

The bootstrap resampling involves the site-wise re-sampling of the aligned sequences with replacement, so that sequences of N sites long will be resampled N times to generate a new set of aligned sequences of the same length, with some sites in the original sequences sampled one or more times while some other sites do not get

sampled at all. The delete-half jackknifing technique will randomly purge off half of the sites from the original sequences so that the new set of aligned sequences will be half as long as the original. Such resampling procedure will typically be repeated a large number of times to generate a large number of new samples.

Each new sample (i.e., new set of aligned sequences), no matter whether it is from bootstrapping or jackknifing, will then be subject to regular phylogenetic reconstruction. The frequencies of subtrees will then be counted from reconstructed trees. If a subtree appears in all reconstructed trees, then the bootstrapping or jackknifing value is 100% for that sub tree, i.e., the strongest possible support for the subtree.

Note that results from resampling (either bootstrapping or jackknifing) will typically not be the same, especially with a small number of resampled data sets. The result will be more similar with increasing number of resampled data sets

Although the bootstrap and the jackknife generally produce similar results, there are some subtle differences. Suppose that we have a set of aligned sequences of N sites long. For the bootstrap resampling, the probability of each site being sampled is 1/N, and the mean number of times a site gets sampled in each bootstrapping resampling is simply one. Thus, a site gets sampled 0, 1, 2, ..., N times follows a Poisson distribution with a mean equal to one. This implies that about 37% of the sites will not be sampled, while 63% of the sites will be sampled at least once. In jackknifing, we have 50% of the sites not sampled and the other 50% of the sites sampled just once. Thus, a jackknifed sample is expected to be less similar to the original sample than a bootstrapped sample. Consequently, jackknifed samples may be less similar to each other than bootstrapped samples.

Phylogenetic reconstruction with a global molecular clock

Molecular phylogenetics has two major objectives, i.e., elucidating the ancestor-descendent relationships among different species and homologous genes, and dating speciation events and gene duplication events. Dating assumes the existence of a molecular clock, either local or global. The existence of a global clock simplifies much computation.

There are several methods that can generate a tree with a global clock. These include the distance-based methods such as UPGMA and Kitsch (in the PHYLIP package) and maximum likelihood methods such as DNAMLK (in the PHYLIP package). A tree with a molecular clock allows its branches to be calibrated by dated fossils.

OBJECTIVES

Distance-based, MP and ML methods

Different phylogenetic reconstruction methods, with different criteria of choosing the tree, may produce different trees, and are useful in different situations. You should keep in mind that all methods are good when they have been used properly. You will develop an empirical appreciation of the strength and weakness of different phylogenetic methods after this lab.

Bootstrap/ jackknife to evaluate subtree reliability

It is always desirable to know how well a phylogenetic tree is supported. There are two approaches to show how a tree is supported. If you have several alternative trees and wish to know the relative statistical support of these trees, then there are a variety of significance tests that can be used. On the other hand, if you wish to know how well different subtrees are supported, then bootstrap or jackknife values are the most frequently used indices. You will be able to attach bootstrap or jackknife values to subtrees after this lab, by using either distance-based, maximum parsimony or maximum likelihood methods for phylogenetic reconstruction.

Phylogenetics assuming a global molecular clock

The distance-based method UPGMA always assumes a global molecular clock. One may also force a molecular clock in the maximum likelihood framework. You will be able to use the UPGMA method or the maximum likelihood method to construct trees with a global molecular clock after this lab.

PROCEDURES

Two sequences files that we are going to use in this lab are included as sample files in the DAMBE installation package. They contain mitochondrial COI and CytB gene sequences from eight vertebrate species (fish: *Masturus lanceolatus*; human: *Homo sapiens*; cow: *Bos Taurus*; whale: *Balaenoptera musculus*; orangutan: *Pongo pygmaeus*; chimpanzee: *Pan troglodytes*; chicken: *Gallus gallus*; alligator: *Alligator mississippiensis*). The two files are in FASTA file format and can be found in DAMBE installation directory, typically C:\Program Files\DAMBE for 32-bit PC or C:\Program Files (x86)\DAMBE for 64-bit PC:

1. VertCOI.FAS. This file contains aligned mitochondrial COI (cytochrome subunit I) sequences from the eight vertebrate species,

2. VertCytB.FAS: This file contains unaligned mitochondrial Cyt-b (cytochrome b) sequences from the eight vertebrate species. It is for you to practice nucleotide sequence alignment and codon sequence alignment guided by aligned amino acid sequences.

Distance-based method

Phylogenetic reconstruction: To construct the phylogeny of the eight vertebrate species, read into DAMBE the sequences in VertCOI.FAS by clicking 'File|Open standard sequence file' and open the VertCOI.FAS file. Click 'Phylogenetics|Distance methods|nucleotide sequences'. In the dialog box for you to set options, set the genetic distance to the TN93 distance (the default in earlier versions of DABE), or MLCompositeTN93 (default in latter versions), the tree-building algorithm to FastME (default), and *Masturus lanceolatus* as the outgroup. Click the 'Run' button to build the tree. The resulting tree (Fig. 10-2) represents a well-corroborated phylogenetic relationship among the eight species ('well-corroborated' is synonymous to 'almost certainly correct'). You may copy and paste the resulting tree to a PowerPoint slide.

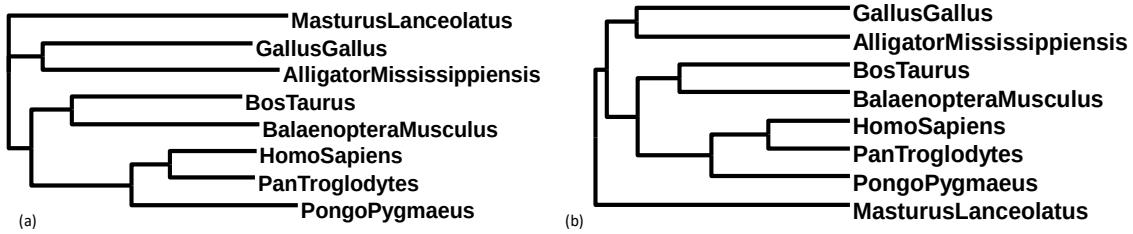

Fig. 10-2. Phylogenetic trees constructed with the TN93 distance, with the unrooted tree (a) from the FastME method and the rooted tree (b) from UPGMA.

Now you may change options in two ways. One is by changing the tree-building algorithm, e.g., from FastME that do not assume a molecular clock to UPGMA which assumes a global molecular clock. The tree built with the UPGMA method is shown in Fig. 10-2b. The other is by changing genetic distances the simplest P distance to the more complicated GTR distance (which is derived from the General Time Reversible substitution model). Do these changes lead to the same tree?

Note that the UPGMA method assumes a global molecular clock, so all OTUs are of equal distance to the root. Before we use any method that assumes a molecular clock, we typically would test the validity of the molecular clock hypothesis first. There are two tests of the clock hypothesis, the relative-rate test and the tree-based test. This topic is covered in another laboratory. If the clock hypothesis is not rejected, then we can use dated fossils to derive divergence time between different species. Dating speciation events or gene duplication events is a subject covered latter in the laboratory manual.

You can copy and paste the tree from DAMBE to PowerPoint slides or any other graphic programs including EXCEL and WORD, either in fixed-resolution bitmapped format or in high-resolution Windows metafile format. The latter should be used for formal presentation or publication. See Appendix 1 Copy trees from DAMBE to PowerPoint slides for details.

In general, a set of sequences with strong phylogenetic signals will often be able to recover the true tree with most combinations of tree-building algorithms and distances. Vertebrate mitochondrial COI is considered to have strong phylogenetic signals and, for this reason, has been used in nearly all barcoding projects for vertebrates.

The distance-based method is typically more resistant to the long-branch attraction problem haunting the maximum parsimony method (Felsenstein 1978; Xia 2007a, pp. 277-279). However, distance-based methods may also become inconsistent when distance estimation is biased. For example, underestimation of distances

will also lead to long-branch attraction for phylogenetic methods using either the minimum evolution criterion or the Fitch-Margoliash criterion (Xia 2006).

A substitution model simpler than the true model will tend to underestimate the genetic distances between OTUs, and such underestimation will be more severe between highly diverged OTUs than between closely related OTUs. This will lead to long-branch attraction and wrong topology. For this reason, we should aim to use genetic distances appropriate for the data to increase the accuracy of the genetic distances.

Bootstrapping and jackknifing: To do bootstrapping or jackknifing using the distance method on vertebrate COI sequences, click 'Phylogenetics|Distance methods|nucleotide sequences'. In the dialog box (Fig. 10-3), set the distance to 'TN93' or 'GTR', outgroup to *Masturus lanceolatus*, and tree-building method to FastME (the default). Check the 'Resample (bootstrap, jackknife' check box, and you will see the default resampling method (bootstrapping) and the default number of resampled data sets (100).

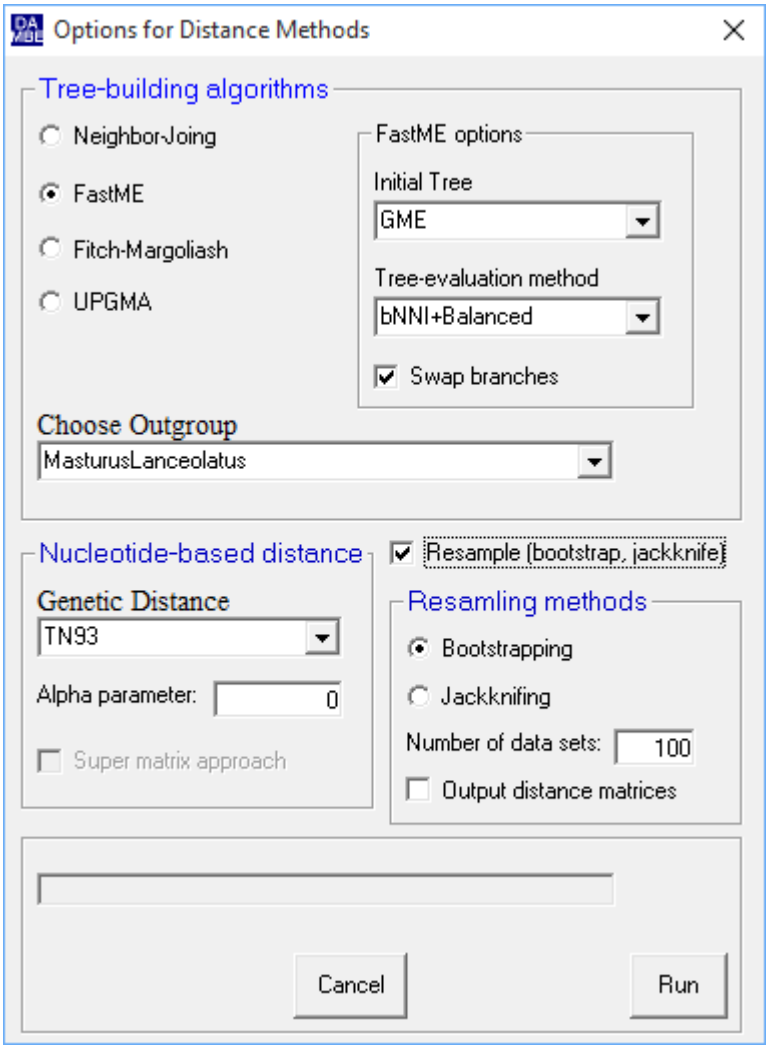

Fig. 10-3. Setting options for generating a tree with bootstrap values.

Click the 'Run' button to obtain a tree with bootstrap values (Fig. 10-4). A value of 90 or higher associated with a subtree is generally taken as strong statistical support for the subtree. You may now do resampling with jackknife for comparison.

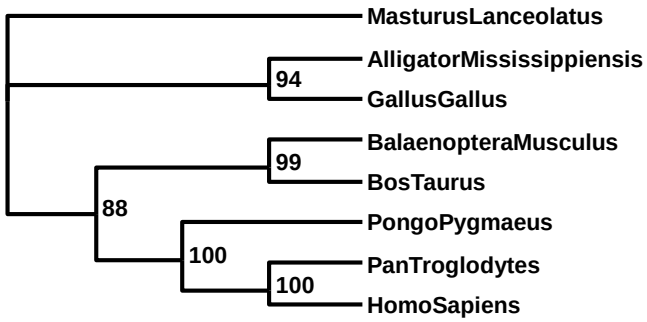

Fig. 10-4. Distance-based tree (FastME on GTR distances) with bootstrap values in percentage.

Maximum parsimony (MP) method

Construct an MP tree: Click 'Phylogenetics|Maximum parsimony|DNAMP'. A dialog box (Fig. 10-5) appears for you to set the parameters. Again set *Masturus lanceolatus* as the outgroup. Don't check the 'Resampling Statistics' check box. Click the 'Go!' button to perform the MP construction. DAMBE will report to have found one most parsimonious tree, with 1427 steps. In terms of topology, this MP tree is identical to Fig. 10-2b.

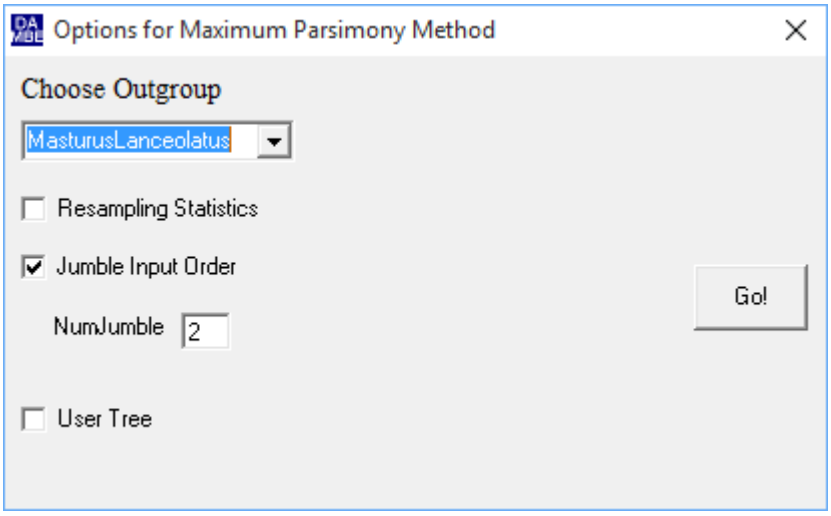

Fig. 10-5. Dialog box for options in MP analysis.

Note that there is no explicit substitution model associated with the MP method because the MP method does not explicitly assume a substitution model. However, sometimes a substitution process is assumed by using a step matrix. The most frequently used step matrix treats transitions and transversions differently.

There is no commonly accepted way of treating indels in the MP and the ML method. The common practice is to delete all indel-containing sites, as shown in Fig. 10-6. However, this approach has two problems. First, DNA sequences often have conserved regions and variable regions. Few substitutions occur at conserved regions which consequently contain little phylogenetic information. Most substitutions occur at the variable region. Unfortunately, variable regions also often experience indel events, and the site-wise deletion of indel-containing sites throws out the baby with the bath water. Second, recall that likelihood-based methods for nucleotide sequences require a substitution model and estimated nucleotide frequencies. The nucleotide frequencies at the variable regions should be the most relevant for computing likelihood. However, site-wise deletion of indel-containing sites leave the nucleotide frequencies dominated by those of the conserved regions that often have nucleotide frequencies different from those at the variable regions. You might also notice that, after deleting the indel-containing sites, Seq1 and Seq3 have become identical, so are Seq2 and Seq4. Any phylogenetic program will now group Seq1 with Seq3 and Seq2 with Seq4, contrary to what we would have expected by inspecting the aligned sequences in the left of Fig. 10-6.

```
Seq1 AAC--GT--ACCGGTT          Seq1 AACGTACCGGTT
Seq2 AAC--GT--ACCAGTT          Seq2 AACGTACCAGTT
Seq3 AACCGGTTAACCGGTT  ------> Seq3 AACGTACCGGTT
Seq4 AACCGGTTAACCAGTT          Seq4 AACGTACCAGTT
```

Fig. 10-6. Site-wise deletion of indel-containing sites.

In this context, the distance-based methods can use more information. For example, the genetic distance between Seq3 and Seq4 (Fig. 10-6) can be calculated with all 16 sites instead of only 12 sites after the site-wise deletion, and the variable sites do contribute to the nucleotide frequencies. How to make the best use of information at indel-containing sites is still a hot research topic.

I should mention that keeping indel-containing sites may also lead to bias. For example, if one sequence has experienced extensive deletion events at its variable sites so that almost all of its variable sites have been lost, i.e., only conserved sites are left. The genetic distance between this sequence and all other sequences will therefore be extraordinarily small whereas pairwise distances among those sequences with their variable sites present will be relatively large. While this is a theoretically possible scenario, the problem has been rarely been demonstrated (Van de Peer, et al. 1993).

Attach bootstrap/jackknife values to an MP tree: To generate a maximum parsimony tree with bootstrap values, click 'Phylogenetics|Maximum parsimony|DNAMP'. In the dialog box for you to set the parameters, set *Masturus lanceolatus* as the outgroup. Check the 'Resampling statistics' check box, as is shown in Fig. 10-7. Click the 'Run' button, and you will get a tree with bootstrap values similar to those in Fig. 10-4.

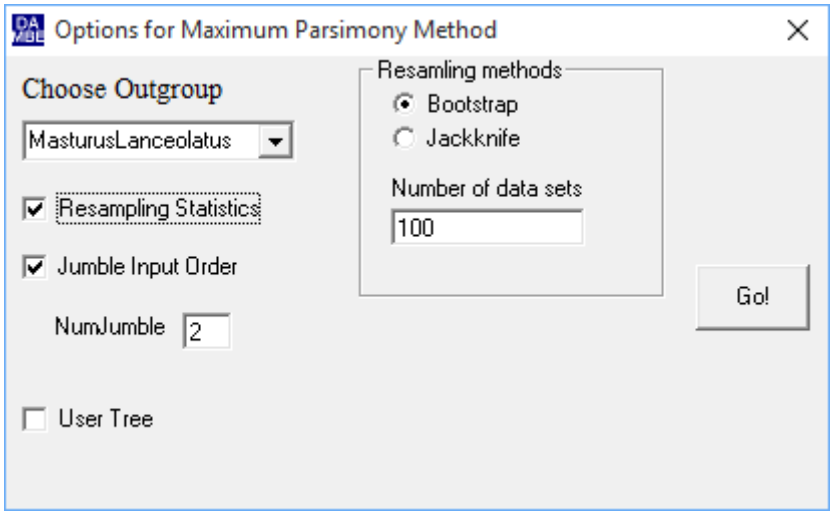

Fig. 10-7. Setting options for producing a maximum parsimony tree with bootstrap values in DAMBE.

Maximum likelihood (ML) reconstruction with bootstrap/jackknife

Read in the 'VertCOI.FAS' file and click 'Phylogenetics|Maximum likelihood|DNAML' to perform phylogenetic analysis with the ML method. The substitution model is F84, which allows different transition and transversion rates in the form of a transition/transversion ratio. You may specify such a ratio or let DAMBE estimate the ratio (Fig. 10-8). Set the outgroup to 'MasturusLanceolatus' sequences. If you wish to produce a ML tree with bootstrap values, you can check the 'Resampling' check box and specify either 'Bootstrap' or 'Jackknife' and the number of resampled data sets. Click the 'Run' button to run to build the tree. You should obtain a tree with topology similar to that in Fig. 10-2a. If you wish to obtain bootstrap values, click the 'Resample' check box before clicking the 'Run' button.

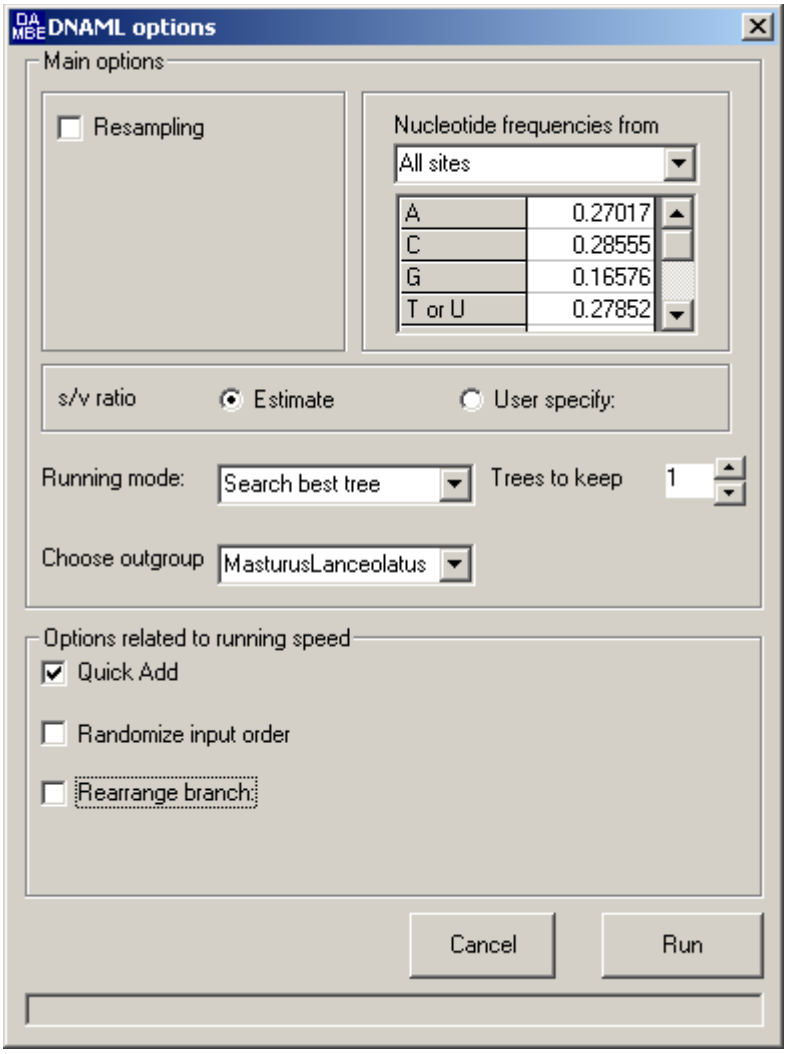

Fig. 10-8. Setting options for phylogenetic analysis with the maximum likelihood method in DAMBE.

Work with the VertCytB.FAS file

The cytochrome-b gene in vertebrates is generally considered to have a weaker phylogenetic signal than the COI gene. You will now explore this sequences by doing the following:

1. Read in the VertCytB.FAS file.
2. Align the sequences by clicking 'Alignment|Align sequences by using ClustalW'
3. Using a distance-based method (e.g., FastME+MLCompositeF84), DNAMP and DNAML to reconstruct the tree. Do the resulting trees show the same phylogenetic relationship as that in Fig. 10-2a?
4. Now read in VertCyb.FAS file again to replace the aligned sequences already in DAMBE's buffer.
5. Translate into amino acid sequences.
6. Align the amino acid sequences
7. Click 'Alignment|Align nuc. seq. to aligned AA seq in buffer' and follow what you have done in a previous laboratory on sequence alignment.
8. Using a distance-based method (e.g., FastME+MLCompositeF84), DNAMP and DNAML to reconstruct the tree. Do the resulting trees show the same phylogenetic relationship as that in Fig. 10-2a?
9. In general, you will find that DNAML is better than the distance-based or maximum parsimony method. Within distance methods, simultaneously estimated distances (e.g, MLCompositeF84 and MLCompositeTN93) are better than independently estimated distances (e.g., F84 and TN93). However, the former takes much longer to compute than the latter.

MORE QUESTIONS

1. By which two categories of parameters do substitution models differ from each other?
   Answer: Frequency parameters and rate parameters.
2. What approaches can we take to determine which substitution model is appropriate for our sequence data?
   Answer: 1) empirical approach by counting the frequencies of different types of identical sites and different sites and check whether transitions occurs more frequent than transversions, whether the two types of transitions are different, etc., and 2) statistical approach for model selection by using information theoretic indices or likelihood ratio test (if the models are nested).
3. Is a genetic distance based on a complicated substitution model always better than one based on a simple model?
4. What are the key differences between UPGMA and FastME algorithms?
5. Use the following distance matrix to manually construct a UPGMA tree with branch lengths indicated on the branches.

	Gene1	Gene2	Gene3	Gene4	Gene5
Gene1	0.00	0.01	0.04	0.16	0.19
Gene2		0.00	0.03	0.14	0.17
Gene3			0.000	0.12	0.13
Gene4				0.00	0.02
Gene5					0.00

6. Given the following distance matrix and the topology for four species designated as S1-S4, evaluate the branch lengths by using the least-square method, and compute the tree length.

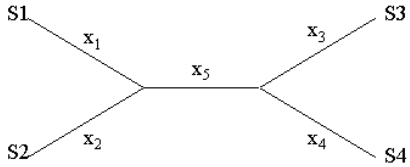

Sp1			
Sp2	0.3		
Sp3	0.4	0.5	
Sp4	0.4	0.6	0.6

7. Does a genetic distance such as the TN93 distance between two molecular sequences measure the divergence time between the two sequences?
8. What does long-branch attraction mean? Is it a problem associated only with the maximum parsimony method?
   Answer: Long-branch attraction refers to the phenomenon in phylogenetics when two highly diverged non-sister taxa are clustered together erroneously as sister taxa. It is associated most frequently with the maximum parsimony method, but can occur with the distance-based or maximum likelihood method as well.
9. In distance-based method, is tree length the summation of all branch lengths or the summation of all pairwise genetic distances?
10. Which four categories of phylogenetic methods are currently used?
    Answer: 1) distance-based, 2) maximum parsimony, 3) maximum likelihood, 4) Bayesian inference.
11. Is transition probability matrix in a Markov chain a matrix of the probabilities of transitional substitutions?
12. Substitution models are the most fundamental in molecular phylogenetics. What are the major differences between the JC69 model and the F84 model in terms of frequency and rate parameters?
13. When you produce your own bootstrapped tree, will the bootstrap values be the same as those in Fig. 4? Explain why the bootstrap values on your tree could be different from those in Fig. 4. Will the difference become smaller or larger when you increase the number of bootstrap samples (e.g., from the default 100 to 500)?
14. A biologist documented the following empirical substitution pattern after building a phylogenetic tree, reconstructing the ancestral sequences, and performing pairwise sequence comparisons between neighboring nodes. The values on the diagonal are number of sites where both sequences have identical nucleotides, and

those off-diagonal ones are number of differences, e.g., the value 20 corresponding to nucleotides A and G means that there are 20 sites where one sequence is A and the other is G. What would be a suitable substitution model for this set of sequences? Give reasons.

	A	G	C	T
A	3333	20	2	2
G		3322	3	3
C			3344	100
T				3323

LAB 11 TESTING THE MOLECULAR CLOCK HYPOTHESES

INTRODUCTION

Molecular phylogenetics has two objectives, one being the characterization of the branching patterns (cladogenic events, specifically the speciation and gene duplication events) in evolution, and the other being the dating of these speciation or gene duplication events. Dating assumes the existence of a molecular clock in which each nucleotide or amino acid substitution is equivalent to a tick in a mechanical clock, although a tick in a molecular clock often takes thousands of years or even longer.

Mutation and substitution

It is important to recognize the difference between mutation and substitution. A mutation is any change to the genetic material such as DNA, whereas a substitution is the process whereby a new mutant allele completely replaces the wild type allele in a population. Obviously, substitutions occur much less frequently than mutations.

Most mutations will be lost after only a few generations. A lethal mutation is lost within a single generation. The probability of a new mutant allele eliminating all the alternative alleles and become 'fixed' is termed fixation probability. The rate of nucleotide substitution is the number of fixations occurring in a species per nucleotide site per unit time. In genetics, a substitution is synonymous to a fixation event and substitution rate is synonymous to fixation rate.

Different mutations may have very different fixation probabilities. If a mutation changes a functionally important amino acid and disrupts the function of a key enzyme, then mutation is deleterious or even lethal, and the mutant will leave few or no offspring (or said to be eliminated by negative or purifying selection). Such a lethal mutation will have a fixation probability of 0. Only those individuals that do not carry the mutation will survive to generate the next generation.

The molecular clock hypothesis

The molecular clock hypothesis claims that the substitution rate is roughly constant over time. However, many factors can contribute to variation in substitution rate. In particular, the same nucleotide site can experience different substitution rates during different geological time (heterotachy) or different nucleotide sites can have different substitution rates (rate heterogeneity over sites).

Heterotachy: Heterotachy refers to the variation in substitution rates over time for a given site or a given group of sites (Lopez, et al. 2002). Changes in functionally important amino acid sites are often deleterious, and substitution rates at these sites are typically very low. However, sometime a dramatic environmental change may favour some amino acid replacements, and these functionally important sites may experience a number of changes in a short period of time in response to the changed selection pressure. Heterotachy is a chief contributor to the violation of the molecular clock hypothesis.

Rate heterogeneity over sites: Functionally important sites typically evolve more slowly than functionally unimportant sites. In protein-coding genes, the second codon position where any change will lead to nonsynonymous substitutions (i.e., amino acid replacement) typically evolve much slower than the third codon position where nucleotide changes will often be synonymous (Xia 1998b). These different sites represent different molecular clocks.

For example, among 190 possible codon substitutions involving a single nucleotide change in the vertebrate mitochondrial genetic code, 54 are transitions and 136 are transversions (Table 11-1). Among the 54 transitions, 26 are at the first codon positions with a mean Miyata's distance (Miyata, et al. 1979) of 1.20. Miyata's distance measures amino acid dissimilarity based on volume and polarity, with a larger value corresponding to greater difference between the two amino acids. In contrast, 28 transitions are at the second codon position with a mean Miyata's distance equal to 2.16. In other words, transitions at the first codon position involve more similar amino acid replacement than those at the second codon position. The same trend is visible with the 136 transversions (Table 11-1).

All transitions at the third codon position are synonymous in vertebrate mitochondrial genomes. For the 24 nonsynonymous transversions at the third codon position, the mean Miyata's distance (= 1.22, Table 11-1) is close to that at the first codon position (= 1.49, Table 11-1). Thus, the second codon position is much more functionally constrained than the third and the first codon positions in vertebrate mitochondrial genomes. Consequently, the substitution rates at the first, second and third codon positions, designated r_1, r_2 and r_3, respectively, are typically in the pattern of $r_3 > r_1 > r_2$.

Table 11-1. Distribution of transitions and transversions at the three codon positions for 190 possible codon substitutions involving a single nucleotide change in vertebrate mitochondrial genomes. Generated from DAMBE.

CP[1]	1	2	3	Subtotal	Prop
s[2]	26	28	0	54	0.2842
MeanD[3]	1.20	2.16	0.00	1.70	
VarD[4]	0.73	0.54	0.00	0.85	
v[5]	56	56	24	136	0.7158
MeanD[3]	1.49	2.36	1.22	1.80	
VarD[4]	1.74	0.76	1.21	1.46	
Sum	82	84	24	190	

(1) CP: codon position
(2) s: transition
(3) MeanD: mean of Miyata's distances
(4) VarD: variance of Miyata's distances
(5) transversion

Rate heterogeneity over sites does not directly violate the molecular clock hypothesis. Whenever some sites are functionally constrained, there is a chance for the sites to be more or less constrained in different lineages experiencing different selection regimes. This will lead to violation of the molecular clock. In contrast, if all sites are not constrained or only weakly constrained throughout evolutionary history, such as the third codon position, then violation of the molecular clock is less likely. For this reason, third codon position should serve as a better molecular clock than first or second codon positions. In any case, we need to test the molecular clock hypothesis instead of assuming it.

Statistical tests of the molecular clock hypothesis

The relative-rate test: A relative-rate test is used when one is interested in testing whether two lineages are evolving at the same rate. In principle, a relative-rate test involves only two ingroup taxa and one outgroup taxon, and consequently does not require a tree. The purpose of the test is to find out whether the two ingroup taxa have evolved at the same rate.

What are ingroup taxa? What is an outgroup? Ingroup taxa are the taxa we are interested in learning more, e.g., the phylogenetic relationship among the taxa, the evolutionary rates among different lineages leading to these taxa, etc. An outgroup is one or more species that does not belong to the ingroup. For example, if our ingroup is made of primate species, then a species that is not a primate would be a valid outgroup (assuming that primates form a monophyletic group). An ideal outgroup is not only an outgroup but also phylogenetic as close as possible to the ingroup. For example, if our ingroup is made of the great apes, then both *Escherichia coli* and Macaca mulatta (Rhesus monkey) are valid outgroups, but Rhesus monkey would make a much better outgroup than *E. coli*. Thus, although a relative-rate test does not require a tree, it is very helpful to have a tree with the two ingroups and species closely related to the ingroup for choosing a good outgroup.

Why should an ideal outgroup be closely related to the ingroup? You may get an intuitive understanding by the following analogue. When I stand by the podium in a classroom, I can see that those students sitting in the front row of seats are physically close to me than those sitting in the back row of seats. However, if I look at the students in the classroom from 100 km away, then all what I see would be a blur, and it would be impossible to tell which student is physically closer to me than others. The outgroup represents the position we stand to view the two ingroups to see which one has evolved faster away from us. If our outgroup is *E. coli*, then the two ingroups such as human and chimp would merge into a blur and the relative-rate test will often fail to give us the correct answer as to which one has evolved faster. However, a rhesus monkey as a an outgroup will substantially improve our resolution.

There are two relative-rate tests implemented in DAMBE, with one based on nucleotide substitution model (Muse and Weir 1992) and the other on codon-based model (Muse and Gaut 1994). For the nucleotide-based model, both the transitional substitution rate and the transversional substitution rate are tested. For the codon-based model, both the synonymous substitution rate and the nonsynonymous substitution rate are tested.

The statistical rationale of a relative-rate test is illustrated in Fig. 11-1, where α and β are used to designate transitional and transversional substitution rates, respectively. Assuming the HKY85 substitution model and a molecular clock, we expect $\alpha_1 = \alpha_2$ and $\beta_1 = \beta_2$. We first test whether this model (Model 2 in Fig. 11-1) is significantly worse than the general model (Model 1 in Fig. 11-1) that does not force $\alpha_1 = \alpha_2$ and $\beta_1 = \beta_2$. It is clear that the two models are nested, i.e., Model 2 is a special case of Model 1 when $\alpha_1 = \alpha_2$ and $\beta_1 = \beta_2$, so a

likelihood ratio test is appropriate. Note that the two models differ in the number of parameters, with Model 1 having four free parameters and Model 2 having only 2.

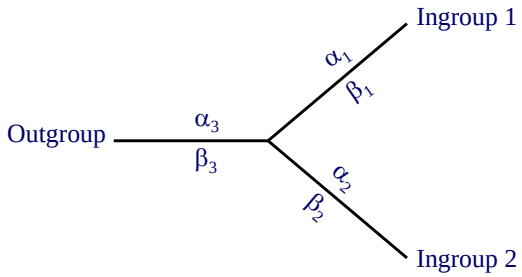

Model 1: General model: $\alpha_1, \alpha_2, \beta_1, \beta_2$ (4 parameters)

Model 2: Constraint both: $\alpha_1 = \alpha_2 = \alpha, \beta_1 = \beta_2 = \beta$ (2 parameters)

Model 3: Constrain α: $\alpha_1 = \alpha_2 = \alpha, \beta_1, \beta_2$ (3 parameters)

Model 4: Constrain β: $\alpha_1, \alpha_2, \beta_1 = \beta_2 = \beta$ (3 parameters)

Likelihood ratio test: $X^2 = 2\Delta\ln L$, DF = ΔParameter

Fig. 11-1. Statistical essence of the relative-rate test.

In carrying out the likelihood ratio test, we compute the log-likelihood (lnL) for Model 1 and Model 2. The statistic equal to $2(\ln L_{Model1} - \ln L_{Model2})$ follows approximately the chi-square distribution when sequences are long, with the degrees of freedom being the difference in the number of parameters between the two models, i.e., 2. The null hypothesis (H_0) being tests is that Model 2 fits the data just as well as Model 1.

If H_0 is not rejected, then we conclude that the molecular hypothesis is not violated, i.e., the two ingroups have similar transition and transversion rates. If H_0 is rejected, then we have three possibilities. First, the two ingroups differ in the transition rate. Second the two ingroups differ in the transversion rate. Third, they differ in both.

In order to narrow down our conclusion, Model 1 is compared to Model 3 and Model 4. Model 3 forces $\alpha_1 = \alpha_2$ but not $\beta_1 = \beta_2$, and Model 4 forces $\beta_1 = \beta_2$ but not $\alpha_1 = \alpha_2$. If both Model 3 and Model 4 are rejected, then we conclude that the two ingroups differ in both transition and transversion rates. If Model 3 is rejected but Model 4 is not, we conclude that the two ingroups differ in the transition rate. If Model 4 is rejected but Model 3 is not, we conclude that the two ingroups differ in transversion rate.

We have previously mentioned that we should prefer an outgroup that is phylogenetically as close as possible to the ingroup. There are two main reasons of which one has mentioned before. The other reason is the test assumes that the outgroup species has evolved with the same substitution process as the two ingroup species, and a closely related outgroup is more likely to satisfy this assumption than a remotely related species.

For protein-coding genes, α and β in Fig. 11-1 stand for synonymous and nonsynonymous substitutions, respectively. The test procedure and the interpretation are the same, although the codon-based test takes much longer to compute than the nucleotide-based test.

Phylogeny-based test: Dating speciation events or gene duplication events requires (1) a phylogenetic tree, (2) either a set of aligned sequences or a matrix of pairwise distances, and (3) one or more calibration points, either based on fossil record or on previous estimates from other data. The most critical assumption for dating is that the sequences accumulate substitutions in a clock-like manner or that the pairwise distance is a linear function of time. This assumption needs to be validated before we can proceed to date speciation or gene duplication events. Validating this assumption requires a phylogeny-based test instead of a relative-rate test.

Take the tree in Fig. 11-2 for example with four species designated by 1, 2, 3 and 4. If we know that T_1 is 9 million years from present based on fossil record, and that the branch length from species 1 and 2 to their common ancestor is 1/3 of the branch length from species 4 to the root, then we may infer $t_3 = T_1/3$, i.e., species 1 and 2 have diverged 3 million years ago. The assumption here is that the lineages leading from the root to the four descendent species have all experienced the same number of substitutions, i.e., the clock along the lineages ticks at the same speed. This is an assumption that needs to be tested with a phylogeny-based test, which can be done either with aligned sequence data or with a matrix of evolutionary distances properly adjusted to be linear with time.

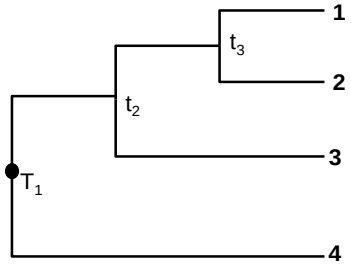

Fig. 11-2. A 4-species tree illustrating dating speciation events.

Sequence-based likelihood ratio test: The likelihood ratio test is also used to perform tree-based test of the molecular clock hypothesis. The rationale is that the tree assuming a molecular clock is a special case of the tree without assuming a molecular clock. The two trees differ in the number of branches that needs to be estimated. With n OTUs (operational taxonomic units), the number of branches is (2n – 3) for a tree without assuming a molecular clock and (n - 1) for a tree assuming a clock (Fig. 11-3). Thus the difference in the number of parameters is (2n-3) – (n-1) = n – 2. Thus, designating the log-likelihood for the tree assuming a clock as $\ln L_{Clock}$ and that without assuming a clock as $\ln L_{NoClock}$, we compute the statistic $\chi^2 = 2(\ln L_{NoClock} - \ln L_{Clock})$ and test for significance with n – 2 degrees of freedom.

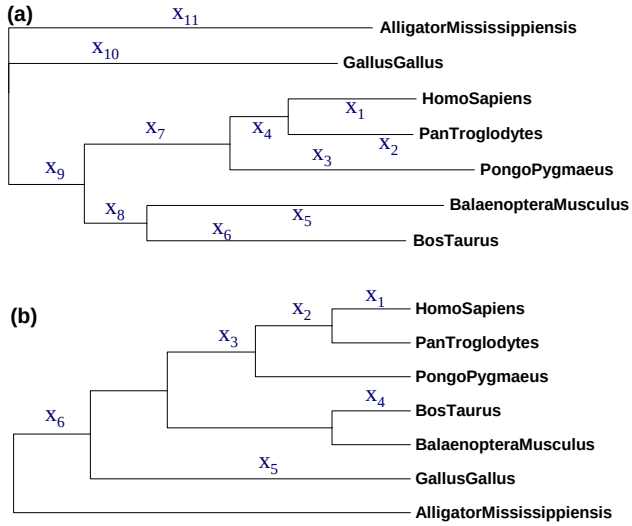

Fig. 11-3. Phylogenetic trees without assuming a molecular clock (a) and assuming a molecular clock (b) for illustrating the likelihood ratio test of the molecular clock hypothesis.

As shown in Fig. 11-3, a tree-based test of molecular clock hypothesis requires two trees: (1) a rooted tree (Fig. 11-3b) with all internal nodes bifurcating and all lineages evolving at the same rate, and (2) an equivalent unrooted tree with a trifurcating root (Fig. 11-3a) and with different lineages allowed to evolve at different rates. The sequence-based likelihood ratio test fits the sequence data to the rooted and unrooted tree by maximizing the likelihood and tests whether the unrooted tree can fit the data significantly better than the rooted tree by the likelihood ratio test. Similarly, the distance-based LS method fits the distance matrix to the rooted and the unrooted tree by minimizing the residual sum of squares and check whether the unrooted tree can fit the distance matrix significantly better than the rooted tree (Xia 2009). Both methods can also use information-theoretic indices such as AIC or its derivatives such as AICc and AICu (Burnham and Anderson 2002; Xia 2009)].

Distance-based least-squares (LS) method: Matrices of evolutionary distances are frequently used in molecular phylogenetic reconstruction. Evolutionary distances arise from many sources. First, distances can be estimated from molecular sequences. Second, it can be computed from many conventional types of data such as DNA hybridization, restriction fragment length polymorphism, and gene frequency data (especially microsatellite data used to characterize genetic differentiation among populations). Third, many so-called whole-genome phylogenetic methods are based on genetic distances such as genome BLAST distances (Henz, et al. 2005; Auch, et al. 2006; Deng, et al. 2006), breakpoint distances based on genome rearrangement (Herniou, et

al. 2001; Gramm and Niedermeier 2002), distances based on the relative information between unaligned/unalignable sequences (Otu and Sayood 2003), distances based on the sharing of oligopeptides (Gao and Qi 2007), and composite distances incorporating several whole-genome similarity measures (Lin, et al. 2009).

An information-theoretic index named AICu as well as an approximate significance test has been proposed to test whether a global clock operates over a phylogeny(Xia 2009). The method is based on the least-squares (LS) framework. We will not bother with the computational or mathematical details of testing the global clock with the LS method, which can be found elsewhere (Xia 2009). However, it is important to get the essence of the conceptual framework behind the test. In general, all tests of the molecular clock involve three steps which are all automated in DAMBE. These steps are detailed below.

First, we need a rooted and an unrooted tree as shown in Fig. 11-3. The trees naturally should be well-corroborated. If you have a good unrooted tree with the root node trifurcating (e.g., the topology in Fig. 11-3a), which is the tree from phylogenetic methods assuming no molecular clock, you can obtain a rooted tree by dragging two of the three daughter nodes to each other (e.g., GallusGallus and the ancestral node for the five mammalian species in Fig. 11-3a). A rooted tree can be made unrooted by 'de-rooting' the bifurcating root node, i.e., by making it trifurcating. We designate the rooted tree by T_c and the unrooted tree by T_{nc}, where the subscript c and nc designate clock and non-clock, respectively.

Second, fit the molecular data (sequence data or distance data) to T_c assuming a molecular clock and to T_{nc} without assuming the clock, and use an index to measure how well the data fit the trees. In the likelihood ratio test, this index is the log-likelihood (designated by $\ln L_c$ and $\ln L_{nc}$, respectively, for fitting data to T_c and T_{nc}). In the test based on the LS criterion, the index is the residual sum of squares (designated by RSS_c and RSS_{nc}, respectively for fitting the distance matrix to T_c and T_{nc}). If the underlying evolutionary process is strictly clock-like, then $\ln L_c = \ln L_{nc}$ and $RSS_c = RSS_{nc}$, i.e., the simpler clock model can fit the data just as well as the more complicated non-clock model. If the underlying evolutionary process is not clock-like, then $\ln L_c < \ln L_{nc}$ and $RSS_c < RSS_{nc}$. The greater the deviation from the molecular clock, the greater the difference between $\ln L_c$ and $\ln L_{nc}$ and between RSS_c and RSS_{nc}. Because of the relationship between the likelihood method and the LS method, we can derive log-likelihood from RSS. We will designate the log-likelihood derived from RSS as $\ln L_{RSS.c}$ and $\ln L_{RSS.nc}$, respectively, for fitting data to T_c and T_{nc}. Thus, if the data fit the two trees equally well, we have $\ln L_{RSS.c} = \ln L_{RSS.nc}$. If not, we have $\ln L_{RSS.c} < \ln L_{RSS.nc}$. Given the reasoning above, a linear function of the difference between $\ln L_c$ and $\ln L_{nc}$ (designated as $\Delta\ln L$) or between $\ln L_{RSS.c} < \ln L_{RSS.nc}$ (designated by $\Delta\ln L_{RSS}$) would seem a good measure of the difference between the clock model and the non-clock model. A large $\Delta\ln L$ or $\Delta\ln L_{RSS}$ indicates a large deviation from the clock model.

Third, in the likelihood ratio test, the linear function is $2\Delta\ln L$ which follows approximately the χ^2-distribution. There is no known distribution for $2\Delta\ln L_{RSS}$ which, however, can be rescaled against $2\Delta\ln L$ in such a way that critical $2\Delta\ln L_{RSS}$ values at 0.10, 0.05 or 0.01 values can be obtained. As such critical values are approximate, we will call them threshold values instead of critical values (e.g., $2\Delta\ln L_{RSS0.10}$, $2\Delta\ln L_{RSS0.05}$, $2\Delta\ln L_{RSS0.01}$). Thus, if the computed $2\Delta\ln L_{RSS}$ value is 20 and $2\Delta\ln L_{RSS0.05}$ is 15, we can conclude that the clock model is rejected at 0.05 level (Xia 2009).

Aside from significance test, one can also use information-theoretic indices for model selection. Among these indices, AICu is the most consistent with the sequence-based likelihood ratio test (Xia 2009). An information-theoretic index is advantageous over a significance test in two ways. First, it does not depend on sample size, whereas the p value in a significance test is always sample size dependent. Second, a significance test alone gives us little information when the null hypothesis is not rejected, but an information-theoretic index such as AICu, being a criterion for model selection, always provides us with information to choose among models.

The minimal input consists of (1) a distance matrix (or data such as aligned sequences or allele frequencies that can be used to generate a distance matrix) and (2) a rooted tree (an equivalent unrooted tree is automatically generated in DAMBE by de-rooting the rooted tree so that the root is trifurcating instead of bifurcating).

One may have a file containing multiple distance matrices, e.g., generated by bootstrapping a set of sequences. DAMBE automatically recognize files with single or multiple distance matrices. If one does not have a distance matrix but have file with a set of aligned sequences, DAMBE can read the file and generate a distance matrix. Many sequence-based genetic distances have been implemented in DAMBE, including distances based on JC69, K80, F84, TN93 and GTR (general time reversible) substitution models, as well as the Log-Det and paralinear distances. Also implemented are simultaneously estimated genetic distances based on the F84 and TN93 substitution models (Xia 2009). These distances are particularly useful for dating with highly diverged sequences that render the conventional independently estimated distances inapplicable.

DAMBE can also read allele frequency data and generate a distance matrix. Three genetic distances are available for conventional allele frequency data: Nei's distance (Nei 1972), the chord distance (Cavalli-Sforza and Edwards 1967), and the distance by Reynolds, Weir, and Cockerham (Reynolds, et al. 1983). For microsatellite data, the distance based on a strict stepwise mutation model (Goldstein, et al. 1995; Slatkin 1995) is implemented.

Here is a list of plain text files that come with DAMBE that you can use to practise the test the molecular clock with the LS method:

1) VertCOI.fas which contains the mitochondrial COI gene from eight vertebrate species in FASTA format.

2) vertCOIRooted.dnd which contains a rooted tree in PHYLIP format.

OBJECTIVES

Learn to use DAMBE to perform relative-rate tests and to test the global clock hypothesis by using (1) the distance-based method in the LS framework, and (2) sequence-based methods employing the likelihood ratio test. The emphasis will be on the proper interpretation of the results rather than computational details.

Given the fact that the first and third codon positions of protein-coding genes are typically less functionally constrained than the second codon position, we will examine whether the first and third codon position will evolve in a more clock-like manner than the second codon position.

PROCEDURES

The sequences that we will use in this laboratory are in the file VertCOI.fas file which is one of the sample files that come with DAMBE. You will find it in DAMBE's installation directory, typically C:\Program Files\DAMBE. The file contains the coding sequence for the mitochondrial COI gene in eight vertebrate species (Table 11-2). The 5'-end and the 3'-end of the coding sequences are difficult to align and have been deleted.

Table 11-2. Eight vertebrate species whose coding sequence for the mitochondrial COI gene are included in the VertCOI.FAS file that comes with DAMBE.

Species	Common name	Accession(1)
Masturus lanceolatus	Sharptail mola	NC_005837
Homo sapiens	Human	NC_001807
Bos Taurus	Cow	NC_006853
Balaenoptera musculus	Blue whale	NC_001601
Pongo pygmaeus	Orangutan	NC_001646
Pan troglodytes	Chimpanzee	NC_001643
Gallus gallus	Chicken	NC_001323
Alligator mississippiensis	American alligator	NC_001922

(1) GenBank accession number of the mitochondrial genome from which the COI gene was extracted.

Start DAMBE and read in the aligned vertebrate mitochondrial gene sequences in the VertCOI.FAS file. Construct a maximum likelihood tree by clicking 'Phylogenetics|Maximum likelihood|DNAML'. Choose *Masturus lanceolatus* as outgroup and click the 'Run' button. You will get a tree that is identical to the one shown in Fig. 11-4. The tree is important for us to choose a proper outgroup in relative-rate test.

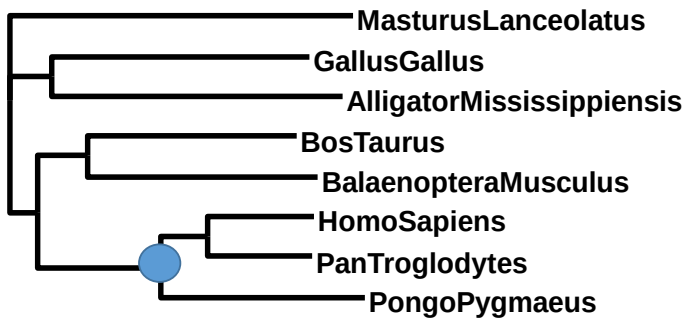

Fig. 11-4. Maximum likelihood tree based on the COI sequences from eight vertebrate species, with the filled circle representing the common ancestor of human (*Homo sapliens*) and orangutan (*Pongo pygmaeus*).

Relative-rate tests

We will address one specific question in this relative-rate test: Do orangutan and chimpanzee evolve at the same rate? You should be able to answer this question after this part of the laboratory. In fact we will perform two separate tests. The first is nucleotide-base and tests whether the two species evolve at the same transitional and transversional rates. The second is codon-based and tests whether the two species evolve at the same synonymous and nonsynonymous rate.

Start DAMBE and read in the VertCOI.FAS file. Click 'Phylogenetics|Relative-rate test'. A dialog box appears for you to specify the test (Fig. 11-5). We want to find out whether the orangutan and the chimpanzee have evolved at the same rate since their divergence. So click the orangutan and chimpanzee sequences to the ingroup box, and highlight an outgroup. Will the fish or the human sequence make good outgroup species? Why?

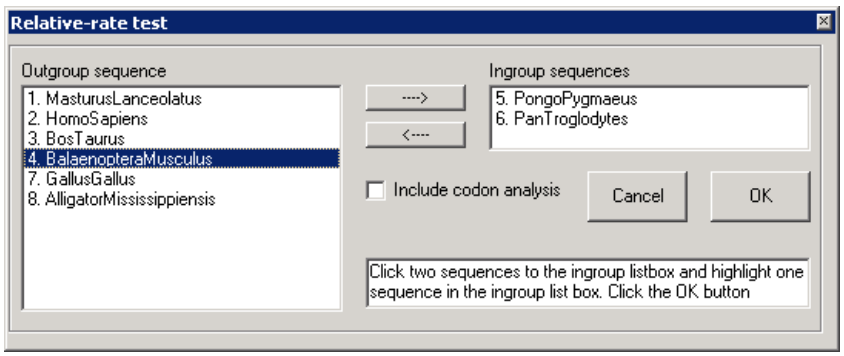

Fig. 11-5. Specifying the relative-rate test in DAMBE. Checking the 'Include codon analysis' checkbox will generate results from a codon-based relative-rate test.

Remember that a valid outgroup is one that does not belong to the ingroup (which means ALL species descending from the common ancestor of the ingroup species). Because human descends from the common ancestor of chimpanzee and orangutan (Fig. 11-4), it is not a valid outgroup.

The fish (*M. lanceolatus*) is a valid outgroup, so are the other four vertebrate species not descending from the common ancestor of chimpanzee and orangutan. Which one would be the best outgroup? Imagine that you are standing at one end of a 100-meter track and watching two athletes, one slow and one fast, running away from you to the other end. If you are not near-sighted, you should be able to see which one is faster. However, if you are standing at a position in Mars, then the two athletes will just blur into one tiny spot and you will not be able to see which one is running faster away from you. An outgroup highly diverged from the ingroup is equivalent to having you standing on Mars. Thus, the best outgroup is an outgroup that 1) does not belong to the ingroup and 2) is closest to the ingroup. The phylogenetic relationship and branch lengths shown in Fig. 11-4 suggest that the cow or the blue whale can serve as good outgroup. Let us use the blue whale as the outgroup first, i.e., highlight it as in Fig. 11-5, and click the 'OK' button (You should choose cow instead).

The computation is instantaneous for nucleotide-based analysis – it will take much longer if you have checked the 'Include codon analysis' checkbox. The core result is duplicated in Table 11-3. The full model shows that the two ingroups appear to differ substantially in transitions (0.34394 vs. 0.19811, Table 11-3) but little in transversions (0.03109 vs. 0.02910).

Table 11-3. Core results from a nucleotide-based relative-rate test.

	Alphas[1]			Betas[2]			lnL[3]
	Ingroup1	InGroup2	Outgroup	Ingroup1	InGroup2	Outgroup	
Full model	0.34394	0.19811	0.35163	0.03109	0.02910	0.21812	-3835.8257
Constrain both	0.27147	0.27147	0.34946	0.03010	0.03010	0.21805	-3839.2045
Constrain α	0.27150	0.27150	0.34959	0.03160	0.02860	0.21796	-3839.1713
Constrain β	0.34407	0.19794	0.35149	0.03010	0.03010	0.21819	-3835.8402

(1) transitions

(2) transversions

(3) log-likelihood of the four alternative but nested models.

The first likelihood ratio test we should do is to test the 'Constrain both' model (which is the model with a molecular clock) against the full model, i.e., the null hypothesis (H_0) that the constrained model can fit data just as well as the full model. If H_0 is not rejected, then we do not need to look at other models with intermediate complexity. See Fig. 11-1 for the meaning of these models.

We compute $\chi 2 = 2 (\ln L_{\text{Full model}} - \ln L_{\text{Constrain both}}) = 6.757$. With 2 degrees of freedom (why 2?), we have p = 0.03409. Recall that, for any significance test, the p value means the probability that we would be wrong if we reject H_0. As the p value is pretty small, we feel quite comfortable to reject H_0 that the 'Contrained both' model is equally good as the full model, i.e., we reject the molecular clock hypothesis. The test detail is also shown in the computer output.

Now that H_0 is rejected, we are left with three possibilities. First, the two ingroups differ in the transition rate. Second, the two ingroups differ in the transversion rate. Third, they differ in both.

In order to narrow down our conclusion, the full model (Model 1 in Fig. 11-1) is compared to Model 3 and Model 4 (Fig. 11-1). Model 3 forces $\alpha_1 = \alpha_2$ but not $\beta_1 = \beta_2$, and Model 4 forces $\beta_1 = \beta_2$ but not $\alpha_1 = \alpha_2$. If both Model 3 and Model 4 are rejected, then we conclude that the two ingroups differ in both transition and transversion rates. If Model 3 is rejected but Model 4 is not, we conclude that the two ingroups differ in the transition rate, i.e., it is the differential transition rates that violate the molecular clock hypothesis. If Model 4 is rejected but Model 3 is not, we conclude that the two ingroups differ in transversion rate, i.e., it is the differential transversion rates that are responsible for the rejection of the molecular clock hypothesis.

The test of Model 3 and Model 4 against Model 1 is also presented in the computer output. However, you are encouraged to compute χ^2, DF and p by yourself using results in Table 11-3. Once you have obtained χ^2 and DF, you can use EXCEL to obtain p. For example, if your $\chi^2 = 6.691$ and DF = 1, then you can obtain p by enter '=chidist(6.691,1)' (without the single quotes) in any EXCEL cell. The test result will allow you to draw specific conclusions as to whether the two in group species differ in transitions, in transversions, or in both.

You should now repeat the relative-rate test by including the codon-based analysis, i.e., by checking the 'Include codon analysis' checkbox in the dialog box in Fig. 11-5. Codon-based analysis is very slow and may take several minutes. Alpha and beta in codon-based analysis refers to synonymous and nonsynonymous substitutions, respectively. Run the test and make sure that you know how to answer the question of whether the two ingroups evolve at the same synonymous and nonsynonymous rates.

Phylogeny-based tests

We will perform distance-based LS tests and sequence-based likelihood ratio tests. The former can be used with either aligned sequences or distance matrices whereas the latter is for aligned sequences only. However, from a statistical point of view, the latter uses more information in the sequences and should outperform the former with aligned sequences. You should keep a comparative perspective when performing the two kinds of tests.

Distance-based method: The distance-based method has the advantage over sequence-based method in that a distance matrix can not only be generated from sequences, but also from a variety of other types of data, including allele frequency data, DNA hybridization data, RFLP data, microsatellite data, as well as genome-based gene presence/absence data. We will compute evolutionary distances from aligned sequences and use a rooted tree as input to test the molecular clock hypothesis by the LS method. A genetic distance matrix will be generated from the aligned sequences for the testing purpose. Using a distance matrix generated from aligned sequences facilitates the comparison between the distance-based and the sequence-based methods.

Start DAMBE. Click 'File|Open standard sequence file'. In the file open dialog box, browse to DAMBE's installation directory (e.g., C:\Program Files\DAMBE), and double-click the 'VertCOI.FAS' file (or single-click to highlight it and then click the 'Open' button). In the next 'Sequence Info' dialog box, click 'Protein-coding Nuc. Seq.' and choose the vertebrate mitochondrial translation table. Click 'OK' and the aligned sequences will be displayed.

Click 'Phylogenetics|Test molecular clock|Least-squares method|Nucleotide sequences'. The next dialog box (Fig. 11-6) is for you to specify the rooted tree and the genetic distance to generate from the sequences. An equivalent unrooted tree will be generated from the rooted tree that you specify.

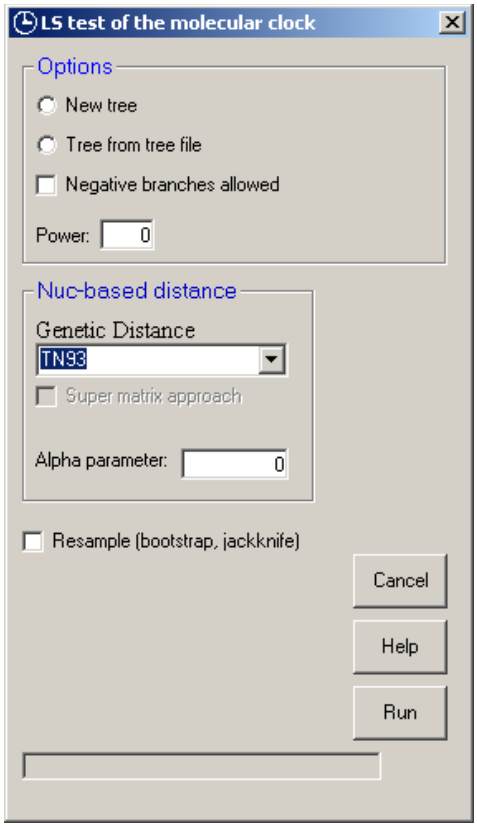

Fig. 11-6. Option dialog box for testing the molecular clock hypothesis by the least-squares method.

You can input a rooted tree in two ways. We will use a tree that has already been generated and saved in the file vertCOIRooted.dnd. However, if you do not have a tree but know what the topology should look like, you can click the 'New tree' option button. This will bring up a tree panel with a star tree with OTUs being the names of the sequences that have been read into DAMBE. You can then drag species or nodes to each other to form a rooted tree.

For the time being, we will use the rooted tree in the vertCOIRooted.dnd file. Click 'Tree from tree file', browse to DAMBE's installation directory (e.g., C:\Program Files\DAMBE), and open the vertCOIRooted.dnd file. The rooted tree will be displayed in the tree panel (Fig. 11-7). Note that it is a rooted tree with all nodes bifurcating. Click 'File|Export and exit' to quit the tree panel. The tree-selection option in Fig. 11-2 is now disabled.

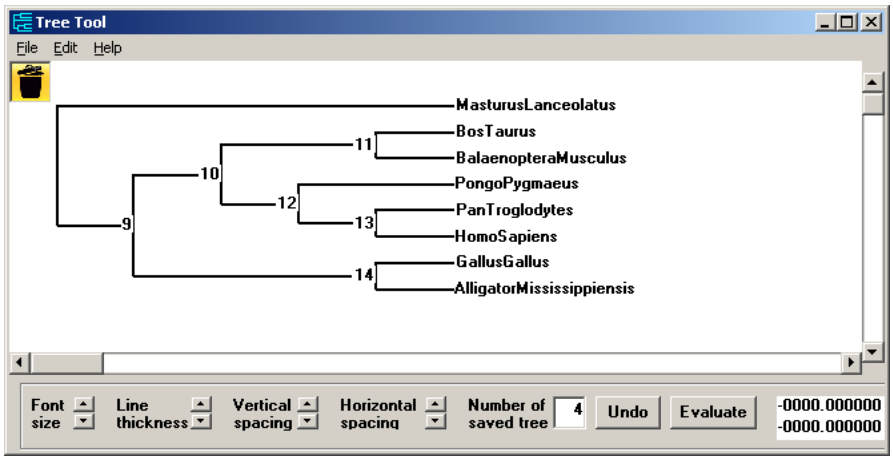

Fig. 11-7. Tree panel for displaying or modifying topologies.

Other than the first two options in Fig. 11-6 related to tree input, there are also several other options that we need to set. You generally should not allow negative branches. The power option in Fig. 11-6 refers to the P parameter in the following equation:

$$RSS = \sum_{i=1}^{n-1} \sum_{j=i+1}^{n} \frac{\left(d_{ij} - e_{ij}\right)^2}{d_{ij}^P} \quad \text{.....(11.1)}$$

where n is the number of species, d_{ij} is the observed distance between species i and j and e_{ij} is the expected distance, also referred to as patristic distances, computed as the length of the path linking species i and species j on the tree. The Fitch-Margoliash criterion or least-square criterion is to find both branch lengths and tree topology that minimize RSS. It is better to leave the default P = 0, i.e., the simple LS method.

For the genetic distance option, I recommend to use one of the four simultaneously estimated (SE) distances, i.e., MLCompositeF84, and MLCompositeTN93 (Xia 2009). If you are using the third codon position only, then you often have no choice other than using these SE distances because the conventional independently estimated distances often become inapplicable with highly diverged sequences.

Two such SE approaches have been implemented, one with the maximum likelihood method and the other with the LS method. For the F84 model, they will estimate the transition/transversion ratio and use it for all pairwise distance calculations. For the TN93 model, they will estimate the two transition/transversion ratio (κ1 and κ2) and use them for all pairwise distance calculations. This approach avoids the inapplicable cases, and produces much more robust distance estimates. These distances are implemented for the F84 and TN93 substitution models and designated 'MLCompositeF84', 'MLCompositeTN93', 'LSCompositeF84', and 'LSCompositeTN93' (where ML stands for maximum likelihood and LS stands for least-squares).

In this first try, we will not do resampling. So leave the resampling checkbox cleared and click the 'Run' button. The output is displayed, with some descriptions, a distance matrix, the re-evaluated rooted and unrooted tree, and finally the result of the test of the molecular clock hypothesis (Table 11-4). The residual sum of squares (RSS) for the clocked model is naturally greater than that for the non-clocked model (Table 11-4). However, the non-clocked model entails more parameters. Can the increased fit of the tree to the distance matrix justify the increased number of parameters? The resulting AICu for the clocked is smaller than that for the non-clocked models, suggesting that the clocked model is better than the non-clocked model, i.e., the increased number of parameters for the non-clock model is not quite justifiable.

Table 11-4. Main output of the test of the molecular clock by the least-squares method based on a genetic distance.

Clock	RSS	NumParam	AICu
Yes	0.003755	8	-6.5804
No	0.000701	14	-6.4015

For your practise, you can now re-run the test by checking the 'Resample (bootstrap, jackknife) check box. The default number of resampled data set is 100. The result (Fig. 11-8) shows that the mean AICu is smaller for the clocked model than for the non-clocked model, although the two are not significantly different (p = 0.19645). Also, 89% of the resampled data favour the clocked model.

```
Mean AICu (Clock)   = -6.097555
Mean AICu (NoClock) = -5.568301
Mean Difference (D) = -0.529254
Std of D:           = 0.409725
z score             = -1.291731
p                   = 0.196450
89% of resampled data supports
the clock model.
```

Fig. 11-8. Output from the test of the molecular clock by the least squares method, with data resampling.

You may also evaluate the molecular clock separately for the first, second and third codon positions. It is often assumed that the third codon position, being relatively free of the amino acid constraint, should evolve in a more clock-like manner than the other two codon positions. You may have noted that, under DAMBE's main menu 'Sequences', there are submenus such as 'Work on codon position 1', 'Work on codon position 2' and 'Work on codon position 3'. These functions allow you to extract specific codon positions for sequence analysis. Once

you have extracted one codon position and have done the analysis with it, you may click 'Sequences|Restore sequences' to restore the original sequences with all three codon positions. Keep in mind that, if you use the third codon position to test the molecular clock hypothesis with the least squares method, you should use one of the SE distances, otherwise you will get unpredictable output because of inapplicable cases with distance calculation.

Sequence-based likelihood ratio test: Sequence-based likelihood methods use more information than distance-based methods and are typically more accurate. As long as sequence data sets are not very large, we should always choose likelihood-based methods over distance-based methods.

Start DAMBE and read in the aligned vertebrate mitochondrial gene sequences in the VertCOI.FAS file. Click 'Test molecular clock|Likelihood ratio test', and a dialog box will (Fig. 11-9) will be shown. Click the option button labelled 'Tree from tree file', and browse to DAMBE's installation directory and open the file 'VertCOIRooted.dnd'. A rooted tree (Fig. 11-7) is shown. Click 'File|Export and exit' to quit the tree drawing panel. When you are back to the dialog box in Fig. 11-9, click the 'Go!' button to proceed.

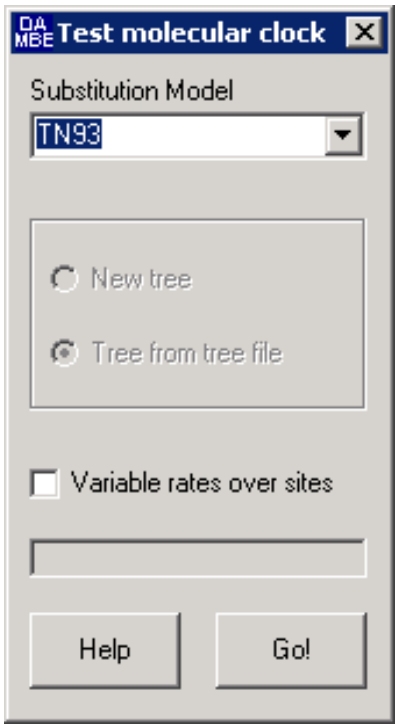

Fig. 11-9. Setting options for a tree-based test of the molecular clock hypothesis.

The output from DAMBE (Table 11-5) shows what the substitution model has been used, $\ln L_{\text{No clock}}$, $\ln L_{\text{Clock}}$, as well as the likelihood ratio χ^2 which is equal to $2(\ln L_{\text{No clock}} - \ln L_{\text{Clock}})$, associated degree of freedom (= n – 2) and the p value. Should we reject the null hypothesis with the p value of 0.0543? Recall that the null hypothesis is that the clock model and the non-clock model are equally good for the data, the p value is the probability that we will observe the likelihood ratio chisquare if the null hypothesis is true. The significance level in science is often set at 0.05 or 0.01, so we do not have enough evidence to reject the null hypothesis.

Table 11-5. Output from a likelihood ratio test of the molecular clock, based on all three codon positions of the vertebrate mitochondrial COI sequences.

Substitution model:	TN93
Log-likelihood with no clock:	-8066.0868
Log-likelihood with clock:	-8072.2697
Likelihood ratio chisquare:	12.3658
Degree of freedom:	6
Prob.:	0.0543

If you do not have a rooted tree, you can draw one from a star tree (a tree with all leaves branching off from a shared root). While the COI sequences are still in DAMBE, click 'Phylogenetics|Draw user tree'. Drag 'HomoSapiens' and drop onto 'PanTroglodytes' (or vice versa) and the two OTUs will be clustered. Drag any species and drop onto another species will cluster these two species. Drag 'PongoPygmaeus' and drop onto the parental node of Homo sapiens and Pan troglodytes so that Pongo pygmaeus becomes the sister species of the common ancestor of H. sapiens and P. troglodytes. Continue this process until you arrive at a rooted tree similar to Fig. 11-7 with all nodes bifurcating. Click 'File|Save tree' and save the tree with the file name MyVertCOITree.dnd (the file type .dnd is added automatically). You can now use this tree for the tree-based test of the molecular clock hypothesis.

Do functionally unconstrained sites evolve more clock-like than functionally constrained sites?

We have just performed phylogeny-based likelihood ratio test of the molecular clock hypothesis, with all three codon positions included (Table 11-5). We will now perform the same test, but separately for the three codon positions. While the eight sequences of the VertCOI.FAS are displayed (1512 sites), click 'Sequence|Work on codon position 1' to get the first codon positions. Note that now you have only 504 sites. Perform the likelihood ratio test on the first codon positions to obtain results similar to that in Table 11-5. To get the second codon position, you need first to restore sequences so that you again will have 1512 sites in DAMBE's buffer, by first clicking 'Sequence|Restore sequences', and then click 'Sequence|Work on codon position 2'. Now perform the likelihood ratio test on the second codon positions. Do the same for the third codon position. The results presented below are obtained with the TN93 model.

Test with the third codon position: Most substitutions at the third codon position are synonymous which implies relatively weak purifying selection compared to first and second codon positions. For this reason, evolutionary biologists tend to think that the third codon position should evolve in a more clock-like manner than the first and second codon positions. Here we examine whether the third codon position of the COI gene sequences evolve in a clock-like manner.

Read in the VertCOI.FAS file if you have not. Click 'Sequences|Work on codon position 3'. You will note that the aligned sequences are now only 1/3 of the original length because only the third codon positions are shown. Click 'Phylogenetics|Test molecular clock' as before and use the same rooted tree file 'VertCOIRooted.dnd' to test the molecular clock.

Based on your test result, which should be similar to that in Table 11-6, what is the probability that we would be wrong if we reject the null hypothesis? Keep in mind that most substitutions are at the third codon position. Everything being equal, the third codon position should have greater statistical power to reject the null hypothesis that the first and third codon positions. The observation that the null hypothesis is not rejected confirms our prediction that the third codon position should evolve in a clock-like manner.

Table 11-6. Output from a likelihood ratio test of the molecular clock, based on the third codon position of the vertebrate mitochondrial COI sequences.

Substitution model:	TN93
Log-likelihood with no clock:	-4006.4459
Log-likelihood with clock:	-4010.8672
Likelihood ratio chisquare:	8.8426
Degree of freedom:	6
Prob.:	0.1826

Now repeat the test by using the distance-based LS method. Do you reach the same conclusion?

Click 'Sequences|Restore Sequence' to restore all three codon positions. Note that the sequences are again 1512 bases long.

Test with the first codon position: Recall that the first codon position is intermediate between the third and the second codon positions in term of functional constraints. Most substitutions at the first codon positions are nonsynonymous, but these synonymous substitutions involve more similar amino acids than those at the second codon position.

Click 'Sequences|Work on codon position 1'. You will note that the aligned sequences are again only 1/3 of the original length because only the first codon positions are shown. Click 'Phylogenetics|Test molecular clock' as before and use the same rooted tree file 'VertCOIRooted.dnd' to test the molecular clock. Based on your test result (Table 11-7), is the molecular hypothesis rejected?

Table 11-7. Output from a likelihood ratio test of the molecular clock, based on the first codon position of the vertebrate mitochondrial COI sequences.

Substitution model:	TN93
Log-likelihood with no clock:	-1784.8591
Log-likelihood with clock:	-1788.7016
Likelihood ratio chisquare:	7.685
Degree of freedom:	6
Prob.:	0.2621

You might ask why the p value (= 0.2621, Table 11-7) for the first codon position is greater than that for the third codon position? Does this mean that the first codon position is even more clock-like than the third codon position? The answer is no. As you might have noticed, the first codon position has much fewer substitutions than the third codon position and consequently has limited power to reject the null hypothesis. However, the result does suggest that the first codon position also evolve in a clock-like manner.

Now repeat the test by using the distance-based LS method. Do you reach the same conclusion?

Click 'Sequences|Restore Sequence' to restore all three codon positions. Note that the sequences are again 1512 bases long.

Test with the second codon position: Recall that the second codon position is the most constrained functionally. Not only is any substitution at the second codon position nonsynonymous, but the nonsynonymous substitutions also typically involve rather different amino acid replacement (Table 11-1). For this reason, we expect the second codon position to evolve in the least clock-like manner.

Click 'Sequences|Work on codon position 2'. You will note that the aligned sequences are again only 1/3 of the original length because only the first codon positions are shown. Click 'Phylogenetics|Test molecular clock' as before and use the same rooted tree file 'VertCOIRooted.dnd' to test the molecular clock. Based on your test result (Table 11-8), is the molecular hypothesis rejected?

Table 11-8. Output from a likelihood ratio test of the molecular clock, based on the second codon position of the vertebrate mitochondrial COI sequences.

Substitution model:	TN93
Log-likelihood with no clock:	-978.2279
Log-likelihood with clock:	-995.916
Likelihood ratio chisquare:	35.3763
Degree of freedom:	6
Prob.:	0

You may have noticed that few substitutions occur at the second codon position, i.e., it should have the least statistical power to reject the null hypothesis, everything else being equal. The fact that the null hypothesis is strongly rejected suggests that the second codon position must have evolved in strong violation of the molecular clock hypothesis.

Now repeat the test by using the distance-based LS method. Do you reach the same conclusion? Which test gives you a smaller p value? With two tests running on the same data, the test that gives you a smaller p value is a more powerful (better) test.

You may also use the FastME method and the MLCompositeTN93 distance to build trees separately for the first, second and third codon positions. Which tree appears to have different lineages evolving at the same rate?

Finally, I should emphasize that the null hypothesis tested in this laboratory is not that of constant evolutionary rate, but is instead that of all extant OTUs are equidistance from the root. Thus, if all lineages increase or decrease their evolutionary rate synchronously (which violates the clock hypothesis), this test will not reject the clock hypothesis. However, one may argue that it must be extremely rare for different lineages to increase or decrease their evolutionary rates synchronously. So the test is still a relevant test of the clock hypothesis.

MORE QUESTIONS

1. Give two reasons why an ideal outgroup should be phylogenetically close to the ingroup.
2. How is the likelihood-ratio chi-square calculated from the model-specific likelihood (or log-likelihood) in the likelihood-ratio test? How is the associated degree of freedom calculated?

3. Use the VertCOI.fas file (containing mitochondrial COX1 sequences) for relative rate test between the cow (*Bos Taurus*) and the whale (*Balaenoptera musculus*). Do the two evolve at the same transitional and transversional rates? Do they evolve at the same synonymous and nonsynonymous rates? List output species and provide statistical evidence for your conclusion.What kind of substitutions tend to violate the molecular clock hypothesis?
4. Does molecular clock calibration always require dated fossils?
   Answer: No. Tip-dating does not require dated fossils. Sometimes geographic events can also be used for dating. For example, if we know the time of Africa-South America split to be 140 million years ago, then species that originally were present at the border region would be split into two and have diverged independently on the two continents 140 million years (assuming that they do not travel from one continent to the other).
5. Do the tests of molecular clock we learned in this lab really test the molecular clock hypothesis? (Consider the following scenario. Suppose all lineages evolve rapidly in one time period, and all evolve slowly in the next period. This would violate the molecular clock hypothesis, but will our tests reveal such synchronous increase or decrease in evolutionary rate?)

LAB 12 DATING WITH THE LEAST-SQUARES METHOD

INTRODUCTION

When did the vertebrates conquer the terrestrial environment? When did the ancestor of whales go back to the marine environment? When did the haemoglobin gene family originate? When did the gene duplication events occur that gave rise to α and β globin family? When did the HIV-1 virus jump the host to human? All these questions can be addressed by dating in molecular phylogenetics.

There are two data-driven types of dating. The first uses fossil records as calibration points in internal nodes, and the second is used specifically for dating rapidly evolving viruses sampled over years. The latter type is typically referred to as tip-dating methods. I will refer to the first type as internal-calibration dating.

Many software packages can perform dating, with the most advanced and complicated being BEAST (Drummond and Rambaut 2007). However, the complicated BEAST gives results similar to simpler distance-based least squares (LS) methods (Xia and Yang 2011). When the 'Relaxed clock' option is used in DAMBE (version 7.0.35), the dating results are nearly identical to that of BEAST. In addition, BEAST performs dating with aligned sequences, not distances, whereas the LS method can be used for both sequence data and distance data. So in this laboratory we will practice the LS method for dating implemented in DAMBE.

Internal-calibration dating

Internal-calibration dating with the least-square method requires three pieces of data (1) a rooted tree, (2) a set of data, either in the form of a set of aligned sequences or a distance matrix, that conform to the molecular clock hypothesis, and (3) one or more calibration points from fossil record (e.g., the common ancestor of the great apes, i.e., human, gorilla, chimpanzee and orang-utan walked on earth about 14 million years ago according to fossil record). The calibration points allow us to translate branch lengths to absolute geological times.

Tip-dating

Tip-dating was originally developed for dating the divergence events in viral strains such as HIV viruses sampled over years. The rationale is that, if the viral sequences evolve in a clock-like manner, then a viral strain sampled in, say, year 1950, should have a shorter branch than its sister lineage sampled in, say, year 2000 from their common ancestor. Thus, the sampling times can be used to calibrate the tree to obtain the divergence time in different viral lineages. The method has been developed and applied successfully in dating HIV-1 sequences and to settle questions concerning whether HIV-1 came to North America via Haiti or the other way round.

Tip-dating in DAMBE is developed in the least-square framework, based on evolutionary distances. Thus, any data that can be used to generate evolutionary distances can be used for tip-dating. Such data include molecular sequences, microsatellite or other allele frequency data, DNA hybridization, genome-based gene-sharing or word-sharing data, etc. The only requirement is that the resulting pairwise distance increases roughly linearly with time.

OBJECTIVES

There are two objectives in this tutorial. The first is to learn simple dating techniques to date speciation events, gene duplication events or virus divergence events by using the LS method implemented in DAMBE. The second is to learn how to attach confidence intervals to the estimated divergence time by using resampling methods (bootstrap or jackknife).

PROCEDURES

Internal-calibration dating

We will need to use four files: two sequence files and two tree files. These are all included in the DAMBE installation package. They can be found in DAMBE installation directory, typically C:\Program Files\DAMBE:

mtDNAPri3.NEX: This file, in NEXUS format, contains third codon positions of the 12 protein-coding genes collinear with the L-strand of vertebrate mitochondrial genome for seven great ape species. The sequences are used in Rannala and Yang (2007), with two reasonably good calibration points.

mtDNAPri3F84SE.DIS, and mtDNAPri3F84SEMult.DIS: These two files, in PHYLIP format, contain simultaneously estimated distances based on the F84 model from sequences in the mtDNAPri3.NEX file.

mtDNAPri3F84SE.DIS contains a single distance matrix, whereas mtDNAPri3F84SEMult.DIS contains 100 distance matrices each derived from a bootstrapped sample from sequences in the mtDNAPri3.NEX file. You can generate these two files yourself by using the mtDNAPri3.NEX file mentioned above.

mtDNAPri.DND: This is a tree file in PHYLIP format containing a rooted tree for the seven ape species. The tree is used in conjunction with the three files above for dating the speciation events of the great apes.

PrimateOnly.NEX: This file, also in NEXUS format, contains 26 primate species with three reasonably good calibration points. They are used in Yang and Yoder (2003).

PrimateOnlyBEAST.dnd: This file contains a rooted tree for the 26 primate species in the PrimateOnly.NEX. It is used in conjunction with the PrimateOnly.NEX file for dating the speciation events of the primate species.

Dating with aligned sequences: We will first perform a simple dating, and then estimate variability of the estimates.

Simple dating: Click the DAMBE icon to start DAMBE. Click 'File|Open standard sequence file'. In the dialog box Fig. 12-1, click the 'File of type' dropdown box to select 'PAUP/NEXUS' format. All files with file types '.nex', '.pau', '.paup' will be displayed (Fig. 12-1). Double-click mtDNAPri3.NEX to open it (or just single-click to highlight it and then click the 'Open' button). If you want to try some sequence files in other format, just click the 'File of type' dropdown box and choose your file type. If you are not sure of your sequence format, choose 'Unknown' to let DAMBE decide.

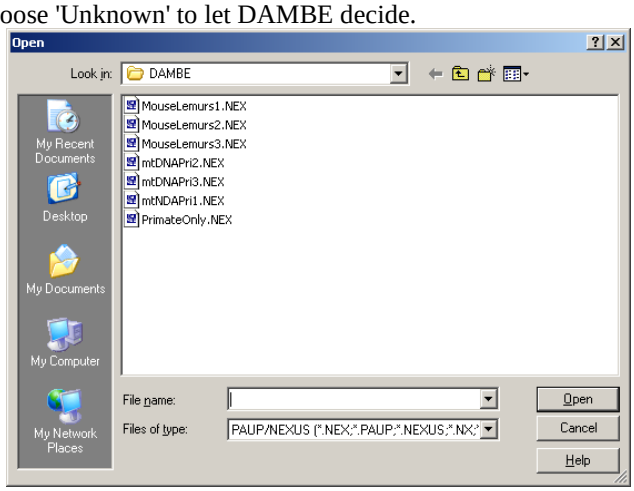

Fig. 12-1. File open dialog box in DAMBE.

You will be asked for sequence information (Fig. 12-2). Different types of sequences are associated with different analytical methods. 'Protein-coding Nuc. Seq.' means protein-coding nucleotide sequences that can be translated into amino acids. In our case, although the third codon positions are from a protein-coding gene, the sequence as a whole is not protein-coding. So you should keep the default 'Non-protein Seq.' and click the 'Go!' button.

Fig. 12-2. Dialog for sequence information.

The aligned sequences will be displayed. Now click 'Phylogenetics|Distance-based dating'. The next dialog box (Fig. 12-3) is for you to specify the rooted tree and the genetic distance to generate from the sequences. Note that the 'Relaxed clock' checkbox is enabled and checked by default in DAMBE from version 7.0.35. Earlier versions of DAMBE would have this checkbox grayed (disabled).

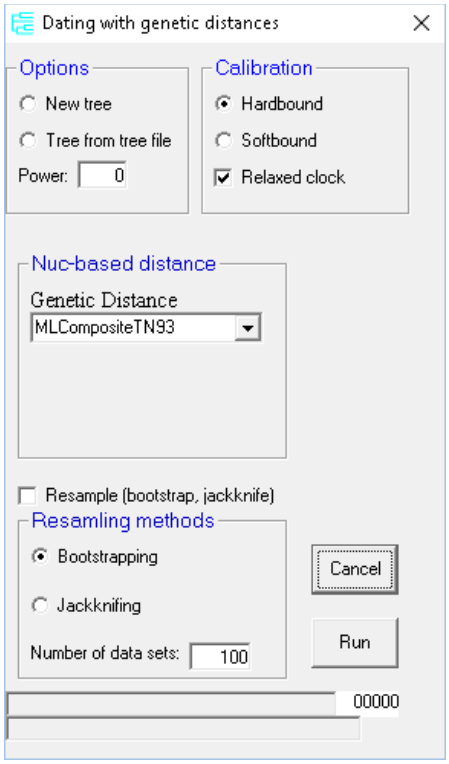

Fig. 12-3. Dialog box to specify options in distance-based dating.

You can input a rooted tree in two ways. We will use a tree that has already been generated and saved in the file mtDNAPri.dnd. Click 'Tree from tree file' at the dialog box shown in Fig. 12-3, browse to DAMBE's installation directory (e.g., C:\Program Files\DAMBE), and open the mtDNAPri.dnd file. The rooted tree will be displayed in the tree panel (Fig. 12-4). Note that it is a rooted tree with all nodes bifurcating.

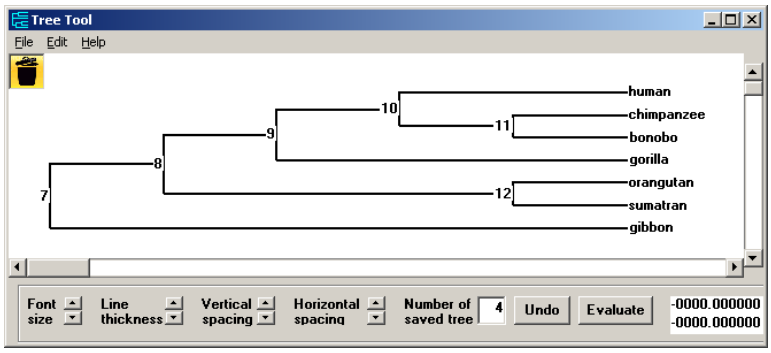

Fig. 12-4. Tree panel for displaying or modifying topologies.

(If you want to use your own tree, make sure that the OTU names in the tree match those in the sequences. If you do not have a tree but know what the topology should look like, you can click the 'New tree' option button. This will bring up a tree panel with a star tree with OTUs being the names of the sequences that have been read into DAMBE. You can then drag species or nodes to each other to form a rooted tree.)

You now need to specify calibration points. Note that all the internal nodes are numbered. Two calibration points have been used for dating this set of sequences (Rannala and Yang 2007), one for the common ancestor of all three great apes and human (node 8), and the other for the common ancestor of human and chimpanzee (node 10). Right-click (Mac users: Enable the secondary click by go to 'System Preferences|Keyboard & Mouse' and set the right button to 'Secondary Button'. The Mac default is to have both the left and right buttons set to the same 'Primary Button'. You may also set the tiny middle button, which defaults to 'dashboard', to the secondary button) the node numbered '8' (including human, two chimp species, gorilla and two orangutan species), and enter 14 (for 14 million years ago) in the ensuing dialog box. Right-click the node numbered '10'

(including human, and two chimp species) and enter 7 (for 7 million years ago). Note that the calibration nodes are now coloured in red. (You can click the tree in many different ways. Different clicks are often associated with advanced dating functions. I have not finalized the interface. So click only as instructed.)

One should be aware of possible inconsistency in calibration points. Take Fig. 12-4 for example, if the common ancestor for human and chimpanzee (node 10) was dated to be 14 million years old, whereas the common ancestor for human, chimp, gorilla and orangutan (node 8) was dated to be less than 14 million years old, then we have inconsistent calibration points. The dating algorithm will fail with inconsistent calibration points.

Click 'File|Export and exit' to quit the tree panel. If you have forgotten to set the calibration points, DAMBE will give you an opportunity to set them. If you have followed the instructions, the tree panel will close and the tree-selection option in the dialog box (Fig. 12-3) will now be disabled because the selection is successful.

We have more options to set in the dialog box shown in Fig. 12-3. If you choose the 'Hardbound' option, then the calibration times will be fixed. If you choose the 'Softbound' option, then the calibration points will be changed to minimize the residual sum of squares when multiple calibration points are available. The 'Softbound' option will have no effect when there is only a single calibration point.

I suggest that you choose the 'Softbound' option. This is not only because the 'Softbound' option will lead to smaller residual sum of squares, but also because fossil dating is often inaccurate. The 'softbound' option allows the use of observed data to revise the calibration points. In a sense, the original calibration points may be taken as a prior estimate, which is revised to give a posterior estimate by incorporating information from the observed data.

In the genetic distance, the default is 'MLCompositeF84'. This is one of the simultaneously estimated (SE) distances for the F84 substitution model (Tamura, et al. 2004; Xia 2009). It is crucial to use SE distances, especially when using the third codon position, because most of the independent estimation method will generate inapplicable cases due to high sequence divergence.

Two such SE approaches have been implemented in DAMBE, one with the maximum likelihood method and the other with the LS method (Xia 2009). These distances are implemented for the F84 and TN93 substitution models in DAMBE and designated 'MLCompositeF84', 'MLCompositeTN93', 'LSCompositeF84', and 'LSCompositeTN93' (where ML stands for maximum likelihood and LS stands for least-squares). For the F84 model, a global transition/transversion ratio will be estimated and used for all pairwise distance calculations. For the TN93 model, there are two transition/transversion ratios (κ1 and κ2) which are used for all pairwise distance calculations. This approach essentially eliminates the inapplicable cases, and produces much more robust distance estimates.

In this first try, we will not do resampling. So leave the resampling checkbox cleared and click the 'Run' button. The output is displayed in two parts. The first is a tree with divergence time estimates (Fig. 12-5). Note that the two calibration points are not 14 and 7 as we have inputted, but are 14.75 and 5.5, respectively. Had you chosen 'Hardbound' instead of 'Softbound' in the dialog box in Fig. 12-3, the two calibration nodes will show exactly as the input values, i.e., 14 and 7, respectively. The option 'Softbound' allows DAMBE to fine-tune the time of the calibration nodes by minimizing the sum of residual squares.

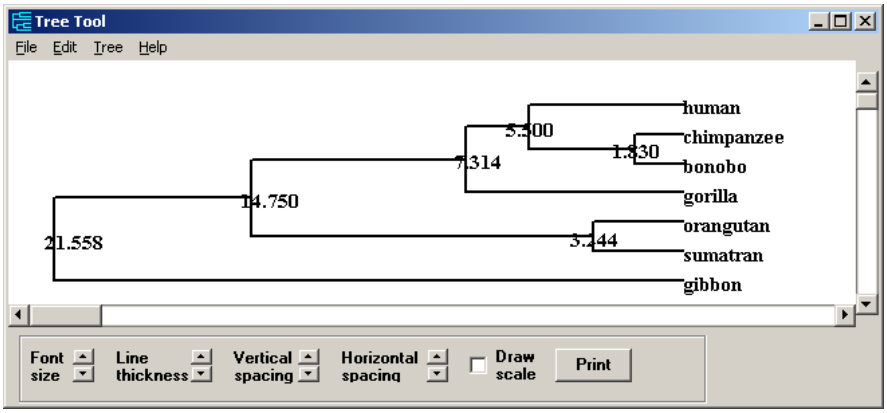

Fig. 12-5. Tree with estimated divergence time.

The tree can be manipulated in many ways and can be exported in low-resolution bitmapped .bmp format or the high-resolution metafile format either for publication or PowerPoint presentation.

The second part is the text output, which includes the distance matrix, the estimated parameters of the substitution model such as the transition/transversion ratio, log-likelihood for the distance estimation, and details of the dating input and results such as the evolutionary rate, the tree with dates and the residual sum of squares (RSS). RSS will be larger if you had chosen the 'Hardbound' option.

You should explore the results from different combinations of 'Hardbound', 'Softbound', 'Strict clock' and 'Relaxed clock' option. 'Strick clock' is used when the 'Relaxed clock' checkbox is not checked.

Estimating variability of the estimated divergence time: Now repeat the procedure until you get to the dialog box shown in Fig. 12-3. Read in the mtDNAPri.DND tree and set the two calibration times as before. Now click the 'Resample (bootstrap, jackknife)' check box. The default resampling protocol is 'Bootstrap' and the default number of resampled data sets is 100. The higher the number, the better the estimates are. For practical research, the number of resampled data sets should be at least 500. Click the 'Run' button.

After DAMBE has bootstrapped the specified number of times, dating results are again presented in two parts: a tree (Fig. 12-6) with divergence times as well as text output. The tree differs from that in Fig. 12-5 in that the standard deviation of the estimated divergence time is also presented.

It is important to keep in mind that the divergence time will be slightly different when you repeat the bootstrapping procedure because bootstrapping randomly samples sites to reconstitute a new set of sequences.

You should now use the second set of sequences (PrimateOnly.NEX) and the associated tree (PrimateOnlyBEAST.NEX) to see how well the distance-based dating method work with a larger data set. Note that this set of sequences contains unresolved nucleotides and DAMBE will ask you how to handle them. You may just leave the default, i.e., '3 leaving them as they are'. This will result in ambiguous codes treated as follows. If it is an R (standing for A or G) and if the nucleotide frequencies of A and G are, say, 0.4 and 0.1, then R will be treated as A with a probability of 0.8 and as G with a probability of 0.2. Of course, if A and G are equal, then R will be treated as 0.5 A and 0.5 G. The same rule applies to other ambiguous codes.

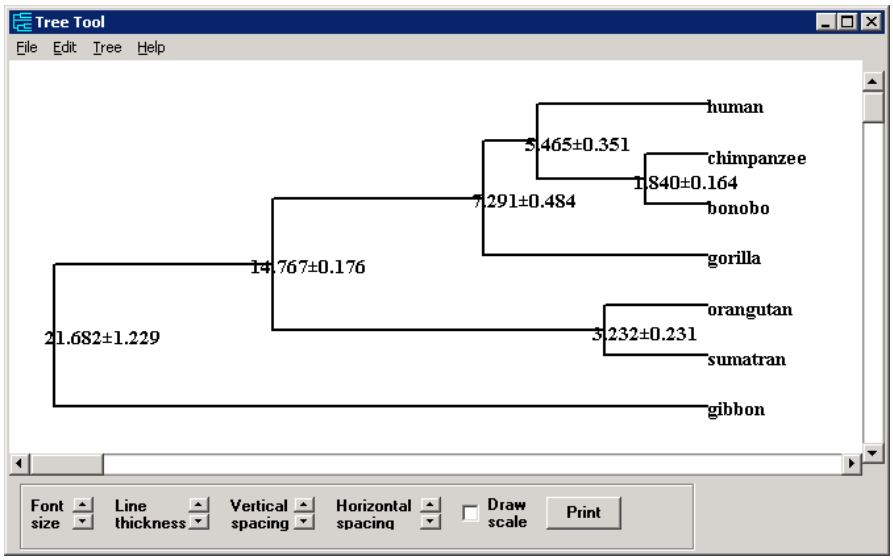

Fig. 12-6. Tree with the estimated divergence time and the associated standard deviation.

You can set three calibration points (Yang and Yoder 2003) when dating this set of sequences, one at the root with 77 million years, one internal node including Homo, Pan, Gorilla, Pongo, and Macaca with 35 million years, and the third node including Homo, Pan, and Gorilla with 10 million years. Continue until you get your dating results.

Dating with distance matrices

When only a single distance matrix is used, then the dating output cannot have any estimate of the variability of the estimated divergence time. With multiple distance matrices, however, each matrix will generate one set of estimated divergence time and a measure of the variability of the divergence times can then be estimated.

Click 'File|Open other molecular data file', choose 'Distance matrix file', and click the 'OK' button. In the 'Open file' dialog box, choose the 'mtDNAPri3F84SE.dis' file and click the 'Open' button. This file contains a single distance matrix and will generate one set of divergence time estimates. In the ensuing dialog box (Fig. 12-7), change the default from 2 (Testing the molecular clock hypothesis) to 3 (Dating). Click 'OK'.

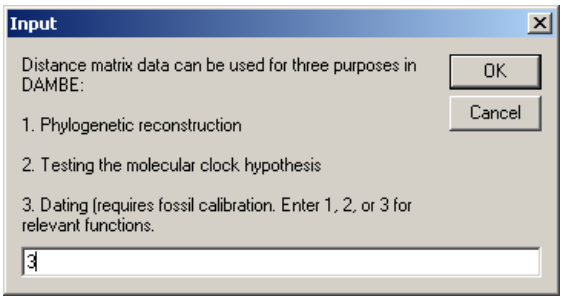

Fig. 12-7. Dialog box for phylogenetic analysis involve distance matrices.

You will be presented with a dialog box similar to that in Fig. 12-3, but without any specification related to the genetic distances. Set the options and click the 'Run' button will generate a dated tree with estimated divergence times.

Dating involving multiple distance matrices is similar. Click 'File|Open other molecular data file', choose 'Distance matrix file', and click the 'OK' button. In the 'Open file' dialog box, choose the 'mtDNAPri3F84SEMult.dis' file and click the 'Open' button. This file contains 100 distance matrices each generated from bootstrapping the seven sequences in the mtDNAPri.nex file. Proceed exactly the same way as before and you will get a dated tree not only with divergence time estimates, but also with the standard error of each time estimate similar to that shown in Fig. 12-6.

You can copy and paste the tree from DAMBE to PowerPoint slides or any other graphic programs including EXCEL and WORD, either in fixed-resolution bitmapped format or in high-resolution Windows metafile format. The latter should be used for formal presentation or publication. See Appendix 1 Copy trees from DAMBE to PowerPoint slides for details.

Tip-Dating

We will use five sample files for demonstrating the tip-dating function in DAMBE:

TipDate8OTU.FAS: A nucleotide sequence file in Pearson/FASTA format, which is the simplest file format exportable from every computer programs used for sequence analysis:

>SeqName1
ACCGTT……
>SeqName2
ACCGTT…..

For tip-dating in DAMBE, the sequence name should be in one of the two following formats. The first is 'Name@Year', e.g., S1@1980, which means that sequence S1 was sampled in the year 1980. If there are multiple '@' in the sequence name, only the last '@' is used.

The second format is 'Name/Year', e.g., 'A/Brisbane/10/2007'. Again, only the last '/' is used. DAMBE will look for '/' only if it does not find '@' in the sequence name.

The 'Year' part can take three forms, e.g., '2007', '2007.56', '02062007' (DDMMYYYY). Thus, sequence names such as 'Brisbane/10/2007', 'H3N2Brisbame@2007.5', 'Brisbane/10/02062007' are all valid sequence names.

You should avoid using the format of 'Name@00' or 'Name/00' for sequences sampled in the year 2000 because it is ambiguous.

DAMBE can read almost all frequently used sequence format, including MEGA, PHYLIP, PAUP/NEXUS, as well as the new NeXML format. The only requirement is that the sequence name should be in the format

of 'Name@Year' or 'Name/Year'. The tip-dating function in DAMBE has an option for resampling (bootstrapping or jackknifing) the sequences to estimate variation of the inferred dates.

TipDate8OTU.dnd for tip-dating with TipDate8OTU.FAS: A rooted tree file in Newick format. Tip-dating needs a rooted tree. You may use DAMBE to generate either a rooted or an unrooted tree. If the tree is unrooted (i.e., with a trifurcating root), DAMBE will display the tree on a tree panel and ask you to drag two child nodes of the trifurcating root to each other to make the root bifurcating.

TipDate6OTU.dis: A distance matrix in PHYLIP format. The OTU name should be in the format of 'Name@Year', and the name and the distance values should be separated by one or more spaces.

TipDate6OTU.dnd for tip-dating with TipDat6OTU.dis.

DistMult8OTU.dis: A file containing 55 distance matrices. Multiple distance matrices allow one to estimate variation of the inferred dates.

Tip-dating with sequence files: Start DAMBE. Click 'File|Open standard sequence file'. The default file input format may be 'Pearson/FASTA' format. If not, click the dropdown box to change the file type to 'Pearson/FASTA', and all files with type .fas, .fasta, .ffn, etc., will be displayed. Highlight TipDate8OTU.FAS and click the 'Open' button. A dialog will appear asking for the type of sequences (binary, non-protein, amino acid or protein-coding nucleotide sequences, with the default being 'Non-Protein'). Keep the default of 'Non-Protein' and click 'Go'. The sequences will be displayed, and you will see sequence names being S1@1980, S2@1965, etc.

Tip-dating with no resampling : Click 'Phylogenetics|Distance-based dating|Tip-dating'. The following dialog (Fig. 12-8) will appear. The first frame has two option buttons: 'New tree' and 'Tree from tree file'. If you don't have a tree, you may click 'New tree' to construct a tree, but you may postpone the exploration of this function later as we already have a rooted tree.

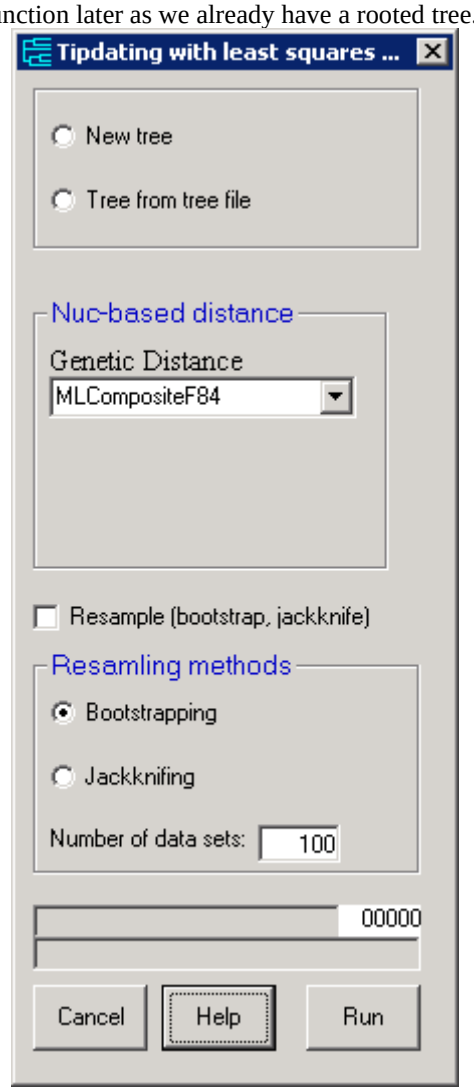

Fig. 12-8. DAMBE's dialog box for tip-dating options.

Click 'Tree from tree file' and read in the TipDate8OTU.dnd. The rooted tree will be displayed (Fig. 12-9). If the tree file happens to contain an unrooted tree, then you should drag two child nodes of the root node to each other to make the root bifurcating instead of trifurcating. Now click 'File|Export/Exit' to close the tree panel. It is very important that you do NOT just close the window by clicking the little red cross at the top-right of the window.

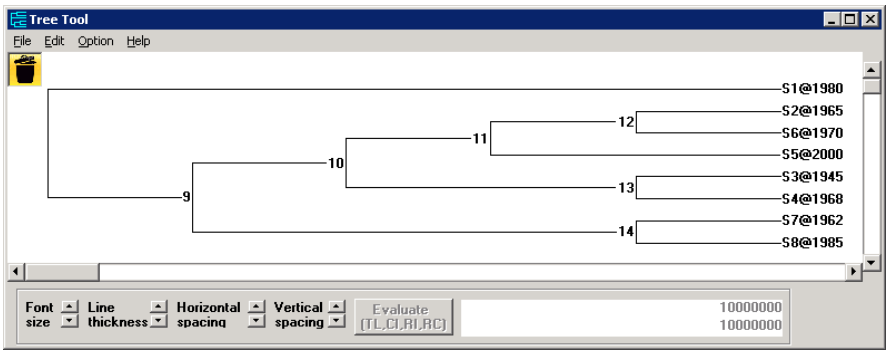

Fig. 12-9. DAMBE's tree display panel. One can drag both internal and terminal nodes to each other to modify the topology.

Now you are back to the dialog shown in Fig. 12-8, except that the option buttons for tree input is disabled, indicating that you have made the selection already. You may now choose a distance for tip-dating. I recommend using either MLCompositeF84 or MLCompositeTN93. These are simultaneously estimated (SE) distances, using information not only between two sequences but also from all other pairs of sequences (Tamura, et al. 2004; Xia 2009). Two approaches have been used for SE distances, one in the likelihood framework (Tamura, et al. 2004; Xia 2009), labeled as MLCompositeF84 (for the F84 substitution model allowing different nucleotide frequencies as well as different transition and transversion rates) and MLCompositeTN93 (for the TN93 substitution model which extended the F84 model by allowing different A↔G and C↔T transition rates) distances in DAMBE, and the other in the least-squares framework (Xia 2009), labeled as LSCompositeF84 and LSCompositeTN93 distances.

The SE distance is computer intensive relative to the independently estimated distances which uses information only from the particular pair of sequences. For example, the MLCompositeF84 distance is much slower to compute than the independently estimated (IE) GTR distance. However, SE distances are much more robust than IE distances (Xia 2009). For this part of the exercise, you may just leave the default distance (which is MLCompositeF84). Below the distance selection is the options for resampling (bootstrapping and jackknifing). We will do this in the next section. So leave the 'Resample' checkbox unchecked.

Click the 'Run' button and the dated tree will be displayed (Fig. 12-10). The terminal nodes show that the sequences were sampled during the period of 1945-2000. The numbers next to the internal nodes are the inferred dates from tip-dating, with the root node dated to year 1766.8. The plotted tree is accurate as long as no branch length is zero, otherwise lineages below the unresolved node will be somewhat displaced to the right. We will learn how to copy a fully editable tree from the tree panel to PowerPoint slides in a later section.

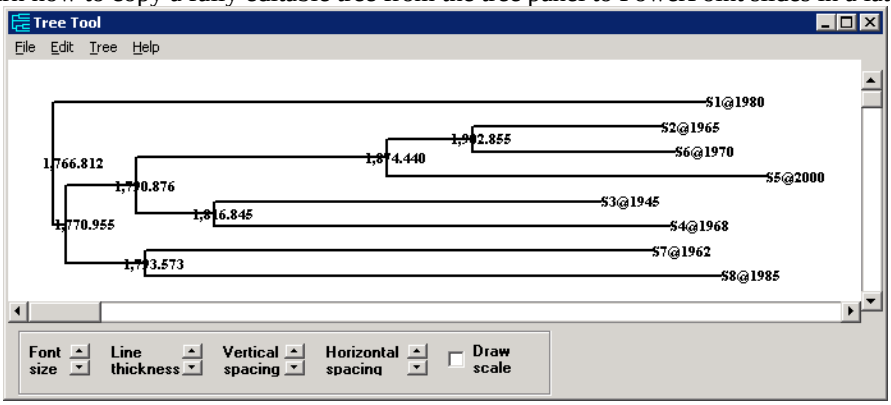

Fig. 12-10. DAMBE's tree display panel, with the numbers next to internal nodes showing the inferred dates.

In addition to the plot of the dated tree, DAMBE also output results in text format (shown below). The results are self-explanatory except for MLCompositeF84, k_F84, TTR_F84 and lnL which you may need to read the section on the simultaneously estimated distances to understand their meanings. 'r = 0.0007' is the estimated evolutionary rate, and RSS is the residual sum of squares.

```
  Tip-Dating based on least-square criterion and distance matrix (Xia, 2012).
  Genetic distance: MLCompositeF84 (Xia 2009) is used, with pair-wise deletion of
indel-containing sites.

   Distance matrix used:

  8
  S1@1980
  S2@1965     0.29443
  S3@1945     0.28447  0.23599
  S4@1968     0.28959  0.25713  0.20092
  S5@2000     0.32437  0.15878  0.26150  0.27683
  S6@1970     0.30416  0.09301  0.24412  0.24834  0.15575
  S7@1962     0.29431  0.27105  0.26710  0.28655  0.29646  0.28972
  S8@1985     0.30888  0.29386  0.28434  0.29944  0.31204  0.28537  0.25885

  Composite lnL maximized after 12 iterations
  k_F84 = 0.7638
  TTR_F84 = 1.2626
  lnL = -18.77469

  Dated tree with the divergence time shown within []:
  (S1@1980:213.18764,((((S2@1965:62.14530,S6@1970:67.14530):[1902.855]28.41514,S5@
2000:125.56044):[1874.440]83.56331,(S3@1945:128.15531,S4@1968:151.15531):[1816.845
]25.96843):[1790.876]19.92118,(S7@1962:168.42681,S8@1985:191.42681):[1793.573]22.6
1812):[1770.955]4.14272);
  r = 0.0007
  RSS = 0.0000
```

Tip-dating with resampling to estimate variation of the inferred dates: Point estimates without associated variation are often not very useful. With molecular sequences, one can use resampling to estimate the variation. In short, each resampled date set will yield a set of point estimates of the dates. N sets of resampled date will produce N sets of such estimates and allow us to obtain the standard deviation for the estimated dates.

To estimate the variation of the inferred dates, simply click 'Phylogenetics|Distance-based dating|Tipdating'. When the dialog in Fig. 12-8 is shown, import the tree in TipDate8OTU.dnd as before. Also keep the default distance which is MLCompositeF84. Check the 'Resample' checkbox, choose whether to do 'Bootstrapping' or 'Jackknifing', and enter the number of date sets to resample (or just leave the default of 100).

Click the 'Run' button, and dated tree is shown with both inferred dates and their standard deviation (Fig. 12-11) in the format of 'MeanDate±SD' where MeanDate is the mean date and SD is standard deviation. MeanDate could be estimated in two ways, one by the average of the N estimates each from a resampled data set ($MeanDate_1$), and the other by the estimate of the date based on the mean distance matrix ($MeanDate_2$). For reasons not yet clear to me, $MeanDate_2$ is almost always closer to the estimate from the original data set than $MeanDate_1$, and is reported as the mean date from DAMBE's tip-dating output. We will learn how to copy a fully editable tree from the tree panel to PowerPoint slides in a later section.

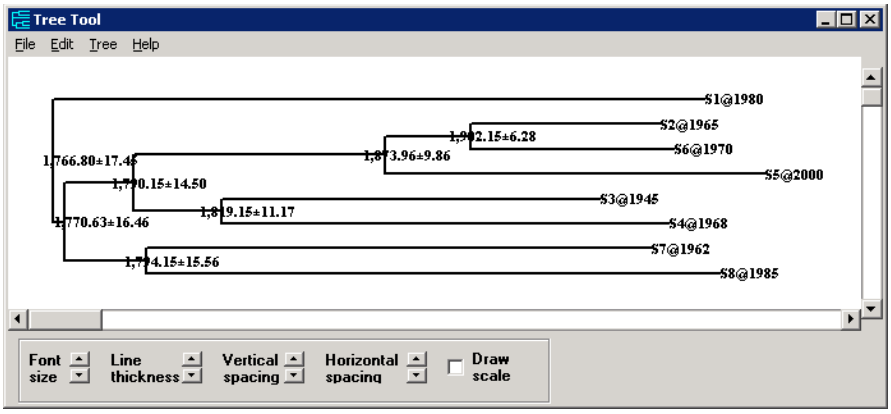

Fig. 12-11. DAMBE's tree display panel, with each internal node showing the mean date and its associated standard deviation in the format of MeanDate±SD.

The text output has a tree with the date estimate and its standard deviation shown in the format of MeanDate±SD.

```
  Tip-Dating based on least-square criterion and distance matrix (Xia, 2012).
  Genetic distance: MLCompositeF84(Xia 2009) is used, with pair-wise deletion of
indel-containing sites.

  Resampling method used: Bootstrapping 55 times.
  Dated tree with the divergence time and standard deviation shown within []:
  (S1@1980:213.19710,((((S2@1965:62.84831,S6@1970:67.84831):[1902.15±6.28]28.19078
,S5@2000:126.03909):[1873.96±9.86]83.81489,(S3@1945:125.85066,S4@1968:148.85066):[
1819.15±11.17]29.01708):[1790.15±14.50]19.51457,(S7@1962:167.84640,S8@1985:190.846
40):[1794.15±15.56]23.52215):[1770.63±16.46]3.82855);
  Mean r = 0.0007
  Std r = 0.0002
```

Tip-dating with distance matrices: If the input is a single distance matrix, then one can only get point estimates, i.e., dates without standard deviation. If a set of OTUs has multiple distance matrices associated with it, then one can obtain both point and interval estimates, i.e., mean dates and their associated standard deviation.

The distance matrix file should be in text format as follows:

```
8
S1@1980
S2@1965    0.29443
S3@1945    0.28447  0.23599
S4@1968    0.28959  0.25713  0.20092
S5@2000    0.32437  0.15878  0.26150  0.27683
S6@1970    0.30416  0.09301  0.24412  0.24834  0.15575
S7@1962    0.29431  0.27105  0.26710  0.28655  0.29646  0.28972
S8@1985    0.30888  0.29386  0.28434  0.29944  0.31204  0.28537  0.25885
```

The only requirement is that multiple entries in a line should have one or more spaces between them. Multiple distance matrices will simply follow each other. In what follows, we will show tip-dating both with a file containing a single distance matrix and a file containing multiple distance matrices.

Tip-dating with a single distance matrix: Start DAMBE, and click 'File|Open other molecular data file'. In the ensuing dialog box, click 'Distance matrix' and click 'OK'. Open in the 'TipDate6OTU.dis' file. A dialog box (Fig. 12-12) appears. Enter 4 (for tip-dating) and click 'OK'. You will see a dialog box similar to that in Fig. 12-8, except that there is no option for distance selection or for resampling. Click 'Tree from tree file' and open the tree file TipDatDis6OTU.dnd. Click 'File|Export/Exit' to export the tree and click 'Run'.

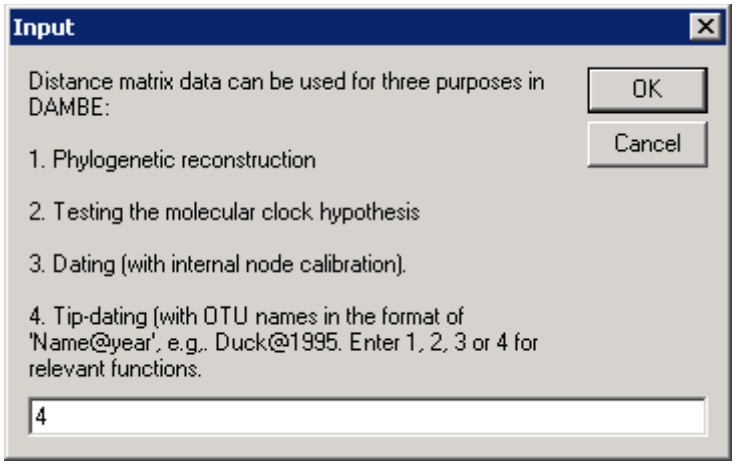

Fig. 12-12. A dialog box for using distance matrices to perform different functions.

A dated tree will be displayed (Fig. 12-13), with the inferred dates shown next to each internal node. It is impossible to attach standard deviation with a single distance matrix.

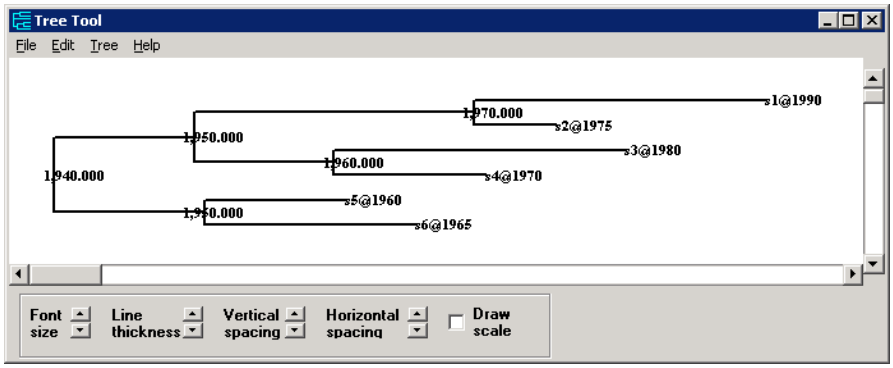

Fig. 12-13. Dated tree from the distance matrix in file TipDate6OTU.dis.

Tip-dating with a file containing multiple distance matrices: The file DistMult8OTU.dis contains 55 distance matrices for the same 8 OTUs, allowing us to obtain not only the inferred dates, but also associated standard deviation. The procedure is similar to running tip-dating with a single distance matrix. Whenever there multiple distance matrices in the file, DAMBE will automatically derive the standard deviation associated with the inferred dates.

MORE QUESTIONS

1. What is the most critical assumption in dating?
2. Why do we need calibration point(s) in dating?
3. Why it is sometimes sensible to use softbound instead of hardbound for calibration points?
4. What are the benefits of multiple calibration points relative to a single calibration point?

APPENDIX 1. COPY TREES FROM DAMBE TO POWERPOINT SLIDES

You can copy and paste the tree from DAMBE to PowerPoint slides or any other graphic programs including EXCEL and WORD, either in fixed-resolution bitmapped format or in high-resolution Windows metafile format. The latter should be used for formal presentation or publication.

To copy a bitmapped tree, click 'Edit|Copy tree as BMP file' when the tree is displayed in the tree panel. Go to PowerPoint or WORD (or any Windows program that can handle graphics) and click 'Edit|Paste' or just press Ctrl-V. Crop the edge of the picture to fit the screen. Note that if your tree is in a small window, then its resolution will be poor when you enlarge it in PowerPoint slides. Instead, you should increase the 'Vertical spacing', 'Horizontal spacing', 'Line thickness' and 'Font size' within DAMBE's Tree Tool window before copy the tree in BMP format.

Copying and pasting the high-resolution windows metafile is a bit more complicated than copying the low-resolution bitmapped graphics, depending on what graphic program you are pasting to. The metafile is in fact a set of drawing instructions to re-draw the picture in the graphic program and different graphic programs treat the instructions slightly differently. The description here is applicable to Microsoft PowerPoint. First, in DAMBE's tree panel with a displayed tree, click 'Edit|Copy tree as Windows metafile'. Go to a PowerPoint slide and click 'Paste|Paste special|Windows metafile'. This is important because the default PowerPoint paste, since Office 2007, is 'Enhanced metafile' instead of 'Windows metafile'.

After pasting, what you will have on the slide is a tiny, almost invisible square. Right-click 'Group|Ungroup' and you will have the tree on the slide. You can click 'Draw|Ungroup' again to edit individual elements of the tree.

REFERENCES

Aerts S, Van Loo P, Thijs G, Mayer H, de Martin R, Moreau Y, De Moor B. 2005. TOUCAN 2: the all-inclusive open source workbench for regulatory sequence analysis. Nucleic Acids Res 33:W393-396.

Ahn HW, Morin RD, Zhao H, Harris RA, Coarfa C, Chen ZJ, Milosavljevic A, Marra MA, Rajkovic A. 2010. MicroRNA transcriptome in the newborn mouse ovaries determined by massive parallel sequencing. Mol Hum Reprod 16:463-471.

Allen A, Flemstrom G, Garner A, Kivilaakso E. 1993. Gastroduodenal mucosal protection. Physiological Reviews 73:823-857.

Altschul SF, Gish W, Miller W, Myers EW, Lipman DJ. 1990. Basic local alignment search tool. Journal of Molecular Biology 215:403-410.

Altschul SF, Madden TL, Schaffer AA, Zhang J, Zhang Z, Miller W, Lipman DJ. 1997. Gapped BLAST and PSI-BLAST: a new generation of protein database search programs. Nucleic Acids Research 25:3389-3402.

Aris-Brosou S, Xia X. 2008. Phylogenetic Analyses: A Toolbox Expanding towards Bayesian Methods. Int J Plant Genomics 2008:Article ID 683509, 16 pages.

Auch AF, Henz SR, Holland BR, Goker M. 2006. Genome BLAST distance phylogenies inferred from whole plastid and whole mitochondrion genome sequences. BMC Bioinformatics 7:350.

Baik SC, Kim KM, Song SM, Kim DS, Jun JS, Lee SG, Song JY, Park JU, Kang HL, Lee WK, et al. 2004. Proteomic analysis of the sarcosine-insoluble outer membrane fraction of *Helicobacter pylori* strain 26695. Journal of Bacteriology 186:949-955.

Baumgartner HK, Montrose MH. 2004. Regulated alkali secretion acts in tandem with unstirred layers to regulate mouse gastric surface pH. Gastroenterology 126:774-783.

Benson DA, Karsch-Mizrachi I, Lipman DJ, Ostell J, Sayers EW. 2011. GenBank. Nucleic Acids Research 39:D32-D37.

Birol I, Jackman SD, Nielsen CB, Qian JQ, Varhol R, Stazyk G, Morin RD, Zhao Y, Hirst M, Schein JE, et al. 2009. De novo transcriptome assembly with ABySS. Bioinformatics 25:2872-2877.

Boettiger C, Lang DT. 2012. Treebase: an R package for discovery, access and manipulation of online phylogenies. Methods in Ecology and Evolution 3:1060-1066.

Brown CM, Stockwell PA, Dalphin ME, Tate WP. 1994. The translational termination signal database (TransTerm) now also includes initiation contexts. Nucleic Acids Res 22:3620-3624.

Bulmer M. (87144571 co-authors). 1987. Coevolution of codon usage and transfer RNA abundance. Nature 325:728-730.

Burge C, Karlin S. 1997. Prediction of complete gene structures in human genomic DNA. Journal of Molecular Biology 268:78-94.

Burnham KP, Anderson DR. 2002. Model Selection and Multimodel Inference : A Practical Information-Theoretic Approach. New York, NY: Springer.

Bury-Mone S, Skouloubris S, Labigne A, De Reuse H. 2001. The *Helicobacter pylori* UreI protein: role in adaptation to acidity and identification of residues essential for its activity and for acid activation. Molecular Microbiology 42:1021-1034.

Carullo M, Xia X. 2008. An Extensive Study of Mutation and Selection on the Wobble Nucleotide in tRNA Anticodons in Fungal Mitochondrial Genomes. Journal of Molecular Evolution 66:484-493.

Cavalli-Sforza LL, Edwards AWF. 1967. Phylogenetic analysis: models and estimation procedures. Evolution 32:550-570.

Chan PP, Lowe TM. 2009. GtRNAdb: a database of transfer RNA genes detected in genomic sequence. Nucleic Acids Res 37:D93-97.

Chang BS, Jonsson K, Kazmi MA, Donoghue MJ, Sakmar TP. 2002. Recreating a functional ancestral archosaur visual pigment. Molecular Biology and Evolution 19:1483-1489.

Chang BS, Kazmi MA, Sakmar TP. 2002. Synthetic gene technology: applications to ancestral gene reconstruction and structure-function studies of receptors. Methods Enzymol 343:274-294.

Chapeville F, Lipmann F, von Ehrenstein G, Weisblum B, Ray WJ, Jr., Benzer S. 1962. On the role of soluble ribonucleic acid in coding for amino acids. Proceedings of the National Academy of Sciences of the United States of America 48:1086-1092.

Chavancy G, Chevallier A, Fournier A, Garel JP. 1979. Adaptation of iso-tRNA concentration to mRNA codon frequency in the eukaryote cell. Biochimie 61:71-78.

Chen MW, Jahn D, Schon A, O'Neill GP, Soll D. 1990. Purification and characterization of Chlamydomonas reinhardtii chloroplast glutamyl-tRNA synthetase, a natural misacylating enzyme. Journal of Biological Chemistry 265:4054-4057.

Chithambaram S, Prabhakaran R, Xia X. 2014a. Differential Codon Adaptation between dsDNA and ssDNA Phages in *Escherichia coli*. Molecular Biology and Evolution 31:1606-1617.

Chithambaram S, Prabhakaran R, Xia X. 2014b. The Effect of Mutation and Selection on Codon Adaptation in *Escherichia coli* Bacteriophage. Genetics 197:301-315.

Coessens B, Thijs G, Aerts S, Marchal K, De Smet F, Engelen K, Glenisson P, Moreau Y, Mathys J, De Moor B. 2003. INCLUSive: A web portal and service registry for microarray and regulatory sequence analysis. Nucleic Acids Res 31:3468-3470.

Coghlan A, Wolfe KH. 2000. Relationship of codon bias to mRNA concentration and protein length in *Saccharomyces cerevisiae*. Yeast 16:1131-1145.

Comeron JM, Aguade M. 1998. An evaluation of measures of synonymous codon usage bias. Journal of Molecular Evolution 47:268-274.

Curnow AW, Hong K, Yuan R, Kim S, Martins O, Winkler W, Henkin TM, Soll D. 1997. Glu-tRNAGln amidotransferase: a novel heterotrimeric enzyme required for correct decoding of glutamine codons during translation. Proceedings of the National Academy of Sciences of the United States of America 94:11819-11826.

Curnow AW, Tumbula DL, Pelaschier JT, Min B, Soll D. 1998. Glutamyl-tRNA(Gln) amidotransferase in Deinococcus radiodurans may be confined to asparagine biosynthesis. Proceedings of the National Academy of Sciences of the United States of America 95:12838-12843.

Dalphin ME, Brown CM, Stockwell PA, Tate WP. 1996. TransTerm: a database of translational signals. Nucleic Acids Res 24:216-218.

Deng Q, Ramskold D, Reinius B, Sandberg R. 2014. Single-cell RNA-seq reveals dynamic, random monoallelic gene expression in mammalian cells. Science 343:193-196.

Deng R, Huang M, Wang J, Huang Y, Yang J, Feng J, Wang X. 2006. PTreeRec: Phylogenetic Tree Reconstruction based on genome BLAST distance. Comput Biol Chem 30:300-302.

Desper R, Gascuel O. (22376423 co-authors). 2002. Fast and accurate phylogeny reconstruction algorithms based on the minimum-evolution principle. Journal of Computational Biology 9:687-705.

Desper R, Gascuel O. 2004. Theoretical foundation of the balanced minimum evolution method of phylogenetic inference and its relationship to weighted least-squares tree fitting. Molecular Biology and Evolution 21:587-598.

Dobin A, Davis CA, Schlesinger F, Drenkow J, Zaleski C, Jha S, Batut P, Chaisson M, Gingeras TR. 2013. STAR: ultrafast universal RNA-seq aligner. Bioinformatics 29:15-21.

Drummond A, Rambaut A. 2007. BEAST: Bayesian evolutionary analysis by sampling trees. Bmc Evolutionary Biology 7:214.

Duret L. 2000. tRNA gene number and codon usage in the *C. elegans* genome are co-adapted for optimal translation of highly expressed genes. Trends Genet 16:287-289.

Edgar RC. 2004a. MUSCLE: a multiple sequence alignment method with reduced time and space complexity. BMC Bioinformatics 5:113.

Edgar RC. 2004b. MUSCLE: multiple sequence alignment with high accuracy and high throughput. Nucleic Acids Res 32:1792-1797.

Efron B. 1982. The jackknife, the bootstrap and other resampling plans. Philadelphia, Pa.: Society for Industrial and Applied Mathematics.

Engel E, Peskoff A, Kauffman GL, Jr., Grossman MI. 1984. Analysis of hydrogen ion concentration in the gastric gel mucus layer. American Journal of Physiology 247:G321-338.

Felsenstein J. 1978. Cases in which parsimony and compatibility methods will be positively misleading. Systematic Zoology 27:401-410.

Felsenstein J. 1985. Confidence limits on phylogenies: an approach using the bootstrap. Evolution 39:783-791.

Felsenstein J. 2004. Inferring phylogenies. Sunderland, Massachusetts: Sinauer.

Felsenstein J. 2014. PHYLIP 3.695 (phylogeny inference package). Seattle: Department of Genetics, University of Washington.

Flicek P. 2007. Gene prediction: compare and CONTRAST. Genome Biology 8:233.

Gao L, Qi J. 2007. Whole genome molecular phylogeny of large dsDNA viruses using composition vector method. BMC Evol. Biol. 7:41.

Garel JP. 1974. Functional adaptation of tRNA population. J Theor Biol 43:211-225.

Garel JP, Hentzen D, Daillie J. 1974. Codon responses of tRNA-Ala, tRNA-Gly and tRNA-Ser from the posterior part of the silkgland of Bombyx mori L. FEBS Lett 39:359-363.
Gene Ontology Consortium. 2008. The Gene Ontology project in 2008. Nucleic Acids Res 36:D440-444.
Gene Ontology Consortium. 2021. The Gene Ontology resource: enriching a GOld mine. Nucleic Acids Res 49:D325-D334.
Ghaemmaghami S, Huh WK, Bower K, Howson RW, Belle A, Dephoure N, O'Shea EK, Weissman JS. 2003. Global analysis of protein expression in yeast. Nature 425:737-741.
Gilbert WV, Zhou K, Butler TK, Doudna JA. 2007. Cap-independent translation is required for starvation-induced differentiation in yeast. Science 317:1224-1227.
Gojobori T, Li WH, Graur D. 1982. Patterns of nucleotide substitution in pseudogenes and functional genes. Journal of Molecular Evolution 18:360-369.
Goldstein DB, Ruiz Linares A, Cavalli-Sforza LL, Feldman MW. 1995. An evaluation of genetic distances for use with microsatellite loci. Genetics 139:463-471.
Gouy M, Gautier C. 1982. Codon usage in bacteria: correlation with gene expressivity. Nucleic Acids Research 10: 7055-7064.
Goya R, Sun MG, Morin RD, Leung G, Ha G, Wiegand KC, Senz J, Crisan A, Marra MA, Hirst M, et al. 2010. SNVMix: predicting single nucleotide variants from next-generation sequencing of tumors. Bioinformatics 26:730-736.
Gramm J, Niedermeier R. 2002. Breakpoint medians and breakpoint phylogenies: a fixed-parameter approach. Bioinformatics 18 Suppl 2:S128-139.
Griffith M, Griffith OL, Mwenifumbo J, Goya R, Morrissy AS, Morin RD, Corbett R, Tang MJ, Hou YC, Pugh TJ, et al. 2010. Alternative expression analysis by RNA sequencing. Nat Methods 7:843-847.
Guindon S, Gascuel O. 2003. A simple, fast, and accurate algorithm to estimate large phylogenies by maximum likelihood. Syst Biol 52:696-704.
Guindon S, Lethiec F, Duroux P, Gascuel O. 2005. PHYML Online--a web server for fast maximum likelihood-based phylogenetic inference. Nucleic Acids Res 33:W557-559.
Haas J, Park E-C, Seed B. 1996. Codon usage limitation in the expression of HIV-1 envelope glycoprotein. Current Biology 6:315-324.
Hamajima N, Goto Y, Nishio K, Tanaka D, Kawai S, Sakakibara H, Kondo T. 2004. *Helicobacter pylori* eradication as a preventive tool against gastric cancer. Asian Pacific Journal of Cancer Prevention 5:246-252.
Hasegawa M, Kishino H, Yano T. 1985. Dating of the human-ape splitting by a molecular clock of mitochondrial DNA. Journal of Molecular Evolution 22:160-174.
Henz SR, Huson DH, Auch AF, Nieselt-Struwe K, Schuster SC. 2005. Whole-genome prokaryotic phylogeny. Bioinformatics 21:2329-2335.
Herniou EA, Luque T, Chen X, Vlak JM, Winstanley D, Cory JS, O'Reilly DR. 2001. Use of whole genome sequence data to infer baculovirus phylogeny. J Virol 75:8117-8126.
Higgins DG, Sharp PM. 1988. CLUSTAL: a package for performing multiple sequence alignment on a microcomputer. Gene 73:237-244.
Hofacker IL. 2003. Vienna RNA secondary structure server. Nucleic Acids Res 31:3429-3431.
Holmes I, Bruno WJ. (21473872 co-authors). 2001. Evolutionary HMMs: a Bayesian approach to multiple alignment. Bioinformatics 17:803-820.
Huelsenbeck JP, Ronquist F. (21415446 co-authors). 2001. MRBAYES: Bayesian inference of phylogenetic trees. Bioinformatics 17:754-755.
Hunt RH. 2004. Will eradication of *Helicobacter pylori* infection influence the risk of gastric cancer? American Journal of Medicine 117:86S-91S.
Ibba M, Curnow AW, Soll D. 1997. Aminoacyl-tRNA synthesis: divergent routes to a common goal. Trends Biochem Sci 22:39-42.
Ikemura T. 1992. Correlation between codon usage and tRNA content in microorganisms. In: Hatfield DL, Lee BJ, Pirtle RM, editors. Transfer RNA in protein synthesis. Boca Raton: CRC Press. p. 87-111.
Ikemura T. 1981a. Correlation between the abundance of *Escherichia coli* transfer RNAs and the occurrence of the respective codons in its protein genes. Journal of Molecular Biology 146:1-21.
Ikemura T. 1981b. Correlation between the abundance of *Escherichia coli* transfer RNAs and the occurrence of the respective codons in its protein genes: a proposal for a synonymous codon choice that is optimal for the *E coli* translational system. J Mol Biol 151:389-409.

International Human Genome Sequencing Consortium. 2001. Initial sequencing and analysis of the human genome. Nature Biotechnology 409:860-921.
Jensen JL, Hein J. 2005. Gibbs sampler for statistical multiple alignment. Statistica Sinica 15:889-907.
Jukes TH, Cantor CR. 1969. Evolution of protein molecules. In: Munro HN, editor. Mammalian protein metabolism. New York: Academic Press. p. 21-123.
Kanaya S, Yamada Y, Kudo Y, Ikemura T. 1999. Studies of codon usage and tRNA genes of 18 unicellular organisms and quantification of Bacillus subtilis tRNAs: gene expression level and species-specific diversity of codon usage based on multivariate analysis. Gene 238:143-155.
Katoh K, Asimenos G, Toh H. 2009. Multiple alignment of DNA sequences with MAFFT. Methods Mol Biol 537:39-64.
Katoh K, Frith MC. 2012. Adding unaligned sequences into an existing alignment using MAFFT and LAST. Bioinformatics 28:3144-3146.
Katoh K, Kuma K, Toh H, Miyata T. 2005. MAFFT version 5: improvement in accuracy of multiple sequence alignment. Nucleic Acids Res 33:511-518.
Kimura M. 1980. A simple method for estimating evolutionary rates of base substitutions through comparative studies of nucleotide sequences. Journal of Molecular Evolution 16:111-120.
Kozak M. 1978. How do eucaryotic ribosomes select initiation regions in messenger RNA? Cell 15:1109-1123.
Kozak M. 1986. Point mutations define a sequence flanking the AUG initiator codon that modulates translation by eukaryotic ribosomes. Cell 44:283-292.
Kozak M. 1997. Recognition of AUG and alternative initiator codons is augmented by G in position +4 but is not generally affected by the nucleotides in positions +5 and +6. Embo J 16:2482-2492.
Kozak M, Shatkin AJ. 1979. Characterization of translational initiation regions from eukaryotic messenger RNAs. Methods Enzymol 60:360-375.
Kridel R, Meissner B, Rogic S, Boyle M, Telenius A, Woolcock B, Gunawardana J, Jenkins C, Cochrane C, Ben-Neriah S, et al. 2012. Whole transcriptome sequencing reveals recurrent NOTCH1 mutations in mantle cell lymphoma. Blood 119:1963-1971.
Kumar S, Stecher G, Tamura K. 2016. MEGA7: Molecular Evolutionary Genetics Analysis Version 7.0 for Bigger Datasets. Molecular Biology and Evolution 33:1870-1874.
Lake JA. 1994. Reconstructing evolutionary trees from DNA and protein sequences: paralinear distances. Proceedings of the National Academy of Sciences, USA 91:1455-1459.
Langmead B, Hansen KD, Leek JT. 2010. Cloud-scale RNA-sequencing differential expression analysis with Myrna. Genome Biology 11:R83.
Langmead B, Salzberg SL. 2012. Fast gapped-read alignment with Bowtie 2. Nat Methods 9:357-359.
Langmead B, Trapnell C, Pop M, Salzberg SL. 2009. Ultrafast and memory-efficient alignment of short DNA sequences to the human genome. Genome Biology 10:R25.
Lawrence CE, Altschul SF, Boguski MS, Liu JS, Neuwald AF, Wootton JC. 1993. Detecting subtle sequence signals: a Gibbs sampling strategy for multiple alignment. Science 262:208-214.
Li W-H. 1983. Evolution of duplicate genes and pseudogenes. Sunderland, MA: Sinauer.
Li WH, Gojobori T, Nei M. 1981. Pseudogenes as a paradigm of neutral evolution. Nature 292:237-239.
Lin GN, Cai Z, Lin G, Chakraborty S, Xu D. 2009. ComPhy: prokaryotic composite distance phylogenies inferred from whole-genome gene sets. BMC Bioinformatics 10 Suppl 1:S5.
Lockhart PJ, Steel MA, Hendy MD, Penny D. 1994. Recovering evolutionary trees under a more realistic model of sequence evolution. Molecular Biology and Evolution 11:605-612.
Lopez P, Casane D, Philippe H. (21624443 co-authors). 2002. Heterotachy, an important process of protein evolution. Molecular Biology and Evolution 19:1-7.
Ma P, Xia X. 2011. Factors affecting splicing strength of yeast genes. Int J Genomics 2011:Article ID 212146, 13 pages.
Mannella CA, Neuwald AF, Lawrence CE. 1996. Detection of likely transmembrane beta strand regions in sequences of mitochondrial pore proteins using the Gibbs sampler. J Bioenerg Biomembr 28:163-169.
Matin A, Zychlinsky E, Keyhan M, Sachs G. 1996. Capacity of *Helicobacter pylori* to generate ionic gradients at low pH is similar to that of bacteria which grow under strongly acidic conditions. Infection and Immunity 64:1434-1436.
Menaker RJ, Sharaf AA, Jones NL. 2004. *Helicobacter pylori* Infection and Gastric Cancer: Host, Bug, Environment, or All Three? Current Gastroenterology Reports 6:429-435.
Mendz GL, Hazell SL. 1996. The urea cycle of *Helicobacter pylori*. Microbiology 142:2959-2967.

Metropolis N. 1987. The Beginnning of the Monte Carlo Method. In. Los Alamos Science (Special issue). p. 125-130.

Miyata T, Miyazawa S, Yasunaga T. 1979. Two types of amino acid substitutions in protein evolution. Journal of Molecular Evolution 12:219-236.

Mobley HL, Hu LT, Foxal PA. 1991. *Helicobacter pylori* urease: properties and role in pathogenesis. Scandinavian Journal of Gastroenterology Supplement 187:39-46.

Morin R, Bainbridge M, Fejes A, Hirst M, Krzywinski M, Pugh T, McDonald H, Varhol R, Jones S, Marra M. 2008. Profiling the HeLa S3 transcriptome using randomly primed cDNA and massively parallel short-read sequencing. Biotechniques 45:81-94.

Muse SV, Gaut BS. 1994. A likelihood approach for comparing synonymous and nonsynonymous nucleotide substitution rates, with application to the chloroplast genome. Molecular Biology and Evolution 11:715-724.

Muse SV, Weir BS. 1992. Testing for equality of evolutionary rates. Genetics 132:269-276.

Muto A, Osawa S. 1987. The guanine and cytosine content of genomic DNA and bacterial evolution. Proceedings of the National Academy of Sciences, USA 84:166-169.

Nakamura Y, Gojobori T, Ikemura T. 2000. Codon usage tabulated from international DNA sequence databases: status for the year 2000. Nucleic Acids Res 28:292.

Nei M. 1972. Genetic distance between populations. American Naturalist 106:283-292.

Neuwald AF, Liu JS, Lawrence CE. 1995. Gibbs motif sampling: detection of bacterial outer membrane protein repeats. Protein Sci 4:1618-1632.

Otu HH, Sayood K. 2003. A new sequence distance measure for phylogenetic tree construction. Bioinformatics 19:2122-2130.

Pearson WR. 1990. Rapid and sensitive sequence comparison with FASTP and FASTA. Methods Enzymol 183:63-98.

Percudani R, Pavesi A, Ottonello S. 1997. Transfer RNA gene redundancy and translational selection in Saccharomyces cerevisiae. J Mol Biol 268:322-330.

Pobre V, Arraiano CM. 2015. Next generation sequencing analysis reveals that the ribonucleases RNase II, RNase R and PNPase affect bacterial motility and biofilm formation in E. coli. Bmc Genomics 16:72.

Prabhakaran R, Chithambaram S, Xia X. 2014. Aeromonas phages encode tRNAs for their overused codons. Int J Comput Biol Drug Des 7:168-182.

Prabhakaran R, Chithambaram S, Xia X. *2015*. *Escherichia coli* and *Staphylococcus* phages: effect of translation initiation efficiency on differential codon adaptation mediated by virulent and temperate lifestyles. J Gen Virol 96:1169-1179.

Ptashne M. 1986. A Genetic Switch: Gene Control and Phage Lambda. Cambridge, MA: Cell Press and Blackwell Scientific.

Qin ZS, McCue LA, Thompson W, Mayerhofer L, Lawrence CE, Liu JS. 2003. Identification of co-regulated genes through Bayesian clustering of predicted regulatory binding sites. Nat Biotechnol 21:435-439.

Qu K, McCue LA, Lawrence CE. 1998. Bayesian protein family classifier. Proceedings of the International Conference on Intelligent Systems for Molecular Biology; ISMB 6:131-139.

Rannala B, Yang Z. 2007. Inferring speciation times under an episodic molecular clock. Syst Biol 56:453-466.

Rektorschek M, Buhmann A, Weeks D, Schwan D, Bensch KW, Eskandari S, Scott D, Sachs G, Melchers K. 2000. Acid resistance of *Helicobacter pylori* depends on the UreI membrane protein and an inner membrane proton barrier. Molecular Microbiology 36:141-152.

Reynolds JB, Weir BS, Cockerham. CC. 1983. Estimation of the coancestry coefficient: basis for a short-term genetic distance. Genetics 105:767-779.

Rice P, Longden I, Bleasby A. 2000. EMBOSS: the European Molecular Biology Open Software Suite. Trends Genet 16:276-277.

Roberts A, Schaeffer L, Pachter L. 2013. Updating RNA-Seq analyses after re-annotation. Bioinformatics 29:1631-1637.

Roberts A, Trapnell C, Donaghey J, Rinn JL, Pachter L. 2011. Improving RNA-Seq expression estimates by correcting for fragment bias. Genome Biology 12:R22.

Roth A, Ding J, Morin R, Crisan A, Ha G, Giuliany R, Bashashati A, Hirst M, Turashvili G, Oloumi A, et al. 2012. JointSNVMix: a probabilistic model for accurate detection of somatic mutations in normal/tumour paired next-generation sequencing data. Bioinformatics 28:907-913.

Rouchka EC. 1997. A Brief Overview of Gibbs Sampling. In: IBC Statistics Study Group, Washington University, Institute for Biomedical Computing.

Sachs G, Weeks DL, Melchers K, Scott DR. 2003. The gastric biology of *Helicobacter pylori*. Annual Review of Physiology 65:349-369.

Saha S, Sparks AB, Rago C, Akmaev V, Wang CJ, Vogelstein B, Kinzler KW, Velculescu VE. 2002. Using the transcriptome to annotate the genome. Nat Biotechnol 20:508-512.

Salemi M, Vandamme A-M. 2003. The Phylogenetic Handbook: A Practical Approach to DNA and Protein Phylogeny. In. Cambridge: Cambridge University Press. p. 430.

Salzberg SL, Delcher AL, Kasif S, White O. 1998. Microbial gene identification using interpolated Markov models. Nucleic Acids Res 26:544-548.

Samso M, Palumbo MJ, Radermacher M, Liu JS, Lawrence CE. 2002. A Bayesian method for classification of images from electron micrographs. J Struct Biol 138:157-170.

Schena M. 1996. Genome analysis with gene expression microarrays. Bioessays 18:427-431.

Schena M. 2003. Microarray analysis. New York: Wiley-Liss.

Schon A, Hottinger H, Soll D. 1988. Misaminoacylation and transamidation are required for protein biosynthesis in Lactobacillus bulgaricus. Biochimie 70:391-394.

Schon A, Kannangara CG, Gough S, Soll D. 1988. Protein biosynthesis in organelles requires misaminoacylation of tRNA. Nature 331:187-190.

Scott D, Weeks D, Melchers K, Sachs G. 1998. The life and death of *Helicobacter pylori*. Gut 43:S56-60.

Scott DR, Marcus EA, Weeks DL, Sachs G. 2002. Mechanisms of acid resistance due to the urease system of *Helicobacter pylori*. Gastroenterology 123:187-195.

Sharp PM, Li WH. 1987. The codon Adaptation Index--a measure of directional synonymous codon usage bias, and its potential applications. Nucleic Acids Res 15:1281-1295.

Shine J, Dalgarno L. 1975. Determinant of cistron specificity in bacterial ribosomes. Nature 254:34-38.

Siavoshi F, Malekzadeh R, Daneshmand M, Smoot DT, Ashktorab H. 2004. Association between *Helicobacter pylori* Infection in gastric cancer, ulcers and gastritis in Iranian patients. Helicobacter 9:470.

Slatkin M. 1995. A measure of population subdivision based on microsatellite allele frequencies. Genetics 139:457-462.

Stingl K, Altendorf K, Bakker EP. 2002. Acid survival of *Helicobacter pylori*: how does urease activity trigger cytoplasmic pH homeostasis? Trends in Microbiology 10:70-74.

Stingl K, Uhlemann E-M, Schmid R, Altendorf K, Bakker EP. 2002. Energetics of *Helicobacter pylori* and Its Implications for the Mechanism of Urease-Dependent Acid Tolerance at pH 1. Journal of Bacteriology 184:3053-3060.

Stingl K, Uhlemann Em EM, Deckers-Hebestreit G, Schmid R, Bakker EP, Altendorf K. 2001. Prolonged survival and cytoplasmic pH homeostasis of *Helicobacter pylori* at pH 1. Infection and Immunity 69:1178-1180.

Stortchevoi A. 2006. Misacylation of tRNA in prokaryotes: a re-evaluation. Cellular and Molecular Life Sciences 63:820.

Swofford D. 1993. Phylogenetic Analysis Using Parsimony. Champaign, IL: Illinois Natural History Survey

Swofford DL. 2000. Phylogeentic analysis using parsimony (* and other methods). Sunderland, Mass.: Sinauer.

Tajima F, Nei M. 1984. Estimation of evolutionary distance between nucleotide sequences. Molecular Biology and Evolution 1:269-285.

Tamai I, Sai Y, Kobayashi H, Kamata M, Wakamiya T, Tsuji A. 1997. Structure-Internalization Relationship for Adsorptive-Mediated Endocytosis of Basic Peptides at the Blood-Brain Barrier. J Pharmacol Exp Ther 280:410-415.

Tamura K, Dudley J, Nei M, Kumar S. 2007. MEGA4: Molecular Evolutionary Genetics Analysis (MEGA) software version 4.0. Molecular Biology and Evolution 24:1596-1599.

Tamura K, Nei M. 1993. Estimation of the number of nucleotide substitutions in the control region of mitochondrial DNA in humans and chimpanzees. Molecular Biology and Evolution 10:512-526.

Tamura K, Nei M, Kumar S. 2004. Prospects for inferring very large phylogenies by using the neighbor-joining method. Proceedings of the National Academy of Sciences of the United States of America 101:11030-11035.

Tavaré S. 1986. Some Probabilistic and Statistical Problems in the Analysis of DNA Sequences. In: Miura RM, editor. Some mathematical questions in biology – DNA sequence analysis. Providence, RI: American Mathematical Society. p. 57-86.

Terasaki T, Deguchi Y, Sato H, Hirai K-i, Tsuji A. 1991. In Vivo Transport of a Dynorphin-like Analgesic Peptide, E-2078, Through the Blood–Brain Barrier: An Application of Brain Microdialysis. Pharmaceutical Research 8:815.

The 1000 Genomes Project Consortium. 2012. An integrated map of genetic variation from 1,092 human genomes. Nature 491:56-65.
The 1000 Genomes Project Consortium. 2010. A map of human genome variation from population-scale sequencing. Nature 467:1061–1073.
Thijs G, Lescot M, Marchal K, Rombauts S, De Moor B, Rouze P, Moreau Y. 2001. A higher-order background model improves the detection of promoter regulatory elements by Gibbs sampling. Bioinformatics 17:1113-1122.
Thijs G, Marchal K, Lescot M, Rombauts S, De Moor B, Rouze P, Moreau Y. 2002. A Gibbs sampling method to detect overrepresented motifs in the upstream regions of coexpressed genes. J Comput Biol 9:447-464.
Thijs G, Moreau Y, De Smet F, Mathys J, Lescot M, Rombauts S, Rouze P, De Moor B, Marchal K. (21835525 co-authors). 2002. INCLUSive: integrated clustering, upstream sequence retrieval and motif sampling. Bioinformatics 18:331-332.
Thompson JD, Higgins DG, Gibson TJ. 1994. CLUSTAL W: improving the sensitivity of progressive multiple sequence alignment through sequence weighting, position-specific gap penalties and weight matrix choice. Nucleic Acids Res 22:4673-4680.
Thompson W, Palumbo MJ, Wasserman WW, Liu JS, Lawrence CE. 2004. Decoding human regulatory circuits. Genome Research 14:1967-1974.
Thompson W, Rouchka EC, Lawrence CE. 2003. Gibbs Recursive Sampler: finding transcription factor binding sites. Nucleic Acids Res 31:3580-3585.
Tomb JF, White O, Kerlavage AR, Clayton RA, Sutton GG, Fleischmann RD, Ketchum KA, Klenk HP, Gill S, Dougherty BA, et al. (97394467 co-authors). 1997. The complete genome sequence of the gastric pathogen *Helicobacter pylori*. Nature 388:539-547.
Trapnell C, Pachter L, Salzberg SL. 2009. TopHat: discovering splice junctions with RNA-Seq. Bioinformatics 25:1105-1111.
Trapnell C, Roberts A, Goff L, Pertea G, Kim D, Kelley DR, Pimentel H, Salzberg SL, Rinn JL, Pachter L. 2012. Differential gene and transcript expression analysis of RNA-seq experiments with TopHat and Cufflinks. Nat Protoc 7:562-578.
Ugalde JA, Chang BS, Matz MV. 2004. Evolution of coral pigments recreated. Science 305:1433.
Valenzuela M, Cerda O, Toledo H. 2003. Overview on chemotaxis and acid resistance in *Helicobacter pylori*. Biological Research 36:429-436.
Van de Peer Y, Neefs JM, De Rijk P, De Wachter R. (94016625 co-authors). 1993. Reconstructing evolution from eukaryotic small-ribosomal-subunit RNA sequences: calibration of the molecular clock. Journal of Molecular Evolution 37:221-232.
van Weringh A, Ragonnet-Cronin M, Pranckeviciene E, Pavon-Eternod M, Kleiman L, Xia X. 2011. HIV-1 Modulates the tRNA Pool to Improve Translation Efficiency. Molecular Biology and Evolution 28:1827-1834.
Velculescu VE, Zhang L, Vogelstein B, Kinzler KW. 1995. Serial analysis of gene expression. Science 270:484-487.
Venter JC, Adams MD, Myers EW, Li PW, Mural RJ, Sutton GG, Smith HO, Yandell M, Evans CA, Holt RA, et al. 2001. The Sequence of the Human Genome. Science 291:1304-1351.
Vlasschaert C, Cook D, Xia X, Gray DA. 2017. The Evolution and Functional Diversification of the Deubiquitinating Enzyme Superfamily. Genome Biology and Evolution 9:558-573.
Vlasschaert C, Xia X, Coulombe J, Gray DA. 2015. Evolution of the highly networked deubiquitinating enzymes USP4, USP15, and USP11. BMC Evol Biol 15:230.
Vlasschaert C, Xia X, Gray DA. 2016. Selection preserves Ubiquitin Specific Protease 4 alternative exon skipping in therian mammals. Sci Rep 6:20039.
Vos RA, Balhoff JP, Caravas JA, Holder MT, Lapp H, Maddison WP, Midford PE, Priyam A, Sukumaran J, Xia X, et al. 2012. NeXML: Rich, Extensible, and Verifiable Representation of Comparative Data and Metadata. Syst Biol 61:675–689.
Weeks DL, Eskandari S, Scott DR, Sachs G. 2000. A H+-gated urea channel: the link between *Helicobacter pylori* urease and gastric colonization. Science 287:482-485.
Wei Y, Silke JR, Xia X. 2017. Elucidating the 16S rRNA 3′ boundaries and defining optimal SD/aSD pairing in *Escherichia coli* and *Bacillus subtilis* using RNA-Seq data. Sci Rep 7:17639.
Wei Y, Silke JR, Xia X. 2019. An improved estimation of tRNA expression to better elucidate the coevolution between tRNA abundance and codon usage in bacteria. Sci Rep 9:3184.

Wei Y, Wang J, Xia X. 2016. Coevolution between Stop Codon Usage and Release Factors in Bacterial Species. Molecular Biology and Evolution 33:2357-2367.
Wei Y, Xia X. 2017. The Role of +4U as an Extended Translation Termination Signal in Bacteria. Genetics 205:539-549.
Wen Y, Marcus EA, Matrubutham U, Gleeson MA, Scott DR, Sachs G. 2003. Acid-adaptive genes of Helicobacter pylori. Infection and Immunity 71:5921-5939.
Williams CL, Preston T, Hossack M, Slater C, McColl KE. 1996. *Helicobacter pylori* utilises urea for amino acid synthesis. FEMS Immunology & Medical Microbiology 13:87-94.
Xia X. 2017. ARSDA: A New Approach for Storing, Transmitting and Analyzing Transcriptomic Data. G3: Genes|Genomes|Genetics 7:3839-3848.
Xia X. 2007a. Bioinformatics and the cell: Modern computational approaches in genomics, proteomics and transcriptomics. New York: Springer US.
Xia X. 2013a. Comparative genomics. Heidelberg: Springer.
Xia X. 2008. The cost of wobble translation in fungal mitochondrial genomes: integration of two traditional hypotheses. BMC Evol. Biol. 8:211.
Xia X. 2013b. DAMBE5: A comprehensive software package for data analysis in molecular biology and evolution. Molecular Biology and Evolution 30:1720-1728.
Xia X. 2018a. DAMBE7: New and improved tools for data analysis in molecular biology and evolution. Molecular Biology and Evolution 35:1550–1552.
Xia X. 2000a. Data analysis in molecular biology and evolution. Boston: Kluwer Academic Publishers.
Xia X. 2021. Detailed Dissection and Critical Evaluation of the Pfizer/BioNTech and Moderna mRNA Vaccines. Vaccines (Basel) 9:734.
Xia X. 1998a. How optimized is the translational machinery in Escherichia coli, Salmonella typhimurium and Saccharomyces cerevisiae? Genetics 149:37-44.
Xia X. 2007b. An Improved Implementation of Codon Adaptation Index. Evolutionary Bioinformatics 3:53–58.
Xia X. 2009. Information-theoretic indices and an approximate significance test for testing the molecular clock hypothesis with genetic distances. Molecular Phylogenetics and Evolution 52:665-676.
Xia X. 2015. A Major Controversy in Codon-Anticodon Adaptation Resolved by a New Codon Usage Index. Genetics 199:573-579.
Xia X. 2020. A Mathematical Primer of Molecular Phylogenetics. New York: CRC Press.
Xia X. 1996. Maximizing transcription efficiency causes codon usage bias. Genetics 144:1309-1320.
Xia X. 2005. Mutation and selection on the anticodon of tRNA genes in vertebrate mitochondrial genomes. Gene 345:13-20.
Xia X. 2000b. Phylogenetic Relationship among Horseshoe Crab Species: The Effect of Substitution Models on Phylogenetic Analyses. Systematic Biology 49:87-100.
Xia X. 2012. Position Weight Matrix, Gibbs Sampler, and the Associated Significance Tests in Motif Characterization and Prediction. Scientifica 2012:917540.
Xia X. 1998b. The rate heterogeneity of nonsynonymous substitutions in mammalian mitochondrial genes. Molecular Biology and Evolution 15:336-344.
Xia X. 2006. Topological bias in distance-based phylogenetic methods: problems with over- and underestimated genetic distances. Evolutionary Bioinformatics 2:375–387.
Xia X. 2018b. Transcriptomics and RNA-Seq Data Analysis. In. Bioinformatics and the Cell: modern computational approaches in genomics, proteomics and transcriptomics. Switzerland: Springer, Cham. p. 113-128.
Xia X. 2013c. Wobble hypothesis. In: Maloy S, Hughes K, editors. Brenner's Encyclopedia of Genetics. San Diego: Academic Press. p. 63-64.
Xia X, Hafner MS, Sudman PD. 1996. On transition bias in mitochondrial genes of pocket gophers. Journal of Molecular Evolution 43:32-40.
Xia X, Holcik M. 2009. Strong Eukaryotic IRESs Have Weak Secondary Structure. PLoS One 4:e4136.
Xia X, Huang H, Carullo M, Betran E, Moriyama EN. 2007. Conflict between Translation Initiation and Elongation in Vertebrate Mitochondrial Genomes. PLoS One 2:e227.
Xia X, Li WH. 1998. What amino acid properties affect protein evolution? Journal of Molecular Evolution 47:557-564.
Xia X, MacKay V, Yao X, Wu J, Miura F, Ito T, Morris DR. 2011. Translation Initiation: A Regulatory Role for Poly(A) Tracts in Front of the AUG Codon in Saccharomyces cerevisiae. Genetics 189:469-478.

Xia X, Palidwor G. 2005. Genomic Adaptation to Acidic Environment: Evidence from *Helicobacter pylori*. Am. Nat. 166:776-784.

Xia X, Xie Z. 2001. DAMBE: Software package for data analysis in molecular biology and evolution. Journal of Heredity 92:371-373.

Xia X, Xie Z, Kjer KM. 2003. 18S ribosomal RNA and tetrapod phylogeny. Systematic Biology 52:283-295.

Xia X, Yang Q. 2013. Cenancestor. In: Maloy S, Hughes K, editors. Encyclopedia of Genetics. San Diego: Academic Press. p. 493-494.

Xia X, Yang Q. 2011. A distance-based least-square method for dating speciation events. Molecular Phylogenetics & Evolution 59:342-353.

Yang Z, Yoder AD. 2003. Comparison of likelihood and Bayesian methods for estimating divergence times using multiple gene Loci and calibration points, with application to a radiation of cute-looking mouse lemur species. Syst Biol 52:705-716.

Zardoya R, Meyer A. 1996. Phylogenetic performance of mitochondrial protein-coding genes in resolving relationships among vertebrates. Molecular Biology and Evolution 13:933-942.

Zhu J, Liu JS, Lawrence CE. 1998. Bayesian adaptive sequence alignment algorithms. Bioinformatics 14:25-39.

Zid BM, Rogers AN, Katewa SD, Vargas MA, Kolipinski MC, Lu TA, Benzer S, Kapahi P. 2009. 4E-BP extends lifespan upon dietary restriction by enhancing mitochondrial activity in Drosophila. Cell 139:149-160.